Intra-annual Variations in Ablation and Surface Velocity on the lower Fox Glacier, South Westland, New Zealand.

Heather Purdie

Thesis submitted in partial fulfilment of the degree of Master of Science in Quaternary Science, at Massey University, Palmerston North, New Zealand.

October 2005

Abstract

This study investigates the intra-annual variations in ablation and surface velocity on the lower Fox Glacier, considering spatial and temporal variability of these processes, and looking at the driving forces behind any variability. Over the years the Fox Glacier has been the focus of little scientific research, with the majority of research being conducted on the neighbouring Franz Josef Glacier, on the premise that the two glaciers, due to their close proximity, would exhibit similar behaviour.

Large variation was recorded between the summer and winter ablation rates, with daily averages of 129 mm d^{-1} and 22 mm d^{-1} respectively. During summer, debris-cover significantly reduced ablation (50%), and ablation suppression increased as debris thickness increased. In winter this ablation suppression was not so apparent, but during heavy precipitation events, ablation under debris cover was only around half of that occurring on the clean ice surface. Variations in climate variables were found to account for over 90% of ablative variability during both summer and winter monitoring. During winter, precipitation was found to exert the most influence to ablation variability, with significant increases in ablation occurring with heavy precipitation events.

Surface velocity on the lower glacier averaged 0.87 m d^{-1} during summer and 0.64 m d^{-1} in winter, a reduction of 26%. However when recent increases to ice thickness are taken into account, this reduction increases to 32%. Reductions in velocity during winter are related to a decrease in water supply. Spatial variations of a similar magnitude were recorded across glacier and upglacier during both field seasons. Unlike ablation, climate variables were not found to exert significant influence on velocity variations. However during winter, precipitation events were found to increase velocity by up to 44%. The surface velocity response to precipitation events could be instantaneous, but on some occasions a time lag was present. This temporal variability in the velocity response is related to either variation in the morphology of the glacial drainage system, affecting the efficiency of water transport to the base of the glacier, and/or to water storage. Both processes influence water pressures in the sub-glacial drainage system, which when increased, can enhance basal sliding.

Acknowledgements

The completion of this project would not have been possible without the help and encouragement from a number of people whom I would like to acknowledge:

- Dr Martin Brook and Dr Ian Fuller for support and feedback both in the field and at the office.
- Mr David Feek for technical/field assistance, and perseverance with a rather temperamental climate station.
- Mike Browne, Kerie Uren and all the team at Alpine Guides Westland, for without their assistance, this project would never have happened. The enthusiasm and help from all the members in the guiding team was amazing, and made my time at Fox Glacier enjoyable and memorable.
- Kim Patterson and all the staff at the Department of Conservation, South Westland, thanks for all your assistance with helping this project.
- Special thanks to Dr Brian Anderson for advice, feedback and support throughout the length of this project.
- Also am also grateful for feedback and assistance received from Drs Jim Salinger, Becky Goodsell, Wendy Lawson, Andrew Mackintosh, Trevor Chinn, Alasdair Noble, Ben Brock and the NZ Snow and Ice Research Group.
- To the New Zealand Metservice, NIWA, NZ Land Information, National Library, New Zealand Aerial Mapping and The Guiding Company (Franz Josef Glacier) for assisting with data and information.
- Support and feedback from a number of colleagues in both the Geography and Earth Science Departments has been greatly appreciated. Special thanks to Matt Irwin for assistance with the GIS component of the project, and to Sina Schneider for field assistance during January 2005.
- All my friends from the PNTMC who have had to put up with my musings of the Fox Glacier during tramping trips into the Ruahine's.
- Financial support from the Massey University Masterate Scholarship, the Federation of Graduate Women (Manawatu Branch) Scholarship, and the Massey University Department of Geography.
- Mum, Dad, Fiona and Julie for support and encouragement.
- Finally to Jason, for making 2005 a very special year.

Table of Contents

List of Figures

List of Tables

Chapter 1: Introduction

1.1 Introduction

Glaciers are highly dynamic features in the landscape. They cover approximately 10% of the Earth's surface, and lock up around 80% of the world's fresh water, the volume of which could raise global sea levels by 70-80 metres (Benn and Evans, 1998). Glaciers provide one of the clearest signals of climate change, advancing and retreating in response to changes in temperature and snowfall (Benn and Evans, 1998; Chinn, 1999).

Due to their dynamic nature, glaciers can be studied on a range of temporal and spatial scales, ranging from long-term climate studies over the entire Earth, down to daily or even hourly studies of complex glaciological processes on a very small section of an individual glacier. Glaciers are of interest not only to the scientific community, but also to the general public. Glacier-based tourism is well established globally, and is of particular importance in the South Island of New Zealand. Understanding the complex relationships between climate fluctuations and glacial response on a variety of timescales is therefore important not only in predicting future glacier behaviour, but also to the safety and management of those people who live and work with these dynamic features.

1.2 Description

Fox Glacier is located on the west coast of the South Island of New Zealand at 43°30"S and 170°10"E (Figure 1.1). South Westland is a thin coastal strip, sandwiched between the Tasman Sea and the Southern Alps. Uplift of the Southern Alps began in the Pliocene (Tippett and Kamp, 1995) and has since created a barrier in excess of 3000 metres, which intercepts the dominant westerly airflow resulting in around 11 to 15 metres of precipitation per year at the top of the range (Adams, 1985; Coates and Chinn, 1992).

The Fox Glacier névé at 2700 m a.s.l is one of the largest in New Zealand, encompassing a collection area of 25 km^2 (Sara, 1970). From this large catchment, the glacier extends 12.7 km, terminating at an altitude of 270 m a.s.l, only 17 km from the present coastline.

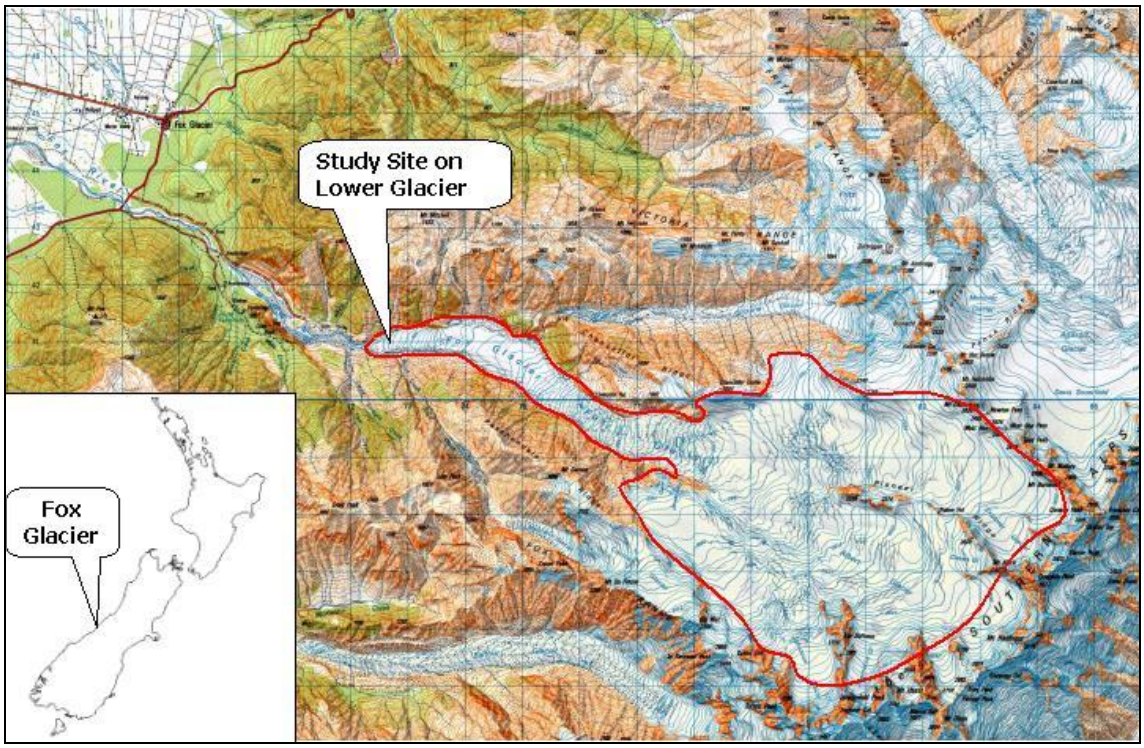

Figure 1.1 Location map of Fox Glacier on the South Islands west coast, highlighting the whole glacier and lower glacier study site. NZMS 260 H35/H36, scale 1: 50 000.

From its high névé, the Fox Glacier initially descends in a north-westerly direction down a steep icefall, the slope then lessons as it reaches its former confluence with the Victoria Glacier. From this corner, the glacier descends more steeply again down another icefall, but now has a more westerly aspect as it flows down to the present terminus (Figure 1.2). This research project focuses on the lower Fox Glacier in particular an area 250 m^2 and 400 metres upglacier from its present 2005 terminus (Figure 1.3). Access to the study site is on foot and utilises a track cut into the ice by the local glacier guiding company, Alpine Guides Westland.

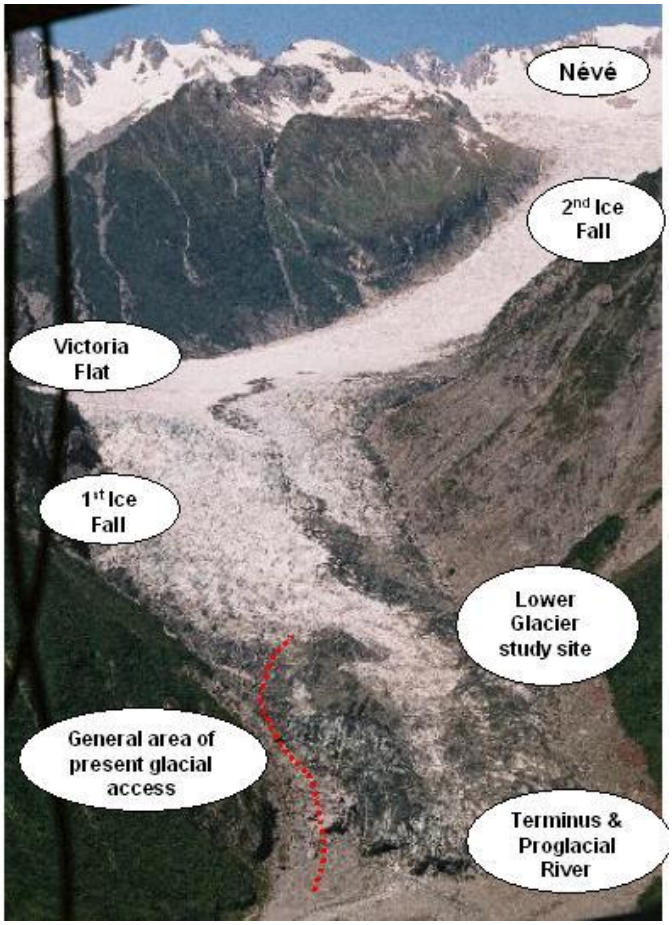

Figure 1.2 General overview of the morphology of the Fox Glacier including the névé, the two major ice-falls and the lower glacier. Source: H. Purdie.

Figure 1.3 Close up of the study site on the lower Fox Glacier. Source: H. Purdie.

1.3 The Glacier as a System

Glaciers can be thought of as an open system: with inputs of snow, ice and rock debris, and outputs of water (Figure 1.4). Whether or not a glacier advances or retreats depends on the balance between the input of snow and ice in the accumulation area, and the output of water in the ablation area. However, both accumulation and ablation can occur down the entire length of a glacier. The glacier system also interacts with other systems, in particular the atmosphere, rivers, oceans and landscape (Benn and Evans, 1998).

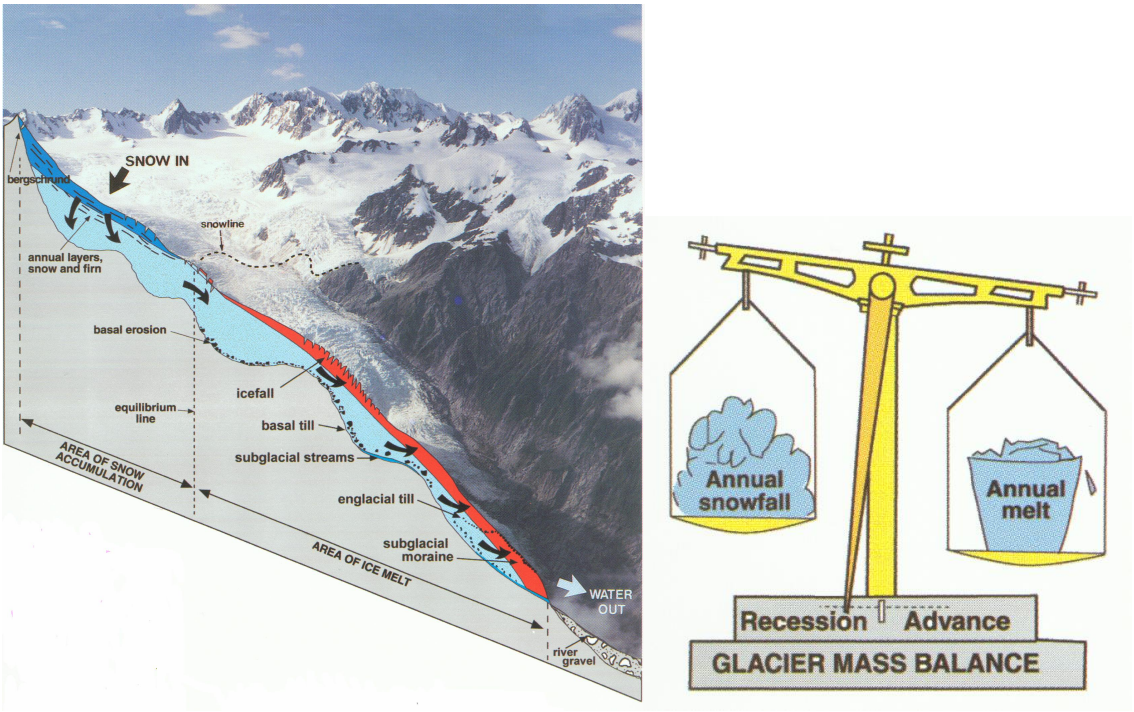

Figure 1.4 The glacier system with inputs of snow and ice in the accumulation area and outputs of water in the ablation area (right). The balance of these inputs and outputs determines whether or not a glacier is advancing or retreating (left). (Coates and Chinn, 1992)

Many inter-relationships exist between various components within this glacier system. This thesis is going to be looking at a smaller scale system on the lower Fox Glacier in the ablation area, involving climate, ablation and surface velocity (Figure 1.5). This study will focus on the inter-relationships between climate parameters and ablation, and climate parameters and surface velocity. It will also be looking to see if any direct links are found between ablation and surface velocity.

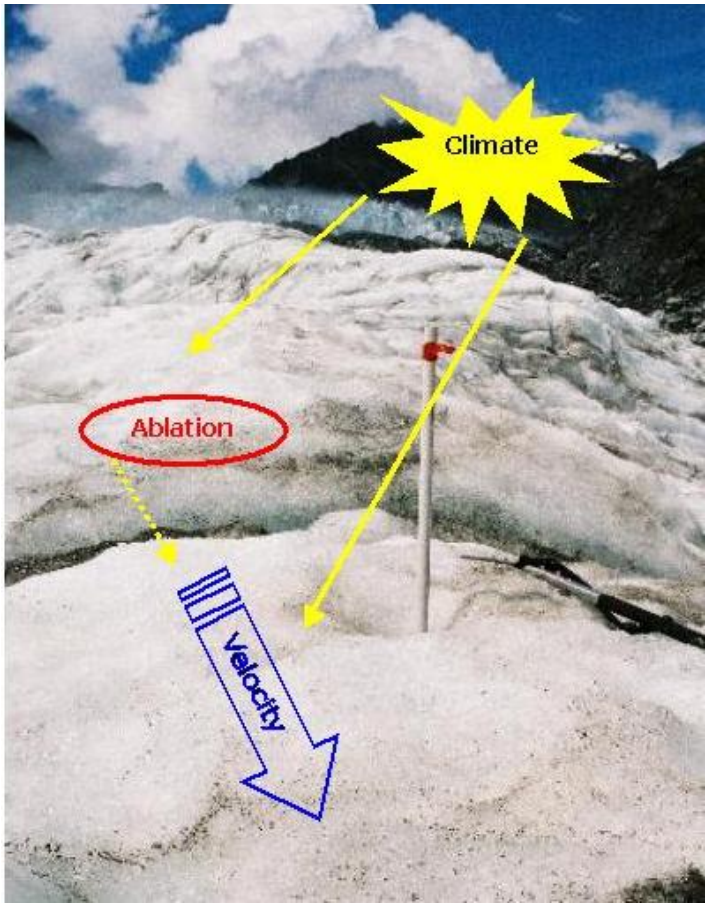

Figure 1.5 Sub-system on the lower glacier involving the interactions between climate, ablation and surface velocity. Source: H. Purdie.

1.4 Thesis Structure

This thesis is divided into eight chapters. The next chapter (chapter two) provides an overview of previous research with particular attention to research conducted on both ablation and surface velocity. Chapter three looks at research methodology, and outlines the techniques used in this study. Chapters four to six report results for climate, ablation and surface velocity measurements respectively. Chapter seven provides discussion on the results gained, and identifies areas for further research. Finally, chapter eight is a summary of key findings.

Chapter 2: Literature Review

2.1 Historical Overview

The Fox and Franz Josef Glaciers have captured the interest of researchers since the late 1800s. At the peak of the Otira Glaciation[1], these major west coast glaciers extended beyond the present coastline, and a considerable amount of research has focused on attempting to reconstruct these past glacial limits (Almond*, et al.*, 2001; Denton and Hendy, 1994; Gellatly*, et al.*, 1988; McGlone*, et al.*, 1993; Mercer, 1988; Suggate, 1990).

Knowledge and interest in these alpine glaciers goes back prior to European discovery and settlement. The Maori name for the Fox Glacier -*Te Moeka o Tuawe*, is derived from the ancestor (tupuna) Tu Awe, who legend tells us, fell to his death when exploring in the area. The bed of the glacier became his final resting place (moeka), and it was the tears of his lover Hine Hukatere, that filled the valley with ice (Alpine Guides Westland, 2005).

One of the earliest European accounts of the glaciers occurred in 1859, during a voyage of the *Mary Louisa.* An entry into the ships logbook recorded "…an immense field of ice, entirely filling up the valley…" (Sara, 1970, p7). Many descriptions of the glaciers followed in the 1860s once gold was discovered in the region, and records began with reports from explorers Douglas and Harper (Douglas, 1896; Langton, 2000; Wilson, 1896).

The Fox Glacier was originally named the Albert Glacier by Haast, but was later changed to Fox, after Sir William Fox, who visited the area when he was Premier of the Colony of New Zealand in 1872 (Sara, 1970). Fox painted a watercolour of the glacier (Figure 2.1), which shows its enormity at this time, with white ice extending down past Cone Rock, some 2.5 km down-valley of the present (2005) terminus. Figure 2.2 is a photograph taken in June 2005 from a similar location that shows the extent of change in the glacier over the years.

[1] The Otira Glaciation spanned Marine Oxygen Isotope (MOI) stages 2-4, around 70-10 ka yrs BP. The peak of this glaciation, often referred to as the Last Glacial Maximum, occurred around 18-20 ka yrs BP with the Kumara 2.2 advance in Westland. During this peak, sea level is estimated to have been 120 m lower than present, and temperatures 4.5 to 5 ^{o}C colder (McGlone *et al.*, 1993)

Figure 2.1 Watercolour of the Fox Glacier in 1872, painted by Sir William Fox. Image provided by the Alexander Turnbull Library.

Figure 2.2 Photograph of Cone Rock (right foreground) with the Fox Glacier visible upvalley and Mt Tasman at the head of the glacier on the skyline, taken June 2005. Source H. Purdie.

Early reports on the Fox Glacier were made by Douglas (1896) and Wilson (1896) (Figure 2.3), with Douglas being one of first Europeans to visit the terminal face (Langton, 2000). Douglas (1896) made an assessment of both the Fox and Franz Josef Glaciers as far as tourist interest was concerned, reporting that:

> "*As a mere mass of ice in a valley, the Fox Glacier cannot compare for a moment with the Franz Josef, its ice-fall is inferior, and the surface of the glacier not so broken up into picturesque pinnacles…" (Douglas, 1986, pp 110)*

However, it was also noted by Wilson (1896) at this time, that access onto the white-ice of the Fox Glacier was much easier.

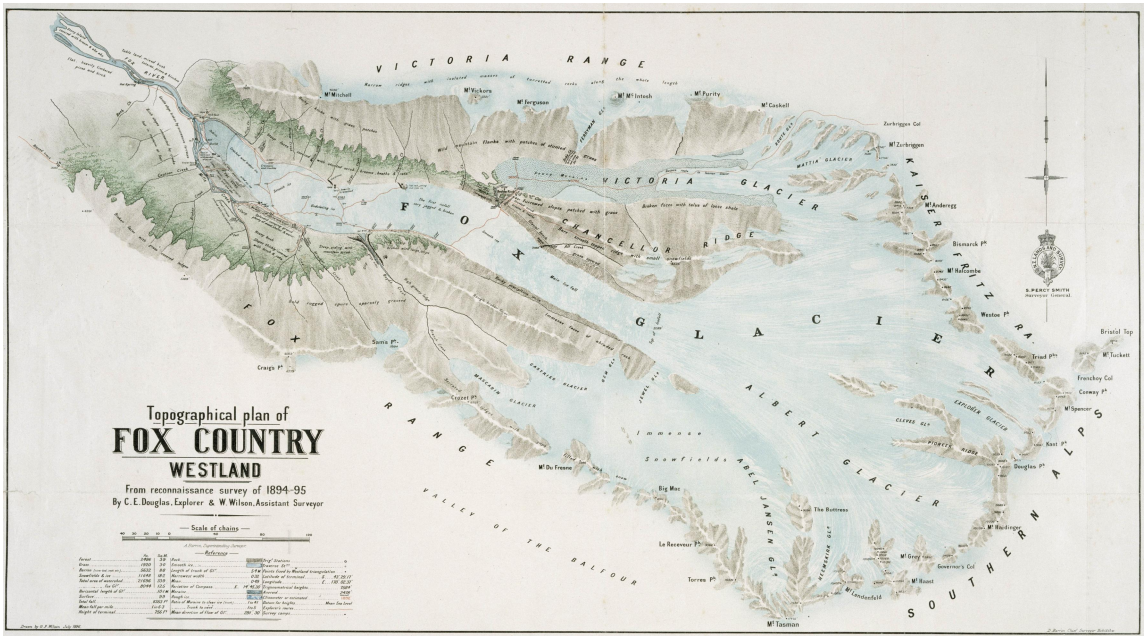

Figure 2.3 Topographical plan of the Fox Glacier prepared by Douglas and Wilson (1896), showing the extent of the glacier and its tributaries. Image supplied by the Alexander Turnbull Library.

Today, both the Fox and Franz Josef Glaciers form important hubs for an increasing tourist industry, with over 400,000 visitors travelling through the Westland *Tai Poutini* National Park each year (Department of Conservation, 2001), and up to 300 visitors taking part in guided walks on the Fox Glacier daily during the summer months. Over the years, the majority of the scientific research has been conducted on the Franz Josef Glacier, with the Fox Glacier receiving only minimal and sporadic attention (Sara, 1968).

2.2 Early Focus on Advance and Retreat

Much of the early research focused on the advance or retreat of the terminal faces of the glaciers, with Franz Josef receiving most of the attention. This has been attributed to the accessibility of the terminal face, the dynamic nature of the glacier, and its aesthetic grandeur (Odell, 1960; Sara, 1968). Suggate (1950) reported how the Fox Glacier had advanced and retreated in a similar way to the Franz Josef Glacier

(although the advance of 1946-47 had not occurred at Fox), and that similar behaviour was expected, due to the similarity in locations between the two glaciers. Sara (1968) noted how minimal observations had been made of the Fox Glacier, but also shared the view that the two glaciers would exhibit similar behaviour. Notably, periods of research interest seem to have coincided with advance phases of the glaciers (Brazier, *et al*., 1992; Fitzharris, *et al*., 1999) with a gap in the literature in the 1970s.

Sara (1970) compiled a terminus map of the Fox Glacier (Figure 2.4) showing various terminus positions since the late 1800s, and more recently Anderson (pers. comm., 2005) annotated photographs that depict historic trim-lines (Figure 2.5). Both the terminus map and the photographs graphically show the extent of retreat since the 1700s.

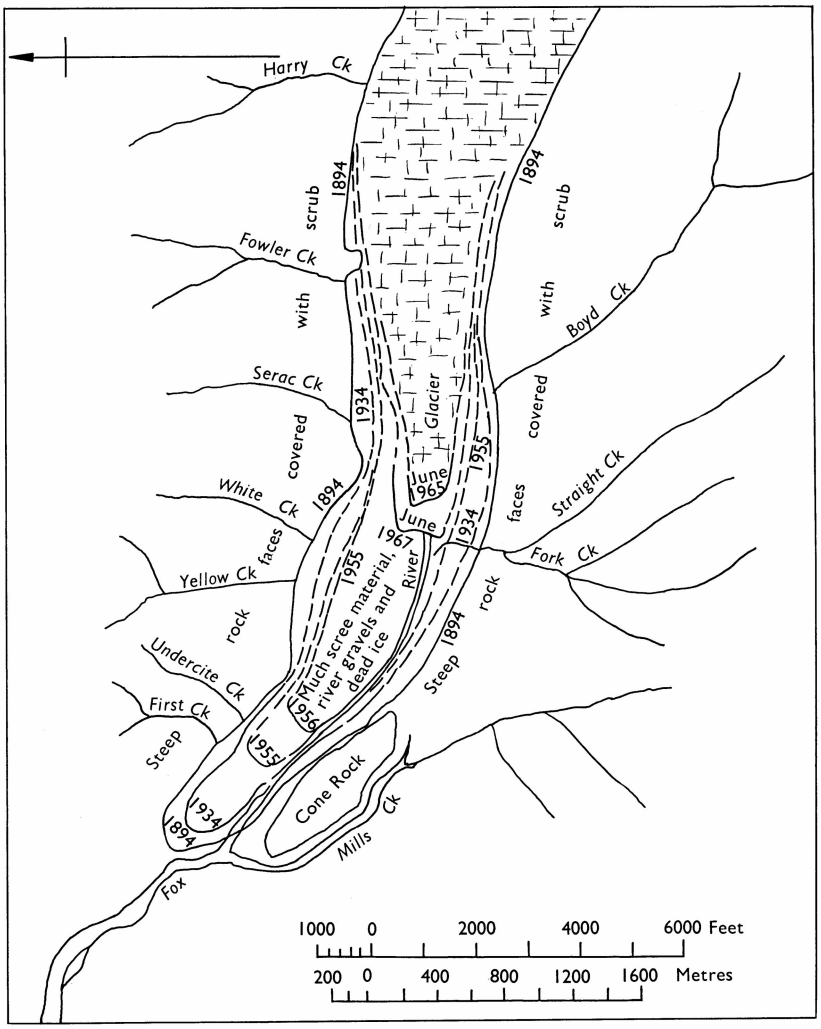

Figure 2.4 Map depicting the historic terminus positions of the Fox Glacier (Sara, 1970).

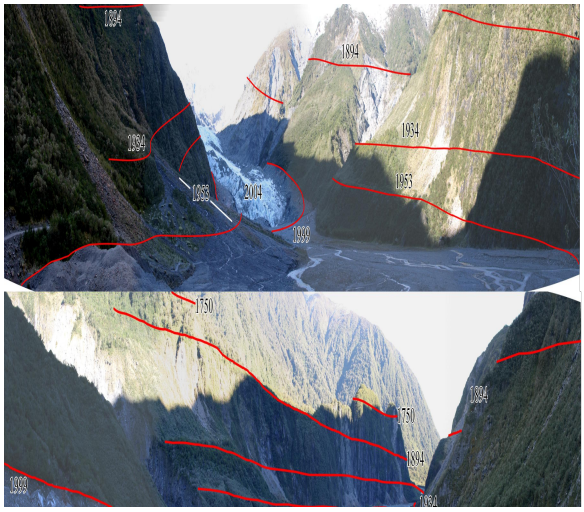

Figure 2.5 Upvalley (top) and down-valley (bottom) photographs of the Fox Glacier showing historic trim-lines, Anderson (pers. comm., 2005).

However, as highlighted by Chinn *et al*. (2002b), the position of the terminus does not simply relate to the changes in volume of a glacier, or its response to climate. Changes in ice thickness and storage create lags in a glaciers response time, resulting in the loss of vital information about relationships between climate change and glacier response. A terminal face could theoretically remain in a static position whilst the height of ice is either reduced or increased. Douglas (1896) noted this phenomenon, reporting that the Fox Glacier appeared to be "dying out" in the middle, but was not retreating from its terminus as expected. Despite this, the position of the terminal face of a glacier is of popular interest, and is a concept that can be readily related to by scientists and the general public alike. Over longer time periods, terminus position does tell a story about climate change.

Figure 2.6 shows the current (2005) terminus as mapped with RTK-GPS survey during this study. The present terminus is 200 metres down-valley of the position shown on the current topographic map (NZMS 260 H35), but still 170 metres short of the push moraine left by the 1998/99 advance. The terminus position used on the NZMS topographic map, is based on information from the 1987 aerial photograph (Land Information New Zealand, pers. comm., 2005), during this period the glacier was at its most retreated in recorded history (Figure 2.7). The current terminus of the Fox Glacier is still some 2.5 kilometres up-valley from the 1894 position.

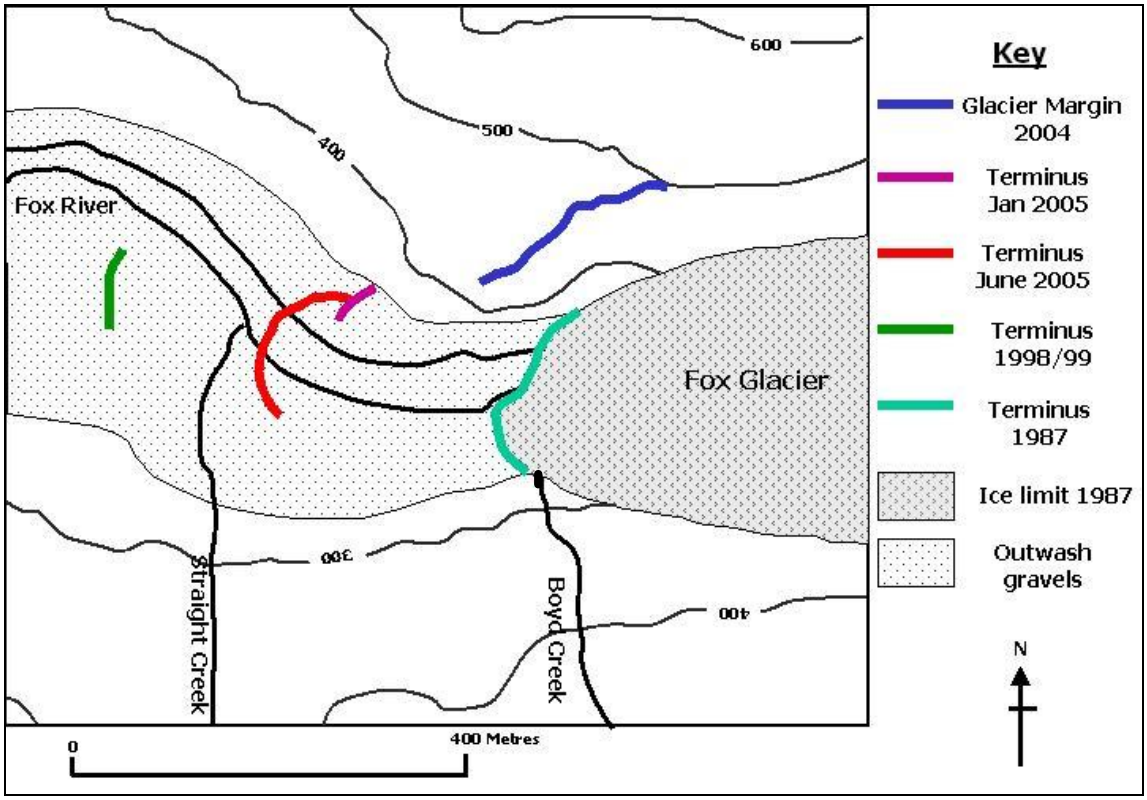

Figure 2.6 Terminus map of the Fox Glacier showing recent terminus positions including the current (2005) position mapped by RTK-GPS survey in June 2005.

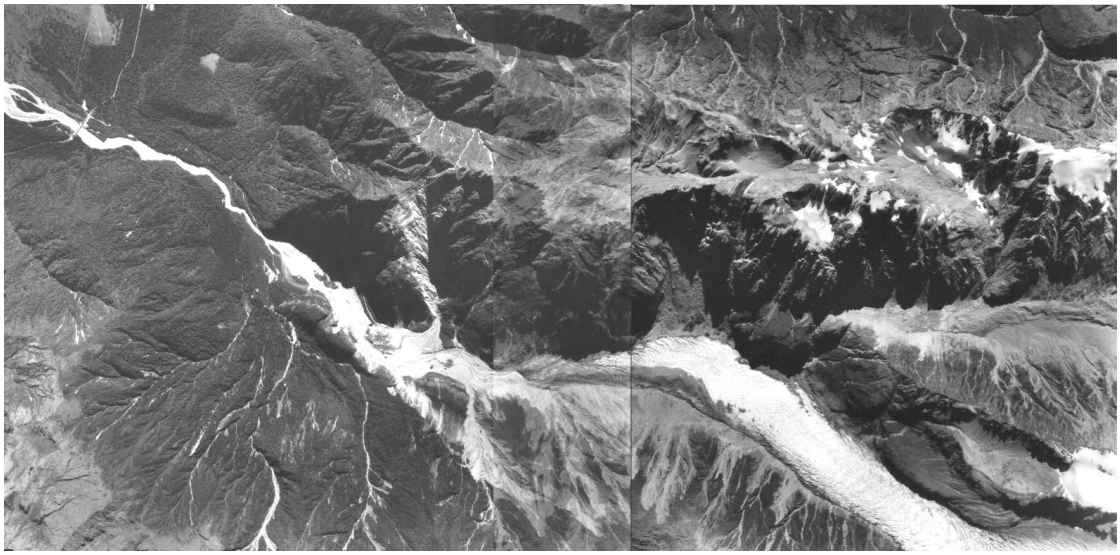

Figure 2.7 Aerial photograph of the lower Fox Glacier taken in March 1985. During this period the glacier was in one of it's most retreated positions since records began. Aerial Photograph SN 8478 G11/G13, NZ Aerial Mapping Ltd.

2.3 Glacier-Climate Interaction

2.3.1 Initial Correlations

Suggate (1950) made tentative correlations between the advance and retreat of the Franz Josef Glacier and precipitation. He suggested that "the amount of precipitation brought by the prevailing westerly winds may, at least in some part, account for the glacier fluctuations" (Suggate, 1950, p427). Following that, there has been some debate over the importance of precipitation versus temperature to glacier behaviour (Gellatly and Norton, 1984; Hessell, 1983; Salinger, *et al*., 1983). More recent modelling of the Franz Josef Glacier seems to indicate that temperature could provide the larger driving force (Anderson, 2003).

The existence of long-term climate databases from Franz Josef township, has meant that this glacier, with its well documented terminus, has been extensively used for glacier-climate correlations, with more recent research focusing on a wide range of climatic variables like changes in the El Niño Southern Oscillation, and sea surface pressure anomalies (Chinn, 1999; Clare, *et al*., 2002; Evans, 2003; Fitzharris, *et al*., 1992; Fitzsimons, 1997; Hay and Fitzharris, 1988; Hooker, 1995; Hooker and Fitzharris, 1999; Tyson, *et al*., 1997). Such an extensive climate record does not exist for the Fox Glacier, and to date, no similar climate modelling has been conducted.

Research by Hay and Fitzharris (1988) on the Ivory Glacier in Westland, found that the general regional synoptic situation had an important influence on the energy balance of snow and ice. They concluded that the long-term behaviour of the glacier was sensitive to the frequency of synoptic situations, and influenced by circulation changes in the southwest Pacific, in particular, the strength of westerlies and blocking anticyclones. It is now recognised that it is a combination of various atmospheric and circulation patterns during both the accumulation season (April-October) and the ablation season (November-March) that exert control on a glaciers mass balance (Chinn, 1999; Clare*, et al.*, 2002; Evans, 2003; Fitzharris*, et al.*, 1992; Fitzharris*, et al.*, 1997; Fitzharris*, et al.*, 1999; Hooker, 1995; Hooker and Fitzharris, 1999; Tyson*, et al.*, 1997).

2.3.2 General Climate of South Westland

New Zealand is located in the mid-latitude westerly zone and consequently the weather is influenced by high-pressure systems tracking westwards from Australia, and intervening cold fronts often generated in the Southern Ocean. A regular cycle of anticyclone, trough, anticyclone can take about a week to pass over New Zealand, with the associated airflow changing from northerly to westerly to southerly respectively (Brenstrum, 1998; Fitzharris, 2001; Sturman, 2001b).

The Southern Alps sit perpendicular to this predominant westerly flow, creating a barrier to the warm moist air arriving across the Tasman Sea. Orographic lifting of these air masses, and associated condensation, results in a strong west-east gradient in precipitation, with the west coast receiving in excess of 10,000 mm annually compared to only 600 mm in the east (Fitzharris, 2001; Griffiths and McSaveney, 1983; Sturman, 2001b).

The Department of Conservation's management plan for Westland *Tai Poutini* National Park describes the climate as "vigorous and diverse and is responsible for the development of the glaciers and the rain forests" (Department of Conservation, 2001). The National Institute of Water and Atmospheric Research (NIWA) has not monitored climate variables at Fox Glacier since 1994, however data gathered between 1966 and 1994 (climate station F30402) showed that the Fox Glacier township receives an average of 4691 mm precipitation per year. The lowest rainfall months are during winter (June to August), with October being the wettest month. Daily temperature averaged 15.4^{o}C, with July the coldest (11.5^{o}C) and February the hottest (19.7^{o}C). Average relative humidity is 94.7%, and vapour pressure 1080Pa (NIWA, 2005).

Sixteen kilometres to the northwest at Franz Josef Glacier township NIWA continues to monitor climate variables (climate station F330312, 1982-2005). Franz Josef appears to have a higher average precipitation at 5878 mm. Average daily temperature is identical to that recorded at Fox, but both humidity and vapour pressures are lower at 89.5% and 1040 Pa respectively. January is the sunniest month (June lowest) and on average, 1199 sunshine hours are received annually (NIWA, 2005).

2.3.3 Glacier Micro-Climates

Although it has been found that the regional synoptic situation exerts an important control on overall glacier mass balance and subsequent behaviour (Evans, 2003; Fitzharris*, et al.*, 1992; Fitzharris*, et al.*, 1997; Hay and Fitzharris, 1988; Hooker, 1995; Hooker and Fitzharris, 1999), glaciers can themselves exert influence on local climate. Each glacier will have a specific microclimate created by its particular location, morphology, and topographic setting (Benn and Evans, 1998; Oerlemans, 2001; Paterson, 1994). The process of glaciation results in a very distinctive landscape, moulding features like glacial troughs, cirques, roche moutonnées and moraine deposits. Some of these features in turn can influence local climate, in particular the glacial trough, where steep valley walls create topographic shading, for example at the Untere Grindelwaldgletscher in Switzerland, the snout receives little solar radiation. It has been found that glaciers occupying such shaded valleys, can penetrate to much lower altitudes (Oerlemans, 2001).

In valleys, there is a diurnal rhythm of anabatic and katabatic wind flow. During the day wind flows upslope due to heating (anabatic wind), but at night, cooler, more dense air flows down valley (katabatic wind) (Sturman, 2001a). The surface temperature of a glacier is lower than the surrounding air, therefore it can disrupt this normal diurnal pattern (Oerlemans, 2001). Research on the Morteratschgletscher in Switzerland, found that irrespective of the time of year, wind flowed down glacier most of the time (Oerlemans, 2001).

2.4 Mass Balance

As mentioned in section 2.2 the earliest method for assessing glacier fluctuations was by monitoring the terminus position, and despite the limitations outlined, this technique has resulted in a comprehensive record of past glacier fluctuations, particularly for the Franz Josef Glacier, and continues to be an important tool for glacier monitoring (Brazier*, et al.*, 1992; Owens, 2005; Suggate, 1990). However, in order to establish a clear picture of climate change, the mass balance of a glacier needs to be examined (Chinn, 1999; 2001).

The mass balance of a glacier is the difference between the annual input of snow and ice and the annual output of water. Over a given balance year (usually taken from March) the mass balance can be either positive or negative (Nesje and Dahl, 2000). The equilibrium line on a glacier is the place where inputs equal outputs, and marks the transition between the accumulation and ablation zones (Figure 2.8).

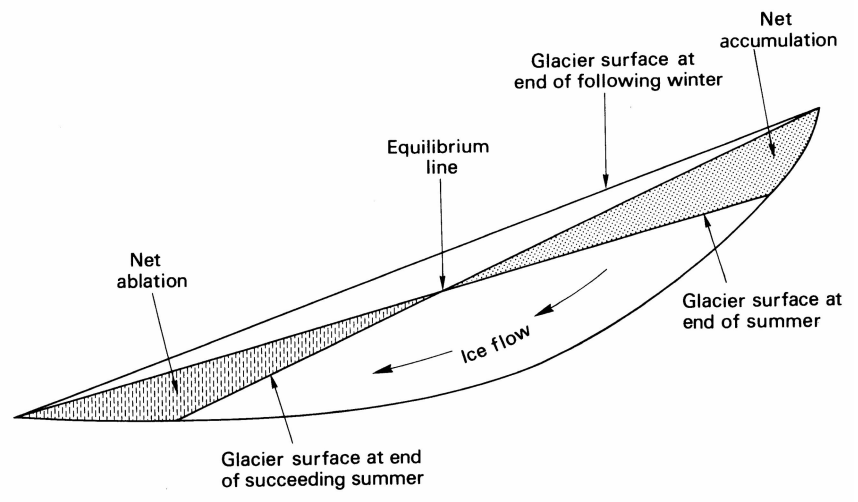

Figure 2.8 Diagram showing the net balance of a glacier, where net accumulation is balanced by net ablation. These two zones are separated in theory by the equilibrium line (Summerfield, 1991).

In Norway, mass balance measurements have been underway for many years with the Storbreen and Nigardsbreen Glaciers being monitored since 1949 and 1962 respectively (Hagen, *et al*., 1998). Likewise, in North America, mass balance measurements on the White and Sverdrup Glaciers began similarly in the 1960s (Ommanney, *et al*., 1998). Measuring mass balance directly is very intensive, requiring large inputs of labour, time and resources. Consequently in New Zealand, very few glaciers have had their mass balances measured directly, although such work has been conducted on the Ivory and Franz Josef Glaciers (Anderson, 2003; Chinn, *et al*., 2002a).

Although annual ablation is quite straightforward to measure (see section 3.2), accumulation is more difficult. Paterson (1994) suggested digging pits or taking ice cores to locate the previous summers surface, where as both Anderson (2003) and Ruddell (1995) used crevasse stratigraphy. Alternatively, meteorological data can be used to numerically model a glaciers mass balance (Anderson, 2003; Braithwaite and Zhang, 2000; Oerlemans, 1997; Woo and Fitzharris, 1992) or, the position of the end-of-summer-snowline (EOSS) can be used as a surrogate for annual mass balance (Chinn, 1995; 1999; Chinn*, et al.*, 2002a; 2003; Clare*, et al.*, 2002).

In New Zealand, an extensive monitoring programme began in 1977, which involves photographing the position of the EOSS for 50 index glaciers from a light aircraft at the very end of summer (usually the end of March). What is determined from the snowline is the departure of the EOSS from the steady state equilibrium line altitude (ELA), thereby giving an indication as to whether the mass balance of a glacier is positive or negative[2]. Photographic surveys can cover a large number of glaciers in a very short period of time, providing regional as well as local information. Both the Fox and Franz Josef Glaciers have crevassed icefalls occurring at their ELAs resulting in these glaciers being unsuitable for monitoring. Therefore, the nearby Chancellor and Salisbury (Almer) Glaciers respectively, are used as alternative indicators (Chinn, 1995).

In 2003 it was noted that all the index glaciers exhibited a positive mass gain and the Chancellor Glacier showed a snowline depression of 186 meters (Chinn*, et al.*, 2003). How representative this is of the actual mass balance of the Fox Glacier is yet to be determined. Anderson (2003) considered whether the EOSS for the Almer (Salisbury) Glacier did actually predict the mass balance of the Franz Josef Glacier. A comparison of the measured Almer Glacier EOSS with the calculated mass balance of the Franz Josef Glacier revealed that there was not a strong relationship between them, therefore the EOSS of the Almer Glacier could not provide an accurate prediction of the mass balance of the Franz Josef Glacier. However, despite limitations for the Fox and Franz Josef Glaciers, this ongoing survey programme provides valuable information on the regional and national trends in glacier behaviour, which can then be correlated with climatic trends.

The effect that any climatic change has on the mass balance of a glacier depends on that glacier's area-altitude distribution or hypsometry. A glacier that has a large proportion of its area close to the ELA (for example the Nigardsbreen, in Norway and the Franz Josef and Fox Glaciers in New Zealand) will experience large fluctuations in mass balance from even small annual climate fluctuations. Conversely, a glacier with a small part of its area close to the ELA will be less sensitive to change (Benn and Evans, 1998; Oerlemans, 2001; Paterson, 1994). So although advance and retreat may be driven by large-scale circulation fluctuations, some glaciers in an area could theoretically be advancing while another retreats. Differences in local climate, size or

[2] When a glaciers mass balance is increasing, it will have a negative EOSS in relation to the steady state ELA resulting from a depressed snowline. Conversely, if mass is decreasing, the EOSS will be positive, with the snowline at a higher altitude than the steady state ELA. (Chinn *et al*,. 2003).

steepness of an individual glacier can result in a different reaction rate to an identical change in mass balance (Paterson, 1994).

2.5 Ablation

2.5.1 Ablation and the Energy Balance

Ablation is the means by which mass is removed from a glacier, and includes melting followed by run off, evaporation, sublimation, avalanching and calving (Benn and Evans, 1998). For the purposes of this thesis, the term ablation is subsequently used to refer to the process of surface melt followed by run off. To fully understand the mechanisms driving ablation, consideration needs to be given to the energy balance at the glacier surface. The energy balance can be defined as the surplus or deficit of energy over a given time frame. Ablation will not occur unless there is an energy surplus (Benn and Evans, 1998).

An important component of the energy budget is the radiation budget, given buy:

$$Q^* = K\downarrow - K\uparrow + L\downarrow - L\uparrow) = K^* + L^* \quad (1)$$

where Q^* is the net radiation; $K\downarrow$ is the incoming short-wave radiation; $K\uparrow$ the reflected short-wave radiation; K* the net short-wave radiation; $L\downarrow$ the incoming long-wave radiation; $L\uparrow$ the emitted long-wave radiation, and L* is the net long-wave radiation (Spronken-Smith, 2001).

The amount of incoming short-wave radiation received at the surface is controlled by both the azimuth and zenith of the sun, while the amount lost from the surface is related to surface albedo. Therefore, site factors like aspect and topographic shading are important to the local energy balance (Benn and Evans, 1998; Spronken-Smith, 2001).

Incoming long-wave radiation is dependent on cloud cover, temperature and the emissivity[3] of the atmosphere, with temperature and emissivity of the surface also influencing the amount of outgoing long-wave radiation (Spronken-Smith, 2001). The lower atmosphere can trap long-wave radiation (The Greenhouse Effect), with water

[3] Emissivity is the ratio of radiant energy emitted from a surface compared to that of a black body.

vapour being particularly efficient at this, resulting in more energy available for heating and ablation (Benn and Evans, 1998).

Snow and ice surfaces have both high albedo and high emissivity. The high albedo results in much of the K↓ being reflected, therefore there is generally only a small surplus in net radiation (Q^*). When considering the energy balance of a glacier, it is the amount of energy available for melting (Q_M) that is most important (Lawson and Fitzsimons, 2001; Spronken-Smith, 2001).

The energy balance of an ice surface can be expressed as:

$$Q_M = Q^* + Q_H + Q_E + Q_P + Q_G \quad (2)$$

where Q^* = net radiation; Q_H = sensible heat flux (resulting from thermal energy exchanges at the surface/atmosphere interface i.e. valley winds); Q_E = latent heat flux (from state changes of water); Q_P = rainfall heat flux; Q_G = conductive heat flux below the ice surface.

All of the fluxes are measured in W/m^{-2} or MJ $m^{-2}d^{-1}$. In general fluxes are positive if they are directed towards the surface and negative if they are sinks (Marcus, *et al*., 1985). During the ablation season, the net radiation is usually positive (heat source) for most glaciers. The latent heat flux can be positive or negative depending on the state change of water. For example, evaporation leads to heat lost from the surface, and condensation heat gain. The rainfall heat flux component is generally very small, and the conductive heat flux is usually considered to be zero for temperate glaciers (Owens, *et al*., 1992). Figure 2.9 shows the variations in the radiative energy fluxes on a surface between day and night.

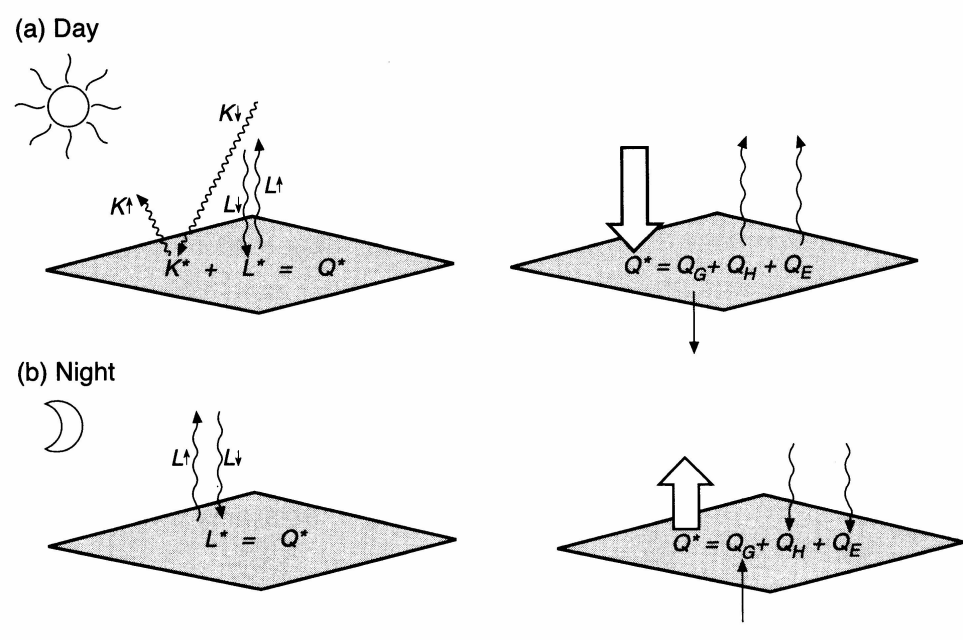

Figure 2.9 Variations in radiative and energy fluxes on a surface between day and night. (Spronken-Smith, 2001).

Generally it is the net radiation (both short and long-wave) that is the most important component of the ablation energy balance (Braithwaite, 1981). However, in maritime climates like western Norway, and New Zealand, the net radiation accounts for only around 10-50% of the energy balance (as opposed to 66% in continental climates). Therefore, energy from sensible heat transfer and latent heat transfer becomes more important, especially when warm moist air moves over the glacier surface (Benn and Evans, 1998; Hay and Fitzharris, 1988).

Each glacier has a specific microclimate created by its particular location, morphology and topographic setting, but this microclimate is embedded within the regional and global climate (Benn and Evans, 1998). Takeuchi *et al.* (1999) compared the ablation characteristics of five glaciers, four in Patagonia and the Franz Josef Glacier in New Zealand. All are situated in the mid-latitudes with a strong humid westerly airflow and high precipitation, and all reported large ablation rates ranging from 49-98 mm d^{-1}.

Takeuchi *et al*. (1999) found that although locally the ratios of the different fluxes varied, with the Franz Josef Glacier and the Soler Glacier (Patagonia) having the highest sensible and latent heat fluxes (Figure 2.10), while the San Rafael had the largest net radiation, overall, the total heat flux was similar, ranging from 240-300 W/m^{-2}. Although not wanting to discuss reasons for this similarity, it was postulated that the total heat flux is related to global radiation and large-scale climatic conditions.

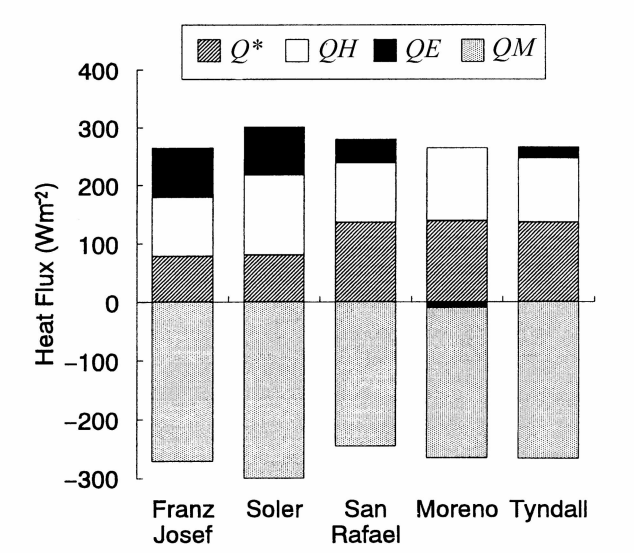

Figure 2.10 Heat balance on mid-latitude glaciers (Takeuchi*, et al.*, 1999).

Variability between the ablation rates of different glaciers is large. Continental glaciers (like the Columbia Glacier in Alaska, and the White Glacier in Canada) can have annual ablation rates ranging between 2.0 and 3.4 m w.e (metres water equivalent) (Oerlemans, 2001; Pelto, 2000). Temperate glaciers with maritime climates like the Nigardbreen (Norway) and the Franz Josef Glaciers, have annual ablation rates of 10 and 20 m.w.e respectively (Anderson, 2003; Oerlemans, 2001).

2.5.2 Spatial Variability in Ablation

Ablation rates on a glacier vary spatially. Because there is a negative linear relationship between temperature and altitude (due to decreasing barometric pressure), it follows that ablation rates will be at a maximum near the terminus and minimum on the upper glacier (Benn and Evans, 1998; Nesje and Dahl, 2000). Previous research on Franz Josef Glacier seems to supports this, and although measured at different times, average melt rates of 30 mm d^{-1} were recorded in the névé at 2150 metres a.s.l (Kelliher, et al., 1996), and 137 mm d^{-1} on the lower glacier at 500 metres a.s.l (Owens*, et al.*, 1992).

Spatial variability in ablation can also result from varying degrees of debris cover. Debris can influence ablation by two mechanisms. First, debris has a lower albedo than clean ice, therefore it absorbs more incoming radiation, heats up, and re-emits long-wave radiation to adjacent ice surfaces. This effect is noticeable in very thin (2-5 mm) or patchy debris cover, and serves to increase the rate of ablation. Second, debris can insulate underlying ice by shielding it from radiation and heat, thereby reducing

ablation. Reductions in ablation occur when debris cover is around 10 mm thickness, and above 30 mm, the debris actually begins to suppress ablation (Benn and Evans, 1998; Nakawo and Young, 1981; Singh*, et al.*, 2000). Figure 2.11 shows these two thresholds where a very thin cover of debris accelerates ablation, but this rate drops rapidly once the debris is thicker than around 10 mm.

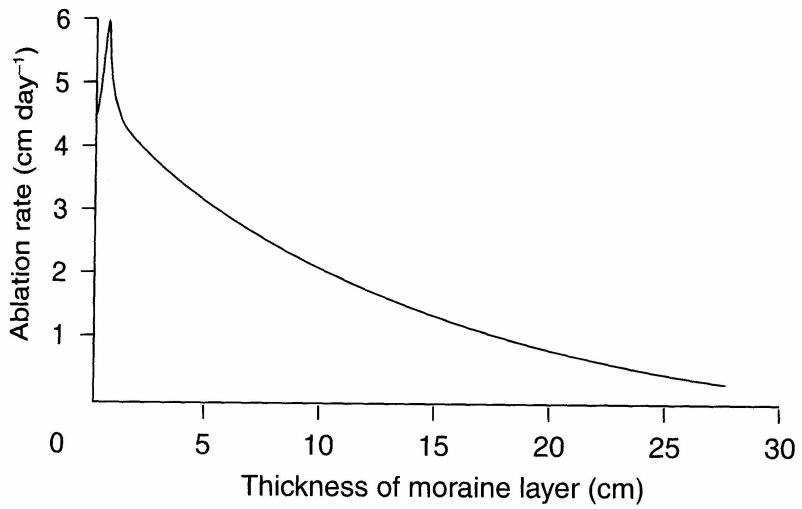

Figure 2.11 Relationship between debris cover thickness and rate of ablation (Benn and Evans, 1998).

The importance of this insulating effect was highlighted by Purdie (1996) in research on the lower Tasman Glacier on the east side of the Southern Alps in New Zealand, where it was found that temperature ranged between 3.3-34.1°C on the heavily debris covered surface, but was only between –0.4-1.2°C at the ice-debris interface at a depth of 1.1 metres. This resulted in ablation rates being suppressed by 93%. Likewise, research conducted by Pelto (2000) on the Lyman and Columbia Glaciers in North America, and by Takeuchi *et al.*(2000) on the Khumbu Glacier in Nepal, found that debris cover (ranging from 100 – 200 mm thickness) suppressed ablation by 30-40%. It was also found that very fine-grained debris cover, consisting of a clay-sand mixture, seemed to provide better insulation in comparison to a cover consisting of larger clast sizes (Pelto, 2000). General observation of the glacier surface can also detect the insulating effect of debris-cover, as these areas tend to have greater vertical relief than surrounding clean-ice areas (Pelto, 2000). Singh *et al.* (2000) tried to detect the albedo effect with their work on the Dokriani Glacier in the Garhwal Himalayas, and found that the presence of a very fine debris cover (2 mm thickness) increased the melt rate on the ice by 8.5%.

Research by Evans (2003) on the lower Franz Josef Glacier found summer ablation to be highly variable with rates ranging from less than 10 mm d^{-1} up to 180 mm d^{-1}. It was concluded that this high degree of variability was a result of varying synoptic conditions and differing characteristics of the glacier surface. Due to problems drilling into the debris-covered ice, most stakes were positioned on clean ice with no comparison being made between the ablation rates of clean ice and debris-covered surfaces. In other work in the Franz Josef Glacier, Marcus *et al*. (1985) determined that surface characteristics like aspect, wind exposure and surrounding topography contribute to spatial variability, and due to these factors, the extrapolation of measurements taken from one site as being representative of the entire ablation area of a glacier can be problematic.

2.5.3 Temporal Variability in Ablation

Seasonal and diurnal variations in ablation have been recorded on the Franz Josef Glacier, with highest rates occurring during summer, and during daylight hours (Ishikawa*, et al.*, 1992; Kelliher*, et al.*, 1996). It was found that the summer mean melt rate was eight times higher than that which occurs during winter (Ishikawa*, et al.*, 1992), with daily rates varying from 8 mm d^{-1} in August up to 72 mm d^{-1} in December (Marcus*, et al.*, 1985). Kelliher, *et al*. (1996) found that in the Franz Josef névé area there was large diurnal variation with 69 mm of melt occurring during the day and only a further 1 mm overnight. Research at a lower altitude (700m) by Marcus *et al.* (1985) found that any diurnal variability was masked by synoptic-scale influences, and the nature of the glacier surface, whilst Braithwaite *et al.* (1998) identified a strong diurnal variability in ablation in the continental climates of North Greenland due to nocturnal cooling by outgoing long-wave radiation and sublimation.

Studies also show that rapid melt can occur at any time, especially during heavy rain when the mechanical and thermal action of running water increases surface melt (Gunn, 1964; Marcus*, et al.*, 1985; Moore and Owens, 1984; Owens*, et al.*, 1992). Marcus *et al*. (1985) recorded a 196 mm surface lowering in 19 hours during an intense rainstorm in June 1981 (306 mm rain in 12 hours) on the Franz Josef Glacier. This melt rate was more then double the previously recorded mean summer rate.

Duration of ablation measurements range from those taken over only a few days (Ishikawa*, et al.*, 1992; Kelliher*, et al.*, 1996; Marcus*, et al.*, 1985; Owens*, et al.*, 1992; Takeuchi*, et al.*, 1999) to more prolonged study periods (Anderson, 2003; Evans,

2003), with the majority of work being conducted during the summer (ablation) season. However, in a maritime climate, ablation should occur all year around, and there has been less research conducted into winter ablation rates on New Zealand glaciers (Anderson, 2003; Ishikawa*, et al.*, 1992; Marcus*, et al.*, 1985). Unlike the Franz Josef Glacier, very little is known about the temporal and spatial variations of ablation on the Fox Glacier, and with the exception of Gunn (1964) and Lawson (pers. comm., 2005) very few ablation measurements appear to have been taken.

Takeuchi *et al*. (1999) found little variation with the overall energy balance for glaciers with a similar climate, likewise Oerlemans (2001) found data from a climate station 9 kilometres from the Morteratsh Glacier in Switzerland could in fact be used to estimate conditions for that glacier. In light of this, and despite microclimate variations, the premise that the Fox Glacier will behave in a similar way to the Franz Josef Glacier (Sara, 1968; Suggate, 1950) may be well founded, as regionally they experience similar climatic conditions (section 2.3.2).

2.5.4 Ablation Measurements on Fox Glacier

Ablation measurements on the Fox Glacier are few (Table 2.1). Gunn (1964) made one of the early attempts to calculate ablation on both the Fox and Franz Josef Glaciers by measuring the height of the ice surface from the bottom of drilled holes at an altitude of 350 m at selected intervals from January to April. Ablation was averaged for both the glaciers at 82 mm d^{-1}. More recently Lawson (pers. comm., 2005) measured summer ablation on the lower Fox Glacier in 1992 recording an average of 118 mm d^{-1}. However, aside from these two studies little is known about the ablation of the Fox Glacier, especially during winter.

Table 2.1 Previous ablation research on the Fox Glacier

Study	Date	Ablation (mm d^{-1})	Location/Details	Notes
Gunn (1964)	Jan- April 1955	82	Measured height of ice surface from bottom of drilled holes 30-40mm deep at 350m altitude	Average from both Fox and Franz.
Lawson (2005	Feb 1992	118	Stake network on lower glacier	Average of 17 stakes over 8 days

2.6 Surface Velocity

2.6.1 The Dynamics of Ice Flow

There are three main processes that can contribute to glacier motion (Figure 2.12). First, internal deformation of the ice occurs due to stress imparted from the weight of the ice body, as well as from the surrounding bedrock geometry. This deformation can occur as creep due to movement between ice crystals, or brittle failure, as for example, when crevasses form[4] (Benn and Evans, 1998; Paterson, 1994). Deformation can also occur in the basal sediments due to pressures from the overlying ice. Fox Glacier, like the Franz Josef Glacier, appears to sit mainly on bedrock, therefore basal sediment deformation is unlikely to be contributing to velocity in a large capacity (Anderson, 2003; Benn and Evans, 1998). Third, depending on the thermal regime at the ice-bed interface, the ice may slide over the bedrock on a thin layer of melt water (Benn and Evans, 1998; Paterson, 1969). In New Zealand, the temperate climate results in ice at the base of glaciers being at the pressure melting point[5], hence basal sliding will be an important component to glacier motion (Ruddell, 1995).

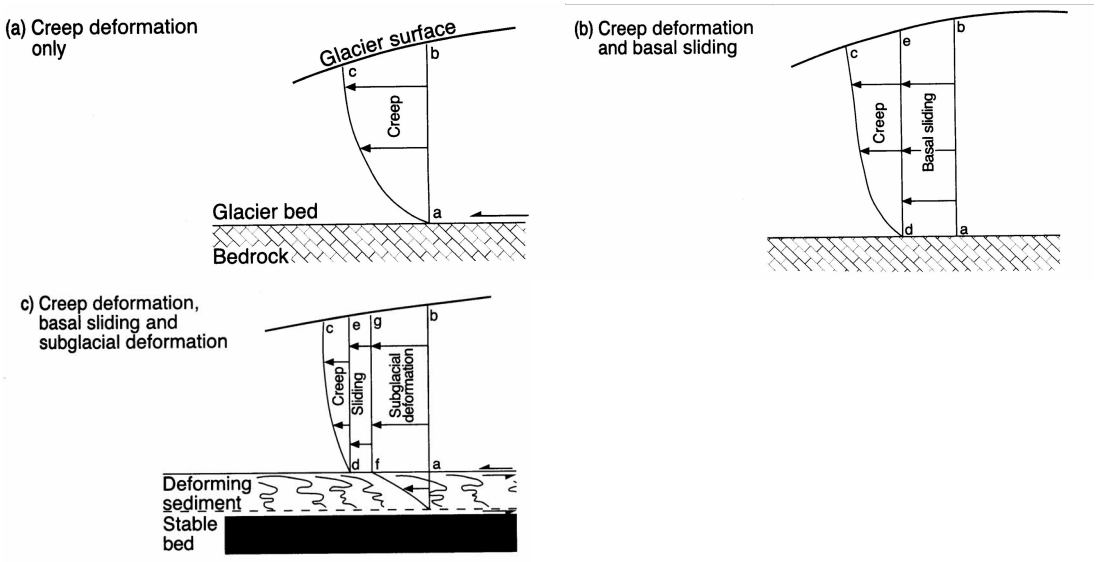

Figure 2.12 Three main processes contributing to glacier motion, creep deformation (a), basal sliding (b) and subglacial basal sediment deformation (c) (Lawson and Fitzsimons, 2001).

[4] The deformation of ice conforms to a power law for flow, known as Glen's Flow Law, defined by $\varepsilon = A\tau^n$, where ε is the rate of deformation, τ the stress applied, n a constant (usually taken to be 3), and A a constant the value of which depends on ice characteristics and environment, like for example water content, impurities and ice temperature (Benn and Evans, 1998).

[5] The temperature at which ice melts is not constant at 0°C, but decreases as the ice is placed under pressure. This occurs at a rate of 0.072°C per million Pascal's (MPa). Therefore the pressure at the base of a glacier 2000 m thick will be at 17.6 MPa, which lowers the melting point of the ice to -1.27°C (Benn and Evans, 1998).

The actual proportions of internal deformation and basal sliding that contribute to total glacier motion can be determined, but the process of direct measurement is not straight forward (Anderson, 2003; Harbor, *et al*., 1997; Willis, *et al*., 2003). However, previous research tends to indicate that on average, sliding may account for around half the movement in glaciers where the basal ice is at pressure melting point (Andreasen, 1983; Paterson, 1969). In some conditions/climates it may be possible to get an indication of the proportion of basal sliding versus internal deformation by looking at the winter daily 'base' velocity. At this time basal sliding should be at a minimum, hence glacier motion will be mainly attributed to internal deformation (Iken*, et al.*, 1983; Ruddell, 1995). Conversely, an increase in velocity during the summer is a strong indication that the glacier is sliding (Paterson, 1994).

Alternatively, the marginal slip rate can give an indication as to the degree of sliding (Anderson, 2003; Andreasen, 1983; Gunn, 1964; Paterson, 1969). Marginal slip looks at the difference between the velocities of two adjacent points on the glacier, one in the middle and one as close to the edge as possible. On the Franz Josef Glacier, Gunn (1964) found the greatest slip rates (68%) occurred where the enclosing valley walls were steepest. Anderson (2003) also considered marginal slip on the Franz Josef Glacier reporting high slip rates (75% and 93%), which indicated a high proportion of sliding on the lower glacier. On the Austre Okstindbre Glacier in Norway, Andreasen (1983) found that sliding velocities increased towards the margin of the glacier and that basal sliding accounted for 50% of the movement at the study site.

Ice thickness and the slope of the surface are the main factors that control velocity, with velocity being proportional to around the fourth power of ice thickness, and the third power of surface slope (Nesje and Dahl, 2000; Paterson, 1969). Over time, the input of mass in the accumulation zone needs to be balanced by ice flowing through the glacier to be ablated in the ablation zone.

2.6.2 The Glacial Drainage System

The glacial drainage system is made up of three main parts; the supraglacial (surface) system; the englacial (internal) system and the subglacial (basal) system (Figure 2.13). The network of surface streams is often well developed in the ablation zone due to the low permeability of the ice. This surface channel network delivers meltwater and surface runoff down moulins and crevasses into the englacial system, which in turn transports the water to the base of the glacier (Benn and Evans, 1998).

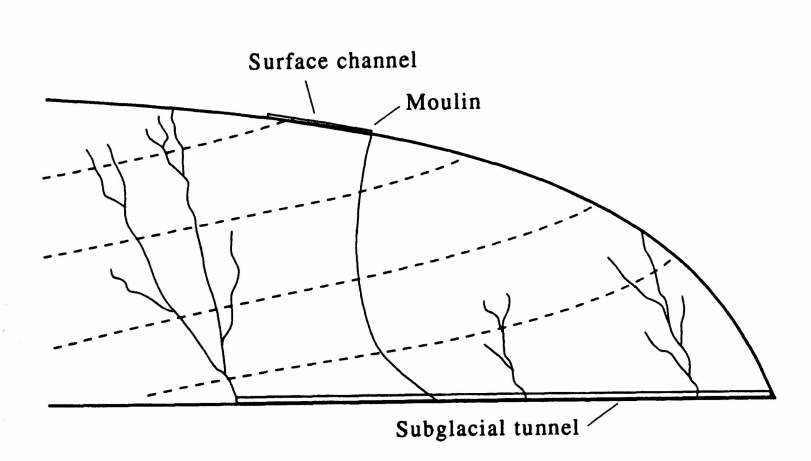

Figure 2.13 The three parts of the glacial drainage system: supraglacial (surface channels), englacial (moulins) and subglacial (tunnel) (Paterson, 1994).

Short-term variations in glacier velocity are strongly linked to the supply of water to the glacial drainage system, in particular, the subglacial drainage system. The subglacial drainage system is made up of various combinations of *discrete* and *distributed* systems. A discrete system contains main channels that can be incised either down into bedrock or sediment, or, upwards into the ice. Channels form a low-density branching network, and transport water efficiently. A distributed system, includes a thin water film at the ice/bed interface, cavities linked via narrow orifices and pore water movement. A distributed system tends to be less efficient at transporting water than a discrete system (Benn and Evans, 1998).

Distinction can also be drawn between hard-bed and soft-bed hydrology. A hard-bed subglacial drainage system is thought to consist of a thin water film (< 4mm) covering the bedrock substrate, a tortuous system of cavities and narrow orifices and a few large and relatively straight channels. In a soft-bed system, channels may be incised down into the sediment, and porous flow will occur though sediment in addition to having the thin water film over the substrate (Willis, 1995). As mentioned in section 2.6.1, Fox Glacier appears to sit mainly on bedrock, so is likely to have a hard-bed subglacial drainage system.

Drainage systems have been found to evolve though the seasons (Harbor*, et al.*, 1997; Mair, 1997; Nienow*, et al.*, 1998; Willis, 1995; Willis*, et al.*, 2003). During winter, the lower water flux can be effectively transported through a distributed system. However, as the ablation season progresses, this system is not efficient enough to cope with the increase in water, and a more efficient channelised system develops (Nienow*, et al.*,

1998; Willis, 1995). During times of low water flux, the small cavities and conduits of the englacial drainage system will close up due to ice deformation (Benn and Evans, 1998). The size of a drainage conduit at any time is determined by two opposing effects; water flowing through the conduit, which enlarges the conduit by melting; and the pressure of the overlying ice, which when it exceeds water pressure, closes the conduit via deformation from ice flow (Paterson, 1994). These processes give the drainage system the capacity to adjust, although not immediately, with the size of the conduits reflecting the average water supply over the preceding one or two weeks (Paterson, 1994).

In addition to conduit and channel evolution, research has also shown that glaciers store water in cavities either within the ice, or at the ice-bed interface (Iken, *et al.*, 1983; Paterson, 1994). For example, Iken *et al.* (1983) reported a 0.6 metre uplift of the Unteraagletscher (Switzerland) at the beginning of the melt season, which they related to water storage in cavities at the bed. They determined that when subglacial water pressures were high enough, a branching network of passageways opens up, connecting the cavities at the ice-bed interface (Figure 2.14). Peaks in velocities were recorded when the cavities were opening up, and as the pressure dropped, water became trapped and stored in the cavities. At the Athabasca Glacier in Alaska, flooding occurred that was unrelated to weather conditions, an indication of water storage (Paterson, 1994).

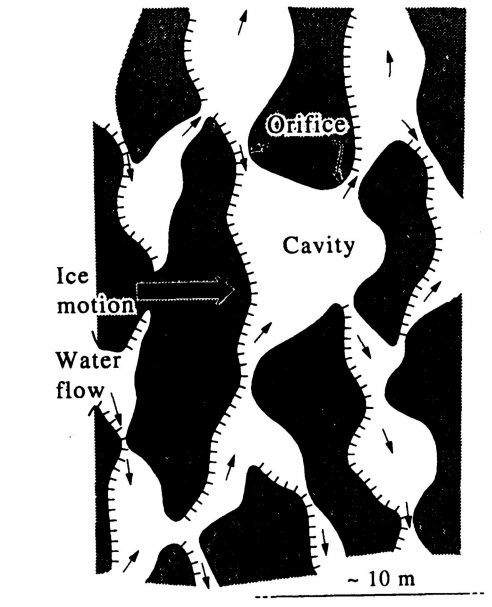

Figure 2.14 Diagram of a linked cavity system at the ice-bed interface, showing areas where water storage can occur. Note that the glacier is only in contact with the bed in the dark areas. (Paterson, 1994)

The rate of evolution of the subglacial drainage system is controlled by not only weather related water supply, but also to the distribution of moulins and crevasses, which provide an efficient means of water transport to the bed. In heavily crevassed areas, numerous entry points to the subglacial drainage system can result in less occurrences when water pressures reach high enough levels to enhance basal sliding (Nienow*, et al.*, 1998). During summer, the lower Fox Glacier has a well-developed system of supraglacial meltwater channels, numerous moulins, and is heavily crevassed, indicating rapid delivery of surface water to the bed.

2.6.3 Spatial Variability in Ice Flow

Glacier velocities vary spatially. In general theory, the velocity of the ice increases steadily from zero at the head of the glacier in the névé area, to a maximum at the equilibrium line, then decreases towards the terminus. There is a downward component to the flow in the accumulation zone, and an upwards component in the ablation zone (Figure 2.15), however this pattern may vary depending on geometry of both the ice and valley sides (Paterson, 1969; Summerfield, 1991). On the Franz Josef Glacier, Anderson (2003) confirmed this spatial variability recording 0.11 m d^{-1} at the head of the névé, 2.3 m d^{-1} below the ELA and only 0.17 m d^{-1} at the terminus.

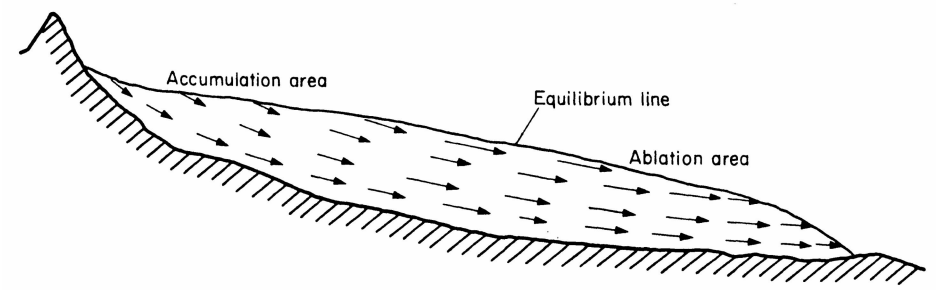

Figure 2.15: Generalised direction of ice flow through a glacier (Paterson, 1994).

Velocity also varies within a glacier cross-section. In a valley glacier shear stress occurs at both the ice-bed interface and at the valley sides. At the bed the shear stress (τ) is a product of the weight of the ice and the surface slope:

$$\tau = \rho_i g h \sin a \qquad (3)$$

where ρ_i the density of ice (usually taken to be 900 kg m^{-3}); g is gravitational acceleration (9.81 m s^{-2}); h is the ice thickness; and a the slope of the surface (Benn and Evans, 1998; Paterson, 1994).

Friction generated by this stress results in a retarding of velocity at these two interfaces. Therefore, valley glacier velocities should increase with distance away from the bed, and away from the valley sides, resulting in the highest velocities occurring along the centreline (Figure 2.16) (Benn and Evans, 1998; Paterson, 1994).

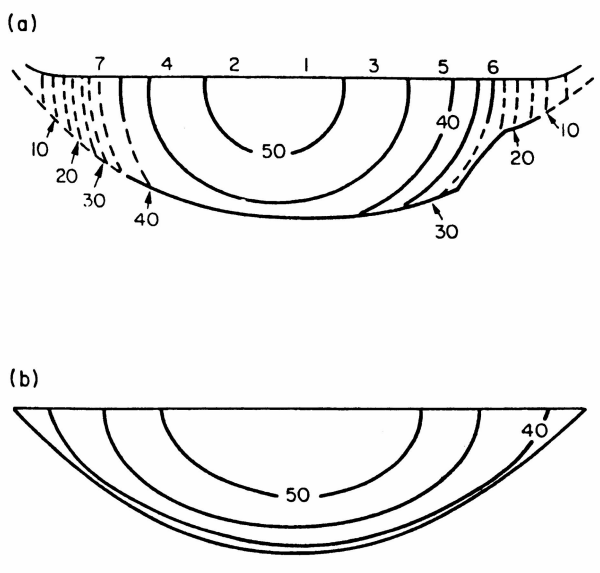

Figure 2.16: Measured (top) and theoretical (bottom) cross sectional velocity profile showing the retarding of velocity at the sides and base of a glacier (Paterson, 1994).

Detecting the spatial velocity variability across the glacier surface can be easily determined by measuring surface velocity along an across glacier transect. However, variation in the vertical velocity profile is not so easy to determine. The vertical velocity profile is influenced not only by basal shear stress, but the various components of glacier flow, in particular internal deformation and basal sliding.

Willis *et al*. (2003) managed to determine velocity profiles on the Haut Glacier d'Arolla in Switzerland by using borehole inclinometry. Holes were drilled right down to the glacier bed, and an inclinometer was used repeatedly to detect the tilt of the borehole at one-metre intervals. At some sites, velocity profiles resembled standard theory, showing a retarding of velocity at the base. However at other sites, basal velocity was in excess of surface velocity. These spatial variations (termed 'sticky' and 'slippery' spots) were found to reflect the changes in the basal water distribution (see section 2.6.4).

Superimposed on this general velocity pattern are variations brought about by changes in mass balance, varying glacier boundaries (i.e. converging valley walls) and flow over a non-uniform bed. Such variations alter the stress and strain on the ice and result in areas of extending or compressing flow (Benn and Evans, 1998; Paterson, 1994).
Detecting such variability in ice flow will depend on the time frame considered, with variations increasing as the time frame considered decreases. Velocity measurements conducted at set points over very short time frames (hours) indicate that movement can occur in a series of small jerks, especially in crevassed areas (Paterson, 1969).

2.6.4 Temporal Variation in Ice Flow

In addition to spatial variability, research has shown that there is also temporal variability in glacier motion (Iken*, et al.*, 1983; Mair, 1997; McSaveney and Gage, 1968; Willis, 1995). Velocity can change on a variety timescales from hourly, to seasonal, to extra-annual variations. One of the most important factors relating to the shorter term changes is the distribution and pressure of basal water (Benn and Evans, 1998; Hooke*, et al.*, 1989; Knight, 1999; Mair, 1997; Mair*, et al.*, 2001; Nienow*, et al.*, 1998; Paterson, 1994; Willis, 1995; Willis*, et al.*, 2003).

Water pressure (P_w) can vary between atmospheric pressure and cryostatic pressure (P_i), which is the pressure exerted by the weight of the ice. Cryostatic pressure is given by:

$$P_i = \rho_i g(h-z) \quad (4)$$

where P_i is the cryostatic pressure; ρ_i the density of ice; g is gravitational acceleration; h is the altitude of the ice surface and z the elevation of the point in question.

If water pressure equals the cryostatic pressure, the water can support the whole weight of the ice, thereby lifting the glacier off its bed. The difference between water pressure and the ice pressure is called the effective pressure (N).

$$N = P_i - P_w. \quad (5)$$

This relationship depends on the magnitude of P_w in relation to P_i. When $P_w = P_i$, the effective pressure equals zero, and the ice can be entirely supported by the water (Benn and Evans, 1998).

At the glacier-bed interface, the point at which the ice separates from the bed is called the separation pressure (P_s) where:

$$P_s = \rho_i - (\lambda\tau/\pi a) \quad (6)$$

where λ is the wavelength of a bump on the bed; τ is the basal shear stress; and a is the bump amplitude.

The separation pressure is high for short wave-length, high amplitude bumps in bed topography and vice versa. Therefore, smooth beds are more sensitive to an increase in water pressure than rough beds (Benn and Evans, 1998). This increase in sliding due to increases in water pressure can reach a critical point (critical pressure, P_c) where positive feedback is created[6] resulting in unstable basal sliding.

A number of factors can influence the amount of water being supplied to the subglacial drainage system and hence the basal water pressure. For example at the Storglaciären in Sweden, an increase in meltwater from enhanced ablation during hot weather resulted in a period of high velocity (Hooke*, et al.*, 1989). Velocity increases during or immediately after periods of heavy rain have been recorded on a number of glaciers including the Unteraargletscher and Franz Josef Glacier (Anderson, 2003; Hooke*, et al.*, 1989; McSaveney and Gage, 1968; Willis, 1995).

Diurnal cycles of glacier velocity have been detected on many glaciers including the White Glacier in Canada, the Storglaciären in Sweeden, the Unteraargletscher in Switzerland, and Variegated Glacier in Alaska. This variation tended to occur on days with large diurnal air temperature fluctuations, which result in large fluctuations in daily meltwater production (Willis, 1995). McSaveney and Gage (1968) attempted to record diurnal variation in flow-rates on the Franz Josef Glacier in 1966. No significant variation was detected during their study. However, it was believed that variation would exist, but was being masked by daily flow irregularities. More recent work on the Franz Josef Glacier by Goodsell (2005) reported no diurnal variability.

[6] Increased in water pressure in cavities results in increased sliding, which in turn results in increased meltwater production, leading to a further increase in water pressure. This positive feedback can result in large velocity increases, which can continue until a more efficient channelised drainage system evolves (Benn and Evans, 1998).

Reorganisation of the basal drainage system can also influence velocity as Nienow *et al*. (1998) found on the Haut Glacier D'Arolla in Switzerland. Here 'Spring Events' were recognised, when early in the melt season, a still inefficient drainage system receives an increase in meltwater, and due to the inability of this system to transport it efficiently, results in increased in basal water pressures, which in turn leads to rapid sliding (Harbor*, et al.*, 1997; Mair*, et al.*, 2001; Willis*, et al.*, 2003). During periods of low water discharge (for example during winter) ice deformation results in the closure of under utilised drainage channels within the glacial drainage system. During these times of low discharge, a hydrologically inefficient distributed drainage system is adequate, however the injection of high discharges into such a system (for example during spring) creates an increase in subglacial water pressures, which in turn leads to enhanced basal sliding (Mair, 1997). Over time, an increase in water supply to a distributed system will result in its evolution to a more efficient channelised system. This in turn results in the threshold for a high velocity event (separation pressure) becoming more difficult to attain as larger channels can cope with higher daily discharges at lower water pressures (Mair, 1997).

Seasonal variations in velocity have been detected on a large number of the glaciers including the Midtdalsbreen in Norway, the Athabasca in Alaska, the Storglaciären in Sweden, and the Haut Glacier d'Arolla in Switzerland. On these glaciers average summer and winter velocities can differ from up to 30%, with faster flows tending to occur during the late spring/early summer (Hooke*, et al.*, 1989; Kamb and Engelhardt, 1987; Krimmell and Vaughn, 1987; Paterson, 1964; 1969; Willis, 1995; Willis*, et al.*, 2003). Such changes can be related to not only to the basal water supply, but also to changes in ice thickness as during the year accumulation and ablation produce variations in thickness (Paterson, 1964; 1969). However in New Zealand, previous work on the Franz Josef Glacier detected no such seasonal variation, but short-term temporal variability in surface velocity was related to changes in the supply of water (Anderson, 2003).

2.6.5 General Glacier Velocity

Velocities tend to be highest on glaciers that have wide accumulation zones that are focused into narrow valleys, and have a steep mass balance gradient[7]. Higher mass balance gradients are found in humid maritime conditions, like New Zealand's west coast or Patagonia, and lower balance gradients are associated with cold based continental glaciers (Benn and Evans, 1998; Nesje and Dahl, 2000).

Normal glacier flow is considered to be at around 10-100 m yr^{-1}; where as fast flowing glaciers may move 100-1000 m yr^{-1}. The Meserve Glacier located in Antarctica's Dry Valleys, has an annual velocity of only 2 m yr^{-1}, the Storglaciären in Sweden moves at 14 m yr^{-1}, and the Glacier San Rafael in Patagonia has a very high velocity, in excess of 7000 m yr^{-1} (Benn and Evans, 1998; Hooke*, et al.*, 1989). Previous studies indicate that the Franz Josef Glacier is New Zealand's fastest flowing glacier, with recorded velocities often in excess of 1 m d^{-1} and on some occasions over 5 m d^{-1} (Anderson, 2003; Goodsell, 2005; Gunn, 1964; Ruddell, 1995; Suggate, 1950), thereby falling into the 'fast' velocity category indicated above. On New Zealand's east coast, average velocities recorded on the Tasman Glacier are around 0.3 – 0.4 m d^{-1} (Brodrick, 1891; Kirkbride, 1995b), and on the Hooker Glacier as low as 0.09 m d^{-1}(Brodrick, 1891). These east coast glaciers are more gently sloping in comparison to the west coast glaciers, and since velocity varies by the third power of surface slope (Paterson, 1994), the lower velocities recorded on the east coast are quite understandable.

On a longer timescale, the velocity of a glacier is influenced by whether or not the glacier is in a period of advance or retreat, due to changes in the primary driving forces of ice thickness and surface slope (where velocity is proportional to the fourth power of ice thickness) (Benn and Evans, 1998; Goodsell, 2005). As the next section will show, a number of the previous direct velocity measurements on the Fox Glacier took place during retreat phases. Due to recent increases in mass (Chinn*, et al.*, 2003; Chinn*, et al.*, 2005), it is expected that surface velocities obtained in this study will be higher than those obtained by Wilson (1896), Speight (1935), or Gunn (1964). However, work done by Lawson (pers. comm., 2005) in 1992 should be comparable as the glacier was advancing at that stage.

[7] Mass balance gradients refer to the situation where annual accumulation and ablation vary systematically with altitude. Accumulation increases with increasing altitude, where as ablation decreases with increasing altitude. The mass balance gradient can be a useful measure of a glaciers activity. Steep gradients result from heavy snowfall in the accumulation zone and high ablation at the snout. Both Fox and Franz Josef Glaciers have a steep mass balance gradient.

2.6.6 Velocity Measurements on Fox Glacier

Wilson (1896) made the first survey of the ice flow of the Fox Glacier in 1894 2.4 km up from the terminus (approximately opposite Yellow Creek, now 600 metres downvalley of the present 2005 terminus position). Using a series of flags, movement was recorded over a period of 28 days, giving average daily rates of between 0.34-0.76 m d^{-1}, with highest values recorded near the middle and the lowest at the sides (Figure 2.17). In 1955 Gunn (1964) monitored flow between Victoria Creek and the terminus finding that the rate decreased from around 1.31 m d^{-1} to 0.05 m d^{-1}. Returning in 1956 Gunn found the glacier had retreated some 300 metres with surface lowering of about 15 metres. Consequently he noted a decrease in velocity, with flow at Victoria Creek only 0.38 m d^{-1}, and commented that "in view of the rapid retreat… is not unexpected" (Gunn, 1964, p 181).

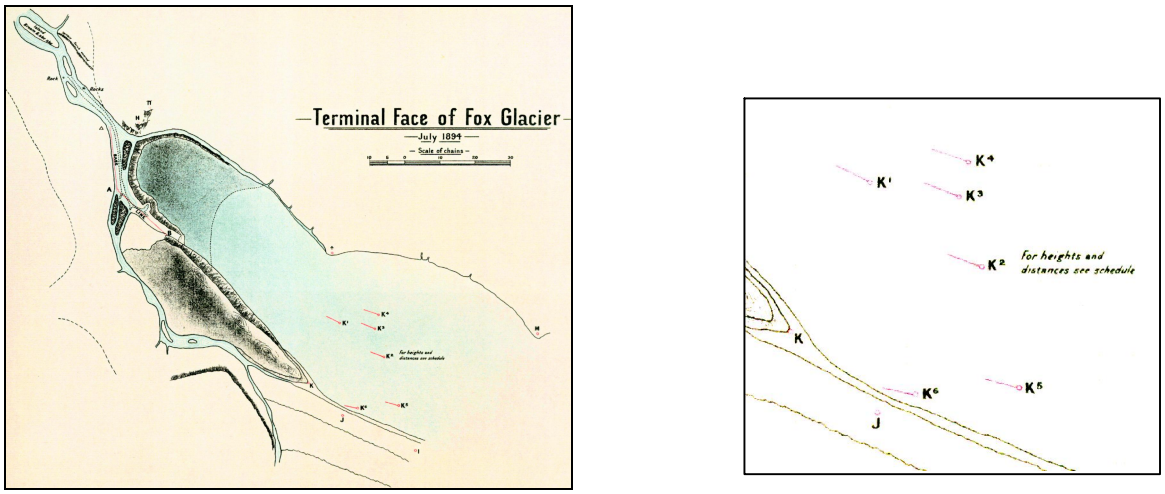

Figure 2.17 Diagram drawn by Wilson (1896), showing position of terminal face and velocity transect (left). Close up of the stake transect used to measure velocity (right). Supplied by the Alexander Turnbull Library.

Ruddell (1995) surveyed velocity on the Fox Glacier, focusing on the névé and the upper icefall. In the névé velocities ranged from 0.28-0.70 m d^{-1}, and in the upper icefall reached as high as 9.3 m d^{-1}. Work by Lawson (pers. comm., 2005) on the lower glacier during the summer of 1992 recorded surface velocities averaging around 0.70 m d^{-1}.

With the exception of Wilson (1896), Gunn (1964) and Ruddell (1995) there has been a considerable dearth in published information on the Fox Glacier (Table 2.2), with the majority of previous and present research focusing on the neighbouring Franz Josef Glacier. Ease of access to the Franz Josef Glacier and the existence of an established database, combined with the two glaciers similar geometry and location (leading to

previous attitudes that the Fox would behave in the similar way), has no doubt influenced the degree of research interest.

With a lesser gradient (4° opposed to 8°), different aspect (W not NW), and larger névé, it is possible that the Fox Glacier may have different velocity dynamics to the Franz Josef. However, more up-to-date measurements would be desirable to confirm whether or not this is the case, or whether as previously thought (Sara, 1968; Suggate, 1950) the Fox Glacier does reflect the activity of the Franz Josef Glacier.

Table 2.2 Previous surface velocity research on the Fox Glacier

Study	Date	Velocity ($m\ d^{-1}$)	Location/Details	Notes
Wilson (1896)	6th July – 3rd August 1894	0.25 0.27 0.24 0.24 0.34 0.08	K1 K2 K3 K4 K5 K6 (Figure 2.15 and Figure 2.3)	Glacier in period of retreat. Transect about 2 km upvalley from terminus at the time of survey and & 600m downglacier from present terminus.
Speight (1935) Mr H.L Hume	9th Sept-30th Oct 1932 & 30th Oct – 6th Dec 1932	0.21 & 0.18 0.30 & 0.25 0.44 & 0.34 0.49 & 0.50 0.54 & 0.54	1 - 65.6m from glacier edge 2 - 119.5m " " 3 - 196m " " 4 - 248.4m " " 5 - 296.3m " "	Glacier possible in advance phase based on FJG Transect approx 1200m up from terminus, which is approx 1km downvalley from present terminus
Gunn (1964)	Jan-Feb 1955	1.313 0.419 0.32 0.127 0.077 0.051	A - Victoria Creek 4.6km from terminus B – Below lower icefall 1.9km up C – Yellow Creek, 914m up D Terminal Moraine, 686m up E Terminal Moraine, 457m up F – Terminal Moraine, 91m up	Glacier likely to be in retreat phase. B appears to be close to present study area. Refer to figure 2.4 for terminus position during this time.
	April 1956	0.381 0.079 0.146 0.216 0.041	A_1 – Victoria Cr, 4.5km up & 224m in from edge C_1 – Yellow Cr, 1km up & 64m in from edge C_2 – Yellow Cr, 1km up & 133m in from edge C_3 – Yellow Creek, 1km up & 230m in from edge D_1 - Term Moraine 600m up & 150 in from edge	
Ruddell (1995)	Feb/Mar 1991	0.28 - 0.70 4.93-9.30	Névé area, Explorer & Albert glaciers Upper Ice fall	Theodolite Survey of poles Theodolite survey of seracs
Lawson (pers. comm., 2005) unpublished	Feb 1992	0.45 – 0.98 Average 0.70	Lower Glacier, similar location to this study	Glacier advancing

2.7 Response Time

The response time is the time it takes for a glacier to adjust to a change in mass balance, whether positive or negative. It represents a time lag, as before any mass balance changes are expressed at the glacier terminus (advance or retreat) the climate signal which drove the mass change needs to be transmitted down the entire length of the glacier (Johannesson*, et al.*, 1989; Oerlemans, 2001; Paterson, 1994). This is an important distinction from the time it might take for a surface object to travel the length of the glacier, which can be much shorter depending on where the object is located on the glaciers surface. The response time is different for every glacier, although previous field research indicates that the response time for a number of valley glaciers is between 10 to 50 years (Oerlemans, 2001). Response times repeated for the Franz Josef Glacier range from as little as 5 to 7 years, based on the correlation of changing terminus positions and precipitation records (Hessell, 1983; Suggate, 1950), between 9 to 13 years, modelled by ablation and thickness (Evans, 2003), and up to 15 to 25 years derived from more complex numerical modelling (Oerlemans, 1997).

Jóhannesson *et al*. (1989) developed two simple models to estimate the general response time of a glacier, one utilising glacier length and terminus velocity, while the other glacier thickness and the annual ablation at the terminus:

$$T_M = fl / u \quad (7)$$

where T_M is the response time; f a factor estimated to be 0.5; l the glacier length; and u the terminus velocity, and:

$$T_M = H / -b \quad (8)$$

where T_M is the response time; H the thickness of the glacier; and $-b$ annual ablation at the terminus.

Further developments to numerical modelling has resulted in more complex ways of determining response times (Hooke, 2005; Oerlemans, 2001). However these models require more measured data like for example a glaciers slope, thickness at the equilibrium line and annual net balance. Therefore equations 7 and 8 are valuable tools for being able to derive a general estimate of response time for glaciers with little previous measurement. To date very little work into estimating of a response time for

the Fox Glacier appears to have been undertaken, although Coates and Chinn (1992) suggested it could be around 6 years (based on the one year delay Fox Glacier is locally observed to have from the Franz Josef Glacier, with a response time estimated of 5 years). Due to the lack of measured data for the Fox Glacier, estimating a response time is complicated.

2.8 Aims and Objectives of Research

It is clear that very little research has been conducted on the Fox Glacier, especially during the winter months. Surface velocity has not been measured for 13 years and with the exception of Wilson (1896), velocity during winter has not been considered, and consequently there is no information on seasonal velocity variations. Research conducted on other glaciers has highlighted the importance of water input to short-term velocity variations (Hooke*, et al.*, 1989; Mair, 1997; Mair*, et al.*, 2001; Nienow*, et al.*, 1998; Willis*, et al.*, 2003). In excess of 10 metres of precipitation is received annually at Fox Glacier, and it could be expected that there will be some variation in daily surface velocity in response to variations in the supply of water.

As this review has shown, even less research has been conducted on ablation rates on the Fox Glacier, and none at all during winter months. Previous research on the Franz Josef has indicated that very high ablation rates can occur even in winter during heavy precipitation events (Marcus*, et al.*, 1985). It would be interesting to see how important such events are to the overall rate of ablation during both summer and winter. In addition, there appears to have been no research conducted on the effect that surface moraine has on the ablation rate of the west coast glaciers.

The sensitivity of glaciers to changing climatic conditions has been well established, especially over longer time periods. How much influence variations in the daily climatic conditions have on glacier ablation has been considered (Evans, 2003; Marcus*, et al.*, 1985), but less work has focused on daily velocity variations, in particular, on glaciers occurring in areas receiving high precipitation, and with high mass turnover, like those on New Zealand's west coast.

Finally, the lack of research on the Fox Glacier has at times been justified by the presumption that its behaviour would essentially be the same as the Franz Josef Glacier. Both glaciers are of similar size and shape, and are located in a similar climate. However, the Fox Glacier has a more westerly aspect, is topographically

shaded in winter, and a lesser slope, and a higher mean elevation, therefore its may respond differently to the Franz Josef Glacier.

Based on the above literature review, the following research questions have been derived:

- What are the intra-annual variations in ablation and surface velocity on the lower Fox Glacier?
- What short-term (daily) fluctuations occur in ablation and surface velocity?
- What are the main factors driving these variations?
- Can the behaviour of the Fox Glacier be predicted by information gathered from the Franz Josef Glacier?

From the above research questions, the following is a list of objectives developed for this research project on the lower Fox Glacier:

i. To investigate the spatial and temporal variations of ice flow on the lower glacier.
ii. To investigate the spatial and temporal variations of ablation (surface melt) on the lower glacier.
iii. To find out what effect surface moraine has on the rate of ablation on the lower glacier.
iv. To consider any possible direct relationships between ablation and surface velocity.
v. To consider how much influence daily climate variables have on both ablation and surface velocity, and the importance of heavy precipitation events on the above processes.
vi. To locate and record the current terminus position of the Fox Glacier and use this up to date location to estimate a response time for the glacier.
vii. To find out whether the behaviour of the Fox Glacier can be estimated from data recorded on the nearby Franz Josef Glacier.

Chapter 3 Methodology

3.1 Meteorological Measurements & Synoptic Observations

3.1.1 General Meteorological Methodology

Local climatic conditions on a glacier can vary from the general regional climate (Paterson, 1994), therefore measurement of standard climate variables (temperature, precipitation, solar radiation and wind dynamics) on, or close to the study site is desirable. The use of automatic climate stations is common practice (Anderson, 2003; Evans, 2003; Ishikawa, *et al*., 1992; Kelliher, *et al*., 1996; Marcus, *et al*., 1985; Owens, *et al*., 1992; Purdie, 1996; Takeuchi, *et al*., 1999) as these can be set up at the study site and programmed to record variables continually, logging averages at the desired interval.

Problems can be encountered however with the use of such equipment in alpine environments. For example, Kelliher, *et al.* (1996) found it difficult to keep sensors stable due to surface melt, and Marcus, *et al.* (1985) had problems keeping equipment working during a storm event. Local wildlife has also created problems on the neighbouring Franz Josef Glacier with Evans (2003) and Marcus, *et al.* (1985) both having equipment tampered with by Kea, resulting in the loss of data.

3.1.2 Meteorological Measurements at Fox Glacier

During each study period an automatic climate station (Figure 3.1) was set up on the clean ice, in a location central to the stake network (section 3.2.2). The climate station was mounted on a tripod one metre above the ice surface at an initial altitude of 430 m a.s.l. It was programmed to record temperature, precipitation, wind speed, wind direction, humidity and solar radiation. In addition to the automated measurements, daily manual measurements of temperature (wet and dry bulb), precipitation, wind speed and wind direction were taken to provide a means of checking the calibration of the climate station, and to provide a back up to the automatic station. During the summer field season the automatic climate station was mounted inside a lightweight cage, this was done to provide protection from possible destruction by Kea. The cage was not used during the winter field season, as it was determined that the risk of damage by local Kea would be very low.

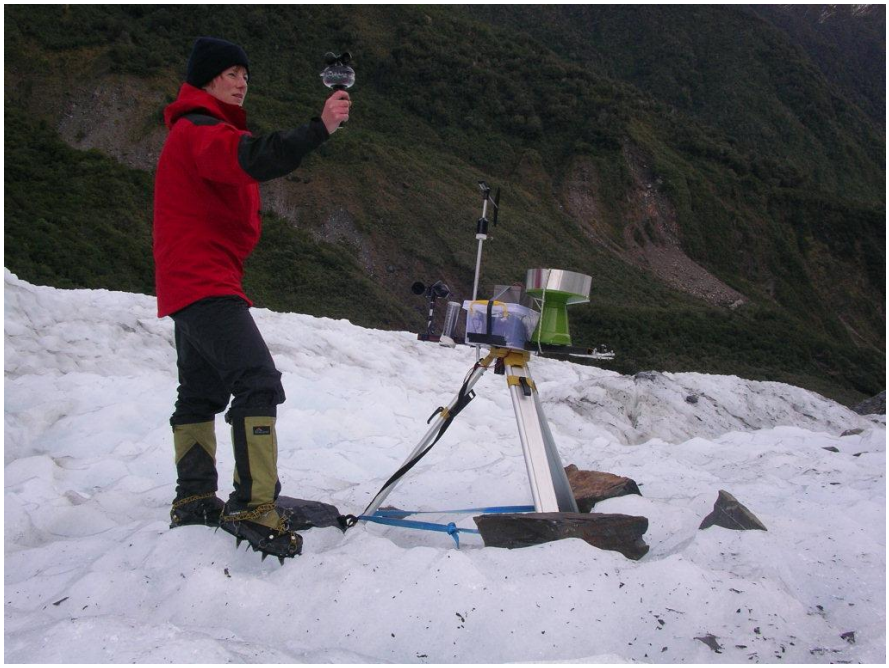

Figure 3.1 Climate station located on the clean ice on the lower Fox Glacier. Daily 'one-off' manual measurements were taken to provide calibration and a backup to the automated system.

During the summer field season precipitation, temperature and wind were recorded by an ENV50, where as humidity and solar radiation were logged by a Campbell Scientific CR10X data logger (Table 3.1). Variables were recorded at fifteen-minute intervals, from which hourly averages were calculated. Problems were encountered with the solar radiation measurements during this first field season due to difficulties in keeping the sensor level. Pyranometers should be kept level for accurate readings, but due to ablation and ice flow, this proved to be difficult. Also, after a brief storm (22-23rd January), the anemometer began working only intermittently until repaired on 26th January. Therefore the one-off daily manual reading is taken as the average wind speed for those days affected.

During the winter field season, all climate sensors were connected to the Campbell Scientific CR10X data logger, which was programmed to log hourly averages. Improvements to the mounting of the pyranometer meant that it could be re-levelled each morning with ease. Problems were encountered with the anemometer readings so post-processing by the regression of the logged data with the one-off daily measurements was conducted to correct the readings. The tipping bucket rain gauge appeared to be only recording every second tip, so the manual measurements for precipitation were used, as these correlated well with data from another rain gauge nearby that was being monitored by Alpine Guides Westland.

Table 3.1 Climate Station Components

Climate Station Component	Meteorological Parameter Measured
ENV50 tipping rain bucket	Precipitation
ENV50 temperature sensor	Temperature
ENV50 anemometer and wind vane	Wind speed & direction
Visala Humitter 50 U	Relative humidity
Apogee Pyranometer Sensor (PYR) & levelling plate	Incoming solar radiation

Daily averages ran from 10:00 am on one day to 9:59am the next day. This meant that data could then be related back to the ablation and surface velocity measurements.

3.1.3 Synoptic Observations at Fox Glacier

Analysis maps of sea surface pressures, prepared by the New Zealand Metservice, were collated to provide information on the synoptic situation that had occurred each day. The synoptic maps were then grouped into one of six general synoptic classifications following the work of Hay and Fitzharris (1988) (Table 3.2).

Table 3.2 Synoptic classifications used in this study, based on the work of Hay and Fitzharris (1988)

Synoptic Classification	Predominant Flow, Description and Observations
I	*South to southwest flow over South Island.* High-pressure system to west. Sunny with light winds. Barometric pressure 1016-1024.
II	*North to northeast flow over South Island.* High-pressure to east. Fine, high cloud, windy. Pressure 1016-1020.
III	*Northwest flow over South Island.* High-pressure to north. Cloudy, patchy rain or drizzle, some sunny patches. Pressure 1016 - 1032.
IV	*Anticyclone over the South Island.* Warm and sunny. Clear skies, light winds. Pressure 1020-1028.
V	*Trough or front over the South Island.* Windy, rain or clearing rain. Cloud or mist. Some sunny patches once front passed.
VI	*Heat Low over the South Island* Very light winds, high temperatures, clear skies. Pressure 1012-1016.

For this study, class IV has been modified to include all days where an anticyclone is situated over the South Island (not only those associated with a weak easterly flow), and class VI was added to account for the situation at the beginning of February where a heat-low developed over the South Island, which resulted in very high temperatures inland (Salinger pers. comm., 2005). Results of surface velocity and ablation could then

be related back to the actual daily synoptic situation. Figures 3.2a to 3.2f give an example of each of the synoptic classifications used in this study.

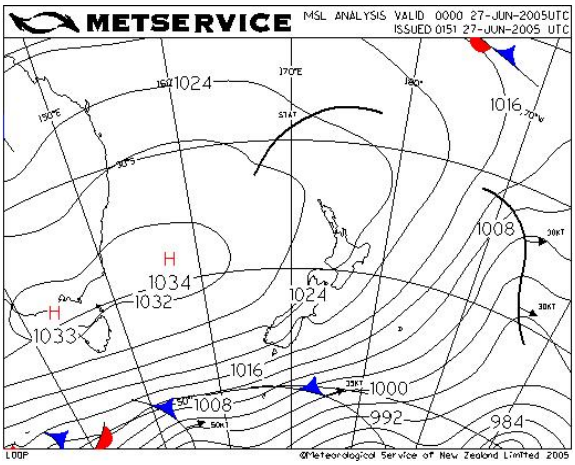

Figure 3.2a (I) South to southwest flow over South Island

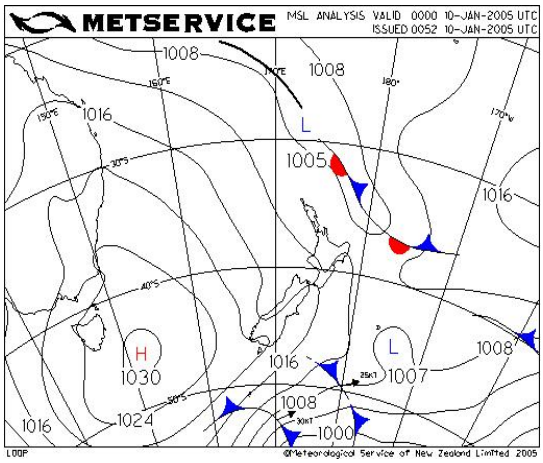

Figure 3.2b (II) North to northeast flow over the South Island

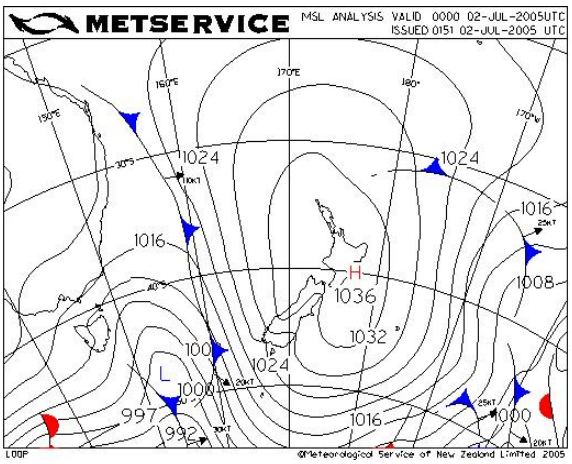

Figure 3.2c (III) Northwest flow over the South Island

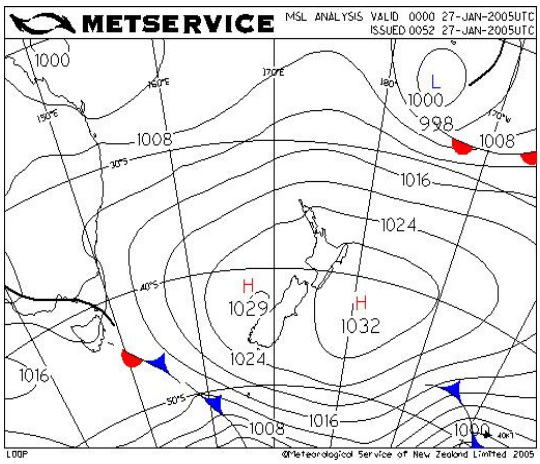

Figure 3.2d (IV) Anticyclone over the South Island

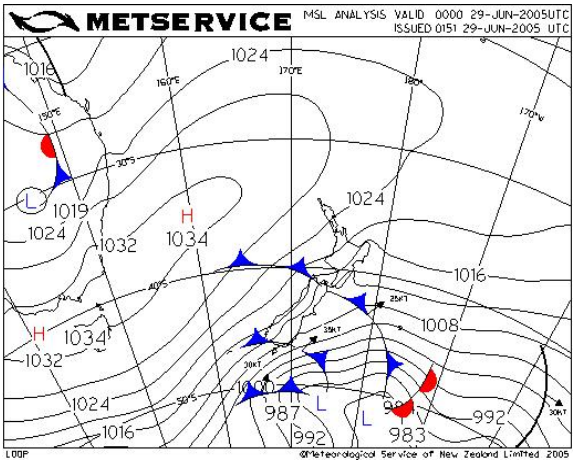

Figure 3.2e (V) Trough or front over the South Island

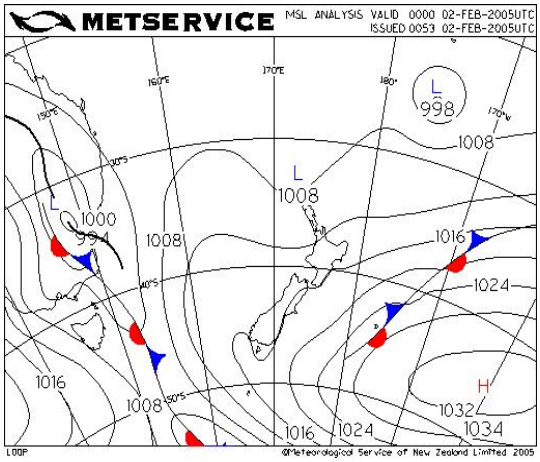

Figure 3.2f (VI) Heat Low over the South Island

Figure 3.2 Examples of synoptic classification used in the study based on the work of Hay and Fitzharris (1988). All analysis maps provided by the New Zealand Metservice.

3.2 Methods for Determining Ablation

3.2.1 Ablation Measurement

Direct measurement by stakes is the most common technique used to measure ablation (surface melt followed by run-off) on glaciers (Anderson, 2003; Evans, 2003; Hubbard and Glasser, 2005; Kirkbride, 1995a; Müller and Keeler, 1969; Paterson, 1994; Purdie, 1996; Willis*, et al.*, 2003). This technique is relatively simple, and involves drilling holes down into the ice into which stakes (usually PVC tubing) are placed. The amount of surface melt can then be measured by the degree of surface lowering relative to the stake. This height difference can, if required, be converted to a mass figure by multiplying by the density of ice (Müller and Keeler, 1969). Melt hollows due to the conductivity of the stakes and complex micro-relief can make measurement difficult, but to address this, the straight edge technique can be used (Figure 3.3). This technique involves placing a round flat disc over the stake and let to rest on the ice surface, the amount of melt can then be read off where the disc intercepts the stake (Müller and Keeler, 1969; Purdie, 1996).

Figure 3.3 Measuring ablation at a stake using the straight edge technique. Note the very blue and glazed surface of the glacier during winter.

Müller and Keeler (1969) conducted research on the possible errors associated with short-term ablation measurement on the White and Sverdrup glaciers the Canadian Arctic. They reported errors averaging ±5 mm with the reading of individual stakes by a straight edge method. This they related to changes in the micro-relief, albedo and physical surface properties of the ice due to weathering. On an ablating glacier surface, a porous layer of ice known as a weathering crust can develop. The porosity of this crust has the effect of masking the true surface lowering. However, during certain weather conditions (i.e. warm and windy weather), this crust will be ablated away leaving a hard, glazed surface, and resulting in what appears to be a rapid surface lowering (Müller and Keeler, 1969). Therefore stake measurements are not considered accurate at timescales shorter than about one week, due to this periodic collapsing of the surface (Brock, pers. comm., 2005).

Large spatial variation was also noted in the amount of surface lowering, even over short distances on what appeared to be uniform ice surfaces (Müller and Keeler, 1969). Despite the above, many researchers still use the stake method to measure ablation (Anderson, 2003; Evans, 2003; Marcus*, et al.*, 1985; Paterson, 1994; Purdie, 1996). The use of lightweight PVC piping helps to reduce conductivity, thereby minimising both melt hollows and the occurrence of stakes melting downwards into the drilled holes (Hubbard and Glasser, 2005; Oerlemans, 2001; Purdie, 1996).

Ablation can also be modelled from climatic data and the technique of combining direct stake measurements with climatic modelling has become common practice, with modelled results seeming to correlate well with the direct measurements (Brock and Arnold, 2000; Evans, 2003; Ishikawa*, et al.*, 1992; Kelliher*, et al.*, 1996; Oerlemans, 2001). Although in some cases, direct measurements proved the more reliable method, due to problems keeping equipment going in harsh environments (Kelliher*, et al.*, 1996; Marcus*, et al.*, 1985).

3.2.2 Ablation Measurement at Fox Glacier

On the lower Fox Glacier daily ablation was measured using a stake network. A Kovacs hand auger was used to drill two metre holes into the ice into which two metre long, grey PVC 25 mm diameter tubes were placed. As outlined above, PVC tubing was used due to it being light and having minimal heat conductivity making them less likely to melt down into the ice under their own weight. Figure 3.4 shows the lower glacier study site and the general location of the stake transects. In summer, seventeen

stakes were placed in the clean ice, with two traverse transects and one longitudinal transect down the mid-line (Figure 3.5). A further five stakes were placed in varying thickness of debris cover in the moraine on the true left to assess possible relationships between debris cover and ablation. For the winter season, nineteen stakes were placed in the clean ice and again another five in debris cover using the same configuration (Figure 3.6). Figure 3.7 shows an example of both a stake placed into the clean ice and one placed in debris cover.

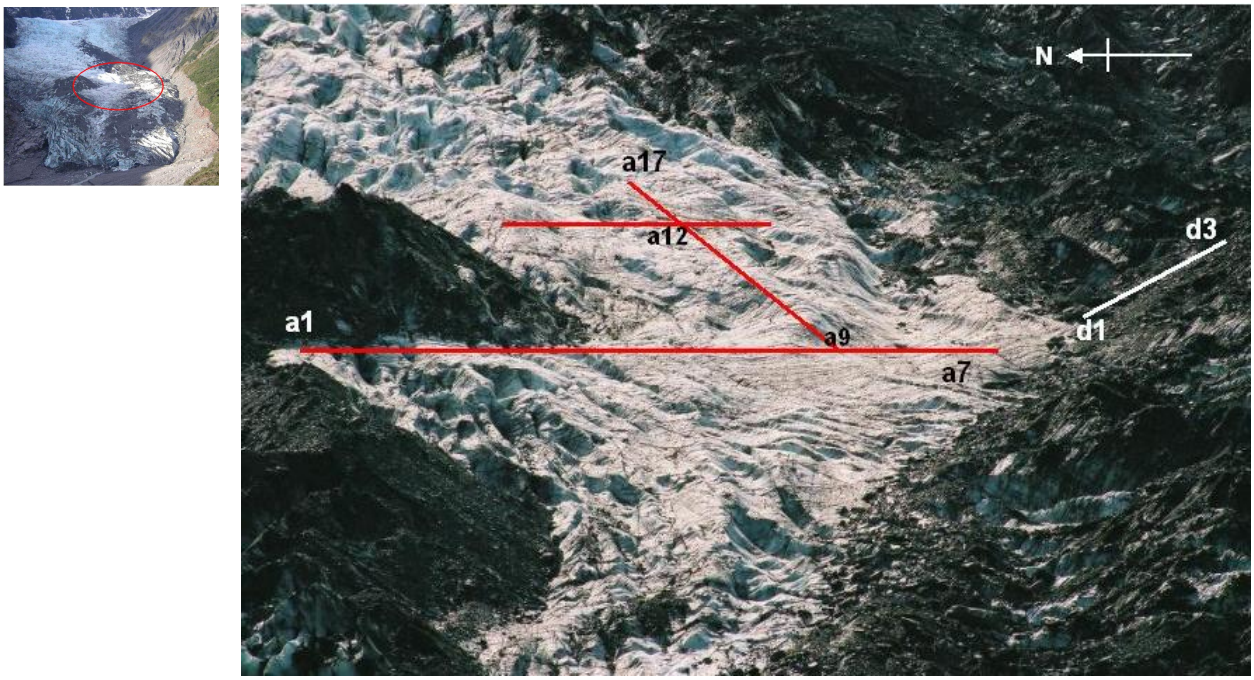

Figure 3.4 Study site on the lower Fox Glacier with the general stake transects highlighted.

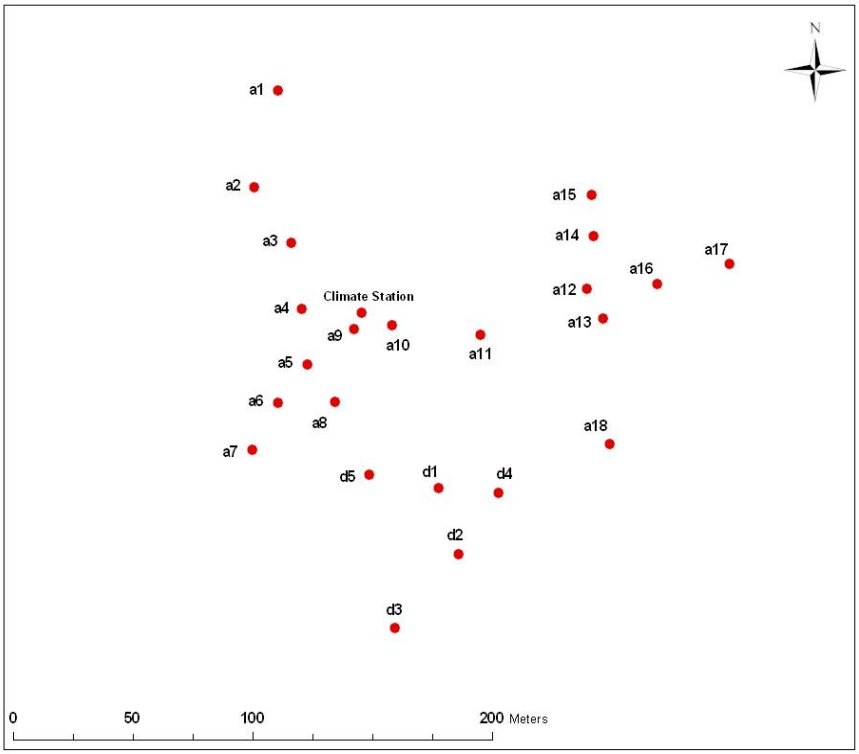

Figure 3.5 Layout of the stake network, including the location of the climate station on the lower Fox Glacier during the summer field season.

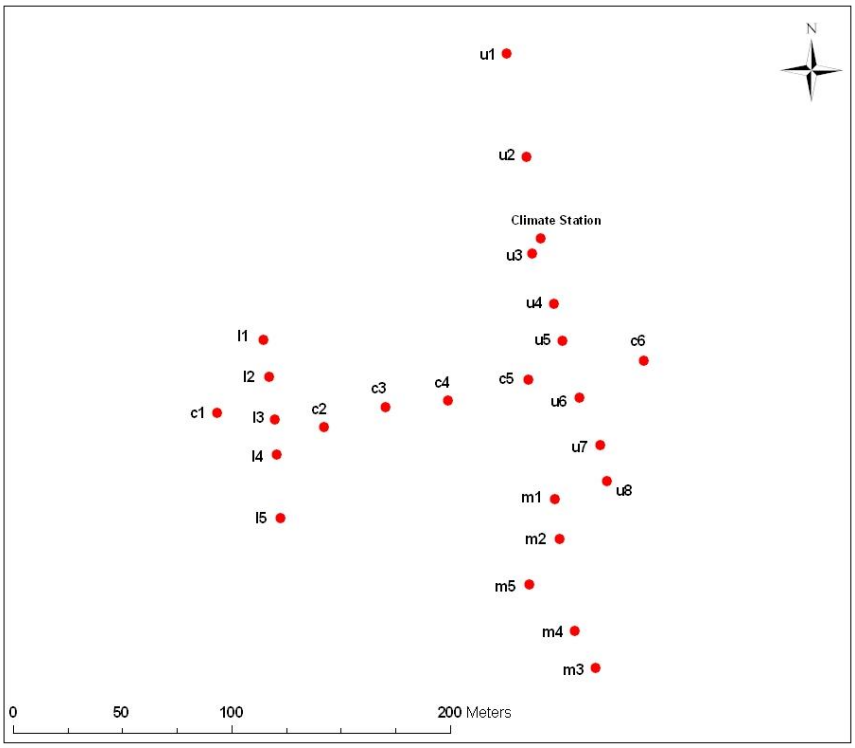

Figure 3.6 Layout of the winter stake network and climate station location on the lower Fox Glacier during the winter field season.

Figure 3.7 Stakes placed in clean ice (u3-left) and into debris cover (m2-right) on the lower Fox Glacier.

Every attempt was made to try and ensure that the winter stake transect was in as similar position as possible to the summer transect. Changes to the surface topography of the glacier and the locations of crevasses made exact same placement in winter problematic. Therefore the winter stake network was on average 3.6 m a.s.l lower, and 23.2 m west (downglacier) of the summer network. The summer network had been on average around 450 m upglacier of the terminus, but during the six months between field seasons the glacier had advanced by around 20 m. This meant that the winter transect, although geographically lower down the glacier was actually positioned on average around 456 m from the terminus, a difference of only 6 metres, giving it a similar morphological position to the summer network.

Stakes were read daily by measuring the height of the stake exposed at the ice surface, using the straight edge technique. Results were recorded in mm d^{-1}, which if required, could later be converted to metres water equivalent (m w.e) by multiplying the daily measurement by the density of ice (assumed to be 900 kg/m^3). Table 3.3 and Table 3.4 provide details of the location, initial altitude, slope and aspect of the stakes. During summer stakes a1-a15 were placed in clean ice on 9th January, and for monitoring ablation under the moraine, stakes d1-d3 were added on 13th January, with d4 and d5 on the 18th January. Finally, on 26th January, a16 and a17 were added at slightly higher altitude, and a18 was put in an area of very fine debris cover. Stake a8 had to be removed on 27th January as it broke through into a crevasse, and was replaced by a8b on the 28th January in the immediate vicinity.

Clean ice stakes were re-drilled on 18th and again on 28th January. This was done to try and keep around half of the stake (one metre) below the ice surface which helps to prevent the stake melting down into the hole, and to helps with stability, preventing excessive movement and possible additional melt (Kirkbride, 1995a; Oerlemans, 2001). Stakes in the moraine were unable to be re-drilled in the same position, due to the amount of debris that fell into each hole. Therefore these stakes were left in position for as long as possible without re-drilling. For the winter field season, the entire stake network was drilled in on the 8th June and due to the much lower melt rate, no re-drilling was required. The debris stakes were shortened to one-metre lengths in order to assist removal at the end of the study period.

Table 3.3 Descriptions of stake placement including altitude, slope and aspect during the summer field season. TR = true right of glacier and TL = true left of glacier.

Stake	Initial Altitude (m)	Slope (°)	Aspect (°)	Notes
a1	426	25	242	TR, edge moraine
a2	424	20	240	Below pyramid moraine
a3	424	22	240	Crevasse TR, small fissures TL
a4	420	22	234	Near centre line, below climate station
a5	423	20	225	
a6	420	14	204	Bound by large crevasses, uplifted block.
a7	417	16	208	TL, edge clean ice, near large rocks (moraine), large crevasses to NW & SE
a8 (a8b)	418	17	137	Gully on TL, initially near drainage channel (later became crevasse)
a9	427	28	248	Lower end of central ridge
a10	430	18	252	Above a9, central ridge
a11	438	19	232	Central Ridge
a12	447	7	64	Depression near ridge top. Moulin's nearby
a13	447	36	230	Steep ridge to TL of central line, moulins each side
a14	450	32	246	Undulating surface between ridges
a15	454	32	258	TR at top of pyramid moraine
a16	450	25	230	Central transect, above a12
a17	458	24	244	Top central transect, flat area bound by steep gullies
a18	434	24	90	TL, in very thin debris band, on ridge between established meltwater channels
d1	425	16	26	Debris depth 20mm
d2	433	22	262	80-100mm
d3	430	10	280	50mm, Furtherest to TL of stakes
d4	425	15	288	2-5 mm, thin surface meltwater
d5	419	14	53	100mm, large clasts

Table 3.4 Description of stake placement including altitude, slope and aspect during the winter field season. TR = true right of glacier and TL = true left of glacier.

Stake	Initial Altitude (m)	Slope (°)	Aspect (°)	Notes
u1	439	19	266	TR, top transect, 150m from valley side
u2	462	20	262	Small valley, near access track
u3	437	19	204	Beside climate station, flat area
u4	437	13	242	Flat depression between ridges, blue ice
u5	436	17	242	Just to TR of centre line
u6	436	29	230	Just to TL of centre line
u7	435	25	212	On ridge line
u8	429	28	206	Between clean ice & TL moraine, channel on TR
l1	410	24	270	TR of lower transect, beside triangle moraine
l2	410	20	210	
l3	413	23	262	Central Ridge, part of both lower and central transect. Also initially in a very fine debris band.
l4	410	26	260	Intermittent channel nearby
l5	410	25	300	Amongst crevasses at edge of clean ice by TL moraine
c1	409	30	210	Bottom lower transect, on ridge line
c2	418	36	218	Crevasse opening on TR
c3	423	14	240	Large moulin to TR, crevassing on TL
c4	425	25	218	Central transect
c5	433	17	210	Central transect
c6	443	21	286	Top of central transect
m1	425	12	240	20mm debris depth
m2	428	20	29	40mm debris depth
m3	439	10	305	60mm, debris depth, closest TL, 90m from valley side
m4	434	20	310	150mm, large clasts
m5	426	5	280	300mm, large clasts

3.3 Methods for Measuring Surface Velocity

3.3.1 Surface Velocity Measurement

The measurement of surface velocity involves standard surveying techniques, where the position of stakes mounted on the glacier surface are repeatedly measured over time (Hubbard and Glasser, 2005; Paterson, 1969). To get a complete picture of surface velocity, both horizontal and vertical components of flow must be taken into account (Paterson, 1969). Measurements undertaken by placing objects on the surface (Odell, 1960; Suggate, 1952) or by observing the movement of surface features such as crevasses (Ruddell, 1995), will only give the horizontal velocity (Paterson, 1969). Because ice moves upwards towards the surface in the ablation zone, net vertical change can be less than estimates made from the movement of surface features. This is called the *emergence velocity*, and is the rate that the ice surface would raise if there were no ablation (Paterson, 1969). Ideally then to get a complete picture of surface velocity in the ablation zone, surface lowering due to melt, must be added back on (Figure 3.8).

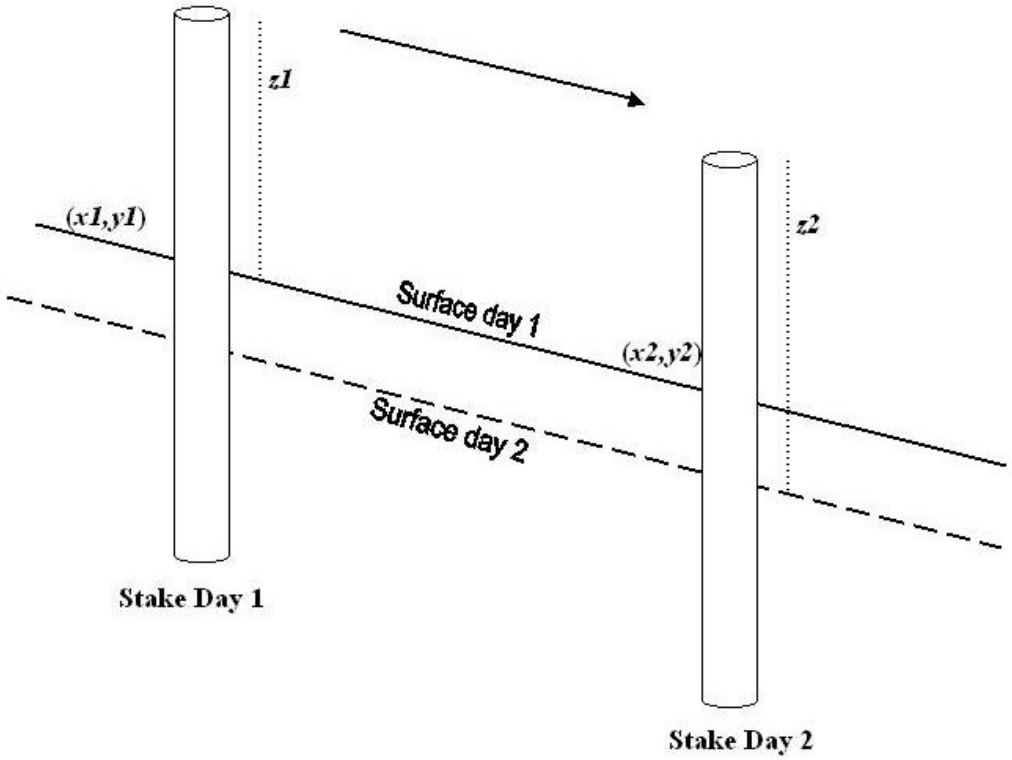

Figure 3.8 Components required for the calculation of surface velocity in the ablation zone of a glacier.

Standard survey techniques involve use of a stake network that is surveyed using a theodolite (McSaveney and Gage, 1968), total station (Goodsell, 2005), or a Global Positioning System (GPS) (Anderson, 2003; Hubbard and Glasser, 2005; Owens, 2005). Stake placement ideally involves a central array with a number of transects crossing at right angles. These transects should reach as close to the edge of the glacier as possible (Paterson, 1969). With the RTK-GPS technique (used for this study) it is important that the base unit is mounted off the glacier on a stable surface, while the roving unit is positioned accurately over each stake on the glacier surface. The temporal resolution of the survey depends on the frequency of measurements (Hubbard and Glasser, 2005). To calculate velocity from the GPS method, the change in the eastings, northings and altitude (including change due to ablation) over the survey time period (i.e. hours, days, weeks) can be calculated using a variation of Pythagorean theory (Hubbard and Glasser, 2005).

3.3.2 Measurement of Surface Velocity on Fox Glacier

On the Fox Glacier the stake networks used for measuring ablation was also utilised for velocity measurement (Figures 3.5 and 3.6). As can be seen in Figure 3.9, the stakes formed three main transects with one running longitudinally up a central ridge, a lower traverse transect at around 410-420 m a.s.l, and a second higher traverse transect at around 440-450 m a.s.l. Due to variations in surface topography and locations of crevasses and moulins, stake lines were not necessarily straight.

A Trimble 5800 Global Position System (GPS) using real time kinematic mode (RTK) was used to record the position of each stake daily from 19thJanuary to 4th February during the summer field season, and from 8th June to 3rd July during the winter field season. The base unit was set up on a debris mound near the carpark (Figures 3.10 and 3.11). Once erected and levelled, the tripod and tribach were not moved throughout the course of the study to maintain positioning. Each day the rover unit and data logger were carried up onto the glacier. The rover unit was placed directly over each stake (Figure 3.11), and stakes were held steady and vertical during measurement. Precision was set at a minimum of 0.015 m horizontal, and 0.020 m vertical. Time taken to achieve this precision varied depending on satellite position and availability, ranging from as little as a few seconds up to around ten minutes.

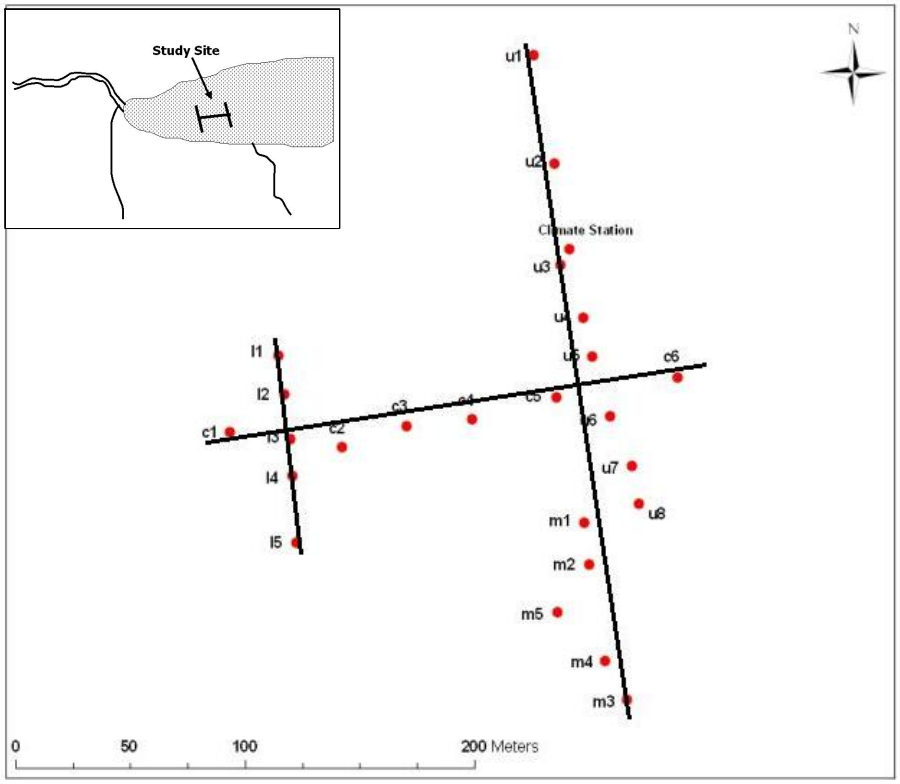

Figure 3.9 The lower (left) upper (right) and central transects used for surface velocity measurements on the lower Fox Glacier. Insert shows the approximate 2005 ice limit and the location of the study site.

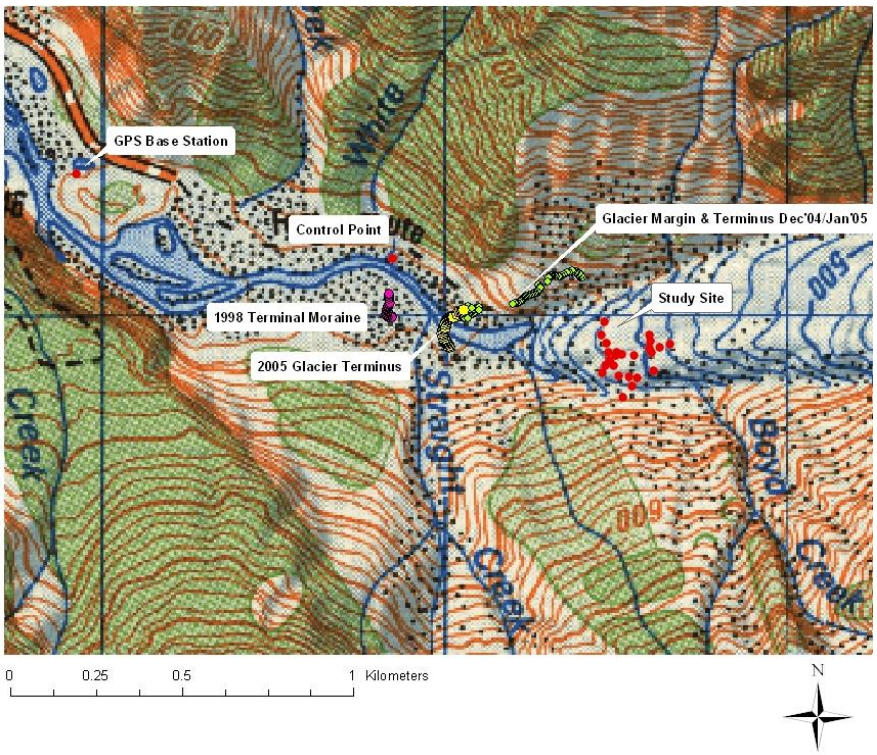

Figure 3.10 Map showing the location of the GPS base station, control point, stake network, the current (2005) terminus position, terminal moraine from the 1998/99 advance and the true right glacier margin mapped in Dec 2004. RTK-GPS data is overlain on the NZMS 260 H35 topographic map.

Figure 3.11 GPS Base unit down valley on debris mound (left) and rover unit positioned over a stake (right) with data-logger sitting on ice beside stake.

During both field seasons it was found that the best time for satellite coverage was between 10am to 12pm daily, so monitoring of the stakes was conducted during this time frame. In addition to the stake network, a control point down in the proglacial zone was measured regularly (Figure 3.10). The GPS method was chosen for this project, as it is the only survey method that can effectively be used by a single person in the field. The GPS errors associated with velocity measurement include horizontal precision of 0.015 m, vertical precision of 0.020 m, and an average variation in x and y at the control point of 0.008 m and 0.007 m respectively. Errors may also arise if the stake was not held completely vertical, Anderson (2003) calculated this error at 0.10 m. Variations in antenna placement were not an issue in this study, as a specially designed attachment for the Rover unit allowed the antenna to be inserted directly into the top of the stake in an identical position each day.

Surface velocity was then calculated daily by looking at the change in the x, y and z co-ordinates provided by the GPS, using an application of Pythagorean theorem and accounting for surface ablation using the following equation (Hubbard and Glasser, 2005; Paterson, 1969):

$$\text{Daily Velocity} = \sqrt{((x_{(t)} - x_{(t)-1})^2 + (y_{(t)} - y_{(t)-1})^2 + ((z_{(t)} + a_{(t)})^2 - (z_{(t)-1} + a_{(t)-1})^2)} \quad (9)$$

where x is the northing co-ordinate; y the easting; z the altitude; a the ablation (all in metres); and t is the time of measurement. It is important to note that although corrections are made for ablation, the above equation gives a surface velocity only and the emergence velocity (or vertical velocity) is not taken into account.

GPS data were also transferred to a GIS (Global Information System), Arcmap ™, so that positions could be overlain on a topographic map and horizontal distances calculated. Flow vectors were also calculated for each stake by digitising polylines from the start and finish positions of each stake during both study periods.

Chapter 4 Results – Climate

4.1 Meteorological Measurements Summer 2005

4.1.1 Introduction

Daily climate variables were measured from 10th January through to the 3rd February 2005, and Table 4.1 provides a summary of this data. Data for temperature, wind speed, wind direction, solar radiation and humidity are daily averages, while precipitation is a daily sum. Unless otherwise stated in the key, measurements have been made by the automatic climate station situated on the white ice of the lower glacier at around 430 m a.s.l.

Table 4.1 Summary of climate variables recorded during Jan/Feb 2005

Date	Temperature (°C)	Wind Speed (m s^{-1})	Wind Direction (°)	Precipitation (mm)	Solar Radiation (W/m^{-2})	Relative Humidity (%)	Synoptic Group (Table 3.2)
09/01	*	*	*	*	*	*	II
10/01	10.00[1]	1.00[1]	73[1]	0.00[1]	*	86[1]	II
11/01	9.44[1]	10.50[1]	*	0.50[1]	*	88[1]	IV
12/01	7.32	0.93	41.06	1.78	*	87[1]	IV
13/01	9.33	2.08	54.52	1.51	*	86[1]	III
14/01	12.73[1]	2.90	42.78	0.00	84.49	821	III
15/01	12.00[2]	*	*	0.00[2]	116.20	87	V
16/01	14.00[2]	*	*	4.00[2]	93.01	91	V
17/01	9.40[1]	4.50[1]	74.00	98.00[1]	72.05	91	V
18/01	6.51	3.90[1]	78.35	2.79	170.28	80.18	I
19/01	7.57	4.50[1]	58.35	0.00	292.51	74.86	I
20/01	8.68	4.00[1]	72.44	0.00	203.00	73.14	III
21/01	8.34	3.50[1]	56.99	1.76	131.47	81.76	III
22/01	10.30	5.00[1]	79.22	114.52	333.31	88.68	V
23/01	9.78	3.00[1]	54.91	6.85	154.68	83.47	V
24/01	9.68	1.00[1]	54.56	0.00	*	78.26	I
25/01	12.04	2.61	58.57	0.00	*	68.24	IV
26/01	12.94	3.94	57.03	0.00	*	58.72	IV
27/01	13.94	3.76	51.38	0.00	*	49.82	IV
28/01	13.83	3.54	47.49	0.00	321.81	49.98	IV
29/01	13.00[2]	*	*	0.00	285.07	70	II
30/01	12.20[1]	11.00[1]	60.00[1]	0.00[1]	200.12	64	II
31/01	13.30[1]	8.00[1]	60.00[1]	0.00[1]	250.84	44	IV
01/02	16.73	6.44	47.95	0.00	353.10	38.15	VI
02/02	15.23	5.06	48.41	0.00	350.80	50.01	VI
03/02	15.82	4.81	47.57	0.00	352.46	52.02	VI

Key:
[1] = manual one off measurement
[2] = Alpine Guides Westland data (Fox Township)
* = No available Data

4.1.2 Temperature

During the summer field season both the maximum and minimum temperatures on the lower glacier were recorded on the 20th January. The minimum of 4.6°C occurred at 3:03 am, while the maximum, 22.5°C, was reached at 2:20 pm. The average daily temperature during this study period was 11.5°C. Table 4.2 shows summary statistics for both the average daily temperature, and for all temperature data logged at fifteen-minute intervals between 12th January and 3rd February.

Table 4.2 Descriptive statistics for temperature data (°C) recorded during the summer field season.

	n	Mean	Max	Min	SE Mean	St Dev	Q1	Q3
Daily Average Temperature	23	11.50	16.73	6.51	3.78	4.60	9.33	13.83
All Temperature Data	1444	11.51	22.50	4.60	0.60	2.86	8.10	14.60

An interval plot of the 95% confidence interval of the mean (two standard errors) of all temperature data shows very little spread (Figure 4.1). The calculation of daily average temperatures does result in a larger margin of error, but does not alter the mean value significantly.

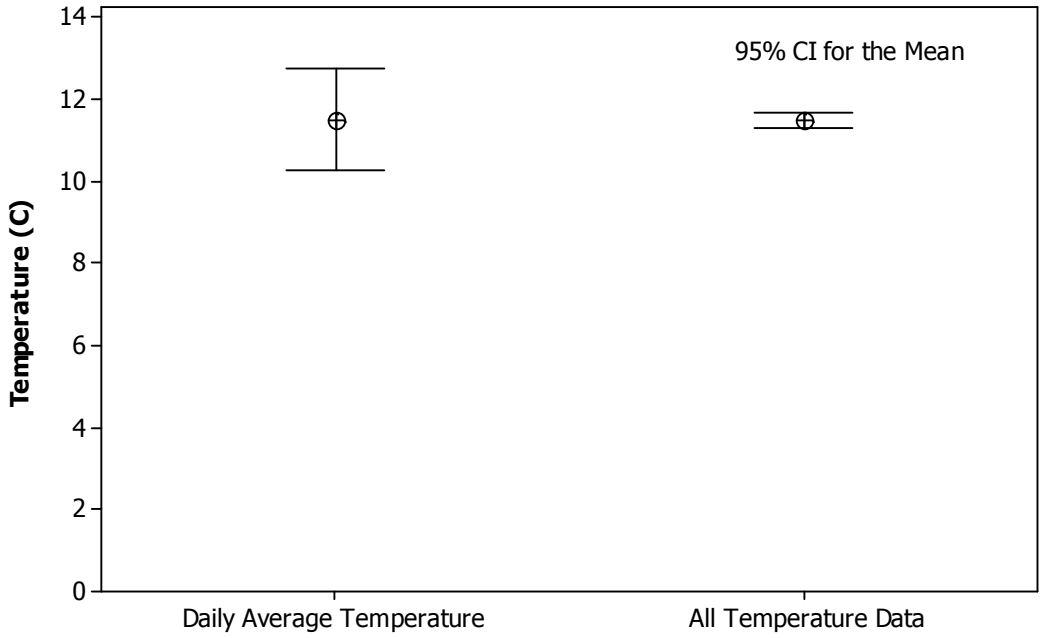

Figure 4.1 95% confidence intervals for both the daily average temperature and for all temperature data recorded on the lower Fox Glacier during the summer study period.

Consideration was given to the diurnal temperature range by looking at the average temperature from 10am to 5pm, and the average evening/night time temperature from 5pm through till 10am the next morning (Figure 4.2). Due to software malfunctions with the climate stations data programme, not all days are represented, but as the graph shows, on some occasions diurnal variability was greater than 5°C, and overall there was a difference of around 3°C (22%) between the temperatures.

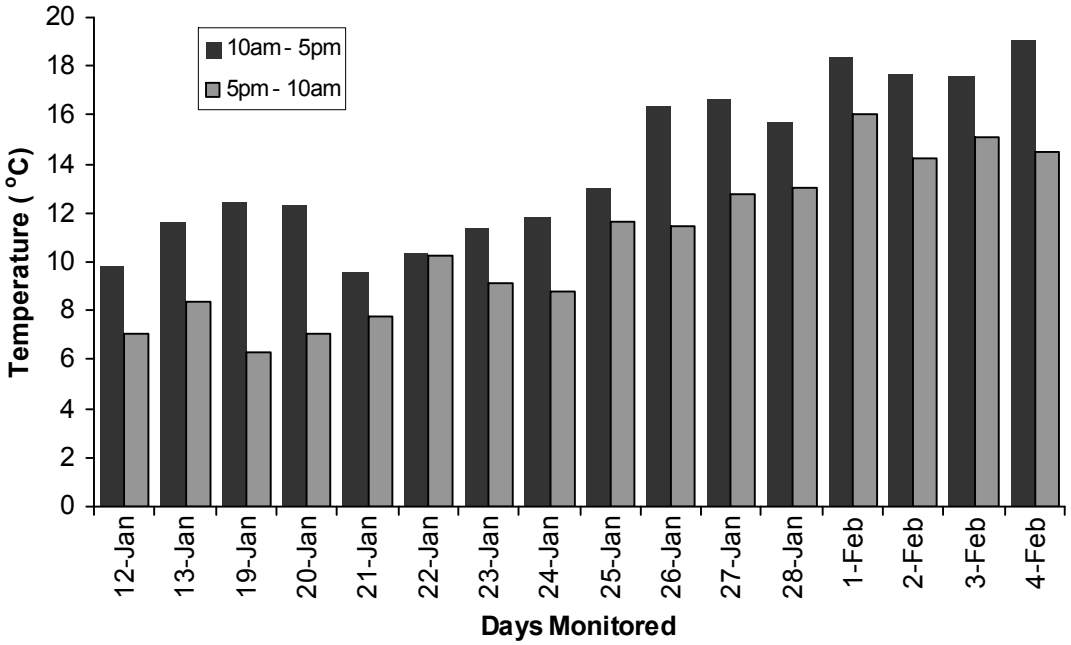

Figure 4.2 Comparison of daily average temperatures recorded on the lower Fox Glacier between 10am and 5pm and between 5pm and 10am the following day during the summer field season.

Figure 4.3 plots the maximum and minimum temperatures recorded. The largest difference occurred on the 20th January when the maximum was 17°C higher then the minimum. The lowest difference occurred on the 12th January when there was only a 4.4 °C difference in temperatures. On average the range between the maximum and minimum temperature was 9.2 °C.

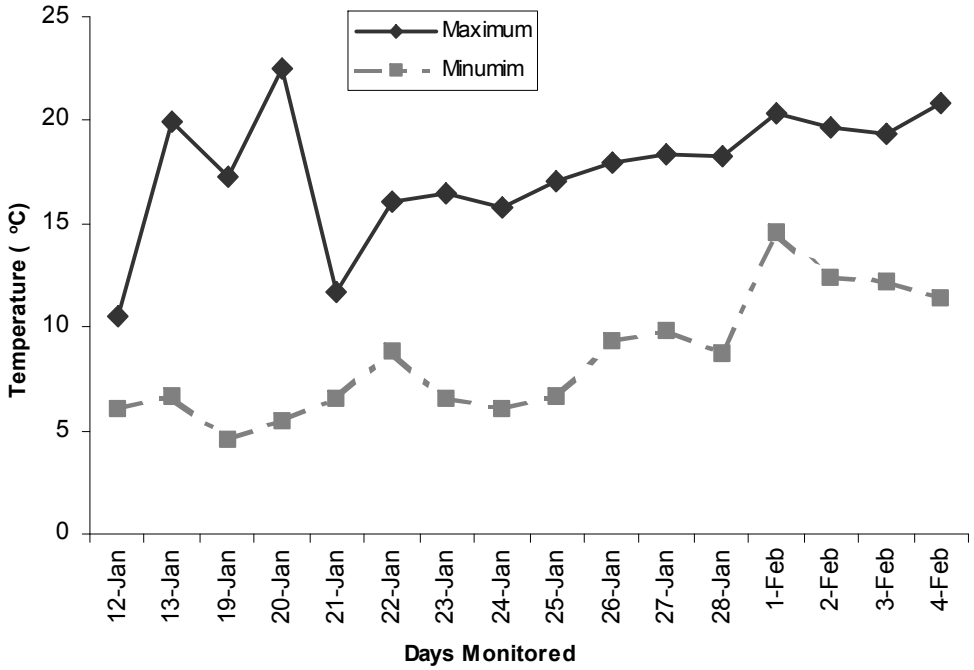

Figure 4.3 Maximum and minimum daily temperatures recorded on the lower Fox Glacier during the summer field season.

A time series for average daily temperature is shown in Figure 4.4. There is a notable drop on the 18th January, and a peak on the 1st February. The drop on the 18th January appears to be associated with the passing of a cold front, and field notes recorded a cool and clear night after a front had passed. The general increase in temperature at the beginning of February (c. 3 °C) is associated with a heat-low that developed in the central South Island.

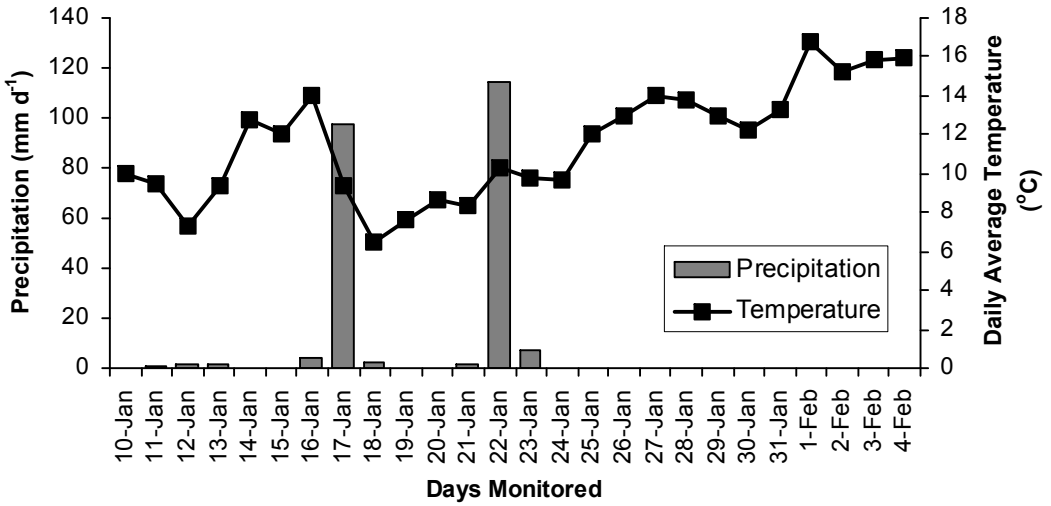

Figure 4.4 Daily average temperatures and net daily precipitation recorded on the lower Fox Glacier during the summer field season.

4.1.3 Precipitation

Precipitation fell on 8 out of the 23 days during which climate variables were monitored. The highest recorded rainfall occurred 22nd January with 116 mm falling over a twenty-four hour period. The other notable rainfall event occurred on the 17th January when 98 mm fell (Figure 4.4). The descriptive statistics for the precipitation data are contained in Table 4.3. Note that for the 'all precipitation data', statistics are based on the fifteen-minute interval log, hence the lower maximum precipitation figure.

Table 4.3 Descriptive statistics for precipitation data (mm) recorded during the summer field season.

	n	Mean	Max	Min	SE Mean	St Dev	Q1	Q3
Daily Average Precipitation	23	10.05	114.50	0.00	6.36	30.51	0.00	1.78
All Precipitation Data	1443	0.90	5.59	0.00	0.01	0.49	0.00	0.00

Due to the large range in precipitation received, non-resistant measures of spread like standard deviations are not very meaningful. As Figure 4.4 demonstrates, on the majority of days monitored, no precipitation fell, instead the bulk of the precipitation which fell, did so on only two days. Therefore, precipitation data do not have a normal distribution so some of the statistics in Table 4.3 like standard deviation have only limited value for describing this climatic parameter over such a short timeframe.

4.1.4 Humidity

Maximum humidity recorded on the lower glacier during the summer field season was 98% at 4:34pm on the 22nd January, with a minimum of 28% occurring at 1:13pm on the 1st February. The daily average humidity was 71%. Table 4.4 contains the descriptive statistics for humidity data. Standard deviations are quite high, at 24% of the daily average humidity mean, and up to 27% of the mean for all humidity data. The maximum and minimum data columns show that there was a large range in humidity during this field season. Figure 4.5 shows the 95% confidence interval of the mean for both the daily average and all humidity data. As can be seen, there is actually very little spread in the data with an overall average of 67% a slightly lower figure than the daily average of 71%, and over time, humidity was lower during late January and early February (Table 4.1).

Table 4.4 Descriptive statistics for relative humidity data (%) during the summer field season.

	n	Mean	Max	Min	SE Mean	St Dev	Q1	Q3
Daily Average Humidity	23	70.83	91.00	38.15	3.47	16.66	32.02	86.00
All Humidity Data	1402	66.70	98.40	28.40	0.49	18.32	51.37	82.63

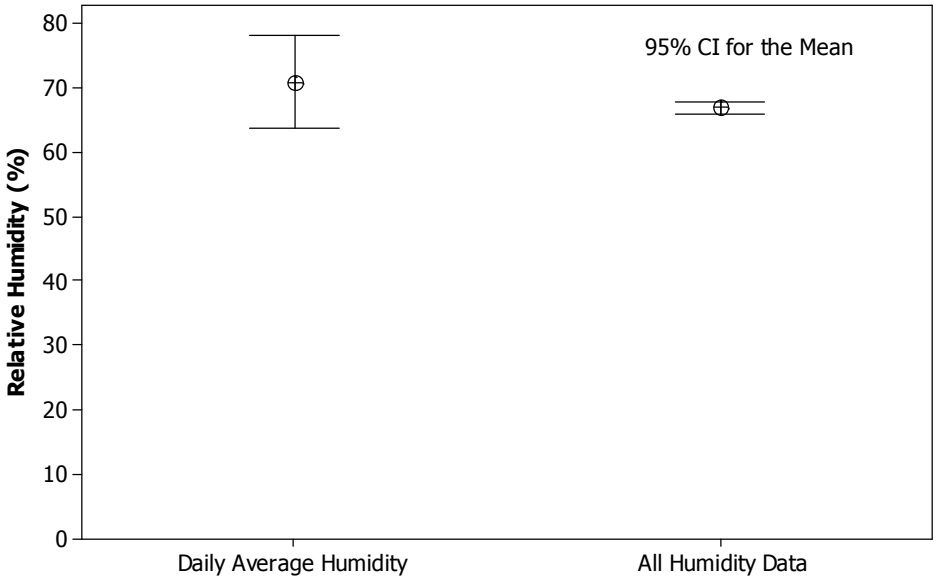

Figure 4.5 95% confidence interval (two standard errors of the mean) for average daily humidity and for all humidity data recorded during the Jan/Feb field season on the lower Fox Glacier.

4.1.5 Wind Speed & Direction

The fastest wind speed recorded during the summer field season was 11 m s^{-1} at around 11am on 31st January, and wind direction, despite the synoptic situation, almost always blew down-glacier from the north-east (57°) due to katabatic influences (see section 2.3.3). Tables 4.5 and 4.6 contain the descriptive statistics for wind speed and wind direction data. As mentioned in section 3.1.2 there was a period when the anemometer began working intermittently, however it is hard to determine exactly which zero velocity figures are genuine and which are due to faulty equipment during this time. This explains why the overall mean based on the fifteen minute data log (all wind speed data) is much lower than the daily average, which uses 'one off' manual anemometer measurements for the days most obviously affected.

Table 4.5 Descriptive statistics for wind speed (m s^{-1}) during the summer field season.

	n	Mean	Max	Min	SE Mean	St Dev	Q1	Q3
Daily Average Wind Speed	20	4.67	11.00	0.93	0.56	2.50	3.13	5.05
All Wind Speed Data	1444	2.36	10.00	0.00	0.06	2.34	0.00	4.00

Table 4.6 Descriptive statistics for wind direction (°) during the summer field season.

	n	Mean	Max	Min	SE Mean	St Dev	Q1	Q3
Daily Average Wind Direction	20	57.28	79.00	41.06	2.48	11.09	48.07	60.00
All Wind Direction Data	1444	55.60	305.00	0.00	0.76	28.87	47.10	57.00

The problems with the anemometer also of influence the standard error of all the wind speed data (Figure 4.6), with the number of zero velocity observations giving the indication of little spread. However, the daily average data incorporating some manual measurements show much larger spread with the standard deviation being 54% of the mean.

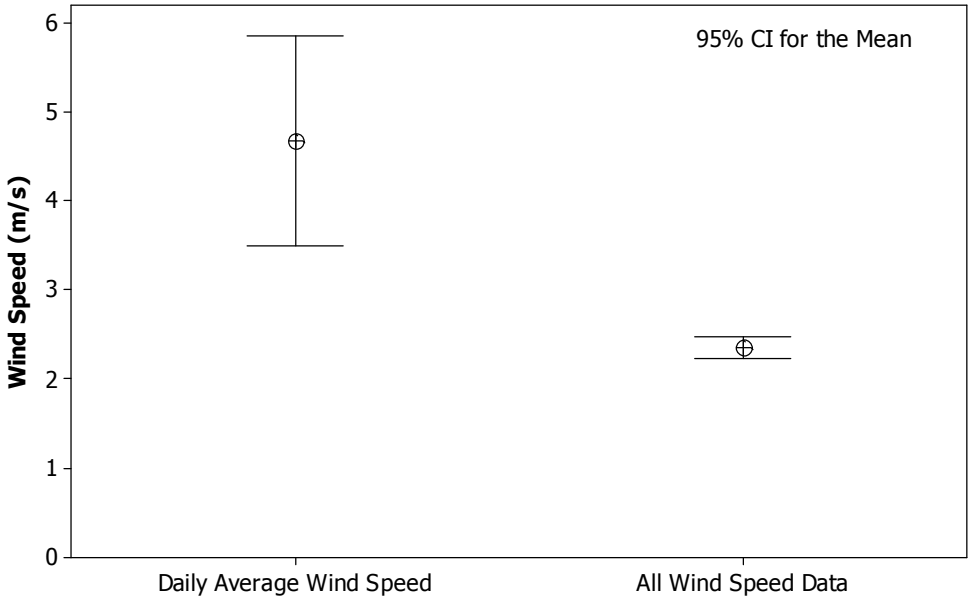

Figure 4.6 The 95% confidence interval of the mean of daily average wind speed and for all the wind speed data (m s^{-1}) recorded on the lower Fox Glacier Jan/Feb 2005.

With wind direction, an observation when wind direction is exactly north (0°), and gusts to the north-north-west (305°) create a lot of spread in the data, but the resistant measures of spread Q1 and Q3 (Table 4.6) show that the majority of the wind blows from the north-easterly sector (Figure 4.7).

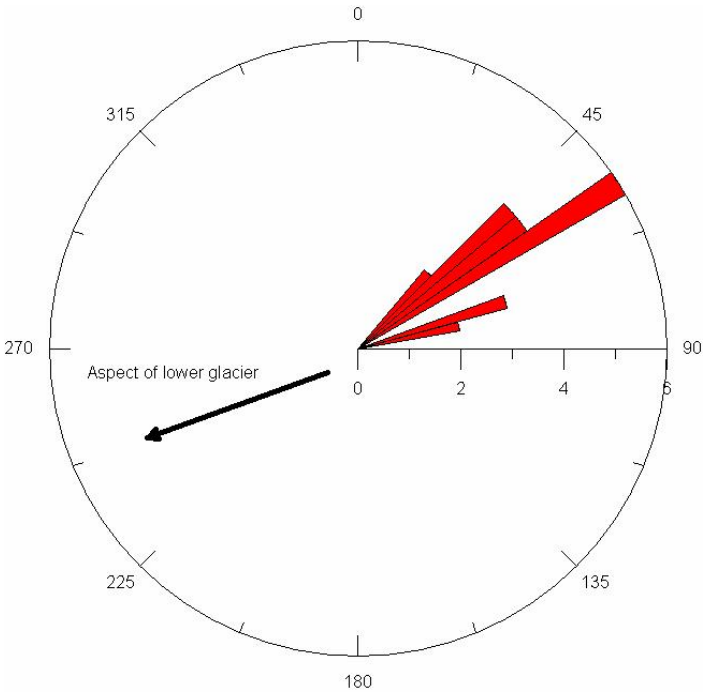

Figure 4.7 Rose-diagram showing average daily wind direction recorded on the lower Fox Glacier during the summer field season.

4.1.6 Solar Radiation

As outlined in section 3.1.2, and seen in Table 4.1, problems with keeping the pyranometer level resulted in gaps in the solar radiation data. However, the days when the sensor was off-level were obvious, due to a –6999 data entry, therefore, it was straight forward to eliminate this data. The means for both the daily average incoming short-wave radiation (ISWR) and for all the valid radiation data are similar (Table 4.7 and Figure 4.8), with the large range in values being captured by the 'all data' row, hence the large standard deviation. The Q1 figure in the 'all data' row is influenced by the large amount of zero values that are recorded each night from around 9:30 pm through until 6:30 am the next day. This results in large diurnal variability in net solar radiation.

Table 4.7 Descriptive statistics for incoming short-wave solar radiation data (W/m^{-2}) during the summer field season.

	n	Mean	Max	Min	SE Mean	St Dev	Q1	Q3
Daily Average Incoming Short-wave Radiation	17	221.5	353.1	72.1	24.9	102.6	123.8	327.6
All ISR Data	893	229.7	1277	0.0	11.3	336.2	0.00	378.2

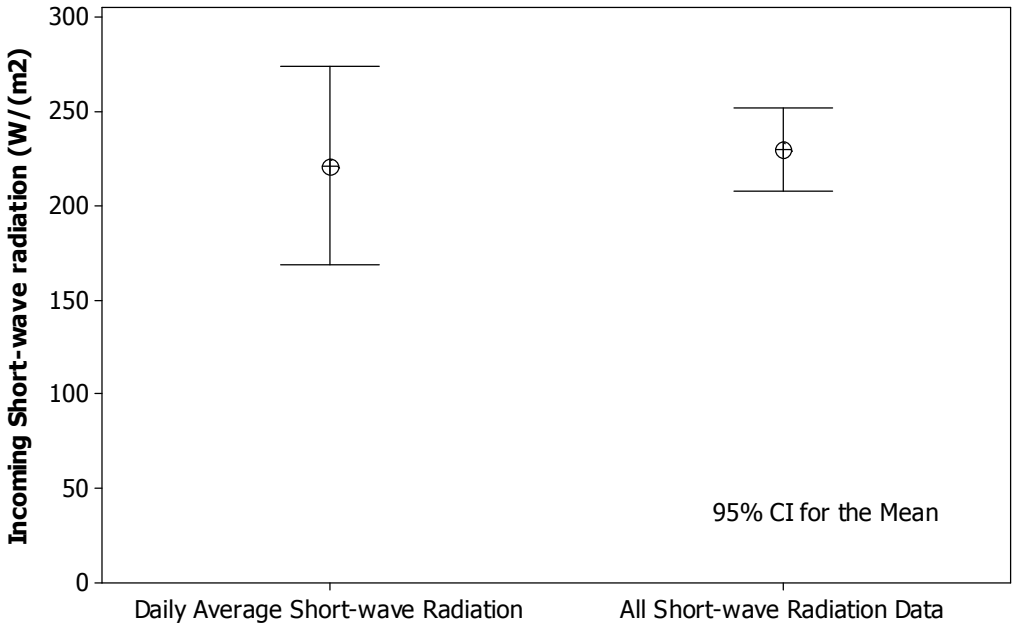

Figure 4.8 The 95% Confidence Interval of the mean for the daily average incoming short-wave radiation and for all short-wave radiation data (W/m^{-2}) recorded on the lower Fox Glacier during Jan/Feb 2005.

4.2 Synoptic Situations Summer 2005

4.2.1 General Patterns

The synoptic classifications in Table 4.1 are based on those developed by Hay and Fitzharris (1988) during their work on the Ivory Glacier (see section 3.1.3). The frequency of each of the synoptic classifications during the summer study period is shown in Figure 4.9. The most common situation that occurred during summer was IV, when an anticyclone was situated over the South Island. The occurrence of a north to north-westerly flows (III) was also quite frequent, with a few passing fronts or troughs (V), and occasional north to north-easterly (II) conditions. A heat-low (VI) developed in early February, and there was a low occurrence of south to south-west flows (I).

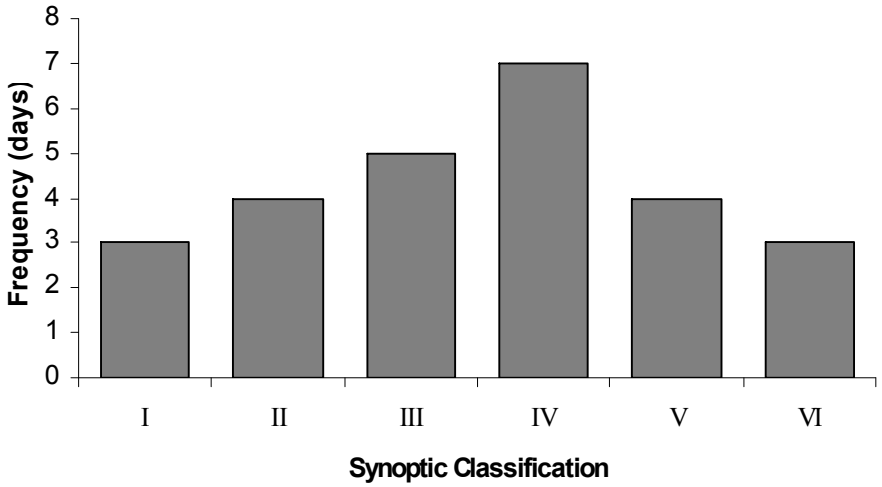

Figure 4.9 The frequency of the different synoptic situations recorded by Metservice that were in place during the summer field season. Classification categories are based on the work of Hay and Fitzharris (1988) with minor modification for this study.

4.2.2 Relationships with other climatic parameters

When considering the average daily temperature and total precipitation associated with each of the general synoptic situations (Figure 4.10), it can be seen that lower temperatures are experienced with north-westerly and south to south-westerly flows (III and I), while higher temperatures occurred with the situation VI, when there was a heat-low in inland areas. The majority of the precipitation fell during the passage of fronts/troughs (V), although very low amounts fell during other synoptic conditions.

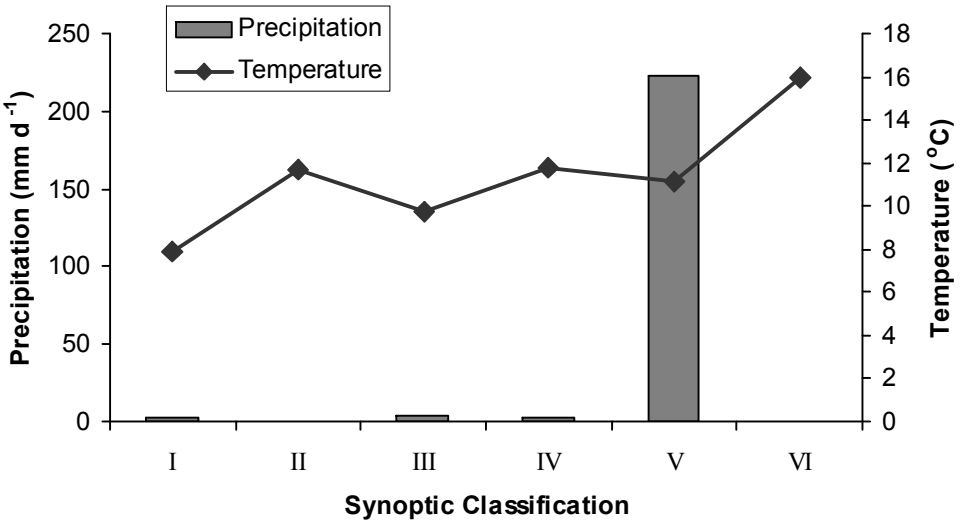

Figure 4.10 Relationship between daily average temperature and total precipitation with the general synoptic situation during the summer field season.

Humidity was highest during the passage of fronts (88%) and low humidity was recorded when anticyclones (IV) were situated over the South Island (64%) and with the occurrence of the heat-low (VI), with an average humidity of only 47% (Figure 4.11). Gaps in solar radiation data makes the correlation with the general synoptic situation difficult, but higher fluxes were received during the heat-low (Figure 4.11). As mentioned earlier, local climatic conditions tend to dominate wind-direction on the lower glacier therefore wind direction was not compared with the synoptic situation.

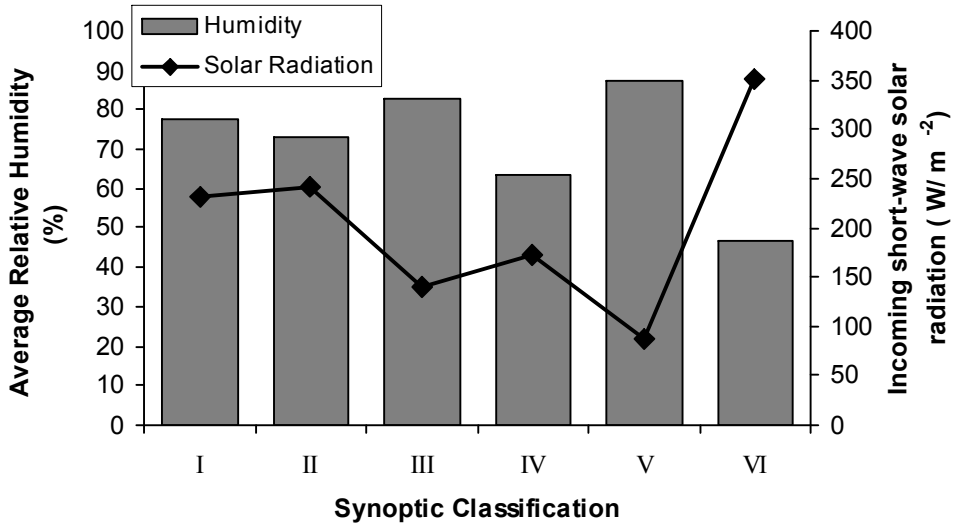

Figure 4.11 The relationship between the synoptic classification and average daily relative humidity and incoming short-wave solar radiation received on the lower Fox Glacier during Jan/Feb 2005.

4.3 Meteorological Measurements Winter 2005

4.3.1 Introduction

During the winter field season daily climate variables were measured from the 8th June through to the 3rd July 2005. Table 4.8 provides a summary of the daily averages (daily sum for precipitation) for the variables measured. All of the variables were measured by the automatic climate station, located on clean ice at 435 m a.s.l, with the exception of precipitation. The precipitation data are based on readings from a manual rain gauge mounted on the side of the automatic climate station.

Table 4.8 Summary of climate variables recorded on the lower Fox Glacier during June/July 2005

Date	Temperature (°C)	Wind Speed (m s^{-1})	Wind Direction (°)	Precipitation (mm)	Incoming Short-wave Radiation (W/m^{-2})	Relative Humidity (%)	Synoptic Group (Table 3.2)
08-Jun	4.13	2.01	38.71	6	27.19	72.07	V
09-Jun	6.52	2.06	40.78	48	15.18	85.41	V
10-Jun	6.25	1.74	43.92	10	25.41	77.75	V
11-Jun	6.41	2.01	43.59	0	22.44	62.71	IV
12-Jun	6.42	2.04	45.19	0	6.55	52.25	IV
13-Jun	7.32	2.76	51.32	0	6.52	46.11	II
14-Jun	6.98	3.66	33.25	0	6.96	45.89	II
15-Jun	7.47	2.56	48.63	0	29.53	39.43	II
16-Jun	6.34	2.59	43.01	2	13.17	59.23	II
17-Jun	6.56	2.70	44.48	113	7.81	94.61	V
18-Jun	6.59	1.40	40.55	18	30.86	79.48	V
19-Jun	5.26	2.76	41.35	2	30.61	73.52	III
20-Jun	5.85	2.62	53.46	100	28.77	82.50	III
21-Jun	5.63	3.04	63.57	20	12.80	84.59	V
22-Jun	4.73	2.71	40.41	0	8.78	64.41	V
23-Jun	3.52	2.01	41.55	0	15.46	63.52	II
24-Jun	3.11	2.34	45.86	0	8.55	55.02	II
25-Jun	2.71	2.47	39.69	0	4.86	51.79	I
26-Jun	2.69	2.06	42.60	0	7.62	59.74	I
27-Jun	3.65	1.44	43.22	0	13.65	69.55	I
28-Jun	5.91	2.05	111.31	116	16.80	92.08	V
29-Jun	3.76	1.52	118.88	4	28.16	77.23	V
30-Jun	3.81	1.86	47.57	0	7.12	62.77	I
01-Jul	5.06	2.21	48.30	0	9.70	64.66	I
02-Jul	5.88	2.58	45.32	24	23.74	75.44	III
03-Jul	6.99	2.59	96.06	220	2.93	94.63	V

4.3.2 Temperature

During the winter field season a maximum temperature of 9.4°C was recorded at 2:00pm on the 15th of June, while a minimum of 1.2°C occurred at 7am on 24th July. Daily average temperature was 5.4°C, a figure that is reflected in both the daily average data, and from all the temperature data recorded (Table 4.9 and Figure 4.12).

Table 4.9 Descriptive statistics for temperature data (°C) June/July 2005.

	n	Mean	Max	Min	SE Mean	St Dev	Q1	Q3
Daily Average Temperature (°C)	26	5.37	7.47	2.69	0.29	1.49	3.80	7.47
All Temperature Data	610	5.42	9.43	1.17	0.07	1.66	4.15	9.43

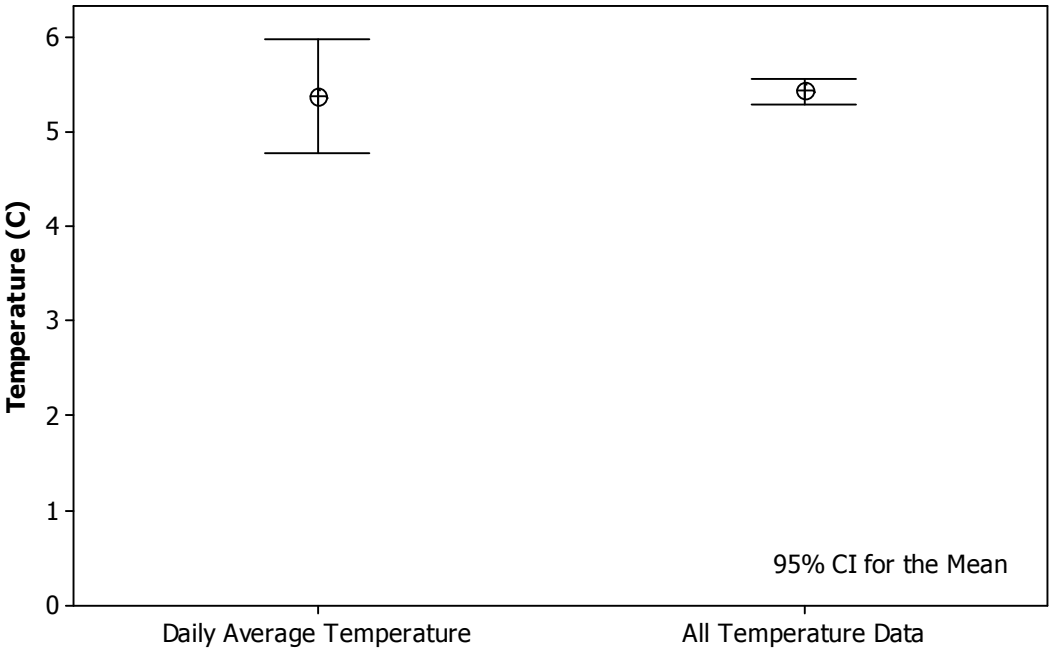

Figure 4.12 The 95% confidence intervals for both the daily average temperature and for all temperature data recorded during the June/July study period.

The diurnal range in temperature was found to be less than during the summer season, with the evening temperature being on average only 0.7°C (12%) lower than the average daytime temperature (Figure 4.13).

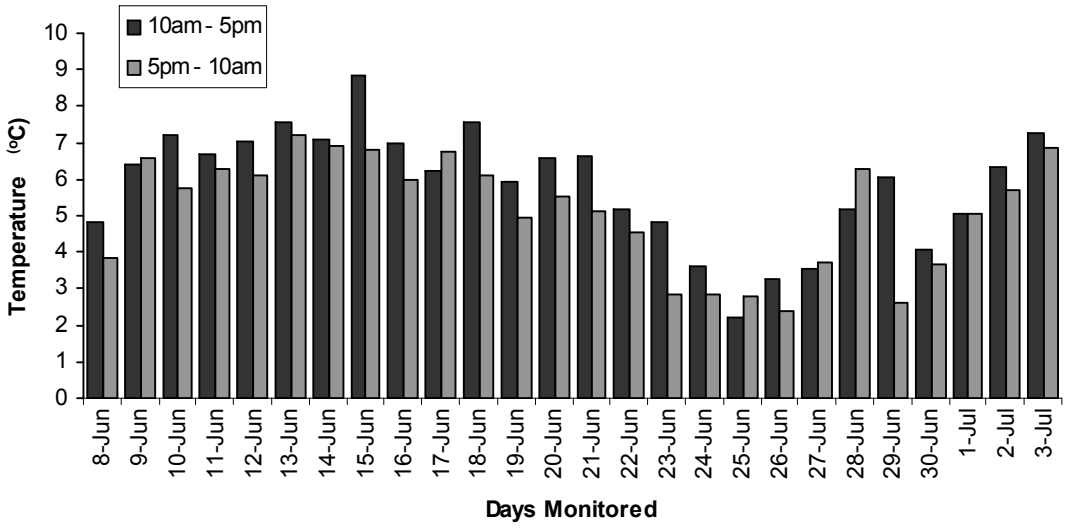

Figure 4.13 Diurnal temperature range during recorded on the lower Fox Glacier during Jun/July 2005

Over time there was quite a large variation in daily average temperature ranging from 2.7°C up to 7.5°C, with a notable low point between 23rd to 26thJune. Field notes record that this was a period of fine frosty weather with very clear skies. On both the 28th June and on the 3rd July temperature is seen to increase with the passing of frontal rain (Figure 4.14).

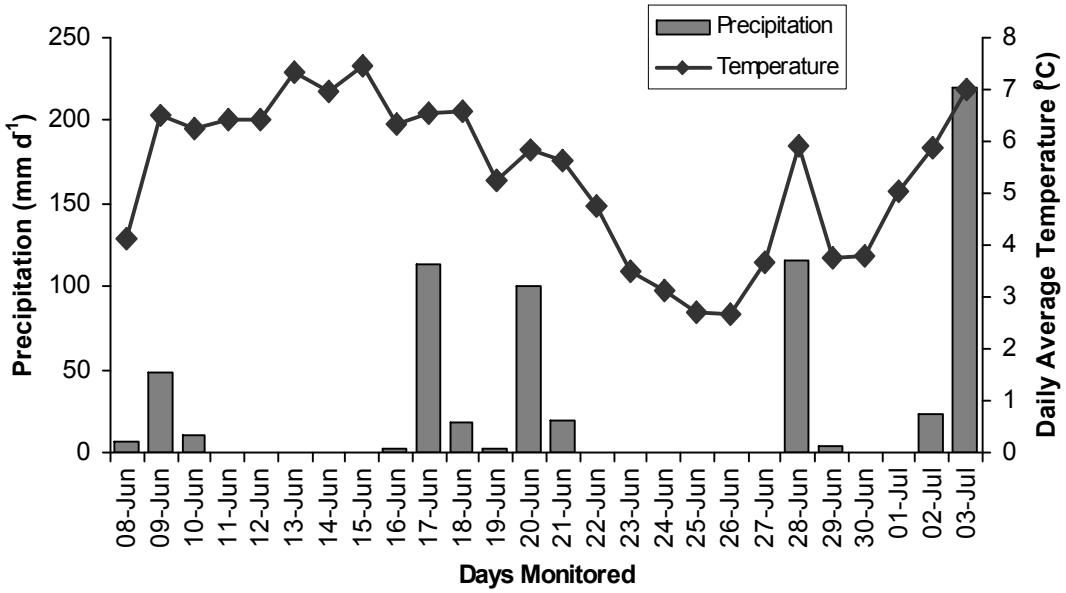

Figure 4.14 Daily average temperature and net precipitation recorded on the lower Fox Glacier during the June/July 2005 study period.

4.3.3 Precipitation

Precipitation fell on 13 out of the 26 days monitored, coinciding with the passage of five frontal systems (Figure 4.14). On four of these occasions an excess of 100 mm was received, and with the event on the 3rd July, an excess of 200 mm was received. Descriptive statistics (Table 4.10) show that non-resistant measures of spread like for example standard deviation are not very informative over such short time frames due to extremes values from days without any rain, to the occurrence of very heavy rainfall events.

Table 4.10 Descriptive statistics for precipitation data (mm) from the winter field season

	n	**Mean**	**Max**	**Min**	**SE Mean**	**St Dev**	**Q1**	**Q3**
Daily Total Precipitation (mm)	26	26	220	0	10.4	53	0	21

4.3.4 Humidity

Table 4.11 contains the descriptive statistics for the winter humidity data. Maximum humidity recorded on the lower glacier during the winter field season was 98.8% at 1:00am on the 3rd July during the very heavy rainfall event. A minimum of 30.8% occurred at 10:00pm on the 15th June. The daily average humidity was 69%. Like during summer, there was a large range (nearly 70%) in humidity conditions on the lower glacier during this field season. Figure 4.15 shows the 95% confidence interval of the mean for both the daily average and all humidity data, with the all humidity data having a much tighter distribution as would be expected with the larger sample size.

Table 4.11 Descriptive statistics for relative humidity data (%) for June/July 2005 field season

	n	Mean	Max	Min	SE Mean	St Dev	Q1	Q3
Daily Average Humidity	26	68.71	94.63	39.43	3.01	15.36	58.18	80.24
All Humidity Data	610	69.03	99.80	30.81	0.71	17.52	55.22	82.88

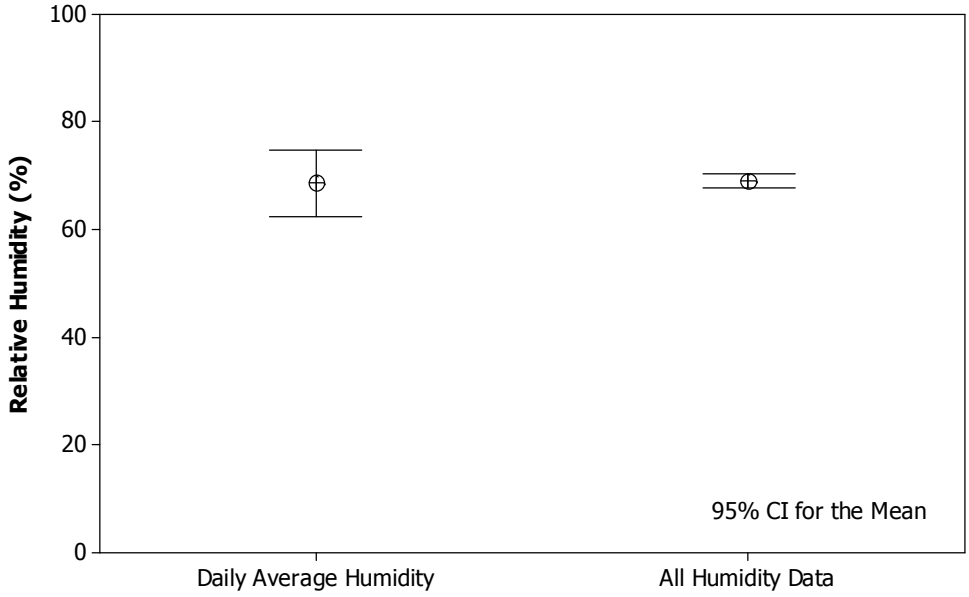

Figure 4.15 The 95% confidence interval (two standard errors of the mean) for average daily humidity and for all humidity data recorded during the June/July 2005 field season on the lower Fox Glacier.

4.3.5 Wind Speed and Direction

As mentioned in section 3.1.2 problems were encountered with the anemometer readings during this field season and corrections had to be made by regressing the one-off manual recordings with the automatically logged value. This process appears to have smoothed the data and true extreme values may have been masked, with the fastest wind speed recorded only 5.5 m s^{-1} (Table 4.12).

Table 4.12 Descriptive statistics for wind speed (m s^{-1}) recorded during the winter field season.

	n	Mean	Max	Min	SE Mean	St Dev	Q1	Q3
Daily Average Wind Speed	26	2.30	3.66	1.40	0.10	0.52	2.01	3.66
All Wind Speed Data	610	2.29	5.54	0.76	0.39	0.96	1.53	2.96

Like during summer, the mean average wind direction was 52°, blowing from the north-east due to katabatic influences (Table 4.13). As mentioned in section 4.1.5 the nature of the wind direction data results in an extreme range and large standard deviations, because both the minimum and maximum figure represents the same general wind direction (northerly). Therefore the resistant measures of spread (Q1 and Q3) provide better information as to the spread of the wind direction data. This general north-easterly or katabatic wind direction can be seen on Figure 4.16.

Table 4.13 Descriptive statistics for wind direction (°) recorded during the winter field season.

	n	Mean	Max	Min	SE Mean	St Dev	Q1	Q3
Daily Average Wind Direction	26	52.02	118.88	33.25	4.29	21.89	41.21	49.30
All Wind Direction Data	610	52.31	359.90	0.00	1.98	48.98	33.74	53.84

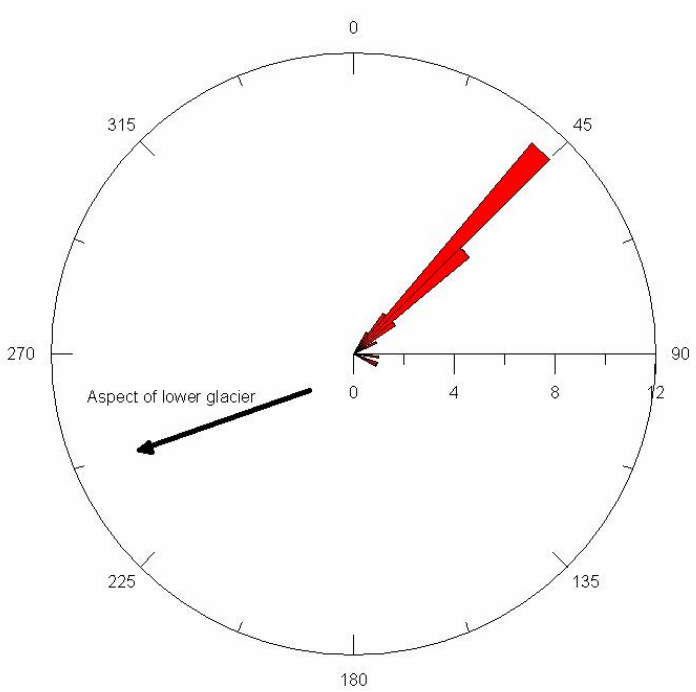

Figure 4.16 Rose-diagram of the daily average wind direction recorded on the lower Fox Glacier during the winter field season.

4.3.6 Solar Radiation

Figures for incoming short-wave radiation (ISWR) were very low over the winter field season. This was to be expected, as most of the lower glacier is topographically shaded during this time and does not receive any direct sunlight. Due to the nature of this climate parameter, in particular the high proportion of zero readings over night, there is large spread in the data (Table 4.14 and Figure 4.17) and resistant measures of spread are not very informative. Again Q1 and Q3 provide good indications about the spread of the solar radiation data during this winter field season.

Table 4.14 Descriptive statistics for incoming short-wave solar radiation data (W/m^{-2}) during the winter field season.

	n	Mean	Max	Min	SE Mean	St Dev	Q1	Q3
Daily Average ISWR	26	15.81	30.86	2.93	1.83	9.35	7.50	25.86
All ISR Data	610	15.99	214.00	0.0	1.36	33.68	0.00	19.09

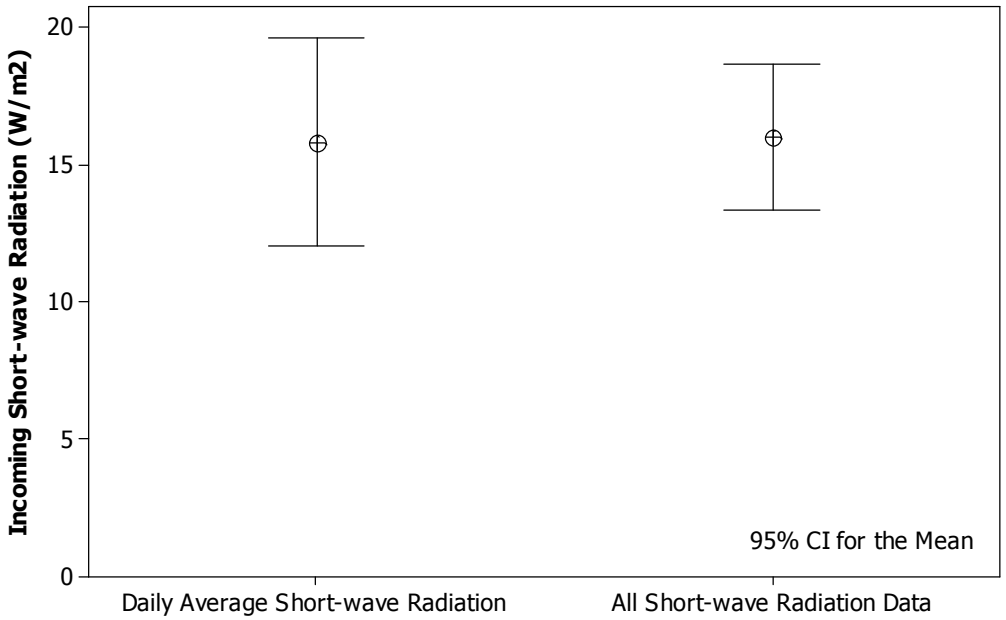

Figure 4.17 The 95% confidence interval (two standard errors of the mean) for average daily incoming solar-radiation and all incoming short-wave radiation recorded on the lower Fox Glacier during the June/July 2005 field season.

4.4 Synoptic Situations Winter 2005

4.4.1 General Patterns

The most common daily synoptic situation during the winter field season was the passing fronts/troughs (V), with south to south-west flows (I) also occurring frequently. North to north-easterly (II) flows and north-westerly airflows (III) were less common, and only on a few occasions was an anticyclone (IV) positioned over the South Island (Figure 4.18 and Table 4.8). There was no occurrence of a heat low (VI) like what was experienced during the summer field season.

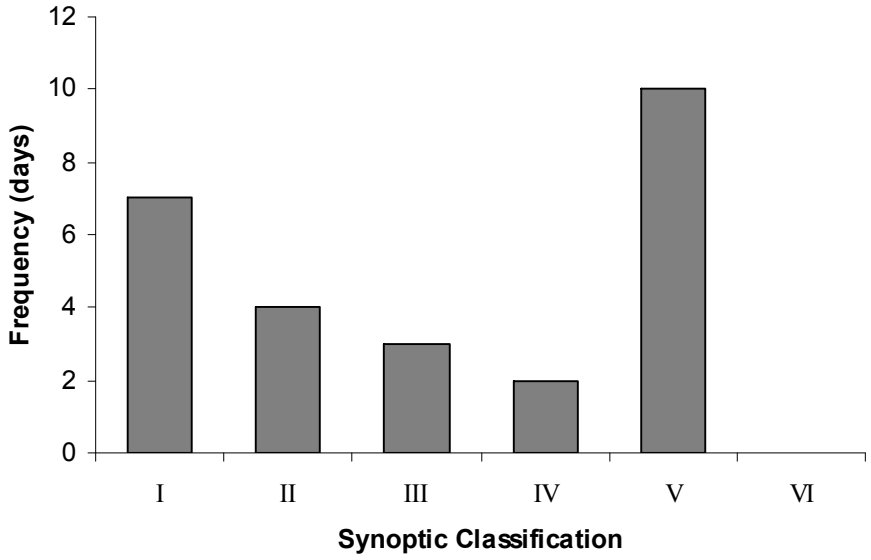

Figure 4.18 The frequency of synoptic situations recorded by Metservice the occurred during the winter field season. Classification is based on the work of Hay and Fitzharris (1988) with minor modification for this study.

Discriminate analysis of the synoptic classes with the climate variables, resulted in 96% correctly grouped. Using cross-validation, 73% of the groups were still correct. Close relationships were identified between groups' III and V (north-westerly flow with a front/trough) and between I and V (south-westerly flow and a front/trough). As mentioned in section 2.3.2 there is a regular pattern to the passage of troughs and anticyclones over New Zealand, resulting in progressive shift from north-westerly airflow through to a southerly airflow (Brenstrum, 1998; Fitzharris, 2001; Sturman, 2001b), therefore it is not surprising that the discriminate analysis identified these relationships. Discriminate analysis of the summer synoptic classifications with measured climate variables was not possible due to the number of gaps in the data for various climate parameters.

4.4.2 Relationships with other Climate Parameters

Looking more specifically at the relationship between the synoptic classification and daily average temperature (Figure 4.19) it is found that north to north-easterly flows (II) brought the warmest temperatures while south to southwest (I) the lowest. Almost all the precipitation fell with passing fronts, and some also occurred with a north-westerly flow (III), which as mentioned earlier is associated with fronts/troughs moving onto the South Island.

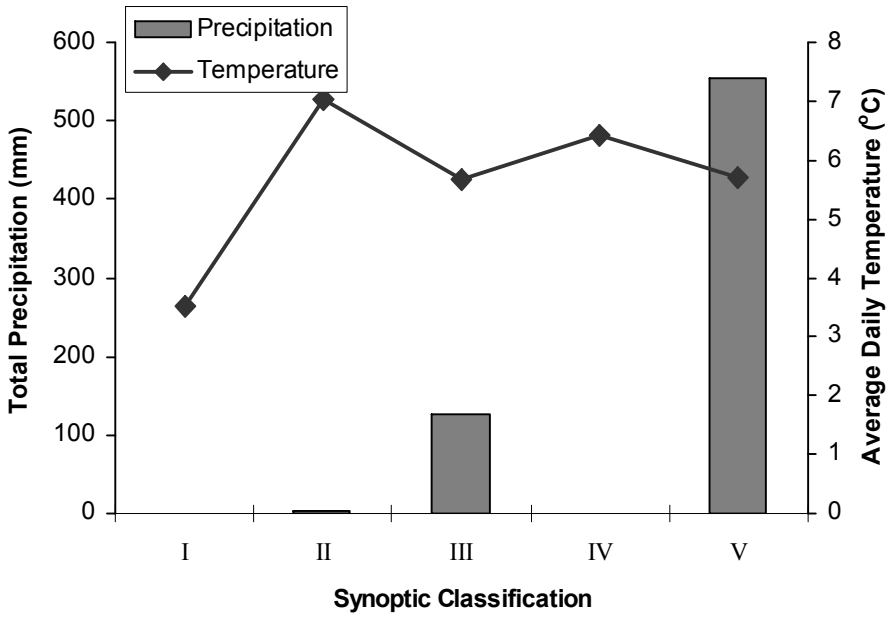

Figure 4.19 The relationship between the synoptic classification, daily average temperature, and total precipitation received on the lower Fox Glacier during June/July 2005.

Although the ISWR was found to be highly variable (section 4.4.6) higher average levels were received during north-westerly flows (III) and lower levels occurred with south to south-west flows (Figure 4.20). High humidity was associated with synoptic groups I, III and V, which is not surprising as these groups are the airflows associated with a passing front and associated precipitation.

Due to the problems with the wind speed data mentioned earlier there is very little difference between daily average wind speeds, and like during the summer field season, wind direction was dominated by local winds (katabatic) so does not appear to be strongly influenced by the changing synoptic situation.

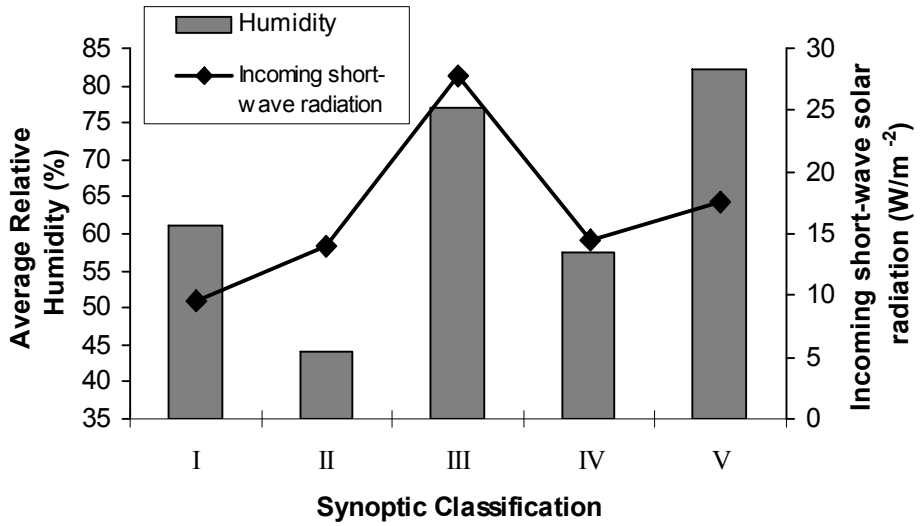

Figure 4.20 The relationship between the synoptic classification and average daily relative humidity and incoming short-wave solar radiation received on the lower Fox Glacier Jun/July 2005.

4.5 Intra-annual variation in Climate

4.5.1 Temperature

There is a clear difference between the daily average temperature recorded on the lower Fox Glacier during summer that recorded during winter, with winter temperatures being on average 47% less than summer (Figure 4.21), in fact, there is basically no overlap between these daily average temperatures. During winter there appears to be less variability of the average daily temperature, and the diurnal range was found to be smaller.

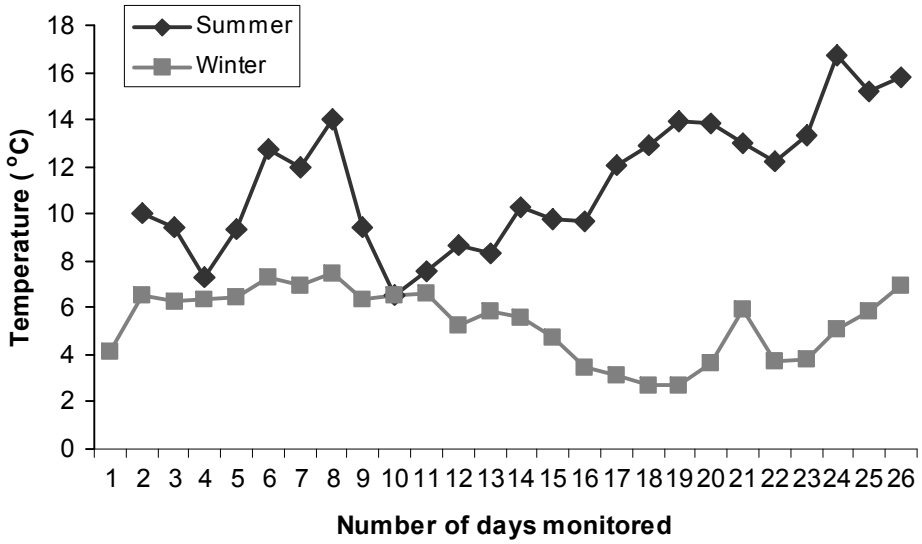

Figure 4.21 Comparison of daily average temperature recorded during both the summer and winter field seasons on the lower Fox Glacier 2005.

4.5.2 Precipitation

The higher occurrence of passing fronts/troughs that occurred during winter understandably resulted in more precipitation being received during the winter field season in comparison to summer (Figure 4.22). However, as outlined in section 2.3.2 longer-term climate data from NIWA reports that June through to August are generally the driest months. The short duration of this study will be of influence to this variation in precipitation data.

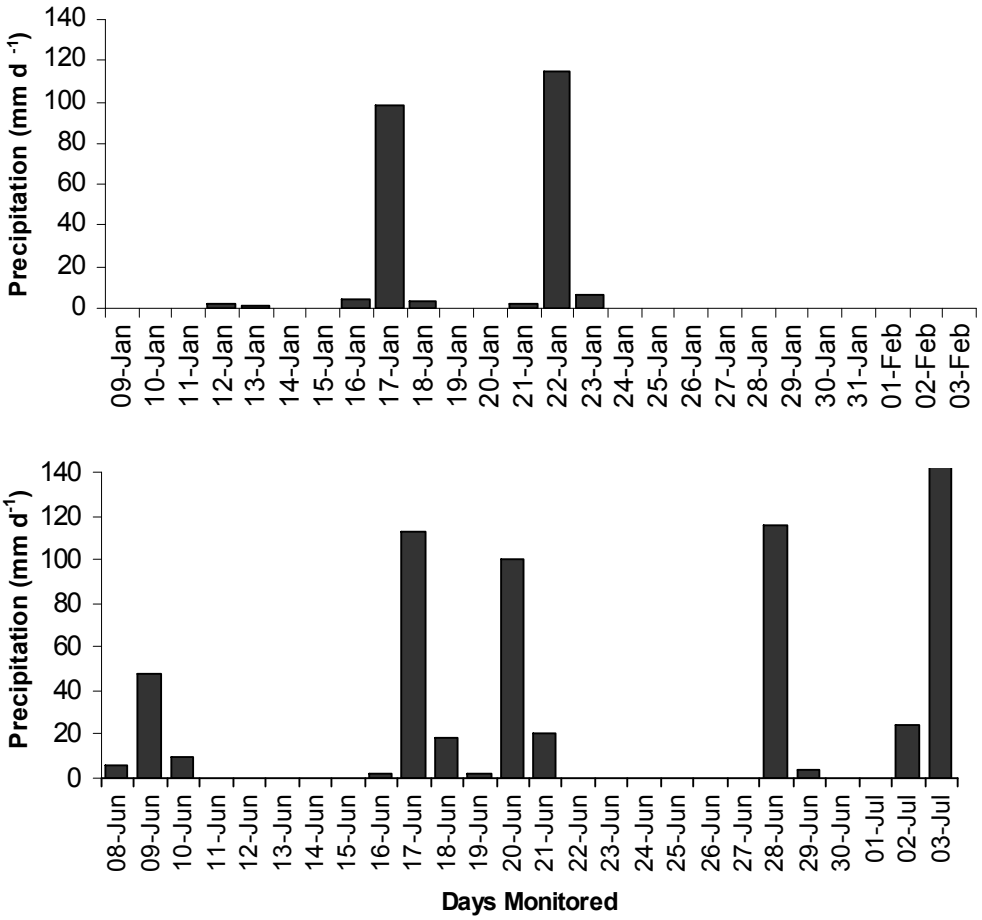

Figure 4.22 Comparison of total daily precipitation received on the lower Fox Glacier during both the summer (top) and winter (bottom) field seasons.

4.5.3 Humidity

Average relative humidity figures were similar during both the summer (67%) and winter (69%) field seasons. In addition, the range in humidity recorded was large and maximum and minimum humidity figures during both field seasons were similar.

4.5.4 Wind Speed and Direction

Average daily wind speed appeared lower during the winter field season than during summer. But as mentioned earlier, problems with the anemometer on both occasions means that this data cannot be deemed to be that reliable. During both field seasons it was found that the local katabatic wind was the dominant wind, blowing down glacier from the northeast regardless of what the regional synoptic situation appeared to be. Only on a small number of occasions did a non-katabatic wind direction dominate, with the occasions on which this occurred generally coinciding with the passage of frontal systems from the north-west or south-west.

4.5.5 Incoming Short-wave Solar Radiation

Despite problems with the solar radiation sensor during the summer field season that resulted in large gaps in the data, there was still a clear difference in the amount of incoming short-wave radiation being received on the lower glacier surface between summer and winter (Figure 4.23). This is likely to be due to the lower sun angle during the winter months that not only results in topographic shading of the lower glacier surface but also means that radiation received is of lower intensity.

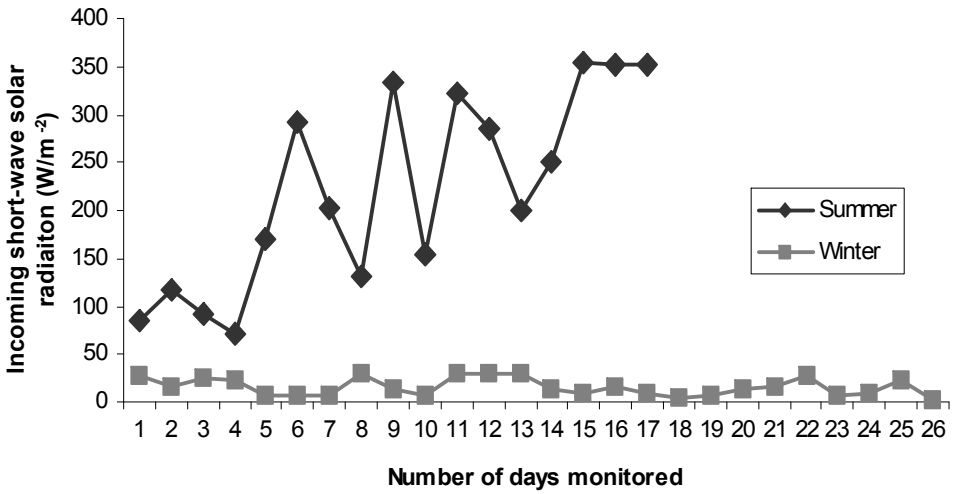

Figure 4.23 Comparison of daily average incoming short-wave radiation received on the lower Fox Glacier during both the summer and winter field seasons.

4.5.6 Synoptic Situations

During the winter field season there was a higher occurrence of passing fronts/troughs (V) than occurred during summer (Figure 4.24), and a much lower occurrence of anticyclones being positions over the south island (IV). South to south-westerly flows (I) were more common during the winter field season, and the frequency of north to north-easterly flows (II) and north-westerly flows (III) during both field seasons was similar. The heat-low experienced during the summer field season (VI) did not occur during the winter field season.

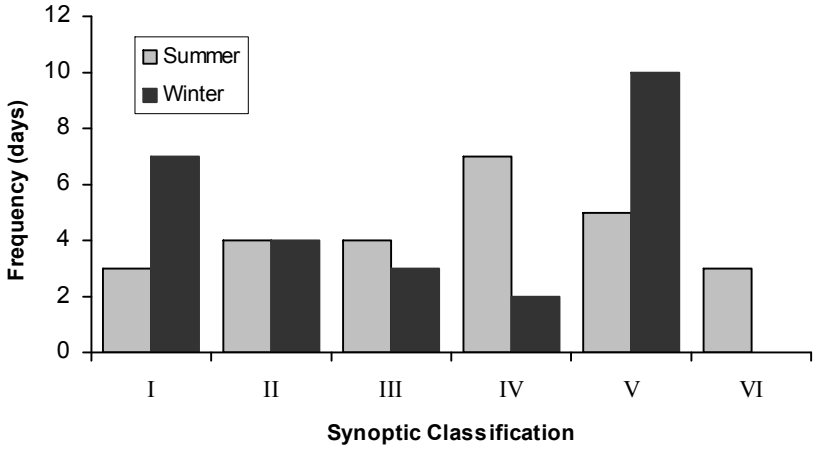

Figure 4.24 Comparison of the frequency of the different synoptic classifications between the summer and winter field seasons.

Chapter 5 Results - Ablation

5.1 Ablation Summer 2005

5.1.1 Clean Ice Measurements

5.1.1.1 General Trends

The average daily ablation recorded across all the clean ice stakes on the lower Fox Glacier during the summer field season is shown in Figure 5.1. Over the first sixteen days of field measurements the average daily ablation was around 100 mm d^{-1}, but in the last ten days of monitoring this value increased to around 150 mm d^{-1}, and on two occasions was over 200 mm d^{-1}. During the study period the overall average daily ablation recorded at the clean ice stakes was 129 mm d^{-1}. Appendix 1 contains full details of ablation data for the summer field season.

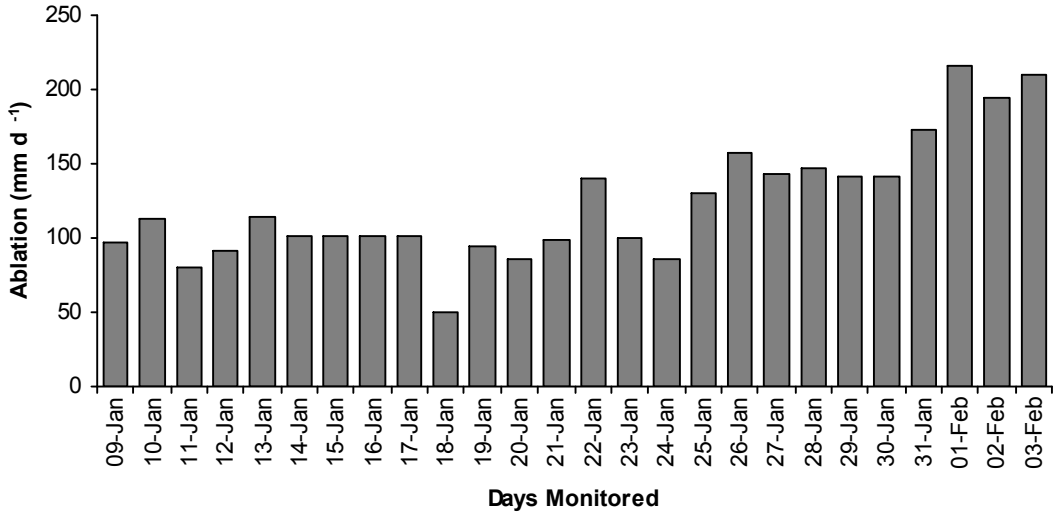

Figure 5.1 The average daily ablation recorded at the clean ice stakes on the lower Fox Glacier during the summer field season.

Average daily ablation between individual clean ice stakes ranged from 102 mm at stake a8 (a8b) up to 176 mm at a17 (Figure 5.2). The higher average melt-rates for a16 and a17 are not surprising, as these stakes were only put in place on the 26th January. They comprise a smaller data set, which only covered a period of warmer weather with an average temperature of 13.9°C compared to a prior average of 9.7°C.

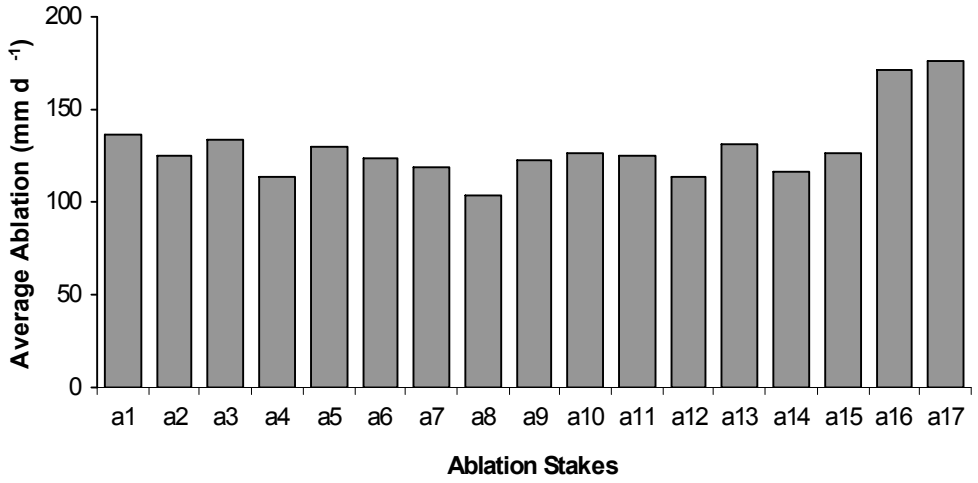

Figure 5.2 The average daily ablation recorded at individual clean ice stakes on the lower Fox Glacier during the summer field season.

Variability in ablation rates across the clean ice stakes on different days was less than that at individual stakes over the entire study period. Standard deviations of the means of daily ablation across all stakes ranged from 9-32% of the mean, with the majority of days falling below 20%. In comparison, data at individual stakes had standard deviations ranging from 13-42% of the mean, with the majority in excess of 20%. Figure 5.3 shows the 95% confidence interval (two standard errors) of the mean ablation at the clean ice stakes on a daily basis, and Figure 5.4 shows the 95% confidence interval of the mean ablation at individual stakes during the entire summer study period. There was less variability in the total amount of ablation per stake (a1-a15), with only 7% variability around the mean total melt of 2.9 m.w.e (Figure 5.5).

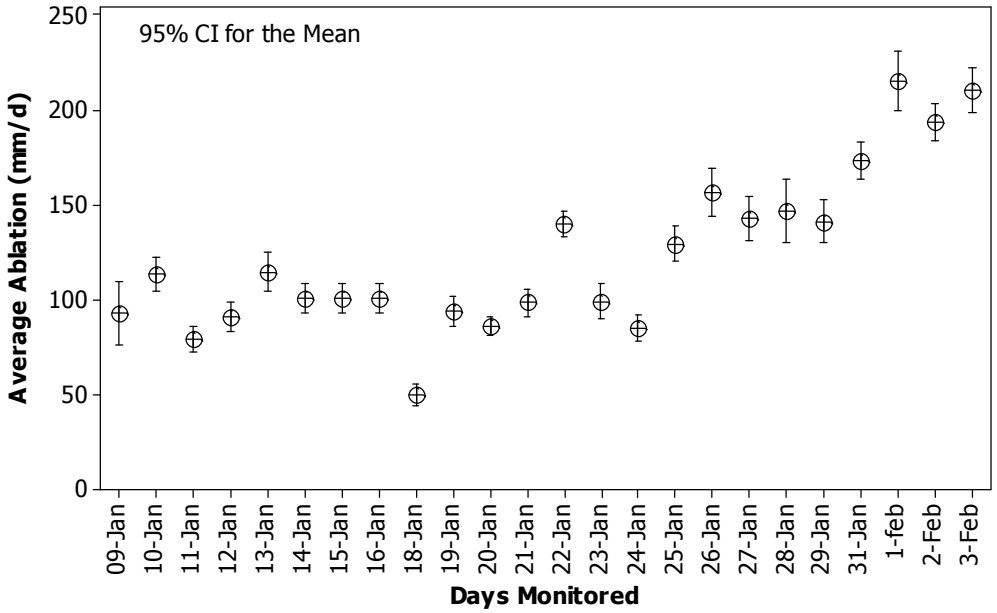

Figure 5.3 The 95% confidence intervals for the mean daily ablation across all clean ice stakes during the summer field season.

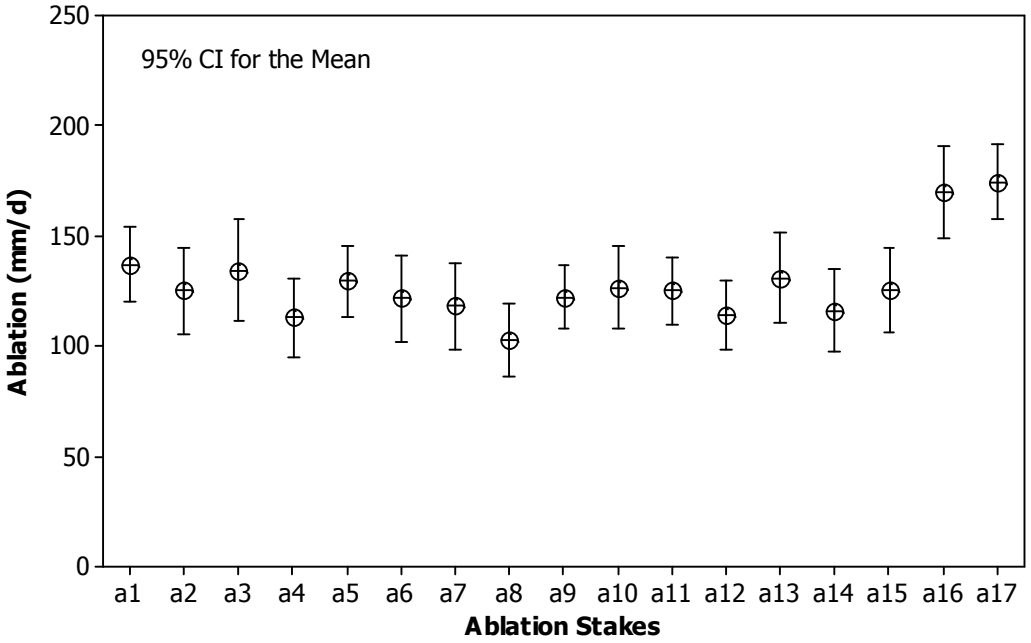

Figure 5.4 The 95% confidence intervals of daily ablation at individual clean ice stakes during the summer field season.

The large variability between the individual stakes could be due to fluctuations in micro-topography (section 3.2.1), whereas the variability between different days could be, as Evans (2003) concluded, be related to synoptic variability. Synoptic variability may also explain why there is less spread in the data on a daily basis compared to at individual stakes over the entire study period.

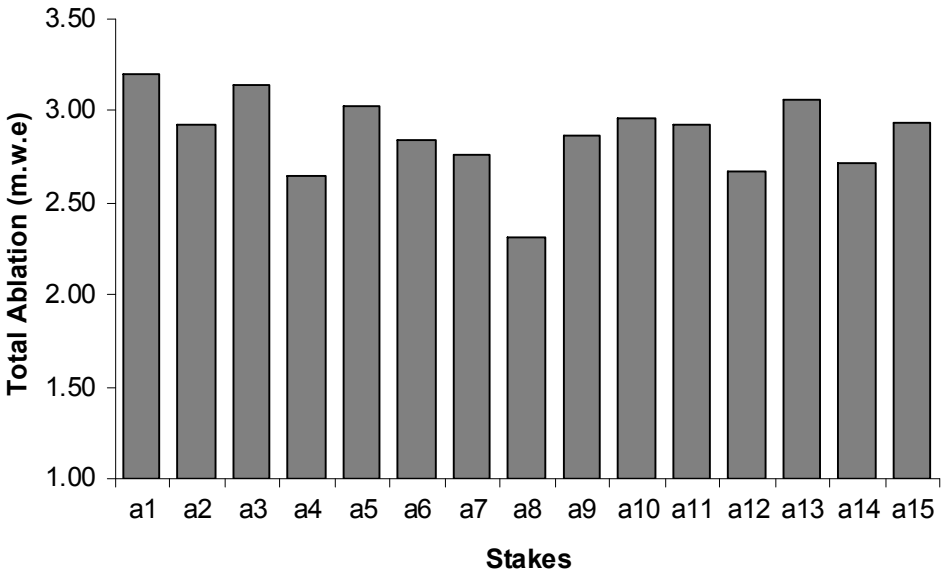

Figure 5.5 Total ablation in metres water equivalent (m w.e) recorded at the clean ice stakes (a1-a15) during the summer field season on the lower Fox Glacier.

5.1.1.2 Spatial Variability

Spatial variability in ablation at the clean ice stakes was detected, in particular at stake a8 (a8b), which had the lowest average melt (Figure 5.2) and the lowest overall melt (Figure 5.5). This stake had a south-easterly aspect (as opposed to westerly) (see Table 3.1) and was situated in a surface depression. These site factors may have resulted in this area of the glacier surface not been subjected to the same amount of direct sunlight or wind velocities as the stakes on more exposed surfaces.

5.1.1.3 Temporal Variability

During the summer study period the ablation rate of the clean ice stakes varied over time (Figure 5.1). Of note is the low rate on the 18th January, and another low recording on the 24th January. On both these occasions a front had just passed over, and field notes recorded a cool clear night after the passing front. Later in the study period there is a gradual increase in the average daily ablation, this coincides with an increase in average daily temperature (from around 13°C up to 16°C) and the occurrence of a heat low over the central South Island. For example, from the 29th to 31st of January and then from the 1st to 3rd February there is a 3°C increase in average temperature and a 27% increase in average daily ablation.

On two separate occasions (24th January and 3rd February), the ablation at the clean ice stakes (a1-a15) was measured twice daily to see if there was any indication of diurnal variability. The first measurement was taken at the usual time (10:00-11:00 am) and the second at around 5pm. On both occasions the melt rate during the first six hours was more than double the rate that occurred over the following eighteen hours (Figure 5.6). This resulted in 36-44% of the total daily melt occurring within the first six hours.

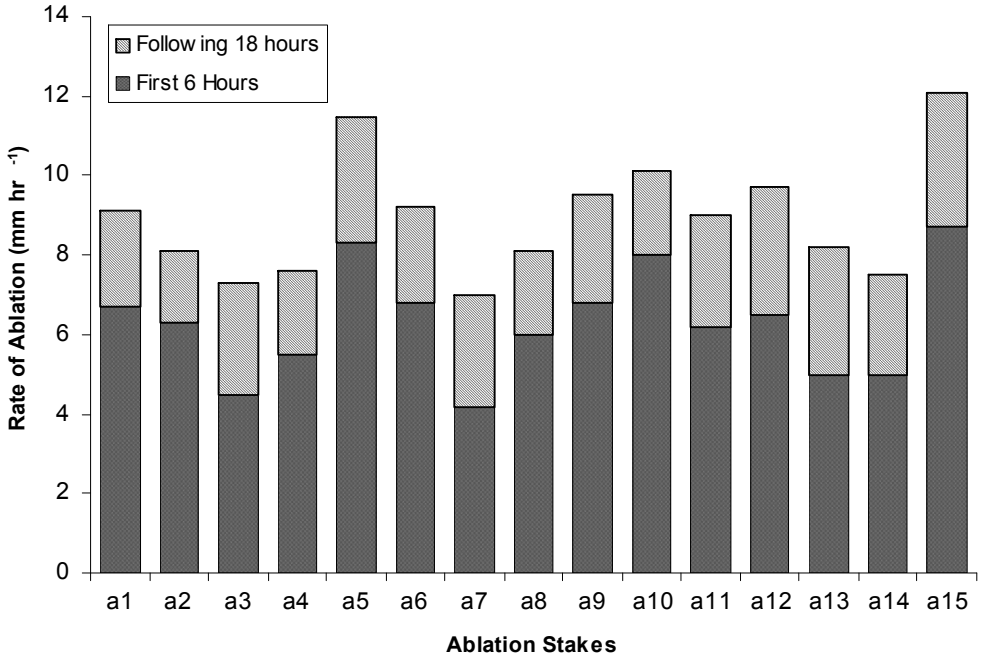

Figure 5.6 Diurnal variability in ablation rates recorded on the lower Fox Glacier on the clean ice on 24th January 2005.

5.1.2 Debris-Covered Ice Measurements

5.1.2.1 General Trends

Six stakes were placed in moraine on the true left side of the glacier (Figure 3.3 and 3.4). Table 5.1 shows details of the debris thickness and clast size around each stake. Stakes d1, d2, d3 and d5 were targeting the insulation effect, while d4 and a18 were placed in an attempt to detect any albedo effect. The ice at d1 had a moraine cover of 20 mm, and although over the study period did record ablation values less than the clean ice average, its melt rate was often as high as that recorded at some of the clean ice stakes. This stake was positioned on a very flat area, which turned out to be regularly inundated with surface melt water later in the afternoon, a factor that may have lead to an increased ablation rate.

Stake d4 was set in an area of thinner debris cover in order to try and detect the albedo effect. The positioning of this stake however turned out to be problematic. Although on placement, there was a very thin layer of debris (c.2 mm), this surface was prone to inundation of melt-water during the late afternoon, resulting in the debris cover being continually reworked, and on some occasions a thicker coverage (c.5 mm) resulted. Eventually all the debris around this stake was washed away after a period of heavy

rain. Ablation values for d4 tended to fall below the clean ice average, but it is impossible to determine the effect the additional melt-water and reworking of the debris had on this rate. Therefore the results of this stake are unreliable and are not included in any of the calculations used for comparison to the ablation rates on the clean-ice.

Stake a18 was put in place on 25th January in a very fine debris band (see Figure 5.7). On four out of the nine days its was monitored, it tended to have one of the highest melt rates, and recorded the highest overall average melt rate of 205 mm d^{-1}. However on some days, a number of the other clean-ice stakes recorded ablation rates as high or higher than a18. The installation of this stake coincided with a period when the overall ablation rate was increasing (Figure 5.1), so although it would appear that this very fine dirt band had some effect in increasing the ablation rate, results need to be treated with caution.

It is also important to note the overall spatial variability that existed between the debris-covered stakes and the clean ice stakes. As mentioned above, the debris covered stakes were placed in surface moraine on the true left side of the glacier (Figure 3.4) so may have been subject to different surface conditions (i.e. wind currents, duration of direct sunlight) than the more centrally located clean ice stakes. This factor needs to be kept in mind with the following comparisons made between the ablation rates of the debris-covered and clean ice stakes.

Table 5.1 Descriptions of stakes placed in varying degrees of debris cover

Stake	**Depth Debris**	**Clast Range** (a-axes measured)
d1	20 mm	20-80 mm
d2	80-100 mm	70-900 mm. Smaller clasts (≤5 mm) forming a matrix on ice surface with larger sized clasts on top
d3	50 mm	Small gravel matrix (clasts ≤5 mm) on ice surface with overlying clasts ranging from 70-200 mm
d4	2-5 mm	Fine debris, near surface melt water
d5	100 mm	Large clasts with air spaces in between 250-500 mm
a18	<1mm	Very fine dirt band in ice

Figure 5.7 Stake a18 in a very thin (< 1 mm) debris band on the lower Fox Glacier.

Overall the average ablation rate for stakes d1, d2, d3 and d5 was 64 mm d^{-1}, with daily averages ranging from as little as 3 mm d^{-1} on the 18th January up to 143 mm d^{-1} on the 1st February. The data for debris-covered ablation is more highly variable than the clean-ice data, a likely consequence of both the smaller data set, and the changing debris conditions mentioned above. There is large spread in the data with standard deviations per stake being at least 31% of the mean, and on a per day basis, ranging from 19 to 87% of the mean. Figure 5.8 shows the 95% confidence interval of the mean for all the debris-covered stakes.

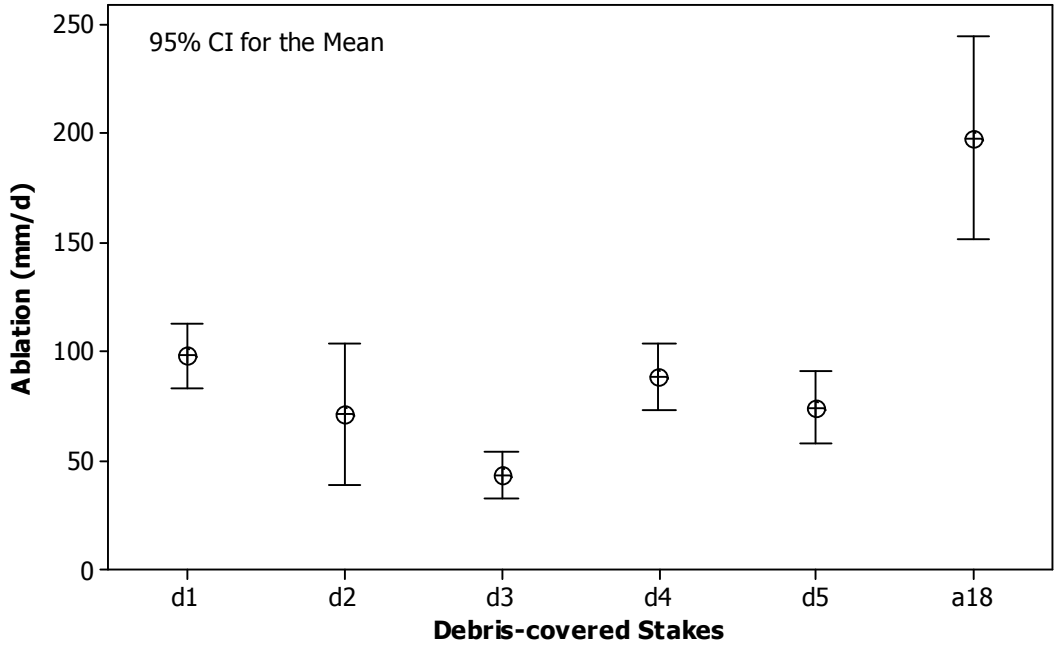

Figure 5.8 The 95% confidence interval for the mean of the debris-covered stakes recorded during the summer field season on the lower Fox Glacier.

5.1.2.2 Spatial Variability

As mentioned in section 2.5.2, previous research has found that ablation is at a maximum when debris is around 5-10 mm thick, and above this thickness, the debris starts to have an insulating effect (also refer back to Figure 2.11). The amount of ablation occurring under stakes d1, d2, d3 and d5 was greatly reduced compared to that on the clean ice (Figure 5.9). The thickness of the moraine around these stakes was 20 mm or above, and at this thickness the debris clearly has an insulating effect. The average surface melt at these stakes in comparison to the clean-ice melt was suppressed by 50%. This suppression figure is larger than those reported by Pelto (2000) and Takeuchi *et al.* (2000) of 30 and 40 % respectively, but lower than Purdie (1996) on the heavily debris-covered Tasman Glacier (1.1 metre debris thickness) where suppression rates of 93% were recorded.

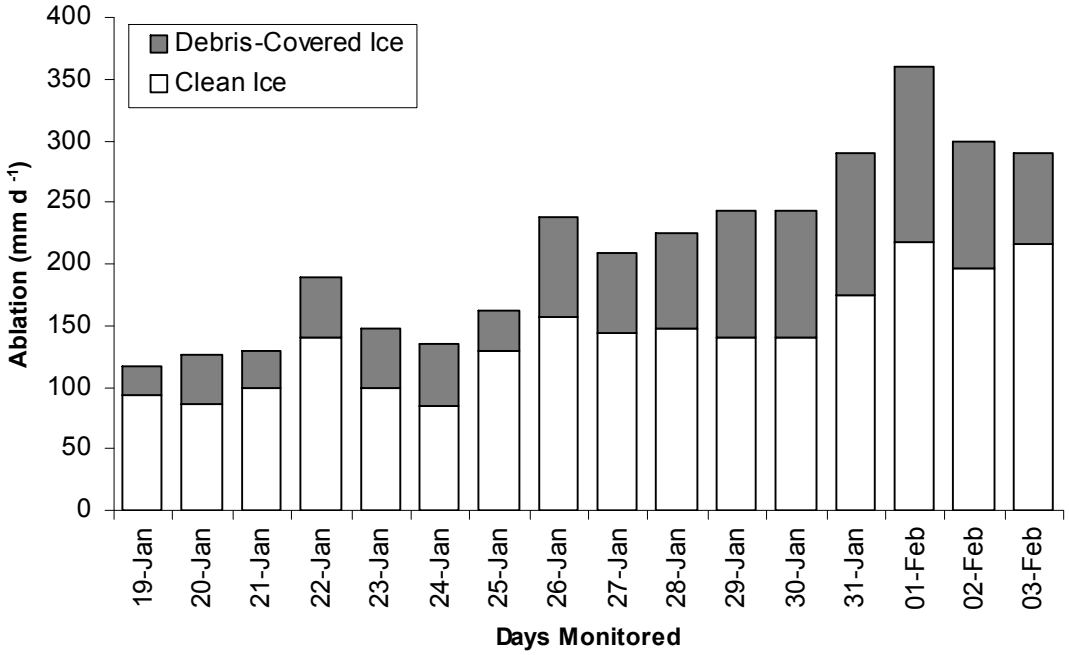

Figure 5.9 Comparison of the average daily ablation at the debris-covered stakes (d1, d2, d3, d5) and the clean ice stakes recorded on the lower Fox Glacier during the summer field season.

Figure 5.10 shows the daily average ablation data for all stakes plotted against debris thickness. A general trend of decreasing ablation with increasing debris thickness (c.>10 mm) can be seen, along with the ablation peak at a18 that was in very fine (c.1 mm) debris-cover. However, what Figures 5.10 and 5.11 also show, is that the relationship between ablation and debris thickness does not appear to be as straight forward as theory suggests (Figure 2.11), as stake d3 reported a much lower average

ablation than either d2 or d5, and the adjusted r^2 of the data is only 38%. Referral back to Table 5.1 shows that both d2 and d3 were reported as having a layer of smaller clasts lying against the ice surface with larger clasts overtop. As mentioned in section 2.5.2, Pelto (2000) found that the finer grained debris cover provided better insulation, and this appears to be the case in this instance, although the grain size of this finer debris cover was not quantified in this study.

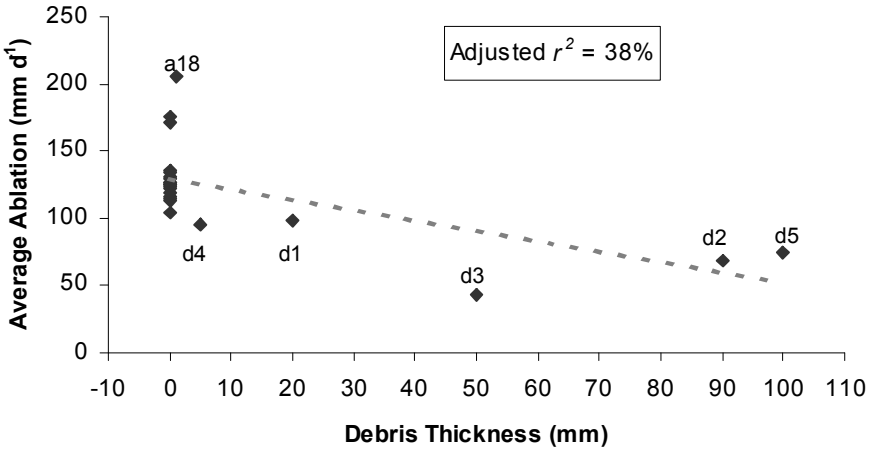

Figure 5.10 Average daily ablation and increasing debris thickness measured on the lower Fox Glacier during the summer field season.

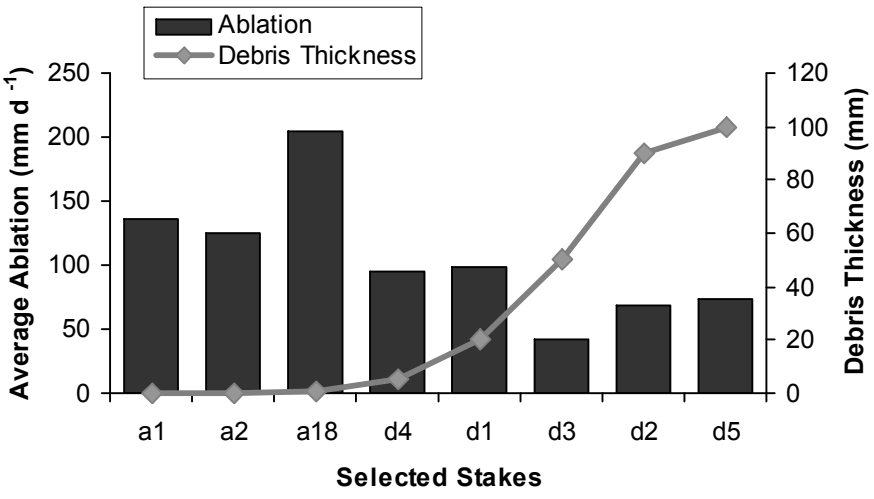

Figure 5.11 Average daily ablation and debris thickness at two clean ice stakes (a1 and a2) and all the debris-covered stakes (a18 and d1 to d5) monitored on the lower Fox Glacier during the summer field season.

General observation of the glacier surface reveals that the debris-covered surfaces do have higher vertical relief than the surrounding clean ice (Figure 5.12), an indication of its insulating properties. In addition, fine dirt bands left by the closing of old crevasses tend to be more depressed than the surrounding clean ice surface (Figure 5.13), a likely indication of the albedo effect. Therefore, these differential ablation rates appear responsible at least in part, for some of the subtle variations in surface topography seen on the lower glacier.

Figure 5.12 Variation in surface relief between clean ice and debris-covered ice on the lower Fox Glacier. Source: H. Purdie.

Figure 5.13 Debris bands showing reduced relief on the lower Fox Glacier. Source: H. Purdie.

A t-test was conducted to test the null hypothesis (H_0) that there is no difference between the ablation rates of the clean ice and debris-covered ice, versus the alternative hypothesis (H_1) that there is a significant difference between the rates. Results of the test gave a t-value of 10.09 and *p*-value of <0.001, with the difference between the two means being 46.79. The 95% confidence interval was 37.49 and 56.09. Therefore, the null hypothesis can be rejected indicating that there was in fact a significant difference between the ablation rates of the clean-ice and debris-covered ice during the summer field season. Figure 5.14 is the plot of the 95% confidence interval for the two data sets that clearly shows this difference in the mean ablation rates.

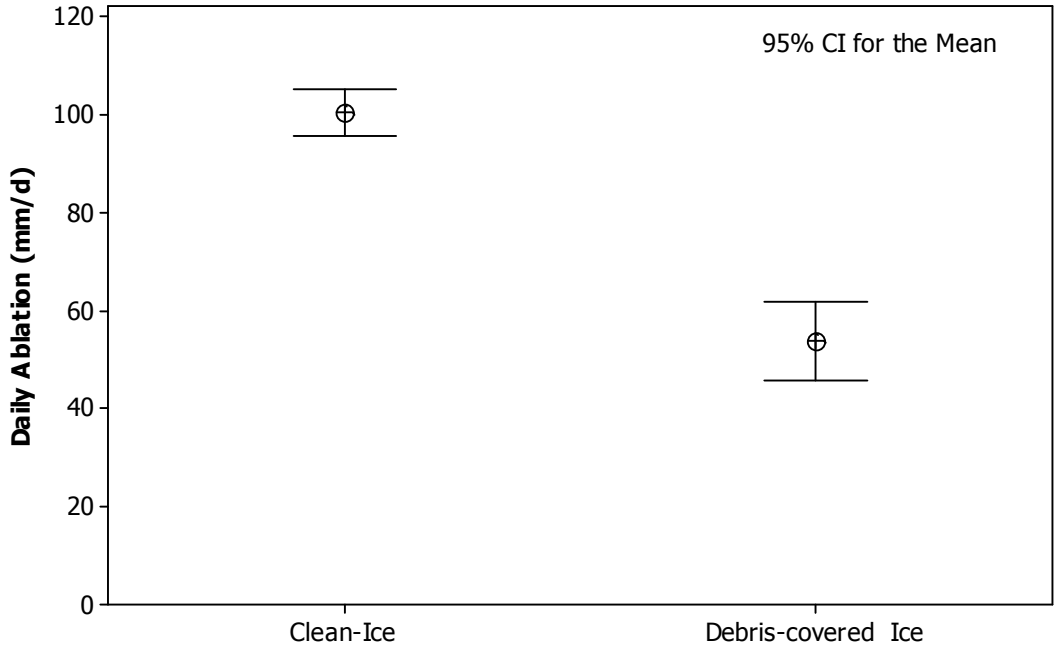

Figure 5.14 The 95% confidence interval of the mean for ablation on the clean ice and that under debris-cover.

5.1.2.3 Temporal Variability

Like the average daily ablation recorded at the clean-ice stakes, there was clear variability over time at the debris-covered stakes during the summer field season (Figure 5.15). The very low rate that occurred on the 18th January on the clean ice was also recorded at the debris-covered stakes. Also the general increase in ablation at the end of January is mirrored. The decrease in ablation seen in the debris-cover on the 2nd and 3rd February when the clean-ice value is still high, is likely to be influenced by those days only consisting of data from stakes d3 and d5 due to the removal of d1 and d2.

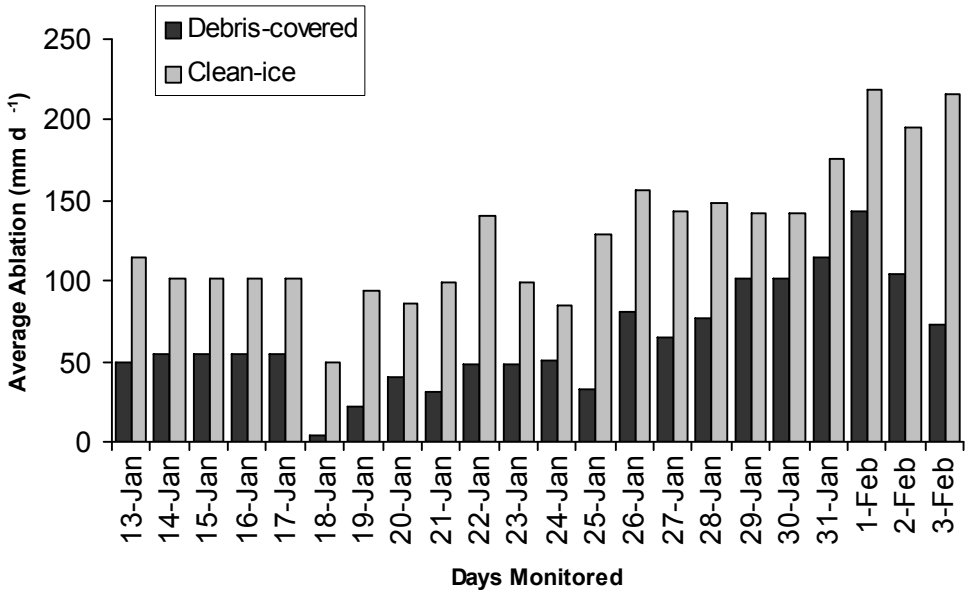

Figure 5.15 Comparison of the average daily ablation over time at the debris-covered stakes (d1-d5) and the clean ice stakes recorded on the lower Fox Glacier during the summer field season.

5.1.3 Ablation and Climate Variables

5.1.3.1 Introduction

To see which, if any, of the climate variables measured had the most influence on daily ablation a Pearson's correlation was conducted to look for any general relationships (Table 5.2), followed by multi-variant regression analysis of ablation and all the measured climate parameters using a general linear model.

Table 5.2 Results from Pearson's correlation analysis between ablation and climate data. The top numbers are the co-efficient, and the bottom numbers the *p*-values.

	Temperature	Precipitation	Humidity	Wind Speed	Wind Direction	Solar Radiation
Ablation	0.849	-0.037	-0.810	0.121	-0.405	0.739
	0.000	0.860	0.000	0.592	0.085	0.001

The multi-variant analysis produced the following equation:

$$\text{Ablation} = 6 + 9.19\,T + 0.451\,P - 0.383\,H + 2.28\,WS - 21.3\,WD + 0.150\,SR \quad (10)$$

(adjusted r^2 90.3%)

where T = temperature; P = precipitation; H = humidity; WS = wind speed; WD = wind direction; and SR = solar radiation.

Correlation identified temperature, humidity and incoming solar radiation as having significant relationships with ablation. Likewise, best subset regression analysis identified temperature as the single most important climate variable, with temperature and solar radiation combining to be the two most influential climate variables. An adjusted r^2 of 90% indicates that climate variable can account for the majority of the variation in daily ablation. The relationships identified above will be looked at more closely in the following sections.

5.1.3.2 Ablation and Temperature

Comparison of average daily temperature with average daily ablation indicates a positive linear relationship (Pearsons r = 0.849, p-value = <0.001), with the temperature trend often being closely mirrored by ablation (Figure 5.16). Ablation increases of between 20-30% were found to coincide with temperature increases of around 2 to 3 ^{O}C. The lack of ablative response shown between the 15th and 18th Jan relates to ablation data for those days being averaged, due to attendance at a conference. Regression analysis of the ablation and temperature data confirms this relationship, with an adjusted r^2 value of 70.9% (Figure 5.17).

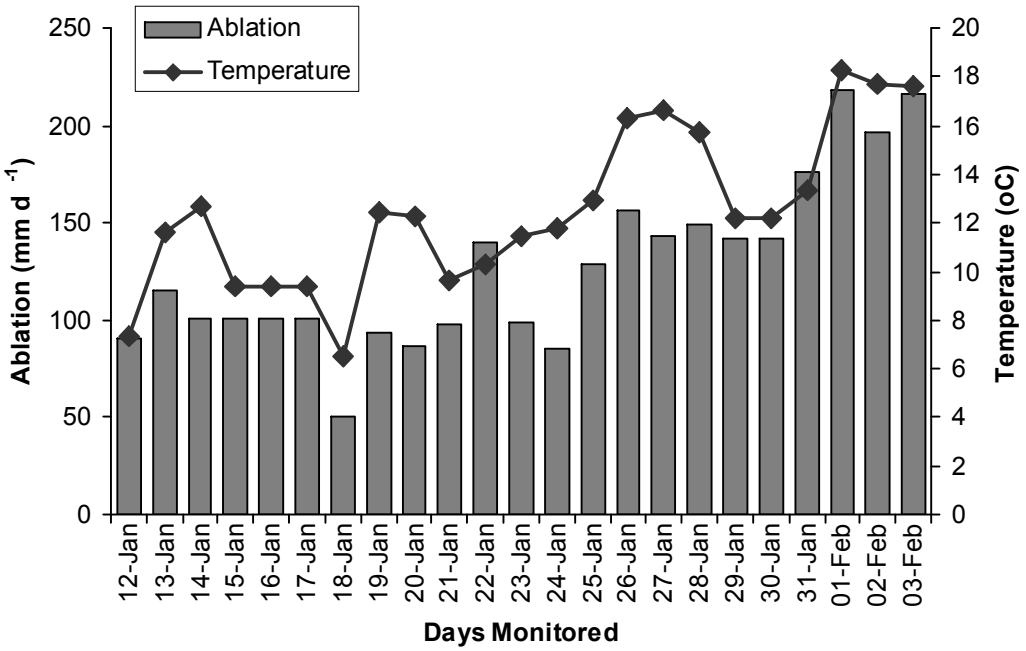

Figure 5.16 Daily average temperature and ablation on the lower Fox Glacier during the summer field season.

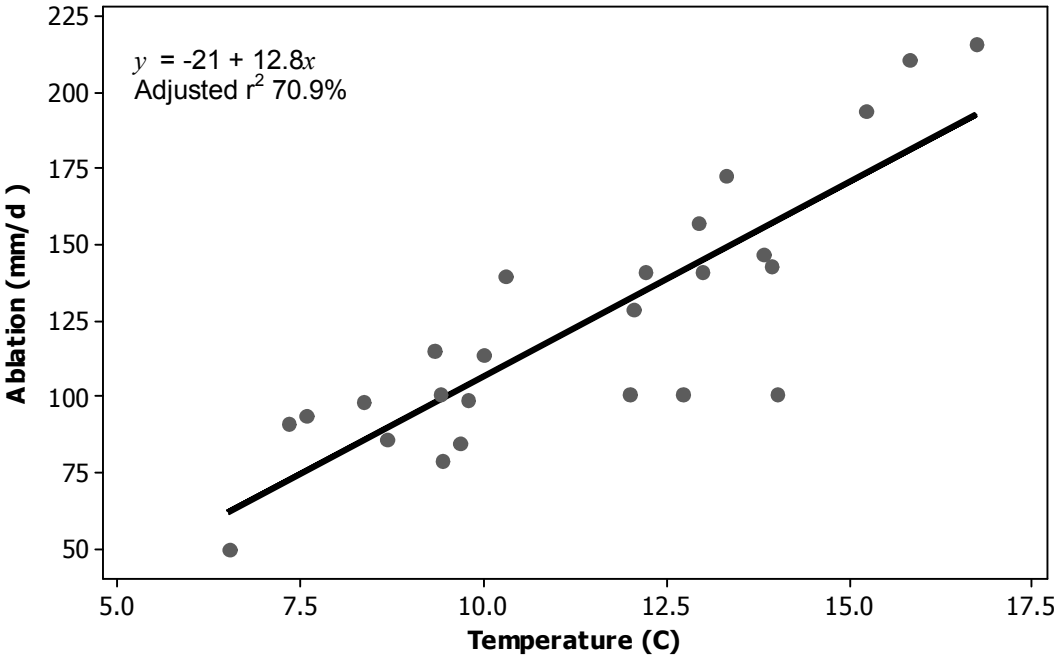

Figure 5.17 Scatter plot with regression of the relationship between daily average temperature and ablation on the lower Fox Glacier recorded during the summer field season 2005.

5.1.3.3 Ablation and Precipitation

A relationship between ablation and precipitation was not very clear, with a *p*-value of only 0.860 (Table 5.2). However, during a heavy rainfall event on the 22nd January a 30% increase in daily average ablation was recorded, increasing from 98 mm d^{-1} on the 21st January up to 140 mm d^{-1} on the 22nd January (Figure 5.18). This was also the highest ablation rate recorded over an eighteen-day period.

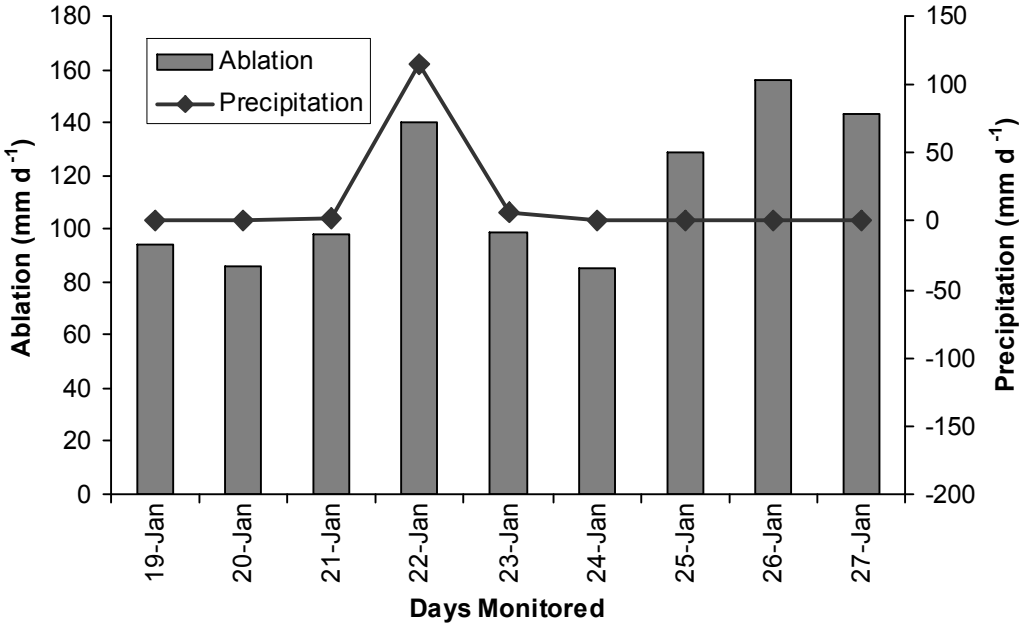

Figure 5.18 Relationship between ablation and precipitation data recorded on the lower Fox Glacier during the summer field season.

Both regression and correlation analysis assume a linear relationship between the data, however as noted in section 4.1.2 the precipitation is non-uniform with a large proportion of zeros values along with a few extreme values. Therefore, this type of statistical analysis is not necessarily very helpful in identifying any possible relationship between ablation and precipitation. In addition, during summer there is a large degree of melt-water in the supra-glacial drainage system so separating the effects of water from precipitation versus water from surface-melt is problematic. As noted in section 2.5.3 previous research on other glaciers indicate that a relationship between the rate of ablation and precipitation does exist. Ideally more precipitation events need to be monitored in order to confirm this relationship on the lower Fox Glacier.

5.1.3.4 Ablation and Humidity

During the summer field season it was found that humidity exhibited a strong negative linear relationship with ablation, with a Pearsons *r* of –0.810 and *p*-value of <0.001 (Table 5.2). This tends to indicate that the processes of evaporation and/or sublimation (in addition to surface melt followed by run off) are important components to the total daily ablation figure. However, during this study, only surface melt followed by run off was being used as a measure of daily ablation.

5.1.3.5 Ablation and Wind Speed and Wind Direction

Neither wind speed or wind direction seemed to have an important effect on the rate of ablation of the lower Fox Glacier during the summer field season, with insignificant correlations (Table 5.2). Like the precipitation data, data for wind direction is clearly non-linear with the two extreme values of 0^{o} and 359^{o} representing the same northerly wind direction. Therefore, for the purposes of correlation analysis, wind direction was group into one of two categories, either katabatic ($30\text{-}60^{o}$) or non-katabatic. Due to the dominant nature of the local winds on the lower glacier, wind speed is therefore also likely to be being influenced by the katabatic wind as opposed to larger scale synoptic winds.

The lack of correlation between ablation and wind speed is surprising, as turbulence from valley winds is a component of the energy required for melt (Q_H), and this climate parameter is used for modelling ablation (Brock and Arnold, 2000; Marcus*, et al.*, 1985). Problems with the anemometer and/or spatial variability of wind turbulence may have resulted in the speeds recorded at the climate station not being a true reflection of wind speed across the entire stake network.

5.1.3.6 Ablation and Solar Radiation

Correlation between ablation and incoming short-wave solar radiation gives a Pearsons *r* of 0.739 with a *p*-value of 0.001 (Table 5.2). As outlined in section 3.1.2 the solar radiation data has a number of gaps due to equipment problems. Therefore this correlation is based on a smaller data set in comparison to other climate parameters. However, it does tend to indicate that there is a relationship between increasing incoming short-wave radiation and increasing ablation. Figure 5.19 presents the most complete sections of solar radiation data plotted with average daily ablation, but despite the relationship indicated by correlation a clear pattern tends not to emerge. However when combined with temperature (section 5.1.3.1), 87% of the variation in ablation during the summer field season can be explained.

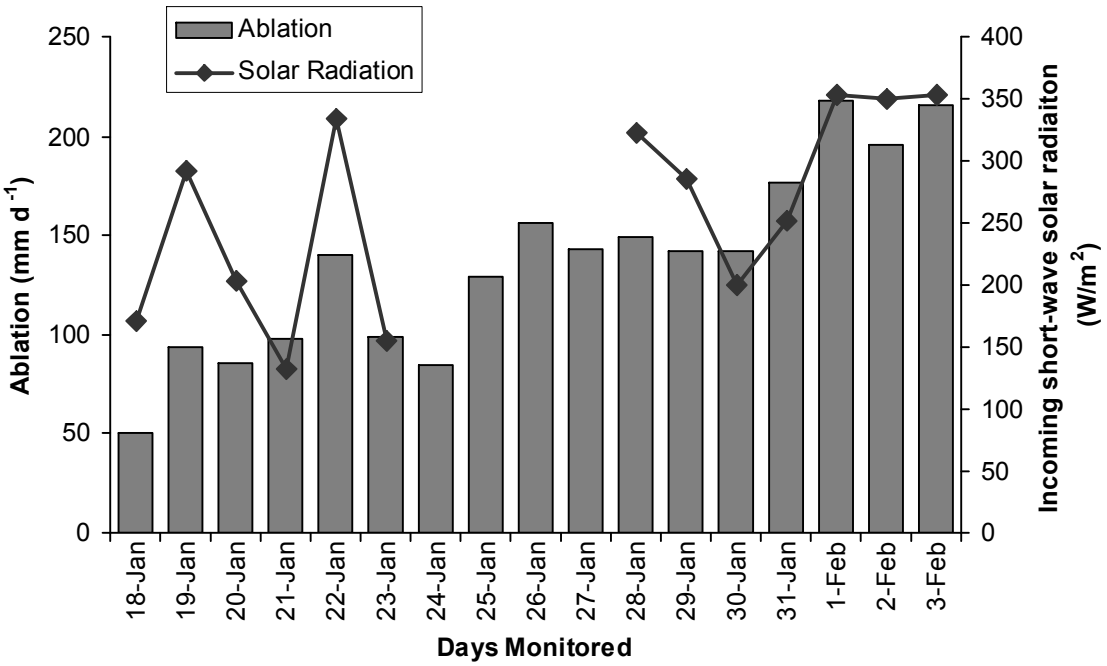

Figure 5.19 Relationship between average daily ablation and incoming short-wave radiation data recorded on the lower Fox Glacier during the summer field season.

5.1.4 Ablation and the Synoptic Situation

When considering the average daily ablation recorded under different synoptic situations (Figure 5.20) it can be seen that higher daily rates were recorded during the heat-low (VI) and when a north to north-easterly flow (II) was in place, with the lowest average ablation coinciding with south to south-westerly (I) conditions. During the heat low in the central South Island, average daily ablation was pushed up by 37%, and north to north-easterly flows resulted in a 27% increase. Conversely the south to south-westerly flows, north-westerly flows and the passage of fronts/troughs resulted in around a 20% reduction in average daily ablation rates.

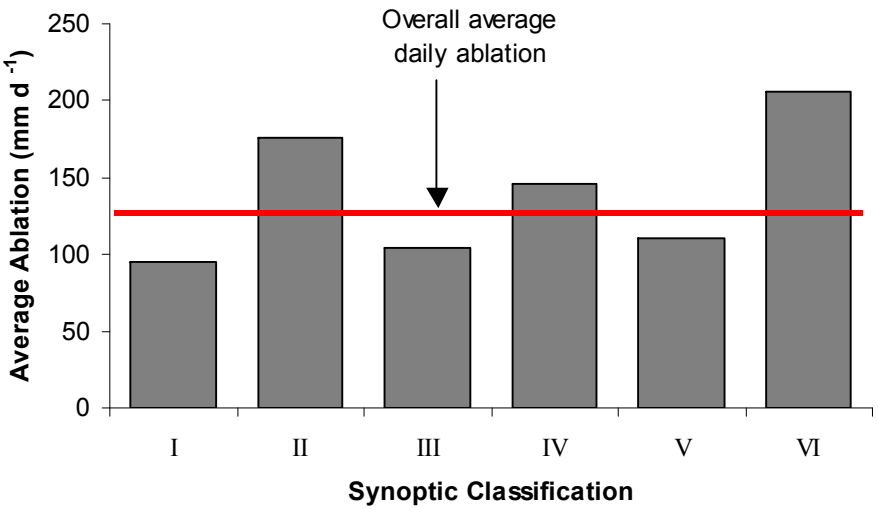

Figure 5.20 Average daily ablation recorded for the six different synoptic classifications experienced during the summer field season.

Figure 5.21 looks at the total amount of ablation recorded during the summer field season under the different synoptic classifications, and although obviously the frequency of the various situations is of importance to the total amount of ablation, it is interesting to note how a lesser occurring situation (VI) was still the third biggest contributor to the total ablation.

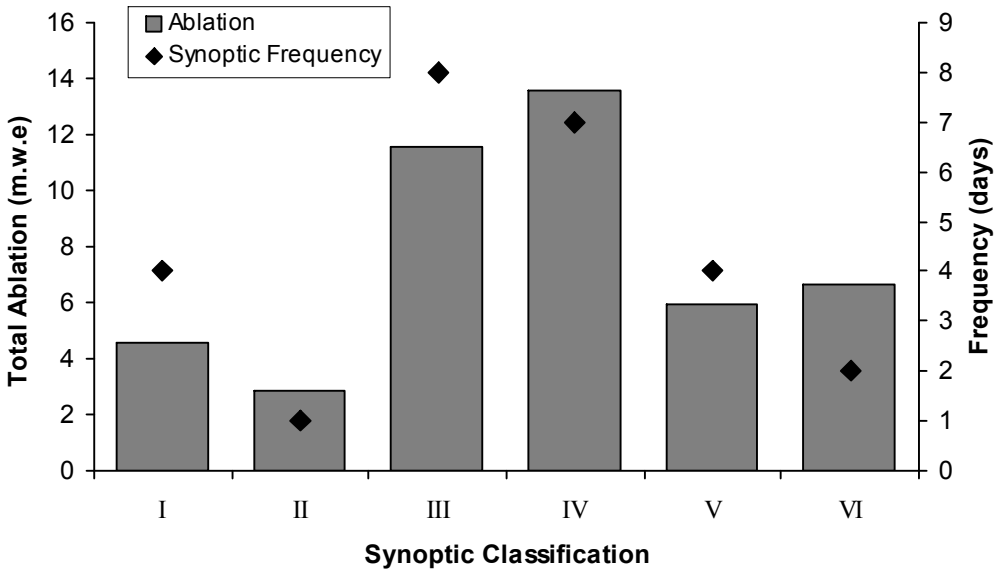

Figure 5.21 Total ablation recorded during the six different synoptic classifications including the frequency of each synoptic classification during the summer field season.

5.2 Ablation Winter 2005

5.2.1 Clean Ice Measurements

5.2.1.1 General Trends

Average daily ablation recorded on the lower Fox Glacier during the winter field season (8th June to 3rd July 2005) is depicted in Figure 5.22 (also see Appendix 3). It is highly variable ranging from as little as –2mm d^{-1} on the 23rd June up to 83 mm d^{-1} on the 3rd of July, and with an overall average of 22 mm d^{-1}. This high degree of variability is reflected in the standard deviations that are often in excess of the mean. Figure 5.23 is an interval plot of the 95% confidence interval (two standard errors of the mean) for the daily average ablation data, showing errors to be lower on days with low average ablation. The occurrence of the negative values may be a reflection of the inaccuracies of the straight-edge technique (as discussed in section 3.2.1), especially when dealing with such small quantities of ablation, and/or due to successive surface melting followed by refreezing resulting in the reorganisation of the ice around the stakes. It is important to note, that on many days, the total amount of ablation recorded is less than the acknowledged error of the straight edge technique (±5 mm).

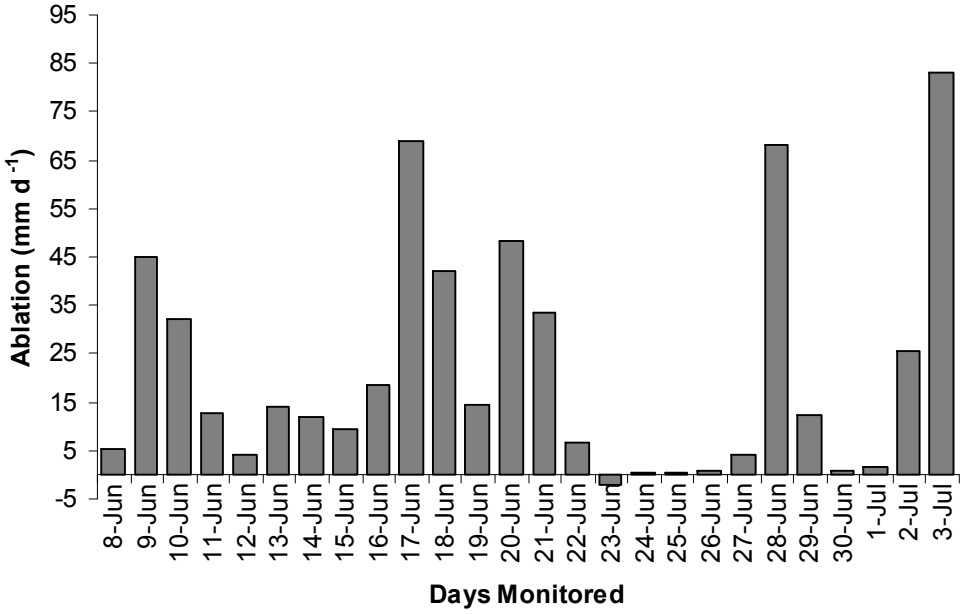

Figure 5.22 Average daily ablation recorded on the clean ice of the lower Fox Glacier during the winter field season.

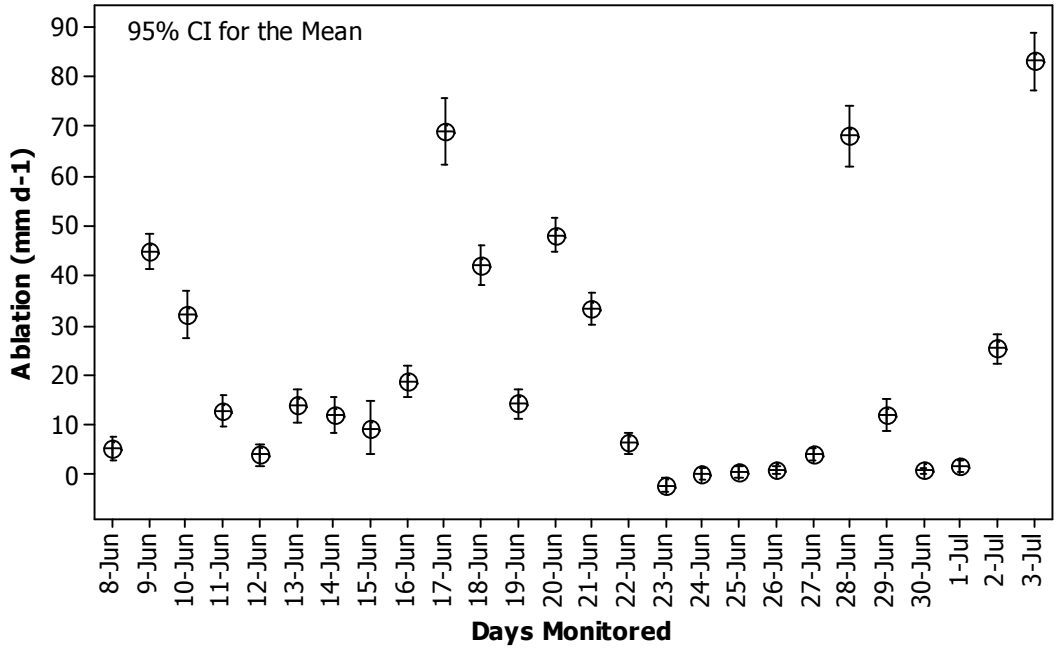

Figure 5.23 The 95% confidence interval of the mean of daily average ablation recorded on the lower Fox Glacier during the winter field season.

Average daily ablation between the individual clean ice stakes ranged from 16 mm d^{-1} at stakes l4 and c4, up to 27 mm d^{-1} at stake u3 (Figure 5.24), with the standard deviations being in the majority occasions, in excess of the mean. This spread in the data can also be seen by the 95% confidence interval of the mean (Figure 5.25) showing the average daily ablation at individual stakes to be even more variable than the daily average across all the clean ice stakes.

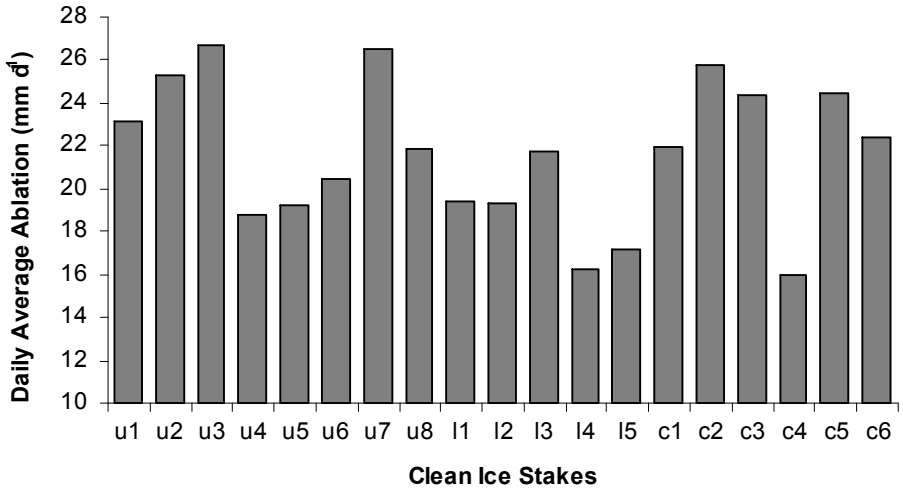

Figure 5.24 Average daily ablation at individual clean ice stakes recorded on the lower Fox Glacier during the winter field season.

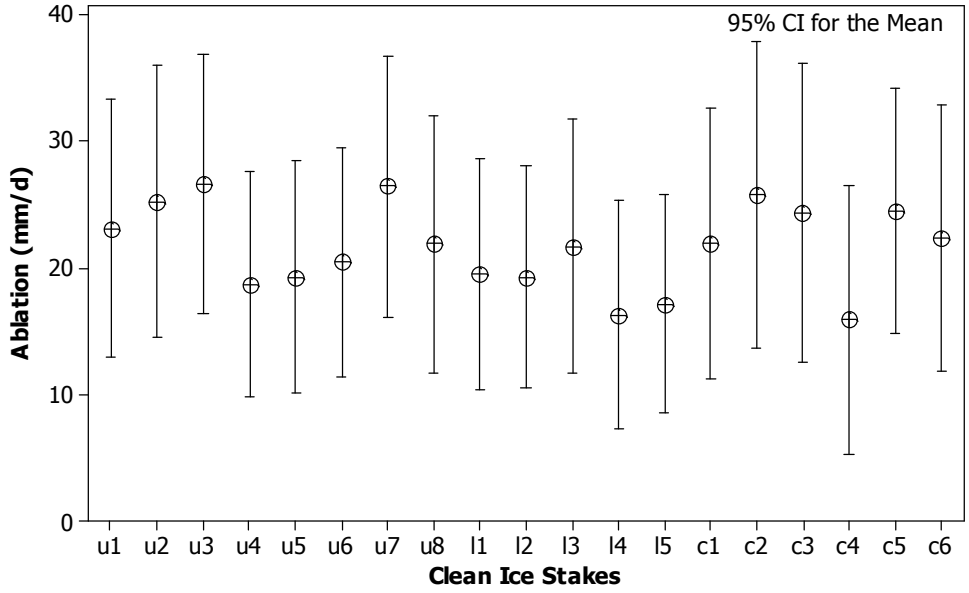

Figure 5.25 The 95% confidence interval of the mean for daily ablation recorded at individual clean ice stakes on the lower Fox Glacier during the winter field season.

5.2.1.2 Spatial Variability

Some spatial variability seems to exist between the individual clean ice stakes (Figure 5.26) with stakes l4 and c4 having the lowest average daily melt rates. The topography and aspects of l4 and c4 (Table 3.4) were not notably different when compared to the other clean ice stakes, with l4 forming part of the lower transect, and c4 mid-way up the central transect. The highest average daily rate was recorded at stake u3 of 27 mm d^{-1}, although a number of stakes recorded average ablation rates not far below this figure.

5.2.1.3 Temporal Variability

Figure 5.26 demonstrates clear temporal variability in ablation during the winter field season. In fact, it tends to portray two extremes, those days when there is little to no ablation (i.e. 22nd to 27th June), and days when ablation is significant like on the 17thand 28th June and the 3rd July. This variability will be discussed in detail in section 5.2.3.2.

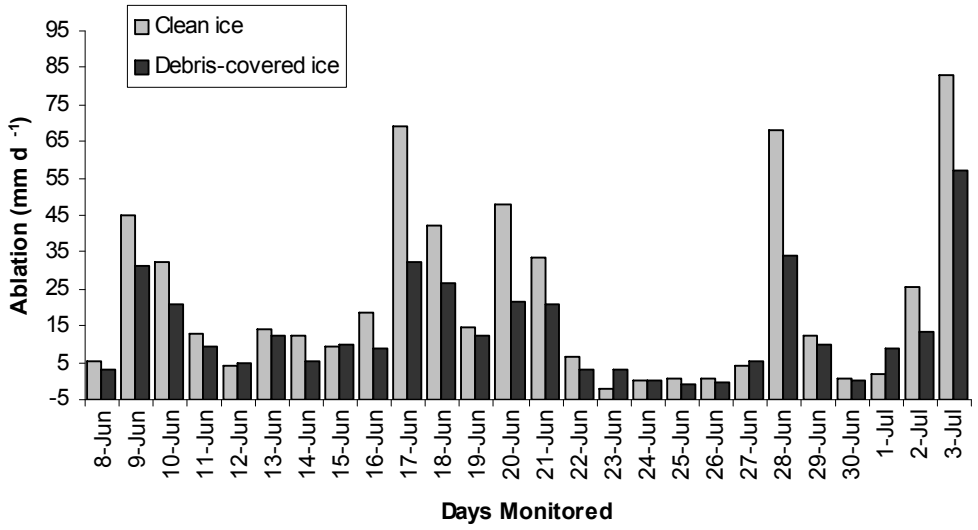

Figure 5.26 Variation in ablation over time recorded at both the clean ice stakes and the debris-covered stakes during the winter field season.

5.2.2 Debris-covered Ice

5.2.2.1 General Trends

Debris thickness ranged from a very thin debris band at stake l3, up to 300 mm thickness at stake m5 (Table 5.3). However, the very fine debris-cover at l3 was quickly washed away during the first substantial rain on the 17th June, so provided insufficient data for detecting an albedo effect. In addition, the lack of sun on the lower glacier during this winter field season, and the very low overall ablation rates resulted in no difference detected between l3 and the other clean ice stakes. Therefore no further consideration is given to any debris-induced albedo effects at l3.

Table 5.3 Descriptions of moraine thickness and clast size at individual debris-covered stakes.

Stake	**Debris Thickness**	**Clast Range** (Measured along the long (*a*) axis)
m1	20 mm	20-120mm long, nil matrix
m2	40 mm	1-40 mm long, matrix
m3	60 mm	1-120mm long, muddy matrix on ice surface
m4	150 mm	c.270mm long, large spaces between clasts, nil matrix
m5	300 mm	>300mm long, large spaces between clasts, nil matrix
l3	< 1 mm	Very thin debris band

Average ablation under debris-cover (m1-m5) ranged from –1 mm d^{-1} on the 25th June up to 57 mm d^{-1} on the 3rd July, with a daily average of 13 mm d^{-1}. Like the clean ice stakes, standard deviations were well in excess of the mean both for the daily average and for the overall stake average ablation. Figures 5.27 and 5.28 depict the 95% confidence of the mean for this data.

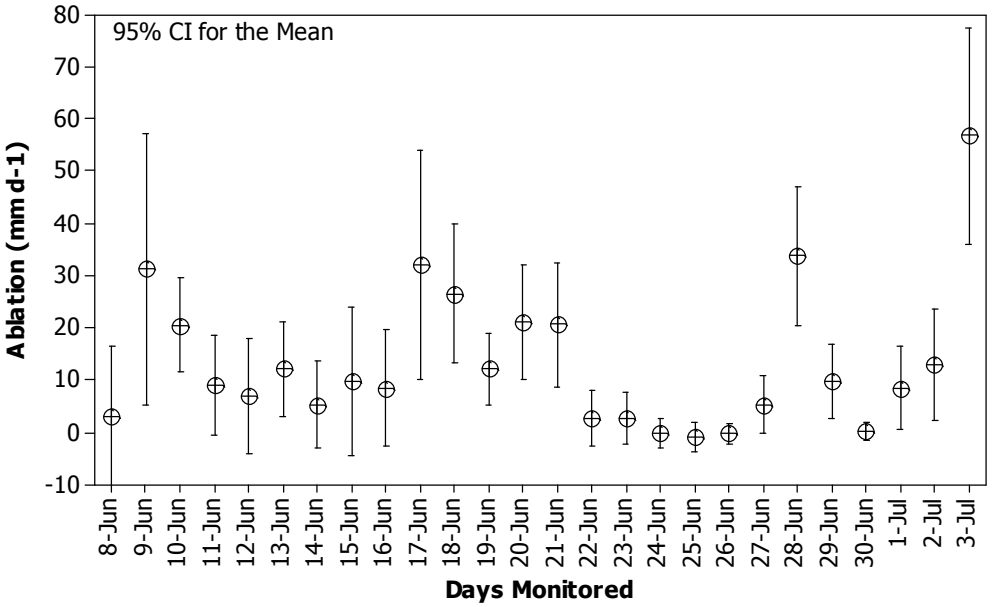

Figure 5.27 The 95% confidence interval of the mean for the average daily ablation recorded at the debris-covered stakes on the lower Fox Glacier during the winter field season.

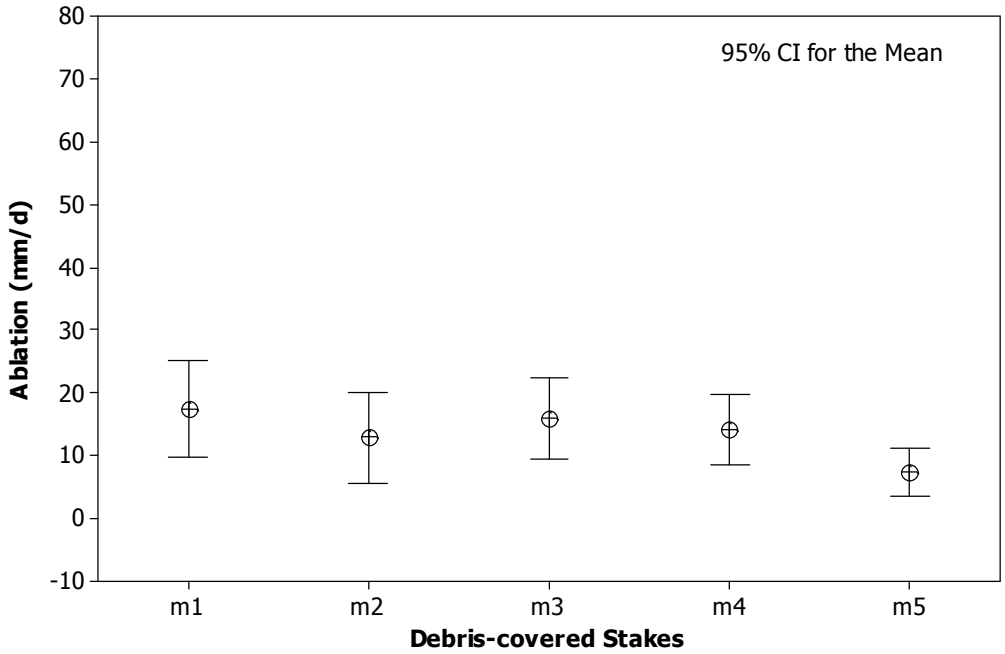

Figure 5.28 The 95% confidence interval of the mean for all ablation recorded at individual debris-covered stakes during the winter field season.

5.2.2.2 Spatial Variability

A comparison of the ablation rates between the five debris-covered stakes shows that stake m5 recorded the lowest daily average and had the thickest debris-cover (Figure 5.29 and 5.30). The graph also shows that the relationship between increasing debris thickness and decreasing ablation is like during summer, quite complex, with an adjusted r^2 of 47%. Referral back to Table 5.3 shows that both m2 and m3 had a matrix of fine muddy debris resting on the ice surface, and, as was discovered during summer, the presence/absence of a matrix of very fine debris at the debris-ice interface can increase the insulation properties of the debris-cover. This factor may have contributed to the lower ablation rate recorded at m2, although the effect does not appear obvious at m3.

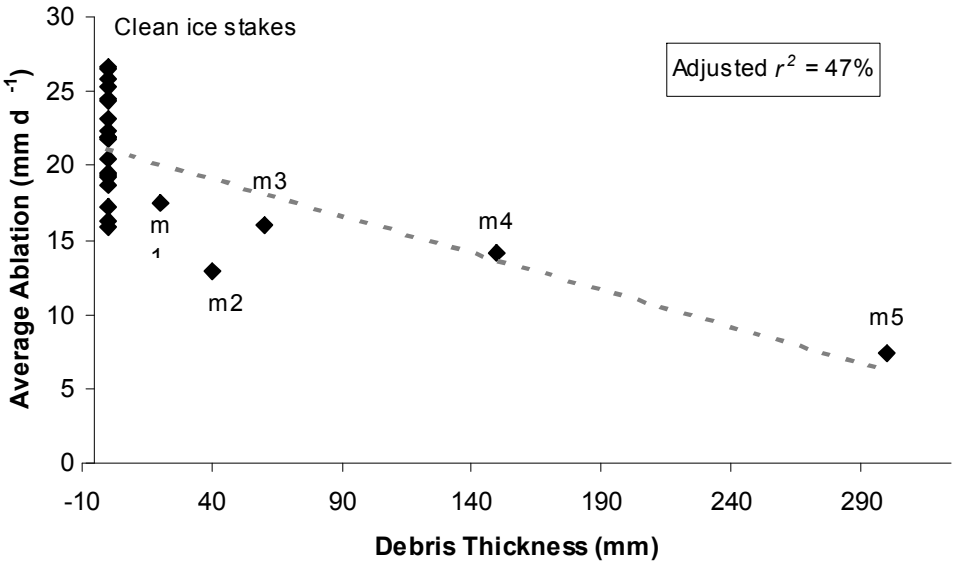

Figure 5.29 Average daily ablation and increasing debris thickness measured on the lower Fox Glacier during the winter field season.

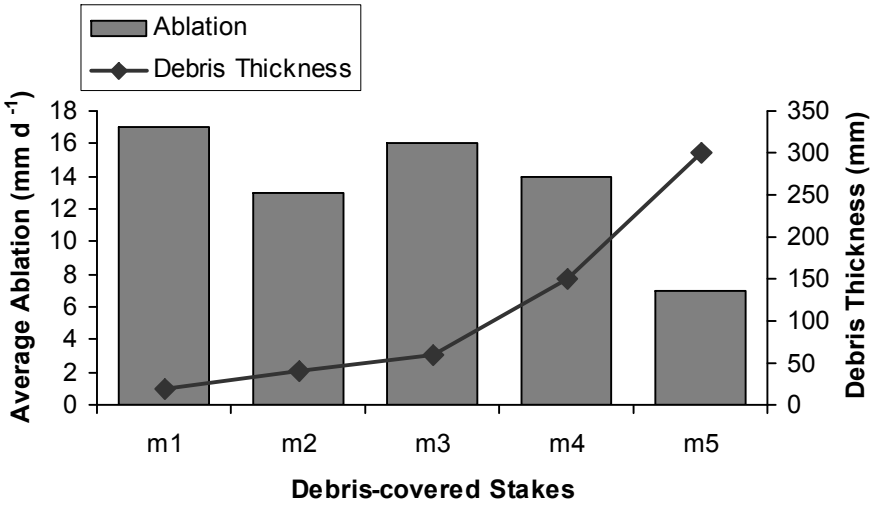

Figure 5.30 Average daily ablation and debris thickness recorded at the debris-covered stakes on the lower Fox Glacier during the winter field season.

Although it was originally thought that the lower glacier received no sun around the winter solstice, it was discovered that a small wedge of sunlight did shine on the lower glacier (Figure 5.31). The nature of the wedge resulted in the debris-covered stakes, and some of the clean ice stakes, receiving from between 15 to 30 minutes of direct sunlight on clear days. During summer a direct comparison between the ablation rates of the clean ice versus the debris-covered ice was made (although spatial variability did exist between the two stake groups), and it was found that ablation under debris was suppressed by as much as 50% (section 5.1.2.2). Before such a comparison can take place with the winter data, it was essential to see what effect if any, this wedge of sunlight was having on the average ablation rates at the various clean ice stakes.

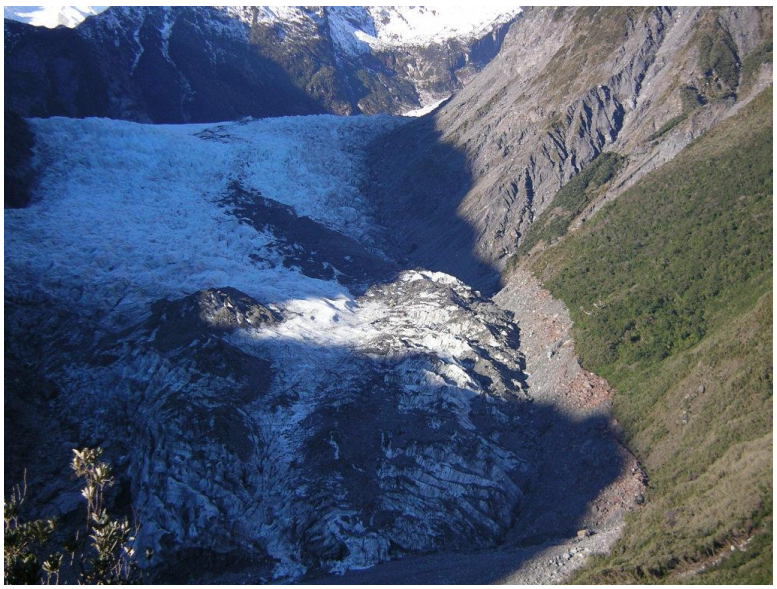

Figure 5.31 Wedge of sunshine across a portion of the study site on the lower Fox Glacier at 2:50pm on the 14th June 2005.

A field survey confirmed that stakes u1 - u5, u8 and c6 received no sun, but stakes u6, u7, c1-c5 and l1to l5 all received a total of around 15 minutes of direct sunlight on clear days. Likewise m1 to m5 also received sun. Due to the more southerly location of m2 to m5, these stakes received at least 20 minutes of insolation, with m3 remaining in sun the longest resulting in around 30 minutes of insolation. Table 5.4 and Figure 5.32 contain comparative data for the groups of stakes that either did or did not receive direct sunlight. As can seen from both the table and the graph the difference between the clean ice stakes either receiving sun or not receiving sun is insignificant as both groups had an average ablation rate of 8 mm d^{-1}, indicating that this very short period of direct sunlight in the afternoon had no significant effect to the average daily ablation on the clean ice.

During winter, the sun angle is very low, so sun intensities would have be less than at the same time during the summer months. Therefore for the purposes of comparison between the ablation rates of the clean ice stakes and the debris-covered stakes, all the clean ice stake data will be combined as it was with the summer data. However, that fact that the debris-covered stakes were receiving the most direct sunlight on clear days may be of influence to the overall ablation rates recorded at these stakes. Therefore the degree of difference between the clean ice and debris-covered ice ablation rates for winter needs to be treated with some caution.

Table 5.4 Comparison of the average ablation of stake groups that either did or did not receive direct sunlight on selected clear days during the winter field season.

Date	Ablation at the "No Sun Stakes" (u1-u5, u8, c6) (mm d^{-1})	Ablation at the "Clean ice Sun Stakes" (u6, u7, l1-l5, c1-c5) (mm d^{-1})	Ablation at the "Debris-covered Stakes" (m1-m5) (mm d^{-1})
11th June	15	12	9
12th June	6	4	7
13th June	16	15	12
14th June	15	10	5
15th June	11	13	10
16th June	18	19	9
22nd June	5	7	3
23rd June	-2	-2	3
24th June	-0.2	0.8	0
25th June	0.8	0.6	-0.8
Average	**8**	**8**	**6**

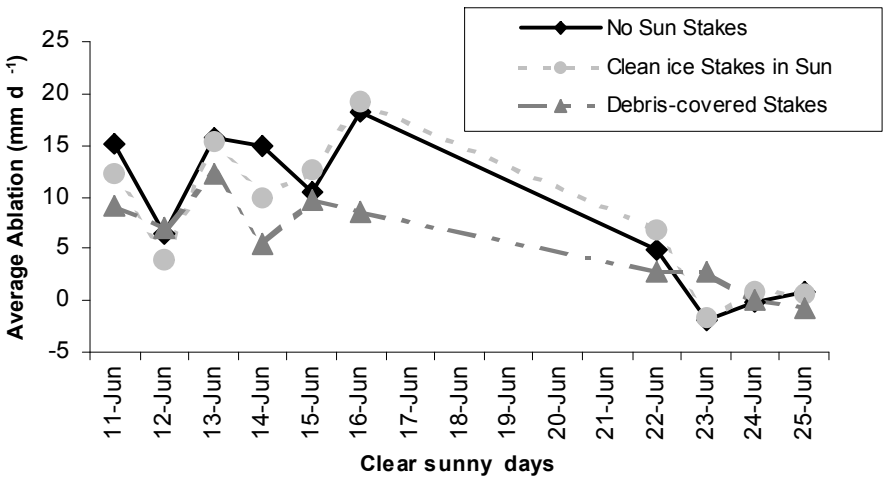

Figure 5.32 Graph of the data from Table 5.4, showing the insignificance in the difference of the average ablation rates between 'no sun stakes' and 'clean ice stakes in sun', and the generally lower rate of the debris-covered stakes.

As mentioned above, during summer there was a significant difference between the daily ablation rate between the clean ice stakes and the debris-covered stakes. During winter conditions however, this large spatial variability was not so apparent with the average ablation at the debris-covered stakes still 83% of that occurring on the clean ice, a suppression rate of only 17% (Figure 5.33). On a number of occasions the ablation under debris-cover was equal to, or even higher than that occurring on the clean ice.

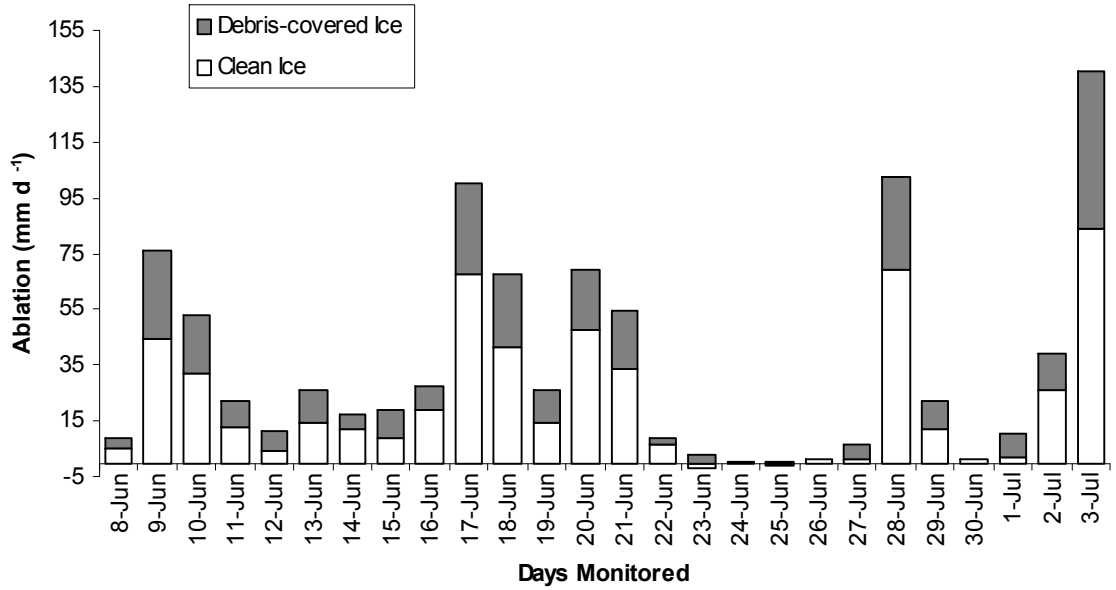

Figure 5.33 Comparison of average daily ablation between the debris-covered stakes and the clean-ice stakes recorded on the lower glacier during the winter field season.

The mean average daily ablation occurring on the clean ice was 22 mm d^{-1} while on the debris-covered ice only 13 mm d^{-1}. A t-test was conducted to test the null hypothesis (H_0) that there is no difference between the ablation rates of the clean ice and debris-covered ice, versus the alternative hypothesis (H_1) that there is a significant difference between the rates. Results of the test gave a t-value of only 1.48 and *p*-value of 0.147, with the difference between the two means being estimated at 8.04, and the 95% confidence interval -2.94 to 19.02. The null hypothesis is therefore accepted in that there is no significant difference between the ablation rates of the clean ice and debris-covered ice during the winter field season.

However, a closer look at the data shows that this small difference in the means seems to evolve due to a larger difference between the ablation rates recorded in conjunction with precipitation as opposed to clear weather, when there is a much smaller difference. Figure 5.34 compares the average ablation rates between the debris-covered ice and the clean ice on days on which precipitation was or was not received.

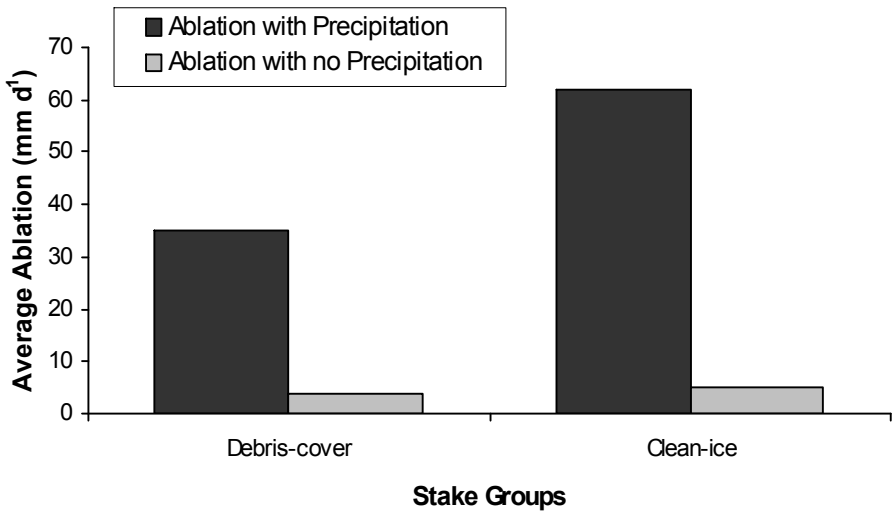

Figure 5.34 Comparison of the average ablation at the debris-covered stakes and the clean ice stakes during precipitation events and during fine weather.

As Figure 5.34 demonstrates, days on which no precipitation is received, the difference between the ablation rates on the clean ice and the debris-covered ice is very small. However, during precipitation events the ablation occurring under debris-cover is only 56% of that occurring on the clean ice. These results would tend to indicate that the debris has some sort of sheltering effect during rain, consequently reducing the ablation rate.

A closer look at ablation under debris during precipitation events indicates that there appears to be a trend of decreasing ablation with increasing debris thickness. Figure 5.35 shows the average ablation recorded at each of the debris stakes and the clean-ice ablation average for the 17th, 20th, 28th June and 3rd July. On these four occasions ≥100 mm of precipitation was received.

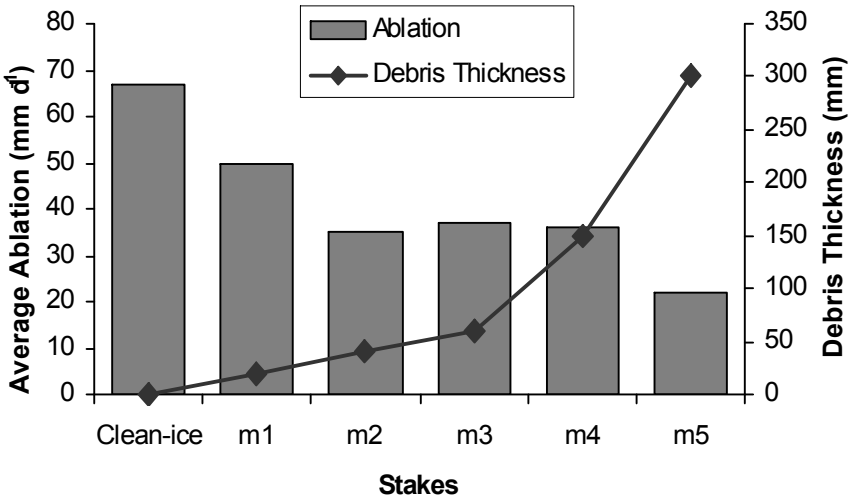

Figure 5.35 Average ablation in comparison to debris thickness recorded during precipitation events ≥100 mm on the lower Fox Glacier during the winter field season.

5.2.2.3 Temporal Variability

On a daily time scale the variability recorded at the debris-covered stakes clearly mirrors that occurring at the clean ice stakes (Figure 5.26). As with the clean ice stakes this daily variability appears to be related to precipitation, which will be covered in section 5.2.3.2. Due to the very small quantities of ablation occurring over a 24-hour period during the winter field season, no attempt was made to try and detect any diurnal variation.

5.2.3 Winter Ablation and Climate Variables

5.2.3.1 Introduction

To see which of the winter climate variables measured most influenced daily ablation, Pearson's correlation (Table 5.5) followed by multi-variant regression analysis using a general linear model of ablation and all the measured climate parameters was conducted.

Table 5.5 Pearson's correlation between ablation and climate variable measured on the lower Fox Glacier (altitude 435 m a.s.l) during the winter field season

	Temperature	Precipitation	Humidity	Wind Speed	Wind Direction	Solar Radiation
Ablation	0.549	0.899	0.795	0.114	0.503	0.051
	0.004	0.000	0.000	0.581	0.009	0.806

The multi-variant analysis produced the following equation:

Ablation = -57.5 + 5.32 T + 0.220 P + 0.653 H + 0.230 WS + 0.160 WD - 0.0.40 SR (11)
(adjusted r^2 93.4%)

This indicates that in winter climate variables can account for 93% of the variation in daily ablation on the lower glacier surface. Correlation indicates the strongest relationship is between precipitation and ablation, this was confirmed by best subset regression analysis which identified precipitation as the single most important climate variable. When considering the two most important variables, the combination of precipitation and temperature, as well as precipitation and humidity were identified. These relationships will be looked at more closely in the following sections.

5.2.3.2 Ablation and Temperature

Unlike during summer, temperature was not identified as being the single most influential climate variable to ablation during the winter field season. However a general plot of daily average ablation and temperature (Figure 5.36), and correlation analysis (Table 5.5), indicates that there is still a positive relationship although this is not as strong as during summer with a Pearson's *r* of 0.549 and *p*-value 0.004. The days on which there was very little to nil ablation average temperature was very low (< 4^{o}C). Ablation peaks on the 9th June, 28th June and 3rd July do appear to coincide with a temperature increase, but this pattern is not seen on 17th June. What is noticeable in Figure 5.37 is the association between temperature and precipitation with ablation. As mentioned, above best subsets regression identified this climatic combination as having influence on ablation with an adjusted r^2 of 84.8%.

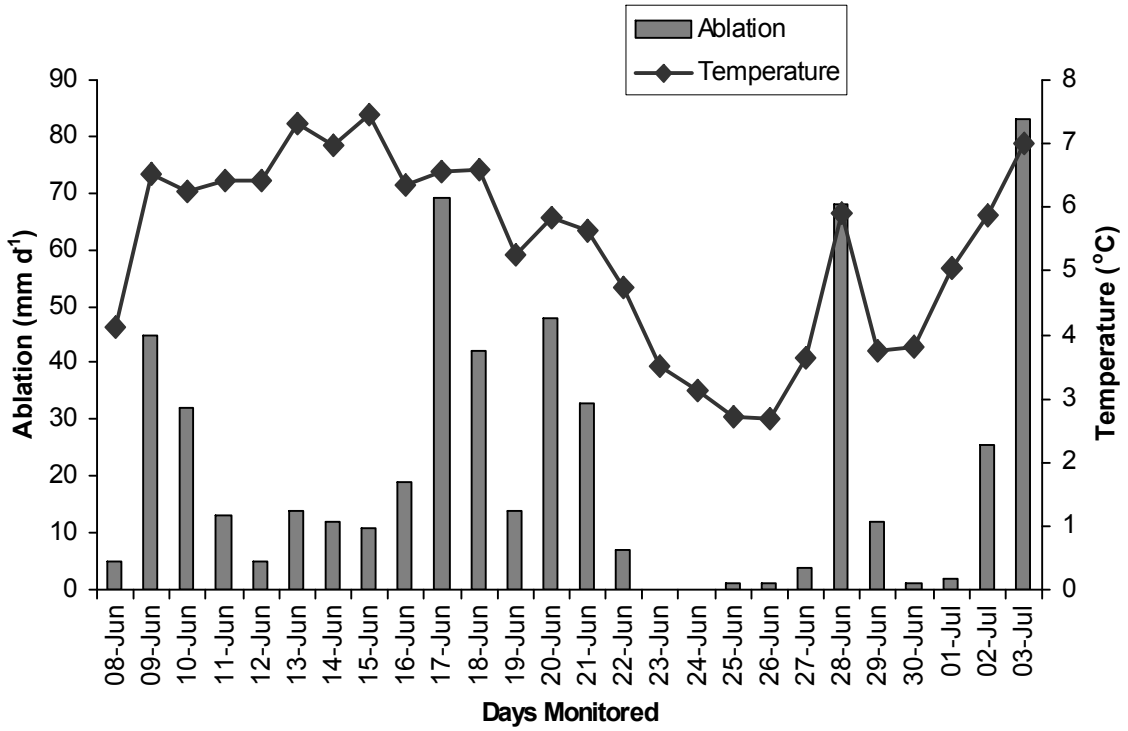

Figure 5.36 Relationship between daily average ablation and daily average temperature during the winter field season on the lower Fox Glacier.

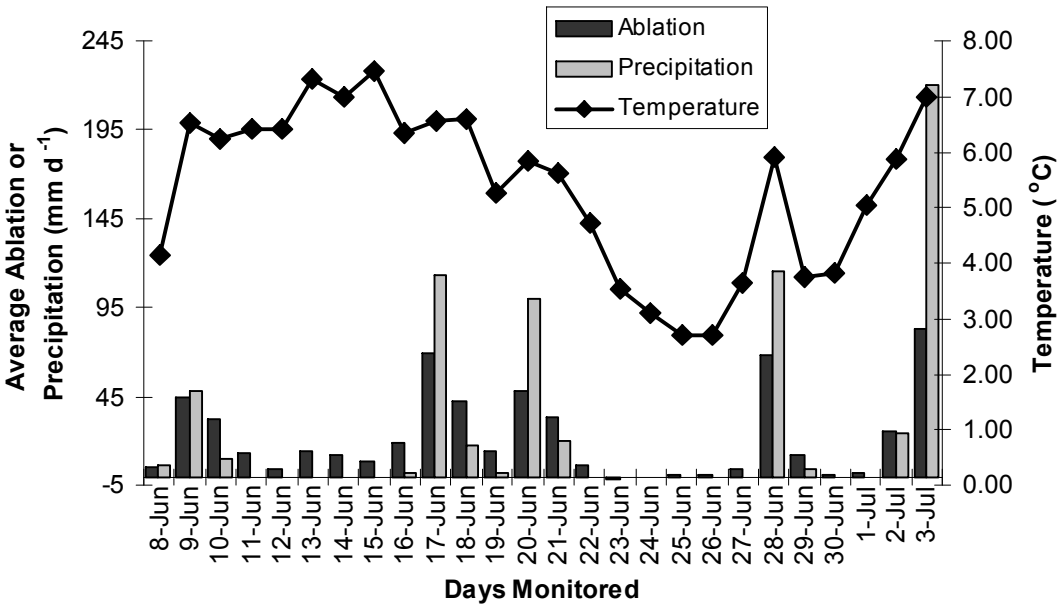

Figure 5.37 Relationship between ablation and temperature and precipitation on the lower Fox Glacier during the winter field season.

5.2.3.3 Winter Ablation and Precipitation

As outlined in section 5.2.3.1 precipitation was identified as the most important climate variable to winter daily ablation. Regression analysis of the ablation data with precipitation data gave the following equation (also see Figure 5.38):

Ablation = 10.8 + 0.407 Precipitation (12)

(adjusted r^2 80%, p-value of <0.001)

This relationship between ablation and precipitation can also be clearly seen in Figure 5.37. On five occasions significant increases in ablation (in excess of 70%) were recorded, all coinciding with heavy rain events, which on four out of the five occasions involved 100 mm or more of rain being received. For example on the 19th and 20th June, 102 mm of precipitation resulted in a 71% increase in ablation, and on the 27th and 28th June 116 mm gave a 94% increase in average daily ablation.

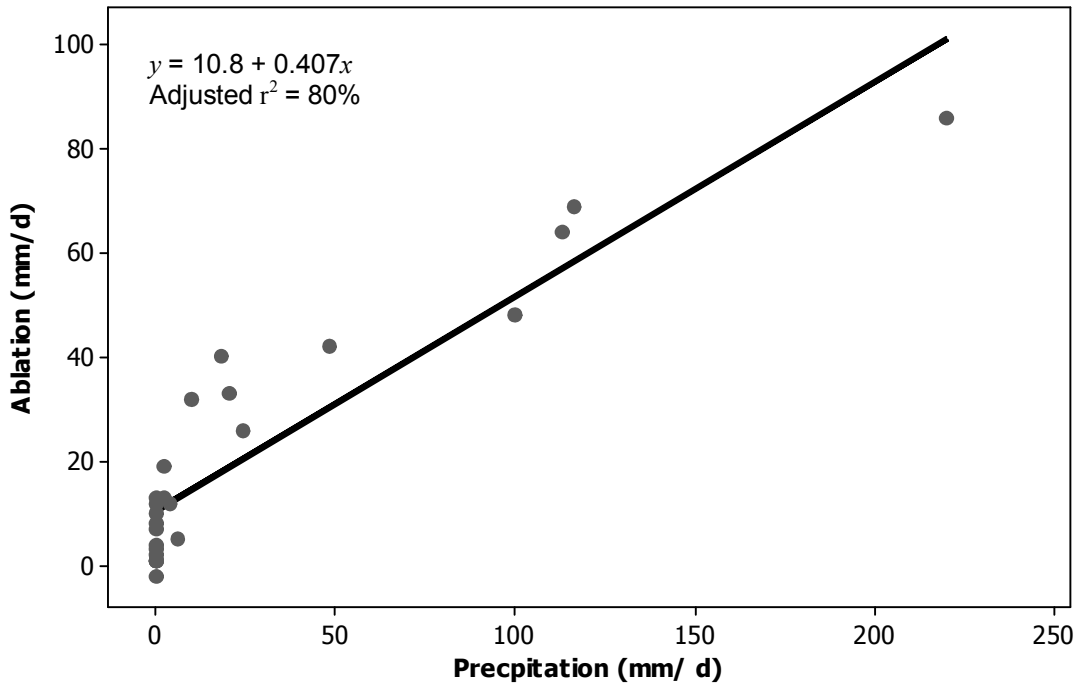

Figure 5.38 Scatter plot with regression showing the relationship between precipitation and ablation on the lower Fox Glacier during the winter field season.

In addition to the combination of temperature and precipitation (section 5.2.3.2), precipitation and humidity were also identified in best subset regression analysis with a combined adjusted r^2 of 85.9%. This relationship between ablation and humidity will be covered below.

5.2.3.4 Winter Ablation and Humidity

During summer it was identified that there was a strong negative relationship between increasing ablation and decreasing humidity. However during winter this relationship is inversed indicating increasing ablation with increasing humidity. Pearson's correlation (Table 5.5) gives a co-efficient of 0.795 and *p*-value <0.001. Like with temperature, this relationship would appear to be related to the importance of precipitation on winter ablation, as humidity tended to increase during precipitation events (Table 4.8).

5.2.3.5 Winter Ablation and Wind Speed and Wind Direction

Wind speed does not appear to have a significant impact to daily ablation on the lower glacier during winter. However as outlined in section 5.1.3.5 wind turbulence is a component of the energy required for melt on an ice surface. Like during summer, problems with the anemometer and/or the location of the climate station may have masked possible relationships between ablation and wind speed.

Correlation does suggest a relationship exists with wind direction, but this is an indirect relationship. As mentioned in section 5.1.3.5 for the purposes of correlation, wind direction data was categorised into two groups, those days that it was katabatic, and those days in which it wasn't. Only on three occasions (Table 4.8) was the average wind direction blowing from a direction other than down glacier, with two of these days being associated with strong westerly fronts and heavy precipitation, hence the correlation between wind direction and ablation. However, like with the temperature and humidity data, this relationship is inextricably linked to the precipitation events, so wind direction alone is not a contributor to daily ablation rates.

5.2.3.6 Winter Ablation and Solar Radiation

Unlike during summer no relationship was identified between incoming short-wave solar radiation and daily ablation. Radiation values were on average 93% lower than they were during summer. However this was not unexpected due to the lack of direct sunlight on the lower glacier.

5.2.4 Winter Ablation and Synoptic Situation

Figure 5.39 shows the daily average ablation occurring under the different synoptic classifications during the winter field season. Clearly both fronts/troughs (V) and north-westerly airflows are associated with higher rates of ablation; where as south-to-south

west flows (III) result in very low rates. Average daily ablation was 44% higher than average during the passage of fronts/troughs, and 31% higher with north-westerly airflows. Conversely, a 95% reduction in average ablation was recorded during south to south-west flows. The total amount of ablation that occurred under different synoptic classifications is shown in Figure 5.40. The large value for (V) is not surprising especially considering the high frequency of fronts/troughs during the winter field season. Of interest is the high frequency of south to south-westerly airflows (I) that still only amounted to very low total ablation.

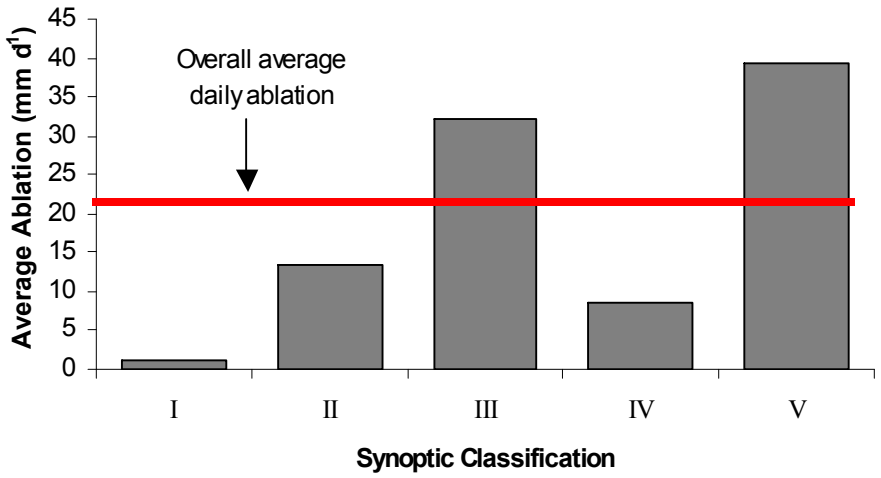

Figure 5.39 Daily average ablation occurring under the different synoptic classifications during the winter field season on the lower Fox Glacier.

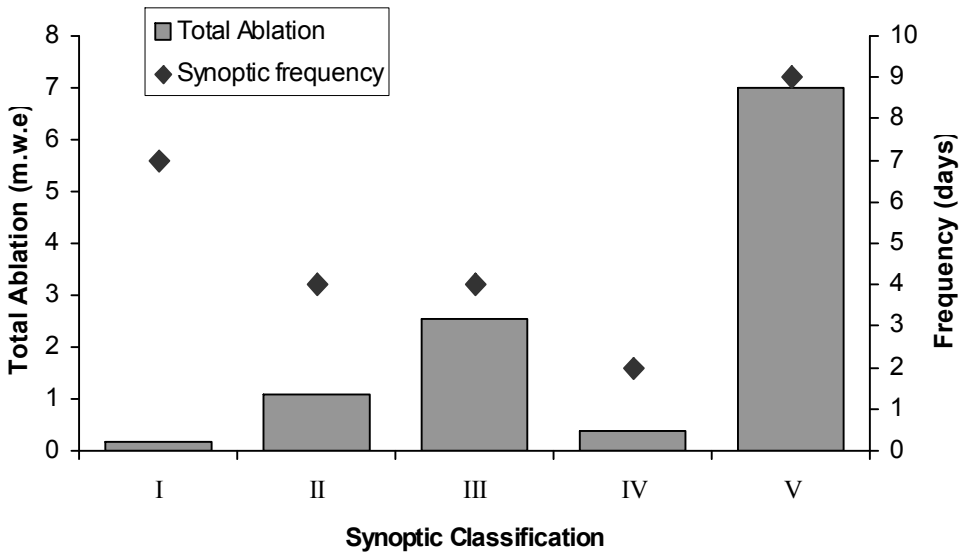

Figure 5.40 Total ablation occurring during different synoptic classifications, and the frequency of those synoptic classifications during the winter field season.

5.3 Intra-annual Variation in Ablation

As figure 5.41 shows there is a large difference in the average daily ablation on the clean ice of the lower Fox Glacier between summer and winter conditions. With the exception of one data point, there is no overlap in the ablation values. The daily average ablation during summer was 129 mm d^{-1} whilst in winter it was only 22 mm d^{-1} an 83% reduction. As outlined above, the winter data was found to have a much larger spread reporting much higher standard deviations than the summer data. This high degree of spread is likely to be related to the combination of negative ablation values (due to either inaccuracies of the straight-edge technique, or the re-freezing of surface melt water around stakes), and synoptic/climatic variability with the only significant ablation values coinciding with heavy rainfall events.

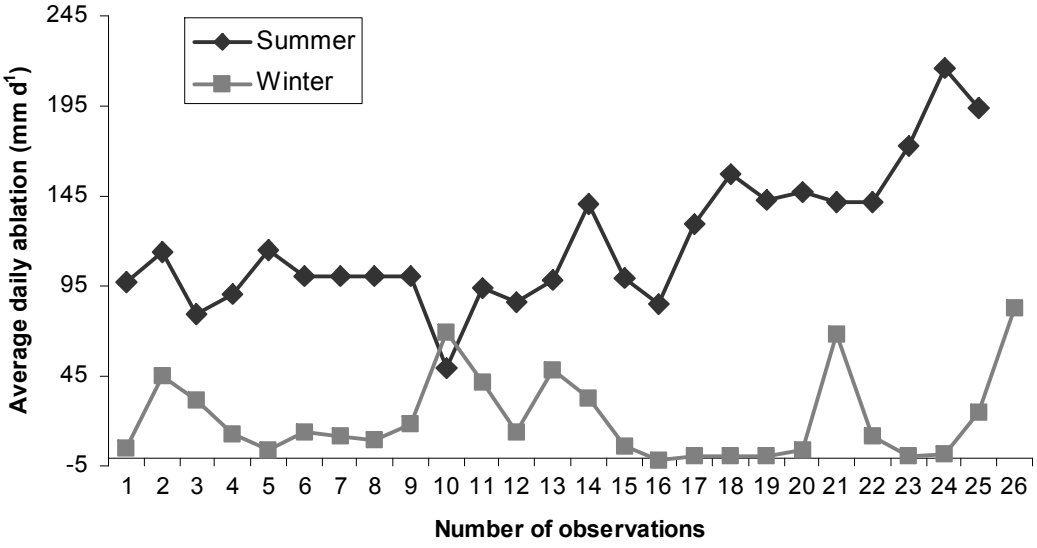

Figure 5.41 Comparison of average daily ablation recorded on the lower Fox Glacier between the summer and winter field seasons 2005.

During summer the spatial variability in ablation between the clean-ice stakes and the debris-covered stakes was significant, with debris-cover suppressing the rate of ablation by around 50%. However during winter this was not as significant, with nil to minimal suppression during fine weather, but during precipitation events, the debris cover suppressed ablation by 44%.

Chapter 6 Results Velocity

6.1 Surface Velocity Summer 2005

6.1.1 Introduction

Surface velocity was measured from 20th January through until the 4th February on a daily basis (Table 6.1, 6.2 and Appendix 2). During this time velocities ranged from as little as 0.52 m d^{-1} at stake d3 up to a maximum of 1.43 m d^{-1} at stake a3. Average daily velocities ranged from 0.75 m d^{-1} on the 22nd January up to 0.99 m d^{-1} on the 4th February, with the overall average during the study period being 0.87 m d^{-1}. No data was gathered on the 30th January due to fieldwork being conducted on the nearby Franz Josef Glacier. Therefore, the data from the survey conducted on the 31st January was averaged over both days. Figure 6.1 shows the general trend in flow direction during the study period, with an average flow vector of 257° or west-by-south-west.

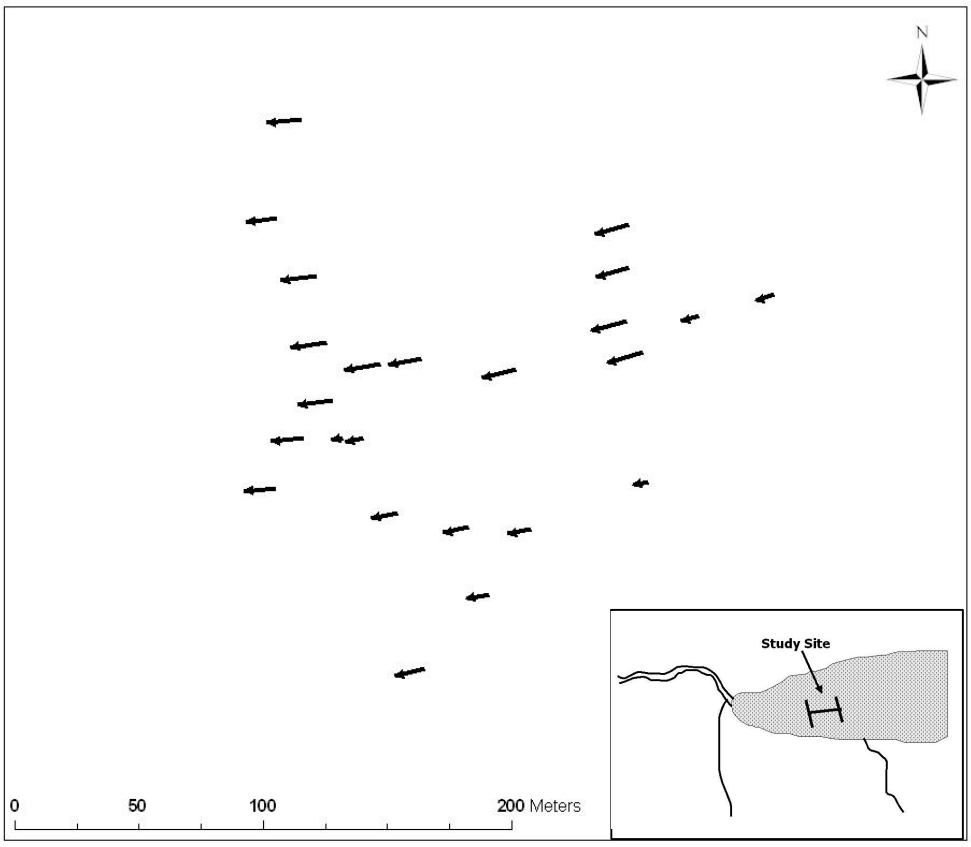

Figure 6.1 Flow vectors of the velocity stakes monitored on the lower Fox Glacier during the summer field season from 18th January to 3rd February. Insert shows the approximate 2005 ice limit and location of the study site.

Table 6.1 Average velocities recorded at each stake during the summer field season.

Stake	Average Surface Velocity (m d $^{-1}$)
a1	0.891
a2	0.892
a3	0.969
a4	0.884
a5	0.885
a6	0.850
a7	0.813
a8	0.845
a9	0.905
a10	0.912
a11	0.919
a12	0.973
a13	0.981
a14	0.970
a15	0.979
a16	1.009
a17	1.035
a18	0.849
d1	0.725
d2	0.645
d3	0.584
d4	0.726
d5	0.742

Table 6.2 Average daily surface velocities during the summer field season

Date	Average Surface Velocity (m d^{-1})
18-Jan	0.895
19-Jan	0.806
20-Jan	0.769
21-Jan	0.748
22-Jan	0.952
23-Jan	0.920
24-Jan	0.894
25-Jan	0.855
26-Jan	0.892
27-Jan	0.863
28-Jan	0.849
29-Jan	0.850
30-Jan	0.850
31-Jan	0.839
1-Feb	0.876
2-Feb	0.880
3-Feb	0.986

There was little spread in the data with standard deviations ranging from 4-17% of the mean on a per stake basis, and from 13-26% of the mean on a per day basis. Figures 6.2 and 6.3 show the 95% confidence interval (two standard errors) of the mean for the data on a per stake and per day basis.

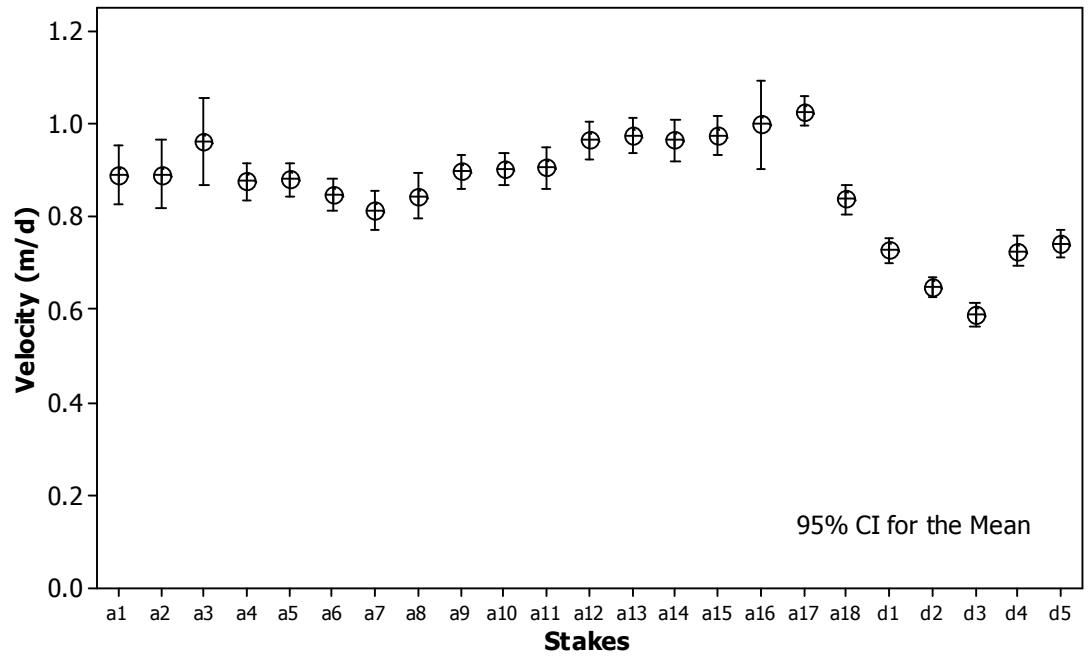

Figure 6.2 The 95% confidence interval (two standard errors) of the mean of the individual stake velocities recorded on the lower Fox Glacier during the summer field season.

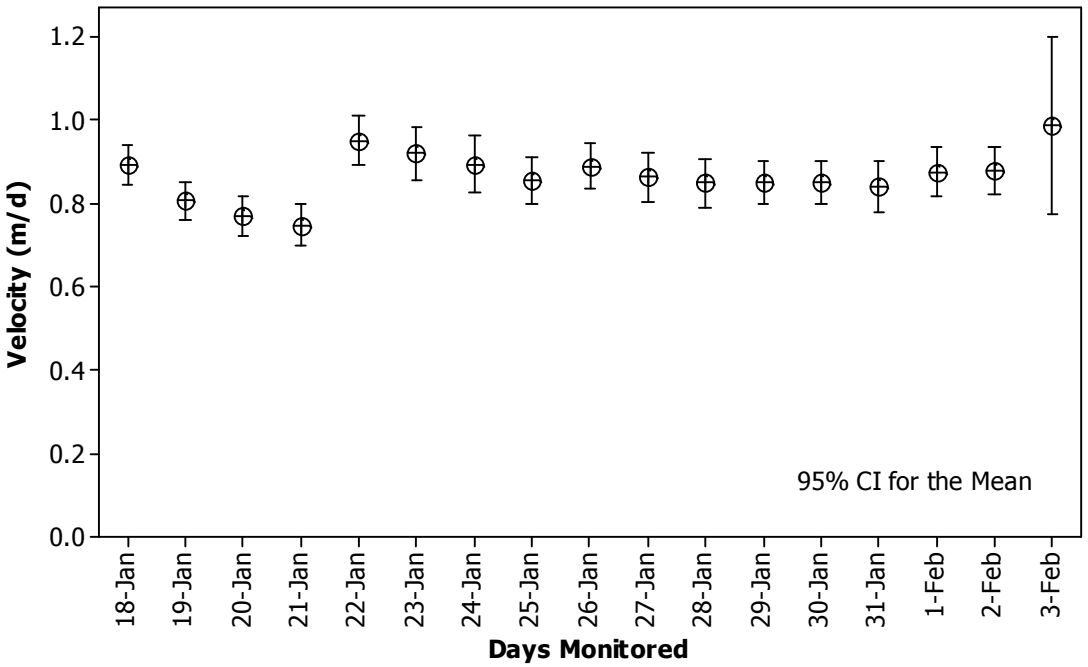

Figure 6.3 The 95% confidence interval of the mean of daily average velocity across all stakes measured on the lower Fox Glacier during the summer field season.

6.1.2 Spatial Variability

Clear spatial variability in surface velocity was identified both across glacier and up glacier. Average daily velocities were found to decrease with proximity to the true left side of the valley (Figures 6.4 and 6.5). Stake d3 was positioned on the true left (south) 83 m from the valley side, and was moving at 66% of the rate of stake a5, located near the centre of the glacier. Due to an area of extensive crevassing (restricting access), stakes were not positioned as close to the true right of the glacier, with stake a1 still being 200 m from the valley side.

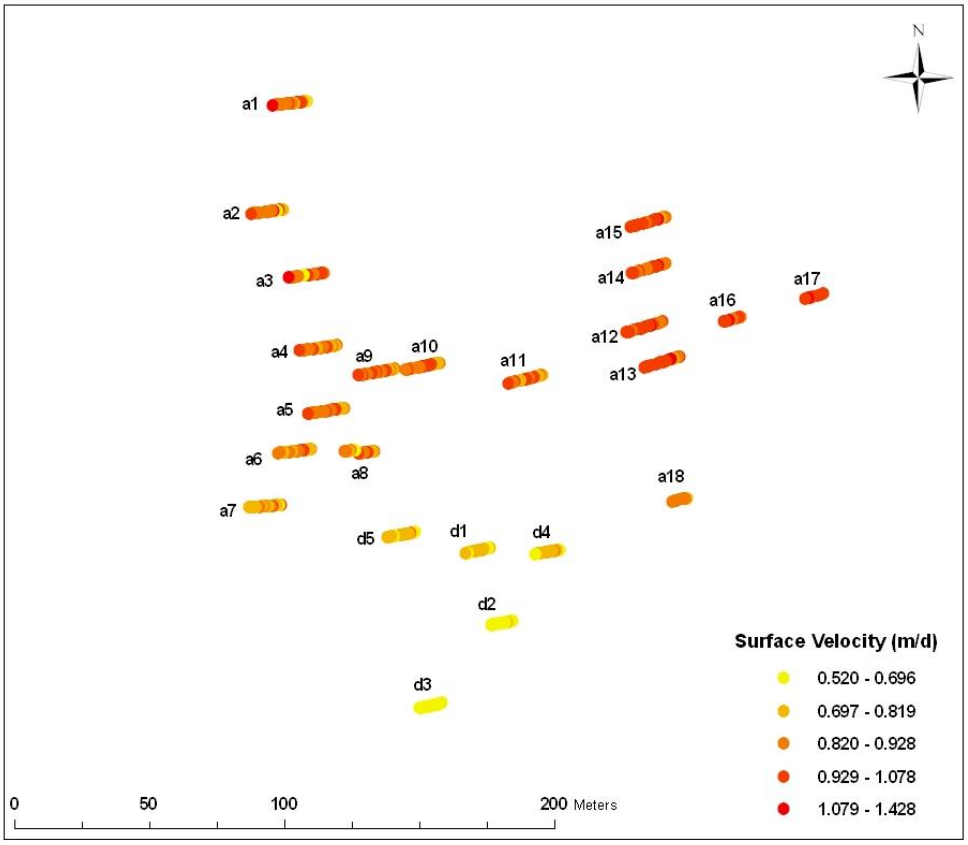

Figure 6.4 Daily velocities at individual stakes recorded on the lower Fox Glacier during the summer field season, showing spatial variability with lower velocities near the true left of the glacier (south) and higher velocities up glacier (east).

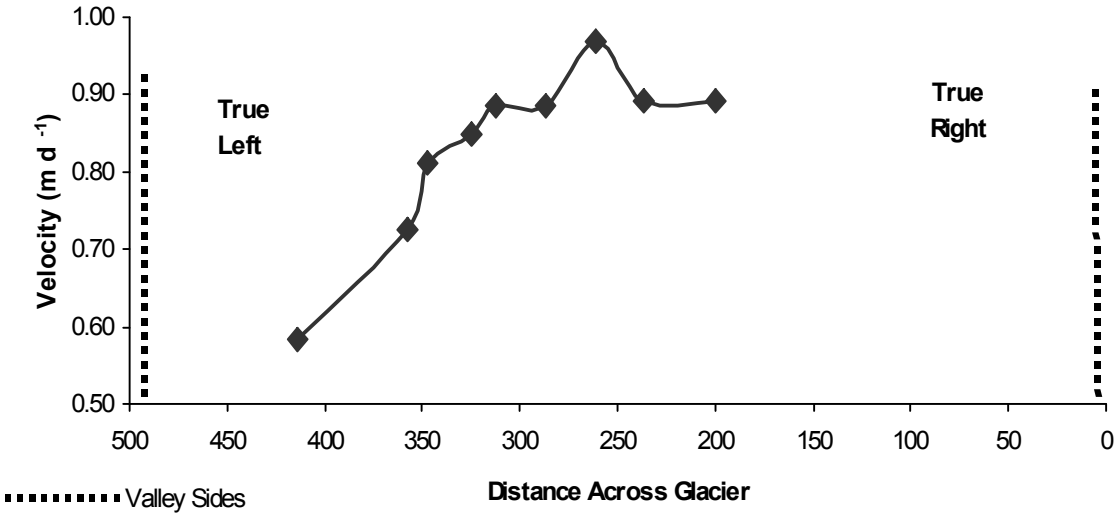

Figure 6.5 Variation in average daily velocity across the lower Fox Glacier based on data from stakes a1-a7 and d1 and d3.

Spatial variability in velocity with increasing distance from the terminus was also recorded, with a 15% increase in velocity from 0.88 m d^{-1} at stake a4 at 370 m from the terminus, to 1.04 m d^{-1} at stake a17, 554 m from the terminus (Figure 6.6). This gave an increase in velocity of 0.16 m d^{-1} over a distance of 184 m with an altitudinal gain of 40 m (Figure 6.7).

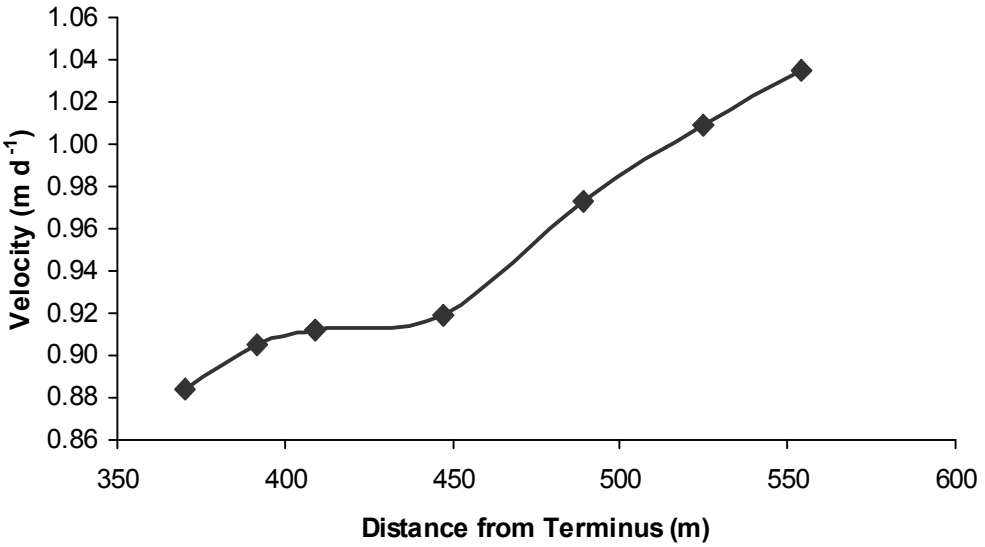

Figure 6.6 Variation in average daily velocity with increasing distance from the terminus based on data from stakes a4, a9-a12, a16 and a17.

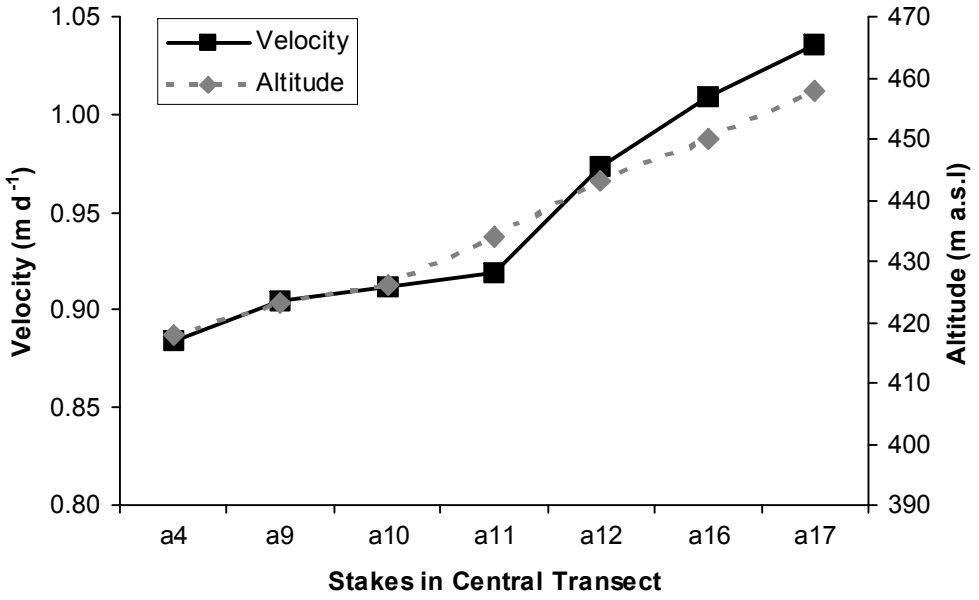

Figure 6.7 Variation in average daily velocity with increasing altitude recorded on the lower Fox Glacier during the summer field season.

On a smaller spatial scale, it was found that stakes a1-a3 were moving with much more variability than stakes a9-a11 whose flow closely resembled the daily average (Figure 6.8). This area of the glacier was undergoing rapid crevassing during this summer field season (Figure 6.9), a factor that appears to have resulted in these stakes moving in surges.

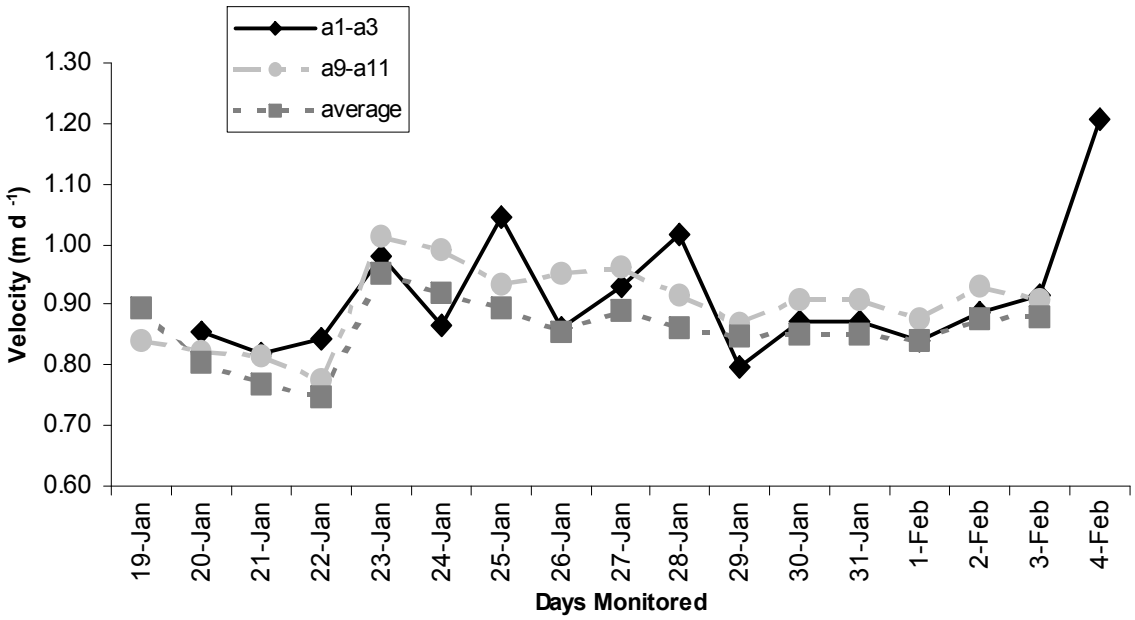

Figure 6.8 Spatial variability in velocity between various stakes monitored on the lower Fox Glacier during the summer field season.

Figure 6.9 Area of rapid crevassing between stakes a1 and a2 on the lower Fox Glacier February 2005. Source: H. Purdie.

6.1.3 Temporal Variability

There was some temporal variability in the average daily velocity recorded on the lower glacier during the summer field season (Figure 6.10). Of particular note is the 20% increase in velocity that occurred between the 21st and 22nd January, which coincided with a heavy rainfall event of 116 mm on the 22nd January. There was also a smaller increase (11%) that occurred on the 3rd February, which appears related to a period of increased temperature (c.3°C) and ablation (27%). These relationships will be discussed in detail in sections 6.1.4.2 and 6.1.4.3.

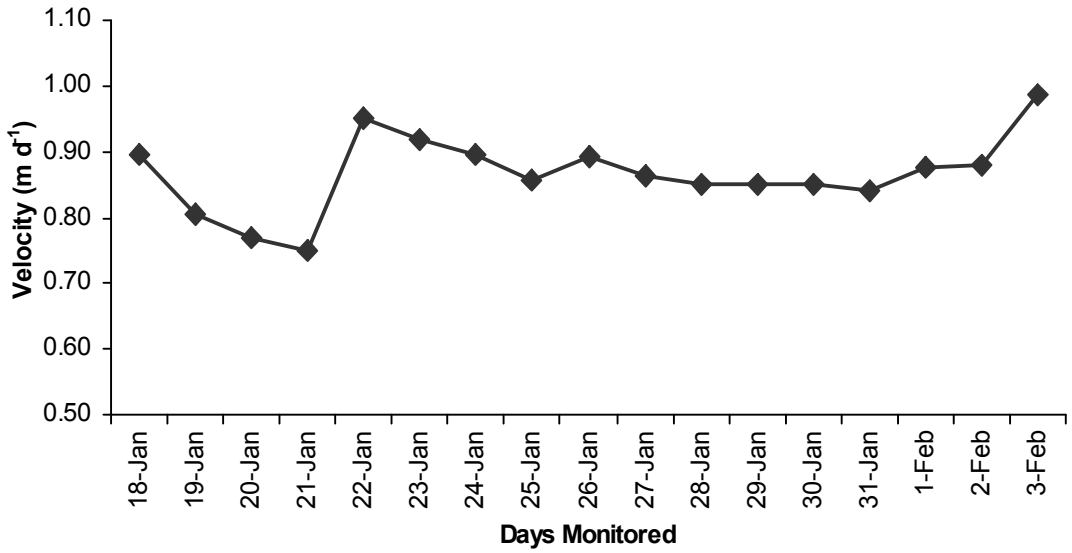

Figure 6.10 Average daily velocity over recorded over time on the lower Fox Glacier during the summer field season.

6.1.4 Velocity and Climate Variables

6.1.4.1 Introduction

To see how much influence daily climate variables had on surface velocity a Pearson's correlation was conducted in order to look for any general relationships between surface velocity and the climate variables measured (Table 6.3). This was followed by multi-variant regression analysis using a general linear model.

Table 6.3 Pearson's correlation of velocity and climate variables measured on the lower Fox Glacier during the summer field season. The top number is the correlation co-efficient and the bottom number, the associated *p*-value.

	Temperature	**Precipitation**	**Humidity**	**Wind Speed**	**Wind Direction**	**Solar Radiation**
Velocity	0.357	0.385	-0.064	0.064	0.142	0.457
	0.160	0.127	0.806	0.814	0.628	0.117

The multi-variant analysis produced the following equation:

$$\text{Velocity} = 0.109 + 0.021\,T + 0.021\,P + 0.004\,H + 0.010\,WS + 0.012\,WD + 0.001\,SR \qquad (13)$$

where T = temperature; P = precipitation; H = humidity; WS = wind speed; WD = wind direction; and SR = solar radiation.

Neither correlation nor the multi-variant regression identified any strong relationships. The above equation gave an adjusted r^2 value of 46.9%, indicating that unlike ablation, variations in daily velocity are only partially influenced by climatic variability. It is important to note however, that both Pearson's correlation and the regression used assume a linear relationship between the variables. Best subset regression analysis identified precipitation and solar radiation as being the two most significant climatic variables influencing velocity. But even then, the adjusted r^2 is only 17% and *p*-value 0.159. When considering individual climatic variables and velocity, temperature has an adjusted r^2 of only 7% and precipitation was 9%.

The lack of correlation between daily average velocity and the climatic variables measured on the lower glacier, and the low regression results, is not surprising since it has already been noted in section 2.6.1 that ice thickness and surface slope are the two factors that exert most influence on velocity. Hence it is only on shorter timescales that climate, or more specifically the supply of water to the base of a glacier, becomes of influence. However, the focus of this study is on short-term fluctuations, so some

influence from climate parameters, in particular those that could most directly influence the supply of water to the base (i.e. precipitation and temperature), might be expected. From the correlation analysis (Table 6.3), and the best subset regression analysis, precipitation, temperature and solar radiation are identified as having most influence, albeit a small one. Therefore, these relationships will be explored in more detail in the following sections.

6.1.4.2 Velocity and Temperature

A first look at Figure 6.11 does not reveal any obvious relationship between surface velocity and temperature. However, close inspection does show that on the 22nd January and on the first three days of February there is an increase in temperature relative to the previous days. In the first case (22nd January), this is an increase of nearly 2°C coinciding with a 20% increase in surface velocity and the passing a frontal/trough in which precipitation fell. In early February there is a 3°C average temperature increase and an 11% increase in surface velocity from the 2nd to the 3rd February. During this time there was also an increase in ablation (see section 5.1.1.3), that is likely to have resulted in more melt water being delivered to the base of the glacier.

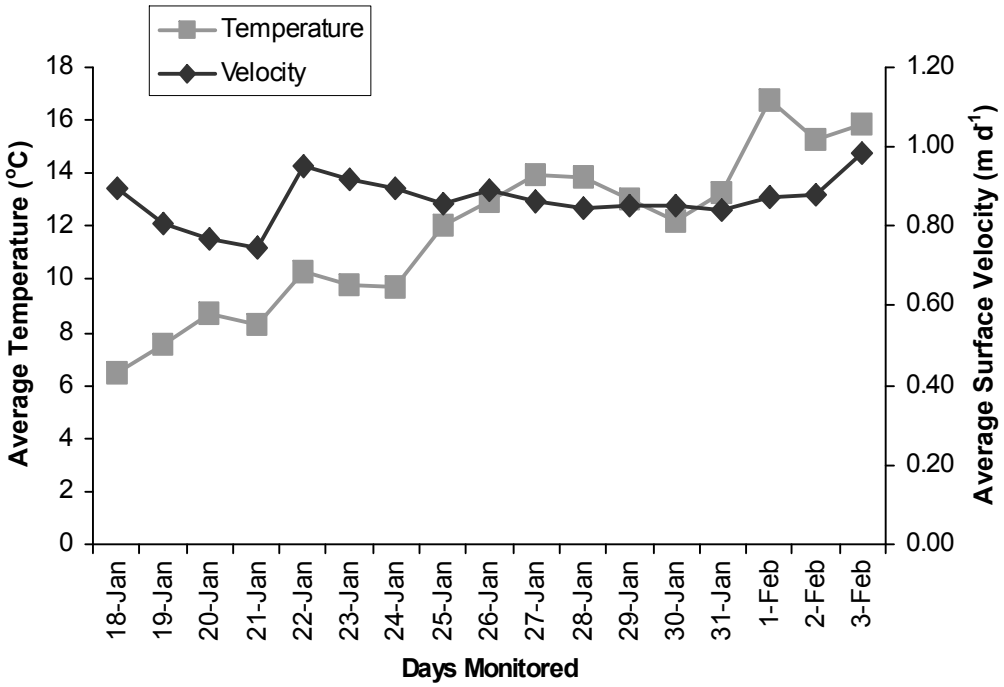

Figure 6.11 Comparison of the average daily surface velocity with temperature recorded on the lower Fox Glacier during the summer field season.

6.1.4.3 Velocity and Precipitation

Because the statistical analysis assumes a linear, time independent relationship, it did not reveal a relationship between precipitation and velocity, however as Figure 6.12 indicates there was a 20% increase in velocity on the 22nd January that could have been related to a heavy rainfall event that delivered 116 mm of precipitation. This precipitation would have been routed via the established drainage system to the base of the glacier, and is likely to have enhanced basal sliding. Nevertheless, drawing conclusions from one heavy rainfall event would be spurious, and in order to confirm if such a relationship exists on the lower Fox Glacier more heavy rainfall events need to be monitored.

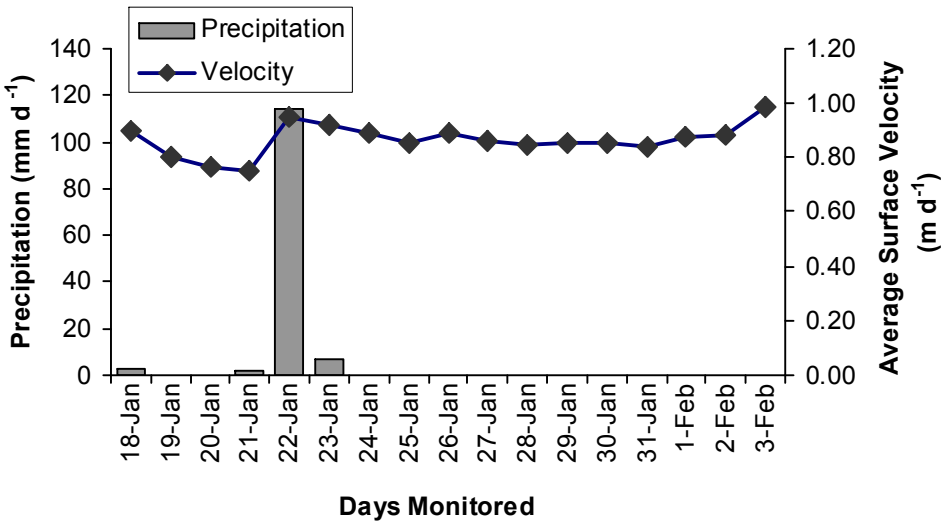

Figure 6.12 Relationship between average daily surface velocity and precipitation received on the lower Fox Glacier during the summer field season.

6.1.4.4 Velocity and Solar Radiation

Although more highly variable than the temperature data, and containing a large break (due to levelling problems), the incoming short-wave solar radiation (ISWR) can be see to have had an increase on both the 22nd January and is also high (> 350 W/m^2) on the first three days of February (Figure 6.13). However, with such an incomplete data set it would be unwise to derive any conclusions from this. Ideally, more data would need to be gathered to confirm or deny any relationship between velocity and ISWR.

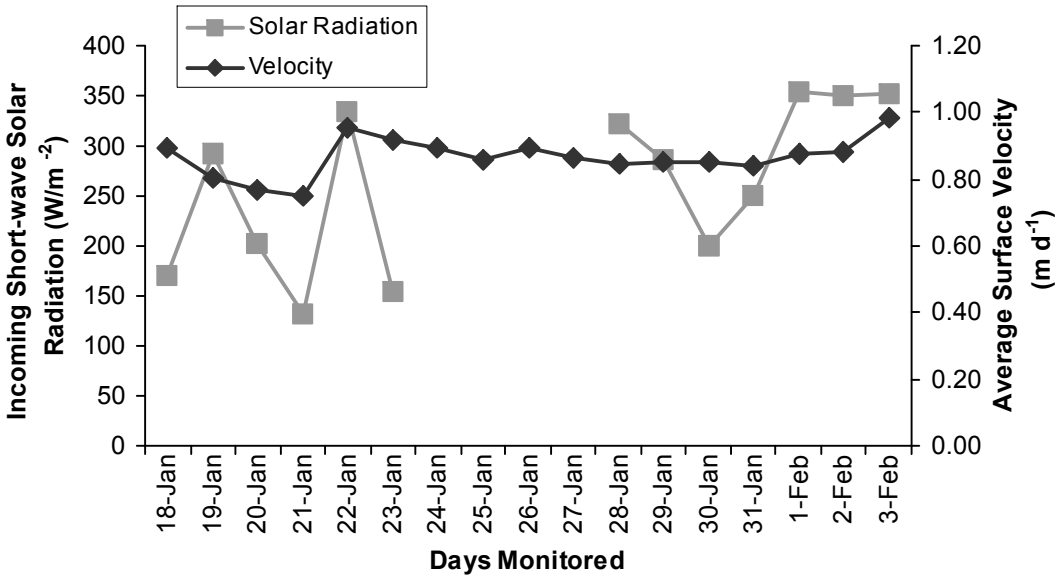

Figure 6.13 Comparison on average daily surface velocity and incoming short-wave solar radiation received on the lower Fox Glacier during the summer field season.

6.1.5 Velocity and Synoptic Situation

Figure 6.14 shows that during both the passage of fronts/troughs (V) and during the heat low (VI) the average daily surface velocity was in excess of 0.90 m d^{-1}. Situations where an anticyclone was present overhead (IV), or a south-to-southwest (I) or northerly flow (II) coincided with velocities close to or just below average (0.87 m d^{-1}), lowest velocities seem to occur while a north-westerly flow (III) is in place. As outlined above, climate parameters did not appear to contribute significantly to average daily velocity during summer, but both synoptic situations V and VI have the potential to influence the amount of surface water occurring on the glacier surface that can consequently influence velocity via basal sliding.

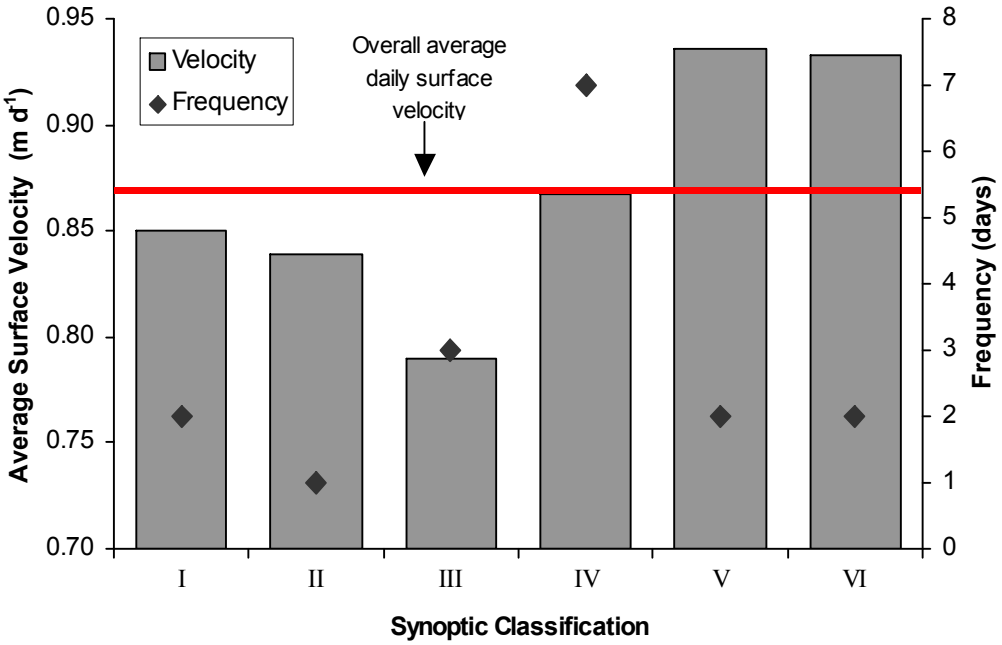

Figure 6.14 Frequency of the various synoptic classifications predicted to occur during the summer field season, and the associated average daily surface velocities recorded on those days on the lower Fox Glacier during the summer field season.

6.2 Surface Velocity Winter 2005

6.2.1 Introduction

General observation and photographic survey of the glacier between the summer and winter field seasons indicated that the glacier terminus had advanced and the lower glacier had increased in thickness (Figure 6.15). A re-survey (using RTK-GPS) of the January stake positions on the 1st and 2nd of July, indicated an increase in height (thickness) of around 3 metres. Only a small number of terminus points had been surveyed with the GPS during summer due to terminus access, but a comparison of those results within those of the more complete winter survey indicated that the terminus had advanced around 20 meters in the between the two field seasons (17 weeks). Local glacier guides have also confirmed this current advance of the glacier (The Press, 2005).

Short-term seasonal terminal advance in winter due to changes in ablation (as opposed to longer term changes in mass balance) have been recorded where the relative magnitudes of velocity over ablation during winter (in comparison to summer) can result in a small advance (Benn and Evans, 1998). However, local glacier guides have not noted this seasonal phenomenon at Fox Glacier and attribute the recorded changes to both ice thickness and the terminus position to changes to the overall mass balance of the glacier (Alpine Guides Westland, pers.comm., 2005).

Figure 6.15 Photographs of the true right edge of the lower Fox Glacier taken during January 2005 (left) and June 2005 (right) showing an obvious increase in size and volume.

During winter, daily surface velocity was measured from 8th June through to the 3rd July. Velocities ranged from 0.42 m d^{-1} at stake m3 on the 16th June up to 1.25 m d^{-1} at stake c6 on the 3rd July, with the overall daily average being 0.64 m d^{-1}. Table 6.3 contains the average surface velocity data for each stake over the entire study period and on a daily basis. The full velocity data set can be viewed in Appendix 4. Data for both the 15th and 16th June is identical due to problems with the GPS data-logger, which resulted in no data being gathered on the 15th, so the measurement taken on the 16th had to be averaged over the two days.

Table 6.4 Average surface velocities recorded at individual stakes on the lower Fox Glacier during the winter field season.

Stake	Average Surface Velocity (m d-1)
u1	0.677
u2	0.692
u3	0.709
u4	0.703
u5	0.700
u6	0.713
u7	0.689
u8	0.657
l1	0.631
l2	0.626
l3	0.621
l4	0.614
l5	0.591
c1	0.616
c2	0.628
c3	0.639
c4	0.654
c5	0.683
c6	0.714
m1	0.620
m2	0.576
m3	0.475
m4	0.493
m5	0.574

Table 6.5 Average daily surface velocities recorded during the winter field season on the lower Fox Glacier.

Date	Average Surface velocity (m d-1)
08-Jun	0.529
09-Jun	0.612
10-Jun	0.597
11-Jun	0.618
12-Jun	0.612
13-Jun	0.556
14-Jun	0.570
15-Jun	0.557
16-Jun	0.557
17-Jun	0.637
18-Jun	0.730
19-Jun	0.702
20-Jun	0.686
21-Jun	0.716
22-Jun	0.657
23-Jun	0.632
24-Jun	0.586
25-Jun	0.605
26-Jun	0.576
27-Jun	0.591
28-Jun	0.633
29-Jun	0.674
30-Jun	0.620
01-Jul	0.604
02-Jul	0.643
03-Jul	1.070

There was generally little spread within the data, with standard deviations ranging from 15-20% of the mean on a per stake basis, and from 9-13% on a daily basis (with the exception of the first day, which was higher at 30%, possible due to the large time differential between measurements due to stake set-up). Figures 6.16 and 6.17 show the 95% confidence interval (two stand errors) of the mean for the data on a per stake and a per day basis.

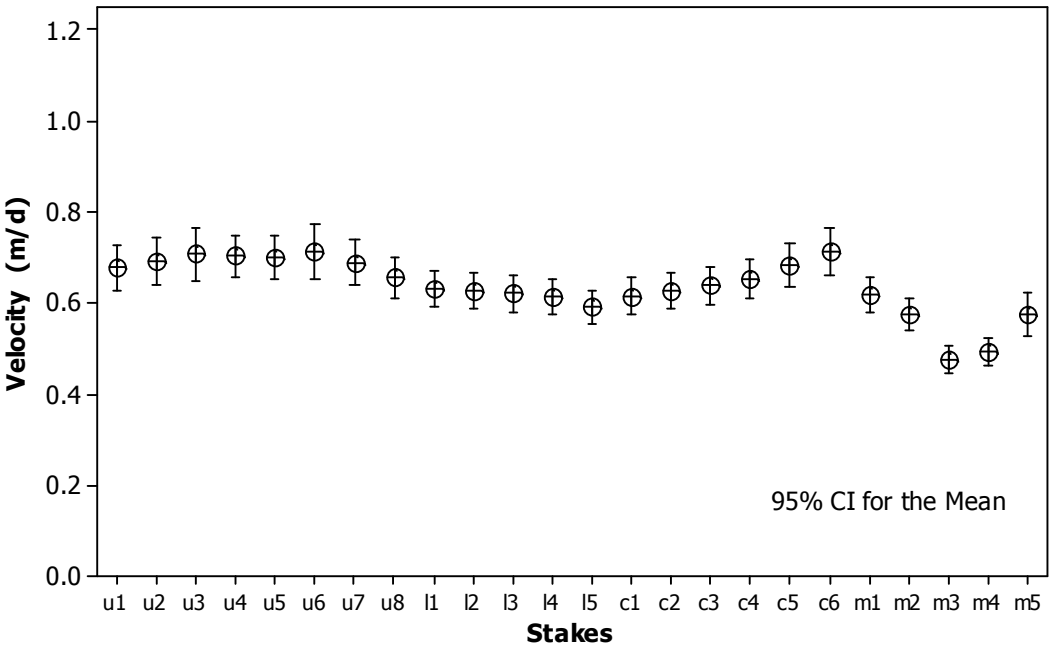

Figure 6.16 The 95% confidence interval of the mean for surface velocity recorded at individual stakes in the lower Fox Glacier during the winter study period.

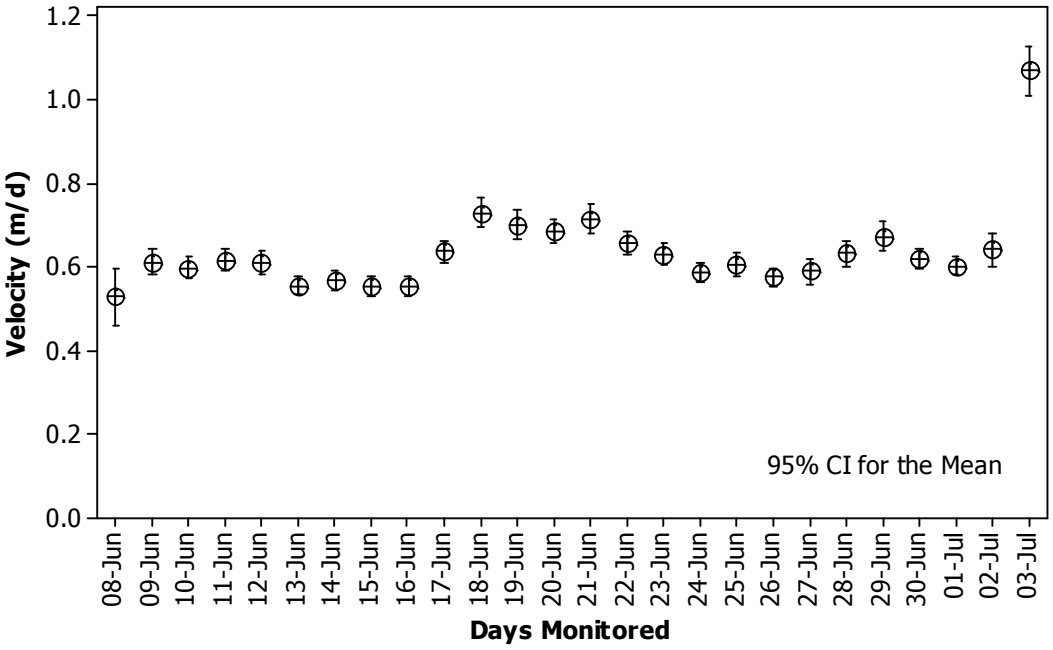

Figure 6.17 The 95% confidence interval of the mean for the surface velocities recorded on the lower Fox Glacier on a daily basis during the winter field season.

The average flow direction (Figure 6.18) of the stakes throughout the study period was 261° (west- by-south-west). This direction is very similar to that which was recorded during the summer field season of 257°.

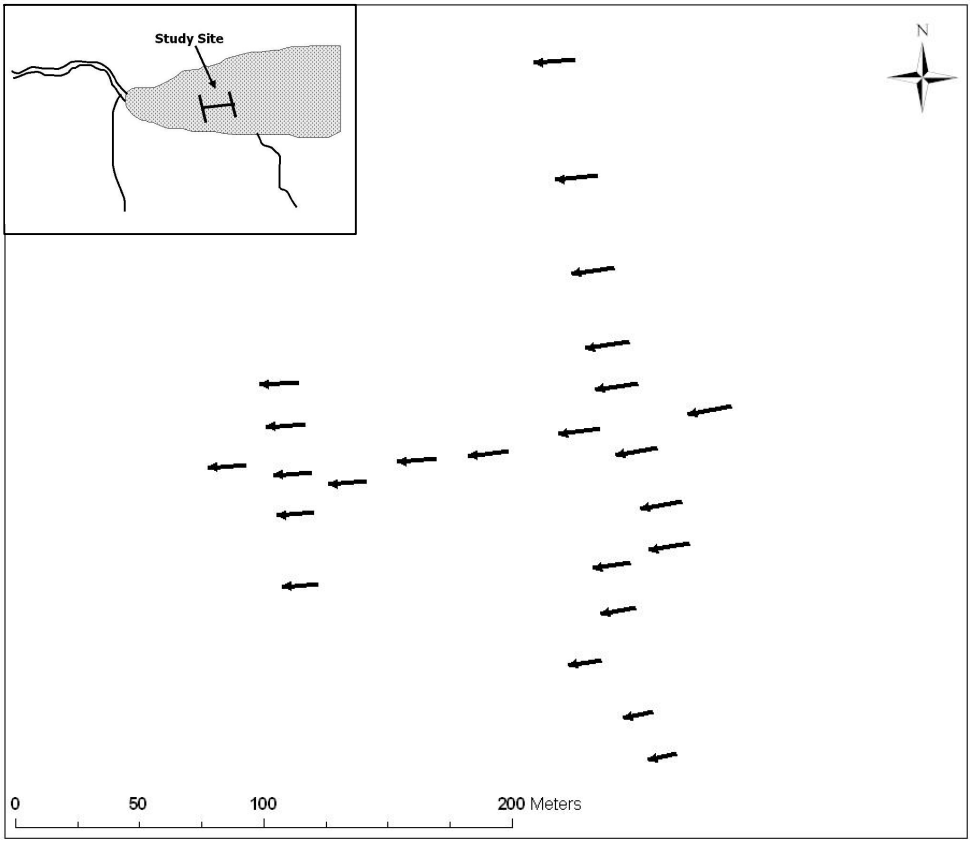

Figure 6.18 Flow vectors for flow direction recorded at individual stakes on the lower Fox Glacier during the winter field season. Insert shows the approximate 2005 ice limit and the location of the study site.

6.2.2 Spatial Variability

As during the summer, spatial velocity variability was recorded across the study site (Figure 6.19) both across glacier and up glacier. Figure 6.20 is a plot of the upper transect (including some debris-covered stakes), which shows the retarding of velocity on the true left side. Stake m3 was positioned closest to this true left side, being only 90 m from the valley wall. This stake recorded an average surface velocity of 0.48 m d^{-1}, and was travelling at only 69% of the velocity of stake u5 located near the centre of the glacier. Slight retardation can be seen at stake u1 on the true right, but as was the case during summer, this most northern stake was still around 150 m from the valley sides due to crevassing, which made access to the true right difficult.

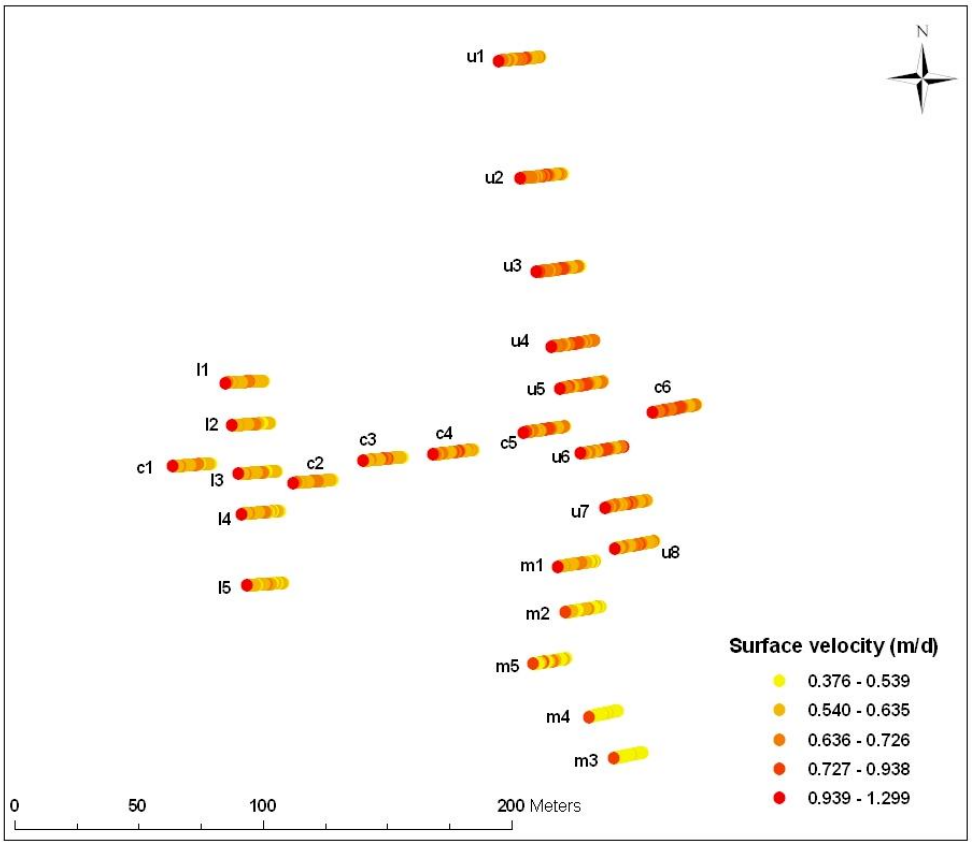

Figure 6.19 Individual daily surface velocity recorded at individual stakes on the lower Fox Glacier during the winter field season.

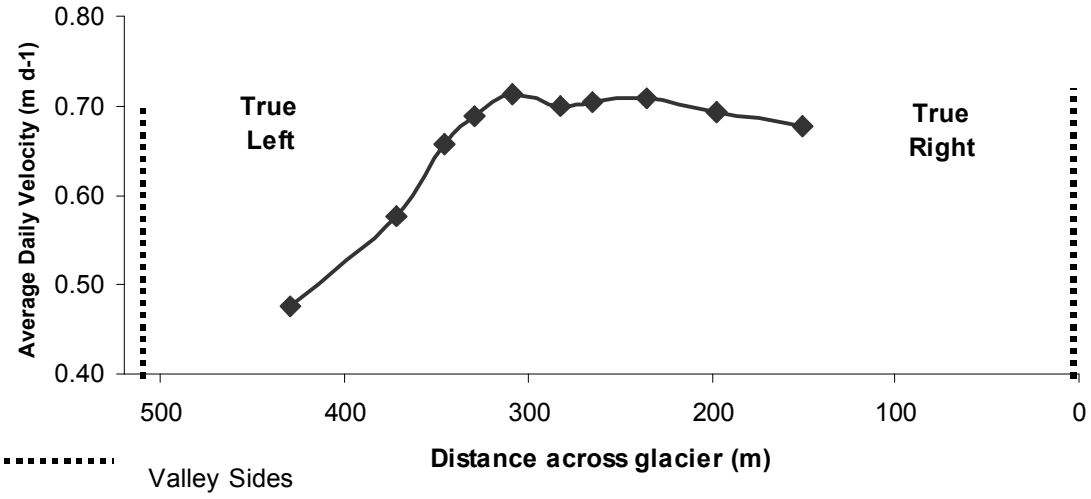

Figure 6.20 Variation in velocity across glacier based on average surface velocities recorded at stakes u1-u8, m2 and m3 on the lower Fox Glacier during the winter field season.

Variation in average surface velocity from the stake lowest and closest to the terminus, stake c1 (408 m a.s.l), to the stake highest and furthest from the terminus, c6 (443 m a.s.l), was 14% (Figure 6.21 and 6.22). With average velocity increasing by around 0.10 m d^{-1} over a distance of 195 m, with an altitudinal gain of 35 m.

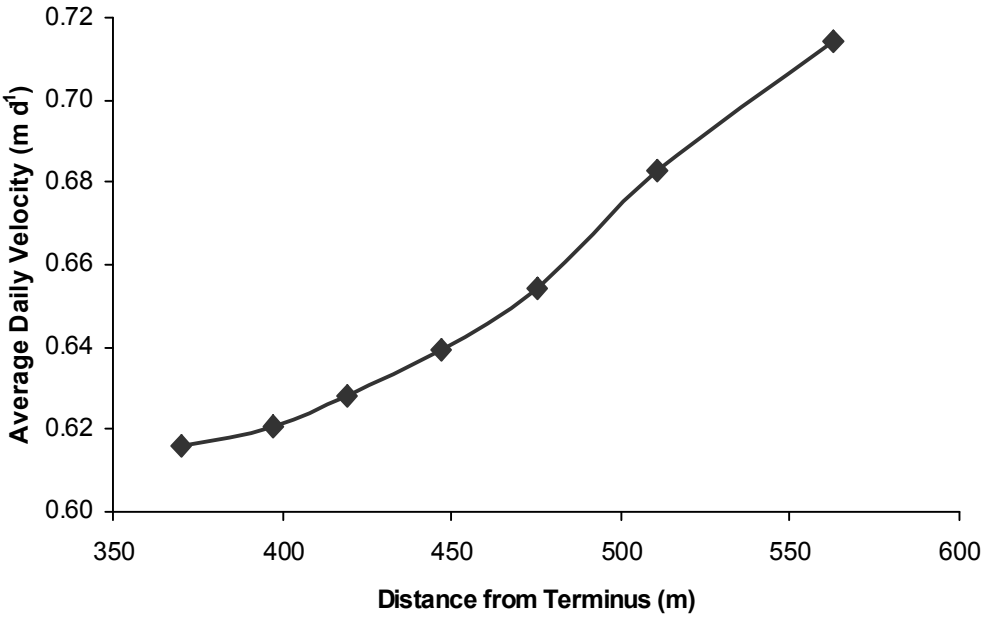

Figure 6.21 Variation in velocity with increasing distance from the terminus based on average surface velocities recorded at stakes c1-c6 and l3 on the lower Fox Glacier during the winter field season.

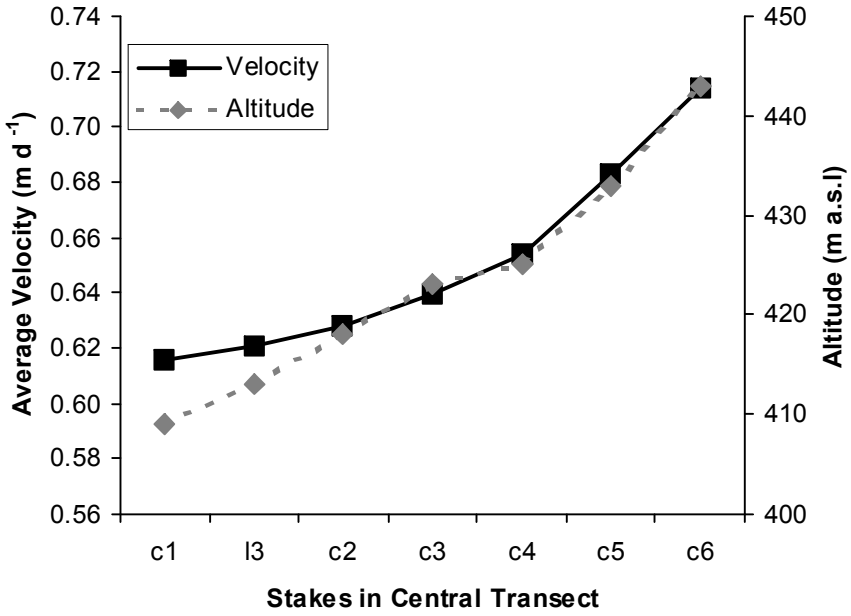

Figure 6.22 Relationship between increasing velocity and increasing altitude along the central stake transect on the lower Fox Glacier during the winter field season.

Spatial variability in surface velocity was also recorded between individual stakes (Figure 6.23) with stake m5 notably moving in surges in comparison to other stakes (i.e. u4), and in comparison to the overall daily trend, and did not appear to be precipitation related (see later). These surges could result in daily velocities varying as much as 0.25 m d^{-1} or 29%. Inspection of the glacier surface around this stake revealed a crevasse opening up about one metre upglacier, so it is likely that the surging velocities were related to crevassing.

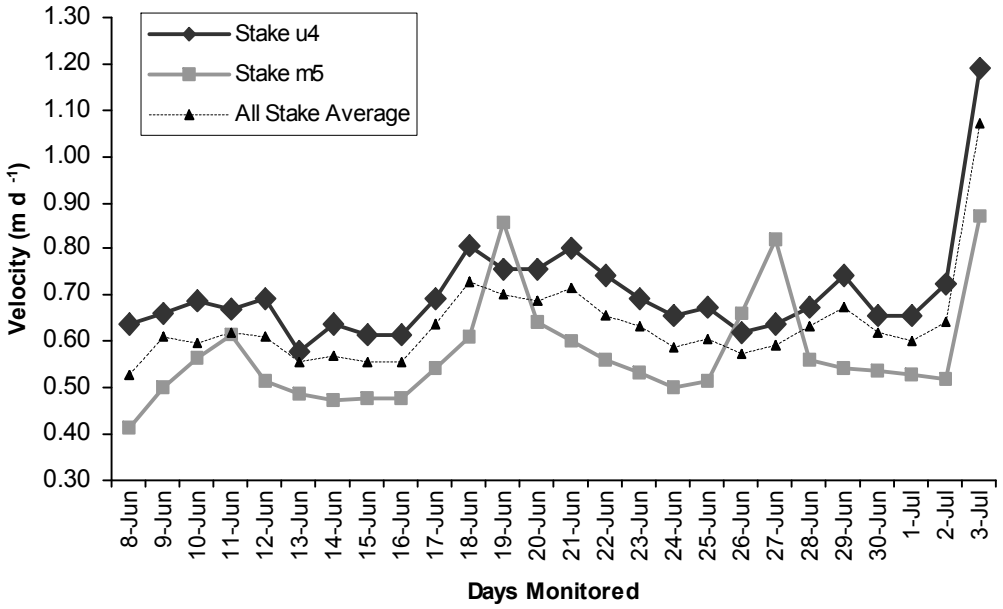

Figure 6.23 short-term variations in average daily surface velocities between different stakes recorded on the lower Fox Glacier during the winter field season.

6.2.3 Temporal Variability

During the winter field season there were temporal variations in ice velocity with distinctive peaks on the 18th and 29th June and 3rd July (Figure 6.24). The peak on the 18th June involved around a 20% increase in velocity compared to the few days prior, and the major peak on the 3rd Feb, involved an increase of over 40% in average surface velocity. All the velocity peaks seen in Figure 6.24 appear to correlate to heavy rainfall events, so this will be dealt with in detail in section 6.2.5.2

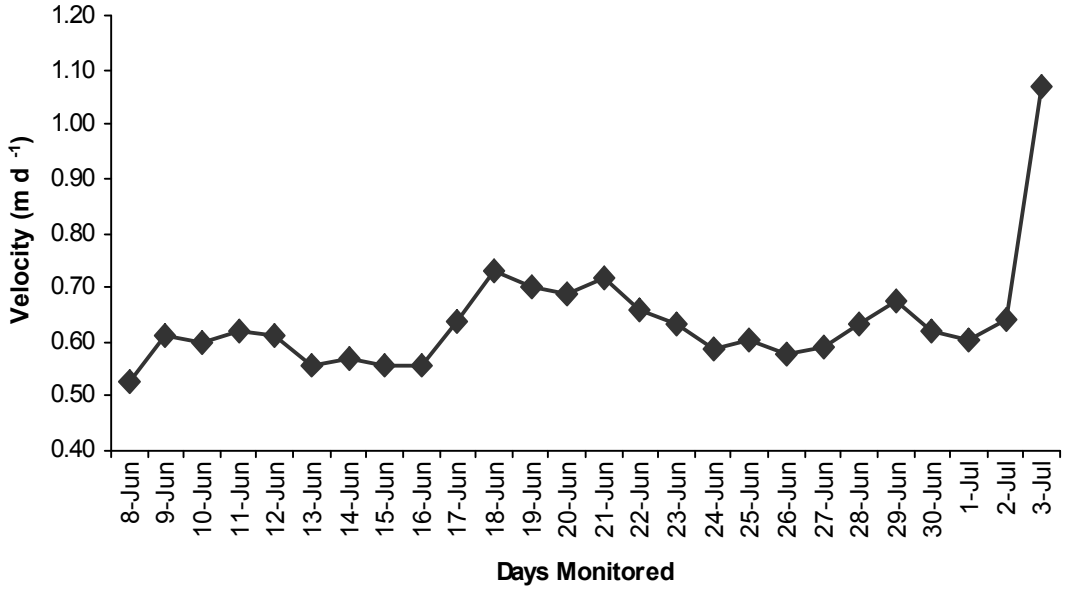

Figure 6.24 Variation in average surface velocity over time as recorded on the lower Fox Glacier during the winter field season.

6.2.4 Velocity and Climate Variables

6.2.4.1 Introduction

To consider how much influence (if any) daily climate variables may have had on surface velocity during winter, Pearson's correlation was conducted between surface velocity and the measured climate variables (Table 6.6), followed by multi-variant regression analysis using a general linear model.

Table 6.6 Pearson's correlation of velocity and climate variables measured on the lower Fox Glacier during the winter field season. The top number is the correlation co-efficient and the bottom number the associated *p*-value.

	Temperature	Precipitation	Humidity	Wind Speed	Wind Direction	Solar Radiation
Velocity	0.206	0.744	0.574	0.065	0.559	-0.076
	0.312	0.000	0.002	0.753	0.003	0.711

The multi-variant regression analysis produced the following equation:

Velocity = 0.542 - 0.002 T + 0.001 P + 0.001 H + 0.010 WS + 0.056 WD - 0.00002 SR (14)
(adjusted r^2 44.5%)

Pearson's correlation (Table 6.3) highlighted relationships between velocity and precipitation (Pearson's r = 0.744, p-value = <0.001), and between both humidity and wind direction, both with co-efficient values greater than 0.550. Likewise best subset regression analysis identified precipitation as the climate variable with the most

influence on velocity variations, with an adjusted r^2 value of 53.5%, and p-value <0.001. The relationships highlighted between velocity and humidity and velocity and wind direction are due to the relationship that both humidity and wind direction were found to have with precipitation events during winter (Table 4.8). Therefore neither of these climate variables has a direct impact on surface velocity variation so no further consideration will be given to these climate parameters.

6.2.4.2 Velocity and Precipitation

A graph of average daily surface velocity plotted against precipitation shows velocity peaks occur either on, or shortly after, precipitation events (Figure 6.25). In Figure 6.26, a 13% increase[8] in surface velocity occurred between the 8th and 9th June with 54 mm of precipitation, a 23% increase with 133 mm between the 16th and 18th June, a small 4% increase with 120 mm between the 21st and 22nd June, a 12% increase with 120mm between the 27th and 29th June, and a large 44% increase coinciding with 244 mm from July 1st to 3rd. During summer (section 6.1.4.3) the 20% velocity increase that coincided with the precipitation event on January 22nd (116 mm) appeared to have an instantaneous effect, as does the increase on the 3rd July. However, the heavy rain events on the 17th and 28th June appear to have a lag, with velocity not peaking until the next day. The very low percentage increase on the 22nd June appears to be an outlier, but as can be seen in Figure 6.25, this precipitation event closely followed one of similar magnitude only three days prior, and velocity still appeared to be elevated from this event, which may have resulted in a smaller percentage increase.

As was highlighted in section 2.6.4 the drainage system on a glacier can be very inefficient in winter, as due to the reduction in surface melt-water, drainage conduits close via ice deformation (Benn and Evans, 1998). This factor could create a lag in the time it takes for surface water to be delivered to the base of the glacier where it can subsequently enhance basal sliding. Field notes on the 18th June record how there was surface water flowing on the glacier, and that some of the crevasses and moulins were water filled, indicating that they were not draining efficiently. This pooling of water in crevasses had not been seen during the summer field season, instead there was a steady flow of surface melt-water down both crevasses and moulins. Such pooling is indicative of an inefficient, poorly developed drainage system.

[8] Percentage increase in velocity was calculated by considering the velocity change recorded on the day prior to precipitation and the velocity peak recorded one or two days later.

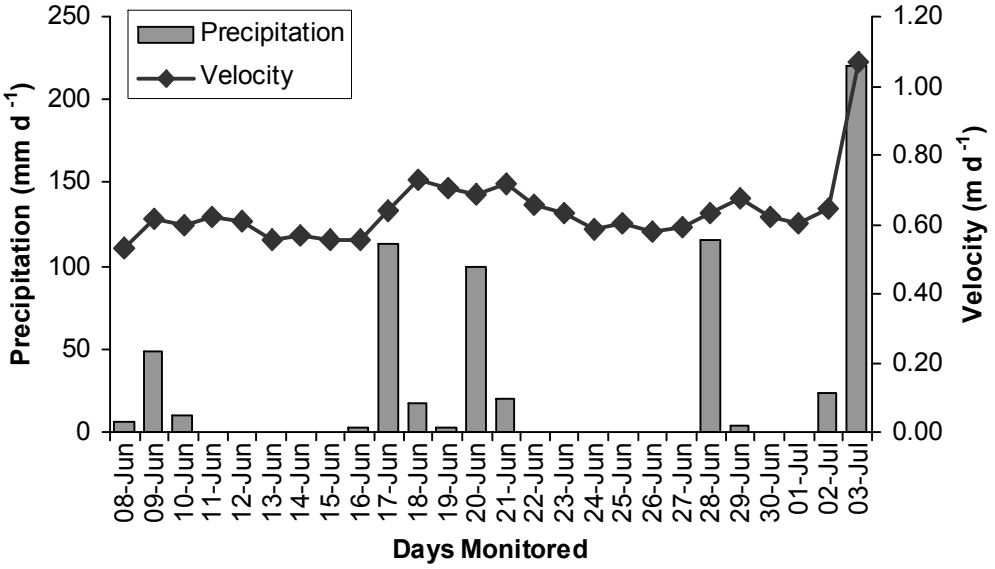

Figure 6.25 Relationships between average daily velocity and precipitation recorded on the lower Fox Glacier during the winter field season.

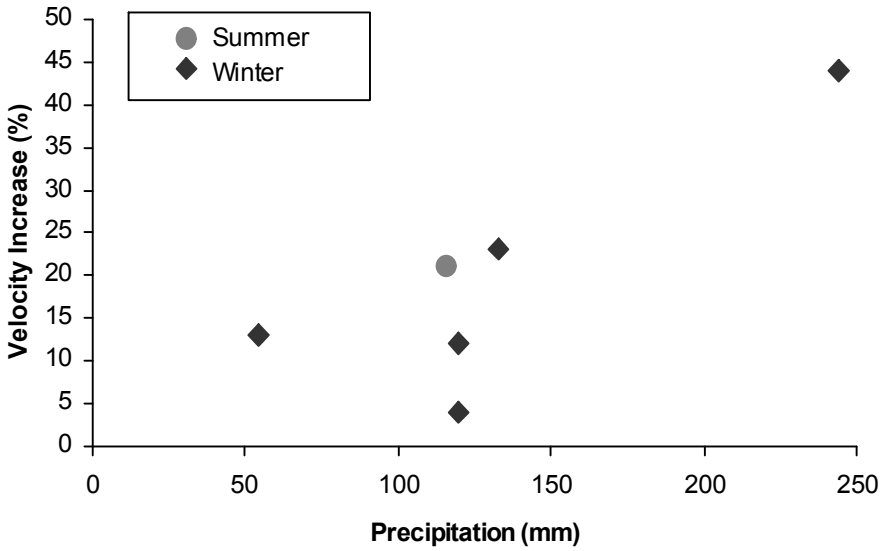

Figure 6.26 Percentage increase in surface velocity with precipitation events on the lower Fox Glacier during both summer and winter monitoring.

Another factor highlighted by the graph is difference in the magnitude of change in velocity with a 24% increase coinciding with 115 mm of precipitation, and a 44% increase with 244 mm of precipitation, equating to around a two fold increase in both velocity with precipitation. However, it appears small amounts of precipitation (18th January and 10th June) can be received with no obvious effect to average surface velocity, indicating that there is a threshold in precipitation that needs to be reached before any change takes place.

6.2.5 Velocity and the Synoptic Situation

When looking at any possible relationship between the daily synoptic situation and average surface velocity (Figure 6.27). It can be seen that higher than average velocities seem to be associated with both north-westerly flows (III) and fronts/troughs (V) and lower then average velocities seem to coincide with north to north-easterly flows (II). Although climate parameters do not appear to exert a large influence on velocity variation, both synoptic situation III and V can be associated with precipitation thereby resulting in this relationship.

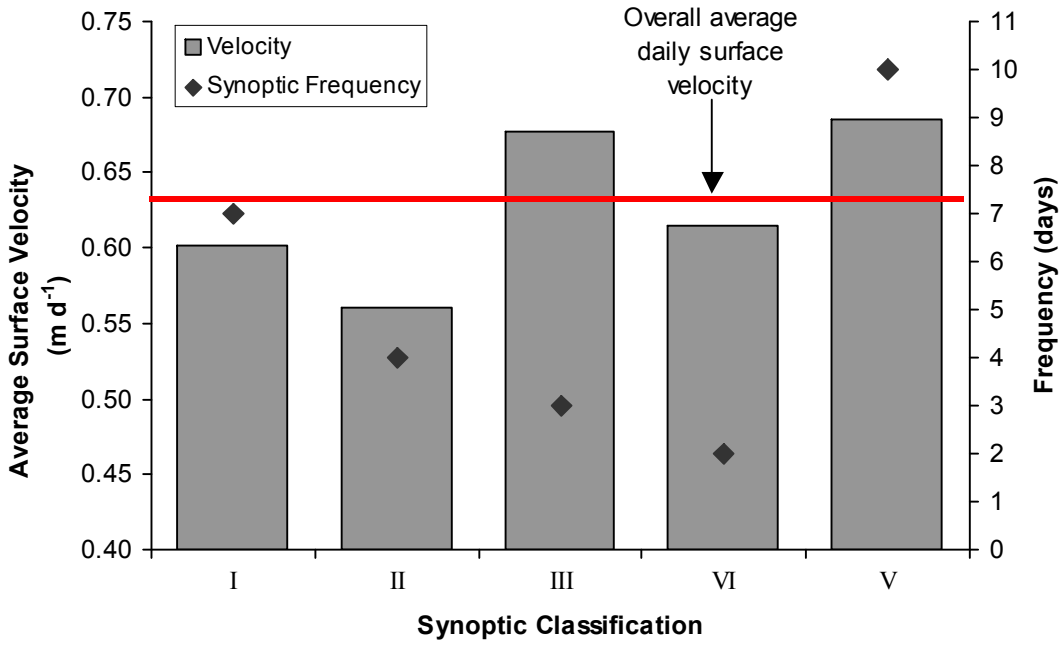

Figure 6.27 Average surface velocity recorded during different synoptic situations and their frequency during the winter field season.

6.3 Intra-annual Variation in Velocity

With the exception of the very high velocities recorded on the 3rd July (coinciding with a very heavy precipitation event), there is absolutely no overlap in the velocity data (Figure 6.28), with an average daily velocity during summer of 0.87 m d^{-1} and for winter 0.64 m d^{-1}. This equates to a 26% decrease in the average surface velocity during the winter, a figure similar to that found on Northern Hemisphere glaciers (section 2.6.4) where a differences of 20% has been recorded.

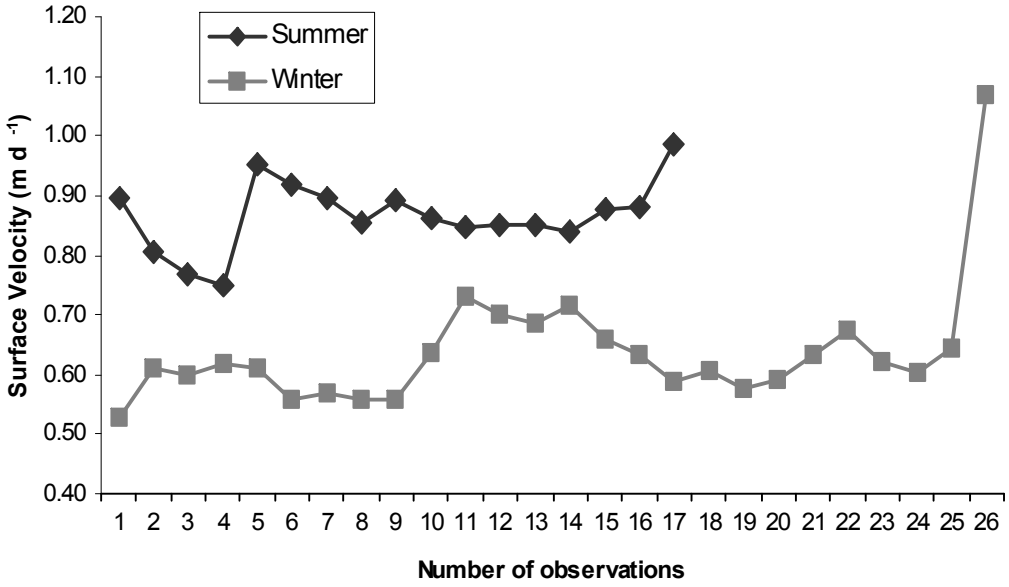

Figure 6.28 Comparison of average daily surface velocity on the lower Fox Glacier during the summer and winter field seasons.

As noted in section 3.2.2 there was a small difference in the overall average geographic location of the summer and winter stake networks, with the summer network being around 23 m upglacier (east) of the winter network. But due to the glacier terminus advancing around 20 m in between the field seasons, the stake networks were in very similar positions in relation to the distance from the terminus. In section 2.6.3 it was outlined how velocity tends to increase as distance from the terminus increases up to a maximum at the equilibrium line. This spatial variation in velocity was recorded in both summer and winter (sections 6.1.2 and 6.2.2), with an averaged velocity increase of 0.0006 m d^{-1} per metre (the average change in velocity upglacier within the study site during both the summer and winter field seasons). Therefore over 6 metres (the difference in average distance from terminus between both field seasons) equates to 0.0036 m d^{-1}, which does not significantly impact on the average velocities recorded during the different field seasons.

During summer the importance of precipitation events to temporal changes in velocity was not overly clear, although on the one occasion when heavy precipitation was received, there was a 20% increase in velocity. However, with only one data set this was by no way conclusive. During winter season five precipitation events occurred with four of these being substantial (>100 mm), and associated surface velocities increased from 14 to 44%. The velocity response to the summer precipitation event appeared to be instantaneous, where as during winter on some occasions it was immediate, but on others a lag appeared to exist (Figure 6.29).

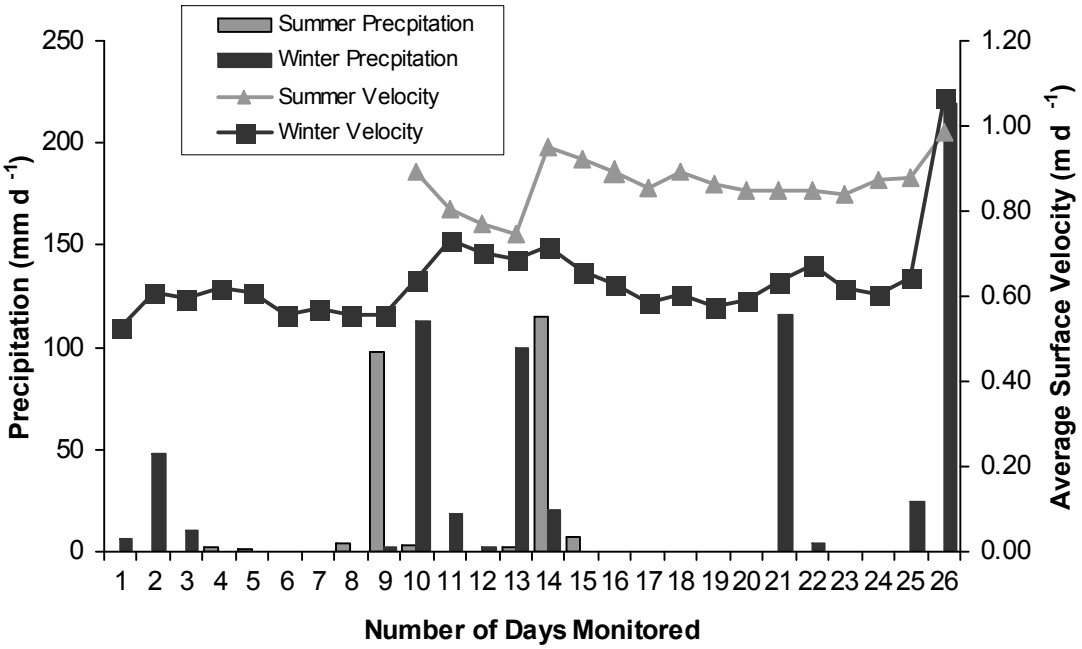

Figure 6.29 Relationship between average surface velocity and precipitation during both the summer and winter field seasons.

The spatial variability in surface velocity recorded during both field seasons was very similar, with a retarding of velocity on the true left side of the glacier. In addition, on both occasions there was a small increase in surface velocity upglacier, as distance from the terminus (and altitude) increased.

6.4 Response Time

As outlined in section 2.7 a general estimate of the response time of a glacier can be calculated by using the terminus velocity and glacier length (equation 7). During summer the stake closest to the terminus (a7), had an average velocity of 0.81 m d^{-1} while in winter, stake c1 averaged 0.62 m d^{-1}. Taking the average velocity of these stakes (0.72 m d^{-1}) and the current (2005) glacier length of 12.7 km the response time of the Fox Glacier using equation 7 would be 8.8 years.

However, Jóhannesson *et al*. (1989) suggest a more robust estimate is to use average thickness and ablation at the terminus (equation 8), a method also used by Paterson (1994). To date, no survey of ice thickness has been conducted on Fox Glacier, but a longitudinal profile estimated by Ruddell (1995) indicates average thickness could be around 200 metres. In addition, no annual survey of ablation has been conducted to give a net balance (negative), therefore the measurements taken during this study are

used for the equation but only provide a general estimate of annual ablation (c.22 m a^{-1})[9]. The above figures for thickness and annual ablation would give a response time of 9.1 years.

Using an application of equation 8, and the results from equation 7, ice thickness can also be estimated by:

$$H = T_M . -b \quad (15)$$

$$= 8.8. 22$$

$$= 194 \text{ metres}$$

This response time for the Fox Glacier of around 9 years, is longer than field estimates for the Franz Josef Glacier (Coates and Chinn, 1992; Suggate, 1950), but shorter than those obtained by more complex numerical modelling of Franz Josef Glacier (Oerlemans, 1997).

[9] Average daily ablation in summer was 116 mm w.e and in winter (excluding days when precipitation fell) was 4.5 mm w.e, giving a possible annual ablation of 22 m w.e.

Chapter 7: Discussion

7.1 Ablation

7.1.1 Spatial Variability

Ablation on the clean ice of the lower Fox Glacier was found to be highly variable, in particular, the variability at individual stakes on a daily basis. This high ablative variability was also recorded on the lower Franz Josef Glacier by Evans (2003), who attributed it to synoptic variability, and differing surface characteristics. Variations in surface topography and aspect were thought to contribute to some of this variability between individual stakes on the lower Fox Glacier, especially during summer, but in winter, high variability between stakes in similar topographic locations seemed to indicate that the causes were more complex. In the future, monitoring climate variables at individual stakes may help determine whether subtle variations in parameters like wind speed or temperature contribute to this variability, or if it is more strongly related to surface irregularities.

Large spatial variability existed on the lower glacier between the ablation rates on the clean ice and under debris-covered surfaces. This variability was particularly significant during the summer with the ablation rate under the debris cover being suppressed by up to 50%. This suppression of ablation is due to the insulating properties that debris cover has been found to have when it is thicker than 10 mm, and previous research has concluded that the degree of suppression increases as debris thickness increases (Benn and Evans, 1998; Nakawo and Young, 1981; Purdie, 1996; Singh*, et al.*, 2000). The relationship between increasing debris thickness and decreasing rates of ablation was apparent on the lower glacier during both the summer and winter, but results also indicate that the relationship was not solely related to debris thickness.

At some of the stakes, the presence of a layer of smaller clasts (≤5 mm) at the debris-ice interface, which were overlain by larger clasts, seemed to enhance the insulation properties of the debris cover. This phenomenon was also noted by Pelto (2000) who observed that finer-grained debris-cover seemed to have a greater insulating capacity. The focus of this study was to measure and quantify variations in ablation between the clean ice and debris-covered ice using debris thickness as the main parameter. Although variations in clast size at each stake were noted, the actual thickness of this

finer layer was not quantified. Clearly further research into the influence that this fine layer has to overall level of insulation of the entire debris layer would be interesting.

In addition to its insulating properties, during the winter, the debris cover was found to have a sheltering effect on the underlying ice during heavy precipitation events, with rates of ablation being suppressed by around 44% in comparison to that occurring on the clean ice surface. Further examination of the days on which ≥100 mm of precipitation was received showed that this sheltering effect was also sensitive to increasing debris thickness, with the thicker debris cover resulting in less ablation.

With the standard insulation effect of a debris cover, it is the ability of the debris to shield the underlying ice from both radiation and heat that leads to a reduction in the heat available for melting. This additional sheltering effect detected during this study is likely to be brought about by the reduction of raindrop impact due to protection by the debris cover, and the debris cover would also provide a buffer to any thermal effects brought about from the water interacting with the ice surface. Further research into this sheltering effect of debris-cover could confirm exactly how, and to what degree, it changes the energy fluxes that contribute to surface melt.

7.1.2 Temporal Variability

This study detected variability in ablation over varying timescales, namely hourly, daily and intra-annual variations. On the shortest of these temporal scales it was found that during summer, 36-44% of the total daily ablation occurred between 11 am and 5 pm, with the melt rate during these first six hours being more than double the rate in the following eighteen hours. Previous research in the Franz Josef névé by Kelliher *et al*. (1996) found that most ablation occurred during daylight hours, and noted that radiation fluxes largely determined this pattern. On the lower Fox Glacier it was found that both temperature (a component of Q_{H}) and incoming short-wave radiation (component of Q^*) had large diurnal variability, and are therefore considered the likely driving forces to the diurnal variability in ablation detected during this study. It is important to note however, that on the lower glacier during summer, ablation occurred continuously over a twenty-four hour period, but the rate of ablation was found to be higher rate during the day.

Previous research has identified links between variations in daily ablation and the prevailing synoptic situation (Evans, 2003; Hay and Fitzharris, 1988; Marcus*, et al.*, 1985; Owens*, et al.*, 1992). This study highlighted how one synoptic situation can have a different effect on ablation at different times of the year. During summer it was found that north to north-easterly flows, the presence of anticyclones and a heat-low all were associated with above average daily ablation rates. However during winter, it was north-westerly airflows and the passage of fronts/troughs that were associated with high rates, and the north to north-easterly flows a lower rate. Therefore the relationship between synoptic situations and daily ablation need to be considered in a temporal setting, as the effects of these systems varies at different times of the year.

Looking more closely at the driving forces behind daily ablative variability it was found that variations in climate parameters measured on the lower glacier could account for 90% and 93% of the variations in daily ablation during summer and winter respectively. During summer it was found that temperature, humidity and solar radiation were the most important parameters with positive relationships existing between ablation and temperature, and ablation and solar radiation, while a negative relationship was found with humidity. However during winter strong positive relationships were identified between ablation and precipitation, and ablation and humidity. Similar results were gained by Evans (2003) on the Franz Josef Glacier, were temperature was identified as the most influencing factor on ablation during summer.

These changes in importance of the various climate parameters during the summer and winter seasons are a reflection of the changes in the energy fluxes driving ablation at different times of the year. The importance of temperature and solar radiation during the summer, is a reflection of the importance that both radiation and sensible heat fluxes have on the energy available for melt (Braithwaite, 1981; Oerlemans, 2001). The strong relationship identified during winter between precipitation and daily ablation demonstrates how heat supplied by the latent heat and rainfall fluxes, although usually considered to be less important, can play a significant role in maritime climates (Benn and Evans, 1998; Marcus*, et al.*, 1985; Takeuchi*, et al.*, 1999). Previous research on the Franz Josef Glacier has also highlighted precipitation as having an important influence on the rate of ablation (Evans, 2003; Ishikawa*, et al.*, 1992; Marcus*, et al.*, 1985; Owens*, et al.*, 1992), therefore it can be concluded that heavy precipitation events can contribute significantly to ablation throughout the year.

Overall this study found that intra-annual variation in average daily ablation on clean-ice surfaces was large, with an 83% reduction in average daily ablation during winter. During winter precipitation was found to exert the most influence on daily ablation, but in summer, temperature and solar radiation were most important. The reduced ablation during winter indicates that on an annual scale, net radiation and sensible heat fluxes appear to be the largest driving forces on daily ablation on the lower glacier.

7.1.3 Comparison with Previous Research

Based on the results from this study the annual ablation of the Fox Glacier is around 22 m w.e. This figure is similar to that reported for the Franz Josef Glacier of 20 m w.e. (Anderson, 2003), larger than the 10 m w.e recorded on the Nigardbreen Glacier in Norway (Oerlemans, 2001) and much larger than rates recorded on glaciers in continental climates (2-3 m w.e.) (Oerlemans, 2001; Pelto, 2000). High rates of annual ablation are associated with glaciers in maritime climates that have high mass balance gradients, where large variation exists between annual accumulation and ablation, resulting in a high mass turnover (Benn and Evans, 1998; Oerlemans, 2001). With annual precipitation in excess of 10 metres and annual ablation around 22 m w.e, it can be concluded that the Fox Glacier has a large mass balance gradient.

Prior to this study being conducted there had only been two other studies on ablation on the lower Fox Glacier. Gunn (1964) reported an average ablation rate of 82 mm d^{-1} , (an average from the Fox and Franz Josef Glaciers) and Lawson (pers. comm., 2005) recording an average surface melt of 118 mm d^{-1} in February 1992 (Table 7.1). This study recorded an overall average in summer daily ablation of 129 mm d^{-1}, a figure higher than both previous studies (although not too dissimilar to Lawson). The longer duration of this study, and the high temperatures experienced in early February may have contributed to this higher average figure. As previous research has indicated (Evans, 2003; Hooker, 1995; Hooker and Fitzharris, 1999; Ishikawa*, et al.*, 1992; Kelliher*, et al.*, 1996; Marcus*, et al.*, 1985; Owens*, et al.*, 1992), and as confirmed in this study, daily climate variables have significant influence to the rate of daily ablation, therefore without knowledge of the climate conditions during the other studies direct comparison is problematic.

Table 7.1 Previous ablation research on the lower Fox Glacier including results from this study.

Study	Date	Ablation (mm d^{-1})	Location/Notes
Gunn (1964)	Jan- April 1955	82	Measured height of ice surface from bottom of drilled holes 30-40mm deep at 350m altitude Average from both Fox and Franz.
Lawson (pers. comm., 2005)	Feb 1992	118	Stake network on lower glacier Average of 17 stakes over 8 days
This Study	Jan/Feb 2005 Jun/July 2005	129 (50 – 216) 22 5* (-2 – 83)	Stake network on lower glacier c. 450 m a.s.l () Range during study *Excluding days when precipitation fell

As mentioned in Chapter 2, the Fox Glacier has over the years been thought to exhibit similar behaviour to the nearby Franz Josef Glacier. This study has found that the average summer ablation rate on the lower Fox Glacier is similar to previous studies on the lower Franz Josef Glacier (Owens*, et al.*, 1992) (Table 7.2). In addition, the Fox Glacier exhibits a large range in daily ablation, as was recorded on the Franz Josef Glacier (Evans, 2003). This similarity in summer ablation rates is likely to be related to the maritime climate of South Westland and glacier geometry, as both glaciers have a long narrow tongue descending to low altitudes.

Table 7.2 Selected key ablation research on the Franz Josef Glacier

Study	Date	Ablation (mm d^{-1})	Notes
Gunn (1964)	Jan-April 1955	82	Averaged from Fox & Franz
Marcus *et al.* (1985)	July 1981 Dec 1981	12 72	Short-term studies of 3 days duration
Owens et al (1992)	Feb 1990	137	5 days
Evans (2003)	January 2003	77 (10 -180)	48 days () Range during study

Prior to this study, no research on the winter ablation rate of the Fox Glacier had been conducted. Research on the ablation rates on the lower Franz Josef Glacier during winter reported 12 mm d^{-1} over three days in July, and 8 mm d^{-1} over three days in August (Marcus*, et al.*, 1985). Due to the longer nature of this study the overall winter ablation rate is somewhat higher (22 mm d^{-1}), a reflection of the five precipitation events that occurred during monitoring. On days without precipitation, ablation was low, ranging from -2 mm d^{-1} up to 14 mm d^{-1}, with an average of only 5 mm d^{-1}. This figure is slightly lower than that recorded on the Franz Josef Glacier, and is most likely related to the more westerly aspect of the lower Fox Glacier that results in topographic shading during winter, preventing the development of surface melt water throughout the day in clear frosty weather.

7.2 Surface Velocity

7.2.1 Spatial Variability

This study considered spatial variability in surface velocity on the lower Fox Glacier in three areas, across-glacier, up-glacier and between individual stakes within the stake network. Across-glacier, or transverse variability in surface velocity, was similar during both the summer and winter field seasons. Retarding of velocity was detected along the true left side, with the southern most stakes moving at 66% (summer) and 69% (winter) of the rate of the central stakes. This reduction in ice flow velocities as distance to valley sides decreases is due to an increase in shear stress along the valley sides (Figure 2.16 and Figures 6.5 and 6.20).

Up-glacier variability in surface velocity was reasonably consistent, with 15% and 14% increases over a distance of just under 200 m during the summer and winter field seasons respectively. Both surface slope and ice thickness tend to increase as distance from the terminus increases, and as already outlined, these two factors are the primary drivers of velocity. Therefore, as with the transverse variability, large-scale influences exert most control on the up-glacier velocity variations.

On a smaller spatial scale, variability was recorded between individual stakes with some stakes moving in noticeable surges in comparison to the general velocity trend. This surging was linked to the proximity of these stakes to developing crevasses. Crevasses are fractures in the ice that open in response to tensile stress, occurring in areas where stress exceeds the strength of the ice (Benn and Evans, 1998; Paterson, 1994). As mentioned in section 2.6.3, ice flow in a glacier is not uniform, but rather a mixture of areas with extending and compressing flow, that in turn create variations in the amount of tensile stress being imparted on the ice. When velocity is averaged over time, these smaller spatial variations are masked by smoothing (Paterson, 1994). Therefore, it is only during more intensive monitoring (i.e. daily) as conducted during this study, that these smaller spatial velocity variations will be detected.

7.2.2 Temporal Variability

Variations in the velocity on the lower Fox Glacier were considered on both daily and intra-annual scales. During the summer field season the overall average daily surface velocity was 0.87 m d^{-1}, and in winter only 0.64 m d^{-1}, equating to a 26% reduction in surface velocity during the winter season. This deceleration in velocity during the winter

is similar to that recorded on a glaciers in both North America and Europe, where seasonal velocity variations of up to 30% were related to changes in basal water supply as well as variations in ice thickness (Hooke*, et al.*, 1989; Kamb and Engelhardt, 1987; Paterson, 1964; 1994; Willis, 1995; Willis*, et al.*, 2003).

On the lower Fox Glacier, this winter velocity reduction is likely to be linked to the former, as ice thickness had actually increased (c.3 m) between study seasons due to glacier growth and advance. This increase in ice thickness could have effectively masked the true seasonal velocity decrease. Altitudes recorded by RTK-GPS survey and valley features from the 1985 aerial photograph (SN 8478 G/11) indicate that ice thickness on the lower glacier is in the vicinity of 150 metres. Since velocity varies by the fourth power of ice thickness this increase in ice thickness, albeit small, should have some effect on velocity.

Ignoring any possible changes to surface slope, a three-metre increase in ice thickness should result in an 8% increase in velocity, which theoretically would have increased average winter velocity by 0.05 m d^{-1}. If this velocity increase due to increasing thickness is taken into account, average winter surface velocity is actually 32% lower than summer. This result is slightly larger than recorded in the literature (Kamb and Engelhardt, 1987; Paterson, 1964; Willis, 1995; Willis*, et al.*, 2003), and indicates that there is a significant reduction in basal sliding on the lower Fox Glacier during the winter months.

Topographic shading of the lower glacier during winter resulted in the lower glacier receiving basically no direct sunlight (with the exception of the wedge outlined in section 5.2.2.2). One of the consequences of this shading was that there was no melt water production, and the ice surface remained very blue and glazed. Ablation measurements conducted during this study recorded an 83% decrease in surface melt during the winter field season. This would lead to a significant drop in the amount of water being supplied to the base of the glacier, resulting in lower water pressures and a subsequent reduction in basal sliding.(Benn and Evans, 1998; Hooke*, et al.*, 1989; Mair, 1997; Mair*, et al.*, 2001; Nienow*, et al.*, 1998; Paterson, 1994; Willis, 1995; Willis*, et al.*, 2003).

Previous research on the Franz Josef Glacier has not detected any seasonal velocity variation, instead short-term changes have been linked to variations in water supply (Anderson, 2003). Due to the more north-westerly aspect of the tongue of the Franz

Josef Glacier (as opposed to the westerly aspect of the Fox Glacier), the surface of the lower glacier still receives direct sunlight throughout winter, and some supra-glacial meltwater channels still flow (The Guiding Company, pers. comm., 2005). Therefore, it is likely that the Franz Josef Glacier does not have as larger seasonal contrast in the supply of meltwater as the Fox Glacier does. It has been suggested that the Franz Josef Glacier could have a well-established sub-glacial drainage system throughout the year, due to year-round melting (Goodsell*, et al.*, 2005), which could also contribute to the lack of any noticeable seasonal velocity variation.

Research on temperate glaciers like the Fox Glacier (where the base of the glacier is at the pressure melting point) has indicated that basal sliding may account for around half of the glaciers motion, thereby being an important component of total velocity (Andreasen, 1983; Paterson, 1969). As outlined in Chapter 2 the process of glacier sliding is inextricably linked to the morphology of the glacial drainage system. Glacial drainage systems have been found to evolve from a highly efficient channelised system during summer, to a less efficient distributed system during winter. During times of decreased water supply (i.e. winter), ice deformation results in the gradual closure of channels and orifices, conversely, an increase in water, will lead to a reopening and expansion of channels and orifices (Benn and Evans, 1998; Iken*, et al.*, 1983; Mair, 1997; Mair*, et al.*, 2001; Nienow*, et al.*, 1998).

Lack of knowledge about the sub-glacial drainage system of the Fox Glacier makes it difficult to ascertain whether or not it does evolve to a more inefficient system during winter, or whether its drainage system remains well-established like what is thought to happen at Franz Josef Glacier (Goodsell*, et al.*, 2005). However, evidence of water pooling on the surface during winter, seems to indicate that on the lower glacier, drainage efficiency is reduced to some degree during the winter season.

On a daily basis, variations in surface velocity during this study were linked to variations in water supply, in particular, precipitation events. Increases in surface velocities ranging from 4% to 44% occurred either in conjunction of, or shortly after, precipitation events. What became apparent during this study was that small amounts of precipitation (i.e.<5 mm) could fall with no noticeable change to surface velocity, but larger amounts seemed to produce a response. Water pressure at the ice-bed interface, rather than water volume, is the controlling factor on basal sliding (Paterson, 1994). Therefore this varying response to precipitation recorded on the lower glacier

during winter, indicates that a threshold level must be reached before any velocity response takes place, this threshold being the separation pressure (section 2.6.4).

This variation in the magnitude of the velocity response to precipitation does not appear to be straightforward, as on one occasion over 100 mm of precipitation was received with very little (4%) velocity response. This lack of response occurred to a precipitation event that closely followed one of similar magnitude only three days prior, and velocity was already in an elevated state. It may be that drainage conduits and channels had already recently adjusted to transport the increased water supply from the earlier event and had not yet begun to be re-closed by ice deformation. This would result in the water from this subsequent event being easily transported within the existing drainage morphology, and therefore not substantially increasing water pressure. Hooke *et al*. (1989) also came to this conclusion with regards to a similar occurrence on the Storglaciären in Sweden. However, it is believed that changes to the sub-glacial drainage system are not that instantaneous, instead reflecting water volumes over the past couple of weeks (Paterson, 1994).

If the glacial drainage system cannot evolve this rapidly, then such short-term velocity variations may be related to processes involving water storage. Velocity peaks have been found to coincide with the growth of storage cavities (Figure 2.14). When water pressure in these cavities exceeds the ice overburden pressure (separation pressure), the glacier is effectively lifted and basal sliding enhanced, for example the uplift of the Unteraargletscher at the beginning of the melt season (Iken*, et al.*, 1983). Daily velocity variations on the Franz Josef Glacier have also been attributed to intense rainfall, and short-term (< 48 hours) storage of water (Goodsell, 2005).

In addition to variations in the magnitude of the velocity response, this study also detected variation in the time taken in which a response was generated. During summer only one heavy precipitation event was measured by velocity survey, but on this occasion there appeared to be an instantaneous response. In winter however, the velocity response did not always seem to be instantaneous, and at times lagged precipitation events by around twenty-four hours, with surface velocity not peaking until the following day.

If the drainage system of the Fox Glacier does evolve to a more inefficient system during winter months, then this change in morphology could create a lag in the time it takes for surface water to be delivered to the base of the glacier. Alternatively, this time

lag may be indicative of water storage, with cavities at the base of the glacier taking time to fill, before water pressures reach separation pressure. The time lag could also be derived from a combination of the above two processes.

The elapsed time in between precipitation events also seemed to be an influencing factor, with a smaller percentage increase in velocity for a precipitation event that occurred in quick succession to another event of similar magnitude. On the two occasions where a lag in response occurred, there had not been any precipitation for at least five consecutive days. Therefore it is feasible that this five day time period is long enough for ice deformation to begin to re-close drainage passages during the winter months, or that sub-glacial water cavities have emptied and require refilling, either process resulting in a delay in the effect that precipitation can have on basal sliding.

Aside from precipitation events driving short-term velocity increases, a small velocity increase (11%) was recorded at the beginning of February that coincided with a temperature increase of around 3^{o}C and an ablation increase of 20-30% (around 0.2 m w.e). This velocity increase represents a direct relationship between ablation (in particular surface melt followed by run-off) and velocity, with the increase in ablation (driven by increased temperatures), supplying more water to the sub-glacial drainage system, increasing water pressures, and subsequently enhancing velocity. This phenomenon was also recorded on the Storglaciären in Sweden (Hooke*, et al.*, 1989).

Surface velocity was found to have an indirect link to the general synoptic situation. During summer higher than average surface velocities were found to be associated with the passage of fronts/troughs and with the heat-low, and in winter it was north to north-westerly flows as well as fronts/troughs that showed enhanced velocity. All these synoptic situations were associated with an increase in the supply of surface water whether by precipitation or enhanced ablation, therefore it can be concluded that it is the supply of water that is the influencing factor to velocity fluctuations, and not the synoptic situations directly.

Clearly any variations in surface velocity cannot be considered in isolation from the time and location at which they occur. The intricate relationship that velocity has been found to have with drainage morphology means that the timing and magnitude of velocity variations will change both throughout the year and around the glacier, depending on the conditions present at the time. However, just how fast the glacial

drainage system can adjust to variations in the supply of surface water could warrant further investigation.

7.2.3 Response Time

A generalised response time of around 9 years was calculated for the Fox Glacier utilising the equations of Johannesson *et al*. (1989) and Paterson (1994), and data gathered during this project. It is important to note that this is a general estimate only, as due to the short nature of this research project, velocities and ablation rates measured during summer and winter had to be extrapolated to annual figures. Clearly more continuous measurements over an entire balance year would be desirable to improve such estimates.

The time lag derived was found to be longer than field estimates for the Fox and Franz Josef Glaciers (Coates and Chinn, 1992; Suggate, 1950), but shorter than those numerically modelled for Franz Josef Glacier (Oerlemans, 1997). Evans (2003) estimated a response time for the Franz Josef Glacier using equation 8 from Johannesson *et al*. (1989) of 9 years, based on glacier thickness of 200 m and a negative net balance of 23 m. Using equation 7 and the Franz Josef's higher surface velocity (c. 1 m d^{-1}) a response time of only 6 years is gained. It is generally considered that the Fox Glacier has a longer response time than the Franz Josef Glacier, and that response at the terminus of the Fox Glacier tends to lag the Franz Josef Glacier by around one year (Chinn, pers. comm., 2005).

When considering data gathered by NIWA in their annual glacier snowline survey (Chinn*, et al.*, 2002b; 2003; Chinn*, et al.*, 2005), it can be noted that in 1995 there was an average depression of the ELA by 150 metres, and from 1992 through to 1997 there was a general increase in mass over the glaciers monitored along the Southern Alps of New Zealand (Figure 7.1). If the response time of the Fox Glacier is in the vicinity of 9 years, this gain in mass in the mid 1990s may well be linked to the current (2005) advance. A response time of 9 years may also explain the advance during the mid 1990s following reasonable mass increases from 1983 to 1985. Following from this, it may be that the full impact of recent mass gains (2003 to 2005) may not be expressed at the glacier terminus until around 2013.

Previous research has correlated glacier advance in New Zealand with changes in the Southern Oscillation Index (SOI), in particular mass gain during periods of a negative

SOI associated with El Niño conditions (Clare*, et al.*, 2002; Hooker, 1995; Hooker and Fitzharris, 1999; Salinger, 2005; Tyson*, et al.*, 1997). Fluctuations in the SOI (Figure 7.1) can be seen to have remarkable similarity to the recorded mean annual snowline departures.

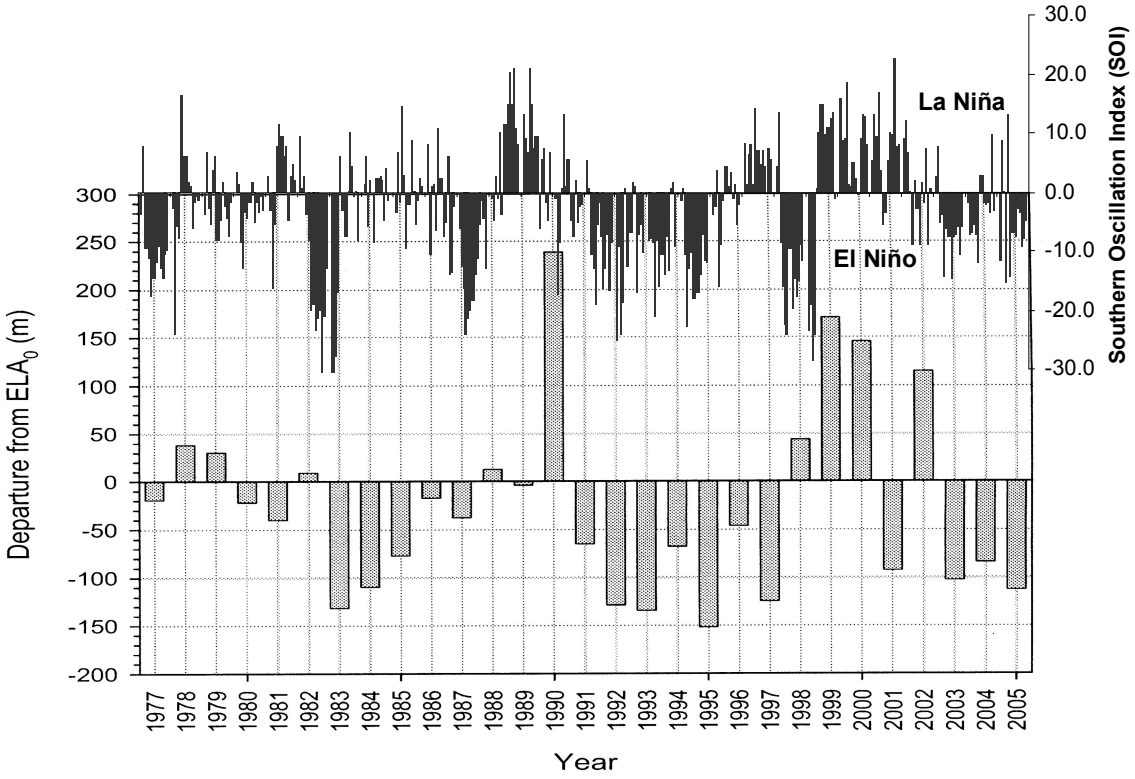

Figure 7.1 Mean annual departures (bottom) from the steady state ELA as monitored by NIWA in the annual snowline survey (Chinn *et al.*, 2005), overlain by variations in the Southern Oscillation Index (top) as recorded by the Australian Government Bureau of Meteorology. (Bureau of Meteorology, 2005). Patterns of El Niño (negative SOI) years show similarity to those with negative snowline departures that correspond to positive mass gains.

The reality of any future advances or fluctuations is of course more complex, as negative mass balances in 1999, 2000 and 2002 will be integrated into the positive balance years as these climate signals are gradually transmitted along the entire length and volume of the glacier. Therefore the whole concept of calculating response times becomes problematic, and results should be regarded as a general estimate.

7.2.4 Comparison with Previous Research

Variations in surface velocity brought about by changes to ice thickness, and distance from the terminus, means that comparison between velocity measurements taken at different temporal and spatial scales can be problematic, especially when consideration

is given to the dramatic change in volume and length of the Fox Glacier since the first measurements were made by Wilson (1896). The low velocities recorded by Wilson (1896) are likely to be related to the lesser slope lower in the valley and the retreating nature of the glacier at this time. Maps and descriptions by Gunn (1964) indicate that his B survey (0.42 m d^{-1}) in Jan-Feb 1955 (Table 7.3) may have been in a similar position to this study, although the terminus was still at least one kilometre further down valley (Figure 2.4). A better comparison can be made between this study and the work of Lawson (pers. comm., 2005) who in 1992 recorded summer velocities ranging from 0.45 m d^{-1} up to 0.98 m d^{-1} with an overall average of 0.70 m d^{-1}. That survey was conducted at a very similar site to this study, and the glacier in 1992, like in 2005, was in a period of advance.

Table 7.3 Previous surface velocity measurements on the lower Fox Glacier including data from this study.

Study	Date of Measurement	Velocity (m d^{-1})	Location/Details	Notes
Wilson (1896)	6th July – 3rd August 1894	0.25 0.27 0.24 0.24 0.34 0.08	K1 K2 K3 K4 K5 K6 (Figure 2.15 and Figure 2.3)	Glacier in period of retreat. Transect about 2 km upvalley from terminus at the time of survey and & 600m downglacier from present terminus.
Speight (1935) Mr H.L Hume	9th Sept-30th Oct 1932 & 30th Oct – 6th Dec 1932	0.21 & 0.18 0.30 & 0.25 0.44 & 0.34 0.49 & 0.50 0.54 & 0.54	1 - 65.6m from glacier edge 2 - 119.5m " " 3 - 196m " " 4 - 248.4m " " 5 - 296.3m " "	Glacier possible in advance phase, based on Franz Josef Glacier. Transect approx 1200m up from terminus, which is approx 1 km downvalley from present terminus
Gunn (1964)	Jan-Feb 1955	1.313 0.419 0.32 0.127 0.077 0.051	A - Victoria Creek B – Below lower icefall C – Yellow Creek D Terminal Moraine E Terminal Moraine F – Terminal Moraine	Glacier likely to be in retreat phase. B appears to be close to present study area. Refer to figure 2.4 for terminus position during this time.
	April 1956	0.381 0.079 0.146 0.216 0.041	A_1 – Victoria Cr C_1 – Yellow Cr C_2 – Yellow Cr C_3 – Yellow Creek D_1 - Term Moraine	
Lawson (pers. comm., 2005) unpublished	Feb 1992	0.45 – 0.98 Average 0.70	Lower Glacier, similar location to this study	Glacier advancing
This Study	Jan/Feb 2005 Jun/July 2005	0.87 m 0.64	Lower Glacier, stake network at c. 450 m a.s.l and c. 450 m from terminus	Glacier advancing

On a global scale the Fox Glacier, like the Franz Josef Glacier, can be categorised as a 'fast' flowing glacier with an annual velocity in the vicinity of 250 m yr^{-1}. Daily velocities on the lower Fox Glacier range between 0.5 to 1.0 m d^{-1}, a rate higher than that recorded on glaciers in continental climates where daily average velocities are generally less than 0.2 m d^{-1}, for example the Haut Glacier d'Arolla in Switzerland, and the Athabasca in Canada (Mair*, et al.*, 2001; Paterson, 1964; Swift*, et al.*, 2005). The maritime climate in which the Fox Glacier is located will contribute to this higher daily velocity, as unlike continental glaciers, the ice at the base of temperate glaciers remains at pressure melting point, so basal sliding can occur year around (Benn and Evans, 1998; Ruddell, 1995). In addition, the steep nature of the west coast glaciers means that they tend to have higher surface velocities than more gently sloping glaciers, for example on the adjacent east coast, where velocities on the Tasman and Hooker Glaciers range from 0.09 to 0.4 m d^{-1}(Brodrick, 1891; Kirkbride, 1995b).

Regionally, recent surveys on the lower Franz Josef Glacier report velocities of around 1.0 to 1.5 m d^{-1} (Anderson, 2003; Goodsell, 2005), a figure higher than either this study or Lawson's work, and the Franz Josef Glacier has also been recorded as having a higher rate of marginal slip (Anderson, 2003). In comparison to the Fox Glacier, the Franz Josef Glacier does have a larger surface slope (8^o as opposed to 4^o) and a higher supply of water from surface melt during the winter season, factors that are likely to be of influence to higher average surface velocities, slip rates, and lack of a noticeable winter velocity deceleration.

Table 7.4 Selected key surface velocity measurements on the lower Franz Josef Glacier

Study	**Date**	**Velocity (m d^{-1})**	**Notes**
Harper (1894) as cited in Anderson (2003)	1893	0.60 – 5.26	600 m a.s.l over 3 days
Speight (1921) as cited in Anderson (2003)	1921	1.0	400 m a.s.l over 200 days
Gunn (1964)	March 1956	0.07 – 0.37	400 m a.s.l. over 24-48 hours
McSaveney & Gage (1968)	April-Aug 1966	0.73 – 1.48	400 m a.s.l over 5 months
Anderson (2003)	2000/2001	0.2 – 1.0	Lower glacier, over a full balance year
Goodsell (2005)	Feb-Oct 2003 Feb – Dec 2004	0.5 – 1.5 1.5 – 7.0	Lower Glacier

7.3 Future Research Opportunities

7.3.1 Ablation Research

From this research project two main areas for future research on ablation have arisen, both in relation to the effect that debris-cover has on the rate of ablation. Firstly it was noted that the presence of a fine matrix of debris at the debris-ice interface seems to have additional insulating properties over and above just increasing debris thickness. This factor was also noted by Pelto (2000) yet there does not yet appear to be any quantification of exactly how fine (clast size), and how thick this matrix needs to be in order to enhance insulation, or to what proportion it contributes to overall insulation in comparison to varying debris thickness.

Secondly, it was noted during the winter field season, that the debris cover appeared to have a role in protecting or shielding the ice from precipitation events, with a 44% reduction in ablation occurring under debris-cover compared to the clean ice surfaces during such events. Whether this sheltering relationship is simply related to debris thickness, or whether clast size and arrangement are also factors, would be worthy of investigation.

7.3.2 Velocity Research

Although much previous research has focused on the relationships between the supply of surface water to velocity response, and that responses relationship to the evolution of the glacial drainage system (Benn and Evans, 1998; Harbor*, et al.*, 1997; Iken*, et al.*, 1983; Mair*, et al.*, 2001; Nienow*, et al.*, 1998; Swift*, et al.*, 2005; Willis, 1995; Willis*, et al.*, 2003), this study has highlighted the importance of time lags, and precipitation thresholds associated with such a response, and whether the glacial drainage system can evolve at shorter (daily) rates than previously believed.

Future research focusing on time lags and looking at how these might change as the glacial drainage system evolves on both a daily and seasonal basis would be of benefit in predicting short and long-term velocity responses to precipitation more accurately. In addition, quantification of a precipitation threshold to velocity response would also assist in the prediction of short-term velocity fluctuations. Both the above factors would need to be considered at varying temporal and spatial scales in order to take into account the changing morphology of the glacial drainage system throughout the year, and variations in response at different parts of a glacier, as drainage morphology will

vary both across-glacier and up-glacier. Before such comparisons could be made, research into the actual drainage morphology of the glacier, and the evolution of the drainage system through out the seasons and on a daily basis would be required. Ideally a series of dye-tracing experiments in conjunction with velocity measurement, should be conducted on the Fox Glacier to not only define its sub-glacial drainage system, but to also consider how, and at what rate the drainage system evolves though out the year.

Chapter 8: Conclusions

8.1 Objectives Revisited

This research project measured ablation (specifically surface melt followed by run off), and surface velocity on the lower Fox Glacier during both the summer (ablation) and winter (accumulation) seasons in order to examine the spatial and temporal variations with these processes. In addition, the interrelationships that both ablation and surface velocity had with climate variables, and with each other, were also considered in an attempt to identify what the major factors driving ablation and surface velocity were.

The research questions being addressed by this thesis were:

- What are the intra-annual variations in ablation and surface velocity on the lower Fox Glacier?
- What short-term (daily) fluctuations occur in ablation and surface velocity?
- What are the main factors driving these variations?
- Can the behaviour of the Fox Glacier be predicted by information gathered from the Franz Josef Glacier?

The following sections provide a summary of the objectives achieved by this project (see section 2.8).

8.2 Ablation

- There was high spatial variability in ablation on the clean ice surfaces, with this variability being linked to variations in surface topography and aspect, and possibly varying local climate conditions.
- There was a significant difference in ablation rates between the clean ice and debris-covered surfaces during summer, with ablation being suppressed by up to 50% by debris-cover.
- During winter, the suppression factor of debris was not as significant, but it was found that during heavy precipitation events, debris cover had a sheltering effect on the underlying ice.
- During both summer and winter, climate parameters were found to explain 90% and 93% respectively of ablation variability, therefore climate, and in particular

temperature and solar radiation, were found to be major driving forces for ablation.

- During winter, heat supplied by latent heat fluxes and rainfall fluxes became more important to ablation variability.
- Heavy rainfall events were found to contribute significantly to ablation on the lower Fox Glacier.
- Although there was similarity between the summer ablation rates of the Franz Josef Glacier and Fox Glacier, the winter ablation rate tended to be lower on the Fox Glacier. This is due to the different aspects of the glacier tongues resulting in little to no melting of the surface of the lower Fox Glacier during winter.

8.3 Surface Velocity

- Spatial variability in surface velocity was recorded both across glacier and up-glacier. These variations were consistent during both summer and winter seasons and were linked to the primary controls on velocity (surface slope, ice thickness and shear stress from valley sides).
- Velocities in winter were on average at least 26% lower than those recorded during summer. This reduction in velocity is likely to be due to a decrease in basal sliding, brought about by a general reduction in the supply of water, that reduces water pressure in sub-glacial cavities and channels.
- Climate parameters were found to account for less than half of the variations in short-term surface velocity. However during winter, a strong relationship was identified between surface velocity and precipitation, with significant increases in velocity occurring in association with heavy precipitation events.
- Time lags in the velocity response to precipitation events could be related to either variation in drainage morphology (in particular the closure of conduits and channels by ice deformation during periods of lower water discharge), or to water storage in sub-glacial cavities, or a combination of both.
- A precipitation threshold appears to exist before a velocity response occurs. This threshold is likely to be influenced by drainage morphology (time of year), magnitude of the precipitation event, and the time elapsed since the last significant event.
- Short-term (daily) variations in surface velocity are strongly linked to variations in the supply of water.

- Average summer surface velocity on the lower Fox Glacier is found to be less than that recorded on the Franz Josef Glacier. This is most likely due to differences in surface slope between the glaciers. Seasonal variations in velocity recorded on Fox Glacier, not apparent on the Franz Josef Glacier, could be due to different aspects and winter melt rates, affecting the amount of water input during cold winter months. Therefore, the velocity of the Fox Glacier should not be estimated from measurements on the Franz Josef Glacier.
- A direct link between ablation and velocity was recorded during summer when an increase in temperature (3^{o}C), drove an increase in ablation, which in turn enhanced surface velocity (11%).

8.4 Summary

- Significant intra-annual variation exists both with average daily ablation and surface velocity on the lower Fox Glacier.
- The present (2005) Fox Glacier terminus is around 200 metres down-valley of the 1987 position, but still some two and a half kilometres up valley of the 1894 terminus position.
- The glacier is at present (2005) in a period of advance, with a terminus gain of around 20 metres, and in increase in height (thickness) of around three metres recorded between February and July 2005.
- A general estimate of the response time of the Fox Glacier using data from this study is 9 years.

This study has demonstrated how highly dynamic the Fox Glacier is. Daily visual change to access tracks and crevasses reinforces this dynamic nature, and therefore highlights the importance of ensuring any results from process studies, like ablation and surface velocity, are kept in context with the time and place at which they were monitored. Significant dynamic relationships were found to exist between precipitation events and the response of both ablation and surface velocity, relationships that warrant further attention. This study focused solely on the lower glacier. It would be of interest to see how the relationships identified manifest further up the glacier at both the Victoria Flat (Figure 1.2) and in the névé area. This project tells a story about what the lower Fox Glacier is doing at present, how it behaves in its lower reaches during an advance phase, and what factors are most influential to variations in daily ablation and surface velocity. Therefore in conclusion, the objects outlined for this research project have been met and areas for future research identified.

Appendix

Appendix 1: Ablation Data (mm d^{-1}) Jan/Feb 2005

Stake	09/01/2005	10/01/2005	11/01/2005	12/01/2005	13/01/2005	14/01/2005	15/01/2005	16/01/2005	17/01/2005	18/01/2005	19/01/2005	20/01/2005	21/01/2005
a1	160	151	90	106	118	*120*	*120*	*120*	*(120)* 479	50	129	98	103
a2	87	136	59	62	90	*106*	*106*	*106*	*(106)* 423	45	102	92	134
a3	109	93	100	99	104	*110*	*110*	*110*	*(110)* 440	45	83	81	111
a4	76	94	70	89	101	*98.5*	*98.5*	98.5	*(98.5)* 394	48	98	102	79
a5	114	126	79	96	84	*119.5*	*119.5*	*119.5*	*(119.5)* 478	68	113	81	93
a6	119	116	73	76	136	*87.5*	*87.5*	*87.5*	*(87.5)* 350	49	91	84	84
a7	105	104	67	71	142	*79.5*	79.5	79.5	*(79.5)* 318	49	80	81	85
a8	92	104	65	86	118	*71.5*	*71.5*	*71.5*	*(71.5)* 286	39	94	79	84
a9	97	119	94	94	116	*110*	*110*	110	*(110)* 440	75	87	90	98
a10	45	122	75	96	111	*113*	*113*	113	*(113)* 453	59	79	74	96
a11	104	94	89	97	132	*112*	*112*	*112*	*(112)* 448	53	93	81	102
a12	87	113	77	87	103	*91.5*	*91.5*	*91.5*	*(91.5)* 366	36	73	80	107
a13	86	111	88	122	147	*92*	*92*	*92*	*(92)* 368	47	104	102	103
a14	31	101	76	93	97	*106*	*106*	*106*	*(106)* 425	42	83	84	97
a15	87	119	88	91	125	*98*	*98*	98	*(98)* 392	39	101	80	101
a16													
a17													
a18													
	98	114	79	91	115	*101*	*101*	*101*	*101*	50	94	86	98
	1399	1703	1190	1365	1724	1515	1515	1515	1515	744	1410	1289	1477
d1					84	*93*	*93*	*93*	*(93)* 371	*0*	75	71	69
d2					45	*24*	*24*	*24*	*(24)* 95	10	29	43	22
d3					18	*47*	*47*	47	*(47)* 188	0	28	26	31
d4										10	96	69	62
d5											10	51	42
					49	55	*55*	55	55	5	36	48	41

22/01/2005	23/01/2005	24/01/2005	25/01/2005	26/01/2005	27/01/2005	28/01/2005	29/01/2005	30/01/2005	31/01/2005	01/02/2005	02/02/2005	03/02/2005
131	104	83	135	177	174	149	*175*	*(175)* 350	141	196	204	233
131	86	70	143	172	116	173	*159*	*(159)* 318	206	223	184	200
142	115	78	126	162	161	184	*163*	*(163)* 325	199	310	236	194
128	59	71	115	145	124	113	*117*	*(117) 234*	180	224	178	216
141	109	108	158	182	143	136	*130*	*(130)* 259	164	215	214	207
132	97	84	122	163	160	145	*117*	*(117*) 254	181	232	201	235
146	111	75	118	216	140	136	*127*	*(127) 253*	167	196	190	219
124	102	73	103	175		59	*102*	(102) 204	149	191	158	188
144	103	90	124	134	127	134	*130*	(130) 260	145	202	197	212
158	123	85	154	163	152	148	*139*	*(139)* 278	187	215	197	224
141	107	87	129	146	141	189	*150*	*(150) 300*	154	186	180	198
153	76	97	109	147	116	154	*139*	*(139)* 277	175	183	168	187
119	85	88	135	126	160	195	*178*	*(178)* 355	187	255	187	235
159	95	75	117	151	123	141	*125*	*(125)* 250	164	220	191	209
155	118	113	154	114	118	129	*135*	*(135)* 270	188	203	228	248
				139	142	159	*155*	*(155) 310*	169	199	191	220
				153	187	153	*162*	*(162) 324*	187	215	194	156
				154	*152*	*176*	*142*	*(142) 284*	*216*	*265*	*221*	*312*
140	99	85	129	157	143	147	*141*	141	173	216	194	211
2104	1490	1277	1942	2819	2436	2673	2545	2545	3159	3930	3519	3893
72	56	67	101	148	141	90	*102.5*	*(102.5) 205*	150	160		
43	53	45	35	55	61	89	*172*	*(172) 344*	198	257		
56	37	31	-10	111	56	53	*55*	*(55)* 110	48	59	66	50
89	79	84	116	135	112	83	*61.5*	*(61.5)* 123	111	114	107	109
47	53	76	62	78	79	88	*76*	*(76)* 152	98	112	142	97
55	50	55	47	98	84	80	101	101	124	147	104	74

Appendix 2: Velocity Data (m d^{-1}) Jan/Feb 2005

	18/01/2005	19/01/2005	20/01/2005	21/01/2005	22/01/2005	23/01/2005	24/01/2005	25/01/2005	26/01/2005	27/01/2005	28/01/2005	29/01/2005
a1		0.860	0.682	0.735	0.972	0.960	0.937	0.815	0.916	0.932	0.867	*0.840*
a2			0.766	0.719	0.960	0.693	1.281	0.877	0.895	0.899	0.914	*0.884*
a3		0.851	1.010	1.078	1.005	0.946	0.916	0.891	0.983	1.214	0.611	*0.897*
a4	0.859	0.766	0.836	0.712	1.013	0.940	0.911	0.892	0.891	0.776	1.001	*0.856*
a5	0.918	0.756	0.792	0.763	0.954	0.989	0.894	0.874	0.996	0.838	0.909	*0.859*
a6	0.911	0.749	0.784	0.734	0.947	0.964	0.841	0.856	0.914	0.809	0.865	*0.830*
a7	0.968	0.676	0.756	0.707	0.932	0.907	0.815	0.793	0.877	0.804	0.863	*0.797*
a8		0.830	0.780	0.729	0.969	0.988	0.889	0.844	0.945		0.690	*0.831*
a9	0.877	0.788	0.842	0.746	1.039	0.984	0.905	0.928	0.948	0.870	0.936	*0.882*
a10	0.890	0.808	0.785	0.799	0.968	0.952	0.988	0.954	1.004	0.902	0.893	*0.899*
a11	0.757	0.870	0.819	0.779	1.030	1.035	0.907	0.972	0.934	0.973	0.782	*0.939*
a12	0.933	0.897	0.821	0.825	1.070	1.097	0.969	1.001	1.007	0.980	0.990	*0.976*
a13	0.940	0.927	0.843	0.816	1.090	1.090	1.015	0.990	1.011	0.937	0.987	*0.978*
a14		0.910	0.847	0.828	1.105	1.043	1.053	1.010	1.003	0.903	0.882	*0.992*
a15		0.909	0.862	0.812	1.122	1.056	1.005	0.997	1.037	0.921	0.982	*0.980*
a16									0.919	0.981	1.008	*0.899*
a17									0.963	0.987	1.057	*1.035*
a18									0.753	0.830	0.885	*0.848*
d1		0.748	0.660	0.677	0.807	0.785	0.719	0.734	0.710	0.747	0.701	*0.728*
d2		0.696	0.617	0.609	0.729	0.680	0.681	0.649	0.656	0.620	0.655	*0.619*
d3		0.660	0.574	0.562	0.685	0.636	0.643	0.582	0.602	0.602	0.560	*0.559*
d4			0.638	0.654	0.793	0.833	0.763	0.705	0.747	0.730	0.755	*0.708*
d5			0.672	0.681	0.852	0.815	0.750	0.741	0.764	0.722	0.730	*0.722*
DailyAv	0.895	0.806	0.769	0.748	0.952	0.920	0.894	0.855	0.892	0.863	0.849	*0.850*

30/01/2005	31/01/2005	01/02/2005	02/02/2005	03/02/2005	StakeAve
0.840	0.859	0.880	0.895	1.227	0.866
0.884	0.835	0.876	0.927	0.964	0.886
0.897	0.828	0.907	0.924	1.428	0.931
0.856	0.859	0.868	0.872	0.983	0.870
0.859	0.841	0.872	0.883	0.953	0.872
0.830	0.813	0.878	0.831		0.844
0.797	0.746	0.782	0.810		0.804
0.831	0.779	0.875	0.843		0.845
0.882	0.851	0.936	0.879	0.945	0.894
0.899	0.891	0.940	0.887		0.906
0.939	0.881	0.914	0.957		0.913
0.976	0.913	0.991	1.001		0.965
0.978	0.957	1.020	1.023		0.974
0.992	0.916	1.010	0.993		0.964
0.980	0.948	1.018	0.989		0.974
0.899	1.254	1.014	1.009		0.996
1.035	1.025	1.087	1.020		1.027
0.848	0.830	0.874	0.832		0.838
0.728	0.643	0.792			0.722
0.619	0.659	0.590			0.653
0.559	0.563	0.531	0.520	0.577	0.589
0.708	0.730	0.736	0.664		0.731
0.722	0.681	0.745	0.722	0.814	0.737
0.850	0.839	0.876	0.880	0.986	

Appendix 3: Ablation Data (m d^{-1}) Jun/July 2005

Stake	08/06/2005	09/06/2005	10/06/2005	11/06/2005	12/06/2005	13/06/2005	14/06/2005	15/06/2005	16/06/2005	17/06/2005	18/06/2005	19/06/2005	20/06/2005
u1	-0.116	0.169	0.028	0.015	0.218	0.017	0.265	0.02	0.027	0.081	0.042	0.014	0.043
u2	0.004	0.106	0.038	0.018	0.172	0.018	0.198	0.013	0.019	0.082	0.053	0.019	0.048
u3	0.015	0.195	0.039	0.016	0.256	0.024	0.298	0.007	0.022	0.077	0.055	0.026	0.044
u4	0.007	0.096	0.029	0.011	0.14	0.012	0.159	0.006	0.011	0.066	0.042	0.017	0.058
u5	0.002	0.107	0.03	0.021	0.161	0.009	0.185	0.007	0.010	0.059	0.040	0.012	0.041
u6	0.004	0.173	0.04	0.011	0.232	0.019	0.253	0.034	0.011	0.058	0.034	0.011	0.040
u7	0.013	0.175	0.038	0.019	0.237	0.029	0.28	0.025	0.028	0.082	0.055	0.020	0.055
u8	0.006	0.092	0.029	0.013	0.132	0.013	0.16	0.015	0.019	0.093	0.055	0.019	0.053
l1	-0.005	0.146	0.034	0.011	0.195	0.013	0.217	0.01	0.011	0.045	0.035	0.012	0.046
l2	0.001	0.063	0.032	0.01	0.103	0.013	0.128	0.016	0.014	0.056	0.041	0.015	0.045
l3	0.005	0.101	0.031	0.021	0.152	0.017	0.184	0.007	0.023	0.061	0.044	0.011	0.052
l4	0.005	0.129	0.013	0	0.128	0.002	0.132	0.003	0.010	0.055	0.033	0.005	0.043
l5	0.001	0.107	0.015	0.005	0.125	0.007	0.14	0.005	0.015	0.052	0.036	0.012	0.040
c1	0.003	0.138	0.032	0.011	0.188	0.011	0.21	0.005	0.020	0.072	0.032	0.013	0.048
c2	0.006	0.112	0.031	0.003	0.155	0.010	0.175	0.008	0.023	0.082	0.047	0.027	0.065
c3	0.008	0.102	0.04	0.019	0.166	0.009	0.203	-0.002	0.023	0.089	0.048	0.002	0.052
c4	0.003	0.311	0.022	0.005	0.335	0.005	0.343	-0.021	0.030	0.057	0.028	0.008	0.040
c5	0.015	0.158	0.059	0.024	0.252	0.023	0.286	0.011	0.020	0.064	0.042	0.014	0.050
c6	0.003	0.16	0.032	0.01	0.211	0.014	0.237	0.01	0.020	0.078	0.038	0.015	0.052
Ave	-0.001	0.139	0.032	0.013	0.187	0.014	0.213	0.009	0.019	0.069	0.042	0.014	0.048
m1	0.002	0.423	0.026	0.011	0.46	0.010	0.47	0.03	0.010	0.060	0.035	0.011	0.036
m2	0.005	0.229	0.024	0.007	0.26	0.009	0.273	0.008	0.002	0.018	0.024	0.014	0.016
m3	-0.01	0.223	0.027	0.015	0.285	0.025	0.313	0.004	0.017	0.038	0.033	0.007	0.017
m4	-0.002	0.206	0.016	0.016	0.25	0.010	0.277	0.005	0.017	0.027	0.032	0.021	0.023
m5	0.02	0.293	0.01	-0.003	0.303	0.007	0.313	0.002	-0.003	0.018	0.009	0.008	0.014
Ave	0.003	0.275	0.021	0.009	0.212	0.012	0.329	0.010	0.009	0.032	0.027	0.012	0.021

21/06/2005	22/06/2005	23/06/2005	24/06/2005	25/06/2005	26/06/2005	27/06/2005	28/06/2005	29/06/2005	30/05/2006	01/07/2005	02/07/2005	03/07/2005
0.029	0.005	-0.001	-0.002	0.002	-0.002	0.000	0.072	0.015	0.000	0.000	0.026	0.082
0.039	0.011	-0.002	0.004	-0.002	0.000	0.005	0.075	0.022	0.000	0.002	0.033	0.086
0.041	0.014	-0.002	0.000	0.003	0.000	0.007	0.078	0.011	0.004	0.010	0.036	0.079
0.030	0.002	-0.002	0.000	0.001	0.000	0.004	0.049	0.006	0.000	0.000	0.016	0.067
0.032	-0.003	0.001	-0.001	-0.002	0.003	0.003	0.058	0.012	0.000	0.000	0.020	0.082
0.028	0.006	-0.003	0.000	0.000	0.003	0.001	0.059	0.013	0.000	0.002	0.024	0.081
0.045	0.007	0.001	0.001	0.002	0.000	0.006	0.060	0.014	-0.001	0.005	0.031	0.090
0.033	0.011	-0.004	-0.004	-0.001	0.003	0.006	0.053	0.008	0.002	0.000	0.018	0.069
0.026	0.012	-0.003	0.003	-0.003	0.003	0.006	0.078	0.016	0.001	0.000	0.025	0.076
0.038	0.007	0.001	0.000	-0.003	0.004	0.005	0.053	0.010	0.000	0.000	0.021	0.080
0.031	0.002	-0.002	-0.001	0.001	0.002	0.002	0.077	0.008	0.000	0.001	0.034	0.081
0.028	0.002	0.000	0.004	0.000	0.002	0.004	0.061	0.010	0.004	0.001	0.020	0.083
0.022	0.007	0.002	-0.001	-0.001	-0.001	0.007	0.056	0.014	0.000	0.000	0.027	0.082
0.035	0.007	-0.002	0.001	-0.001	0.000	0.003	0.081	0.014	0.000	0.003	0.031	0.096
0.039	0.013	-0.005	0.005	0.005	-0.001	0.005	0.062	0.026	0.000	0.007	0.025	0.121
0.044	0.007	-0.007	-0.004	0.004	-0.002	0.008	0.078	0.012	0.000	0.001	0.024	0.092
0.024	0.005	-0.007	0.002	0.000	0.001	0.000	0.094	-0.007	0.002	-0.001	0.014	0.070
0.030	0.008	0.003	0.000	0.002	0.002	0.003	0.063	0.013	0.003	0.001	0.032	0.085
0.039	0.000	-0.005	-0.002	0.003	0.001	0.004	0.087	0.014	0.002	0.002	0.026	0.077
0.033	0.006	-0.002	0.000	0.001	0.001	0.004	0.068	0.012	0.001	0.002	0.025	0.083
0.033	0.005	0.000	-0.003	0.000	-0.002	0.001	0.049	0.013	0.001	0.005	0.025	0.055
0.018	0.004	0.000	0.002	-0.002	-0.001	0.002	0.025	0.013	0.002	-0.001	0.012	0.081
0.027	0.002	0.005	-0.002	0.000	0.000	0.009	0.037	0.015	-0.002	0.014	0.013	0.056
0.008	0.007	0.000	0.002	-0.004	0.002	0.011	0.036	0.001	0.000	0.012	0.015	0.058
0.018	-0.004	0.009	0.001	0.002	0.000	0.004	0.022	0.007	0.000	0.013	0.001	0.034
0.021	0.003	0.003	0.000	-0.001	0.000	0.005	0.034	0.010	0.000	0.009	0.013	0.057

Appendix 4: Velocity Data (m d^{-1}) Jun/July 2005

Stake	08-Jun	09-Jun	10-Jun	11-Jun	12-Jun	13-Jun	14-Jun	15-Jun	16-Jun	17-Jun	18-Jun	19-Jun	20-Jun	21-Jun	22-Jun
u1	0.504	0.701	0.598	0.622	0.680	0.568	0.603	*0.593*	0.593	0.686	0.776	0.745	0.713	0.764	0.699
u2	0.486	0.732	0.593	0.669	0.678	0.588	0.614	*0.604*	0.604	0.686	0.817	0.781	0.718	0.811	0.703
u3	0.496	0.671	0.677	0.643	0.726	0.564	0.623	*0.620*	0.620	0.710	0.802	0.774	0.743	0.788	0.716
u4	0.636	0.661	0.688	0.669	0.694	0.579	0.636	*0.616*	0.616	0.694	0.806	0.755	0.757	0.804	0.745
u5	0.599	0.658	0.674	0.667	0.684	0.600	0.630	*0.616*	0.616	0.699	0.811	0.764	0.750	0.787	0.730
u6	1.213	0.654	0.661	0.680	0.637	0.614	0.606	*0.606*	0.606	0.683	0.803	0.747	0.771	0.761	0.731
u7	0.601	0.663	0.613	0.663	0.652	0.611	0.601	*0.589*	0.589	0.664	0.830	0.695	0.743	0.783	0.698
u8	0.517	0.665	0.590	0.641	0.633	0.591	0.602	*0.564*	0.564	0.686	0.775	0.690	0.720	0.756	0.660
l1	0.499	0.600	0.605	0.603	0.620	0.552	0.560	*0.559*	0.559	0.614	0.748	0.689	0.690	0.709	0.656
l2	0.524	0.573	0.610	0.592	0.601	0.571	0.538	*0.558*	0.558	0.606	0.719	0.704	0.679	0.694	0.645
l3	0.491	0.589	0.604	0.595	0.599	0.543	0.555	*0.539*	0.539	0.610	0.713	0.702	0.672	0.706	0.629
l4	0.508	0.583	0.548	0.639	0.572	0.521	0.597	*0.528*	0.528	0.624	0.703	0.644	0.673	0.694	0.632
l5	0.455	0.561	0.554	0.564	0.553	0.519	0.554	*0.519*	0.519	0.595	0.656	0.634	0.643	0.657	0.617
c1	0.469	0.596	0.558	0.609	0.572	0.559	0.569	*0.526*	0.526	0.650	0.684	0.678	0.676	0.688	0.628
c2	0.486	0.592	0.610	0.584	0.615	0.560	0.544	*0.559*	0.559	0.626	0.713	0.701	0.680	0.716	0.657
c3	0.493	0.607	0.619	0.616	0.621	0.569	0.581	*0.560*	0.560	0.628	0.732	0.706	0.707	0.729	0.661
c4	0.510	0.617	0.639	0.628	0.637	0.579	0.586	*0.571*	0.571	0.665	0.745	0.732	0.694	0.756	0.685
c5	0.509	0.657	0.661	0.671	0.661	0.610	0.599	*0.601*	0.601	0.685	0.780	0.753	0.743	0.787	0.730
c6	0.532	0.699	0.677	0.692	0.686	0.634	0.634	*0.628*	0.628	0.705	0.844	0.781	0.765	0.810	0.730
m1	0.508	0.653	0.531	0.674	0.579	0.537	0.557	*0.555*	0.555	0.620	0.692	0.679	0.642	0.690	0.665
m2	0.485	0.553	0.510	0.557	0.546	0.514	0.538	*0.507*	0.507	0.601	0.636	0.630	0.624	0.634	0.605
m3	0.376	0.440	0.475	0.466	0.440	0.441	0.431	*0.421*	0.421	0.500	0.553	0.494	0.509	0.517	0.491
m4	0.386	0.463	0.476	0.477	0.483	0.444	0.442	*0.440*	0.440	0.514	0.576	0.514	0.514	0.549	0.508
m5	0.416	0.500	0.563	0.617	0.515	0.488	0.475	*0.480*	0.480	0.543	0.612	0.857	0.642	0.601	0.559
Ave	0.529	0.612	0.597	0.618	0.612	0.556	0.570	0.557	0.557	0.637	0.730	0.702	0.686	0.716	0.657

23-Jun	24-Jun	25-Jun	26-Jun	27-Jun	28-Jun	29-Jun	30-Jun	01-Jul	02-Jul	03-Jul	Stake Ave
0.663	0.642	0.663	0.578	0.635	0.686	0.706	0.632	0.651	0.701	1.205	0.677
0.673	0.633	0.700	0.600	0.638	0.696	0.723	0.666	0.654	0.717	1.216	0.692
0.686	0.658	0.683	0.610	0.651	0.714	0.708	0.662	0.666	0.914	1.299	0.709
0.694	0.657	0.675	0.618	0.639	0.675	0.744	0.658	0.657	0.725	1.190	0.703
0.680	0.652	0.687	0.611	0.628	0.672	0.749	0.669	0.655	0.687	1.217	0.700
0.689	0.620	0.653	0.620	0.618	0.700	0.700	0.680	0.616	0.701	1.179	0.713
0.723	0.577	0.641	0.609	0.609	0.718	0.893	0.667	0.623	0.689	1.158	0.689
0.661	0.583	0.634	0.591	0.590	0.665	0.670	0.663	0.611	0.635	1.121	0.657
0.635	0.591	0.587	0.570	0.569	0.631	0.672	0.607	0.629	0.644	1.016	0.631
0.632	0.583	0.583	0.569	0.590	0.595	0.675	0.612	0.616	0.616	1.028	0.626
0.635	0.586	0.580	0.567	0.563	0.618	0.663	0.615	0.605	0.604	1.017	0.621
0.614	0.591	0.581	0.555	0.553	0.599	0.669	0.632	0.557	0.609	1.015	0.614
0.603	0.554	0.560	0.561	0.534	0.601	0.612	0.607	0.569	0.585	0.983	0.591
0.623	0.583	0.596	0.567	0.549	0.621	0.652	0.601	0.617	0.584	1.031	0.616
0.641	0.580	0.591	0.551	0.590	0.615	0.663	0.621	0.608	0.658	1.008	0.628
0.617	0.607	0.598	0.574	0.580	0.615	0.712	0.624	0.627	0.628	1.052	0.639
0.630	0.596	0.628	0.594	0.587	0.640	0.702	0.641	0.614	0.655	1.106	0.654
0.665	0.561	0.656	0.598	0.612	0.698	0.714	0.668	0.617	0.751	1.161	0.683
0.703	0.685	0.677	0.641	0.646	0.729	0.728	0.672	0.666	0.723	1.252	0.714
0.616	0.574	0.584	0.558	0.552	0.618	0.640	0.610	0.606	0.607	1.018	0.620
0.577	0.548	0.524	0.537	0.525	0.572	0.609	0.576	0.551	0.560	0.938	0.576
0.470	0.452	0.459	0.433	0.429	0.473	0.499	0.470	0.463	0.451	0.786	0.475
0.495	0.461	0.468	0.456	0.464	0.474	0.523	0.489	0.481	0.458	0.814	0.493
0.531	0.500	0.513	0.662	0.823	0.561	0.542	0.539	0.527	0.519	0.869	0.574
0.632	0.586	0.605	0.576	0.591	0.633	0.674	0.620	0.604	0.643	1.070	0.637

Bibliography

Adams, J. 1985: Large-scale Tectonic geomorphology of the Southern Alps, New Zealand, in Morisaw, M and Hack, J T, *Tectonic Geomorphology, Proceedings of the 15th Annual Binghamton Symposium*, Allen and Unwin, 105-128.

Almond, P. C., Moar, N. T. and Lian, O. B. 2001: Reinterpretation of the glacial chronology of South Westland, New Zealand, *New Zealand Journal of Geology and Geophysics*, 44, 1-15.

Alpine Guides Westland 2005: 'About Fox Glacier', 12/04/05, http://www.foxguides.co.nz.

Anderson, B. 2003: *The Response of Ka Roimata O Hine Hukatere Franz Josef Glacier To Climate Change*, Doctor of Philosophy, University of Canterbury.

Andreasen, J.-O. 1983: Basal Sliding at the Margin of the Glacier Austre Okindbre, Norland, Norway, *Arctic and Alpine Research*, 15, 333-338.

Benn, D. I. and Evans, D. J. A. 1998: *Glaciers and Glaciation*, Arnold, London.

Braithwaite, R. J. 1981: On Glacier Energy Balance, Ablation and Air Temperature, *Journal of Glaciology*, 27, 381-391.

Braithwaite, R. J., Konzelmann, T., Marty, C. and Olesen, O. B. 1998: Reconnaissance study of glacier energy balance in North Greenland 1993-94, *Journal of Glaciology*, 44, 239-247.

Braithwaite, R. J. and Zhang, Y. 2000: Sensitivity of mass balance of five Swiss glaciers to temperature changes assessed by tuning a degree-day model, *Journal of Glaciology*, 46, 7-14.

Brazier, V., Owens, I. F., Soons, J. M. and Sturman, A. P. 1992: Report on the Franz Josef Glacier, *Zeitschrift fur Geomorphologie Supplementband*, 86, 35-49.

Brenstrum, E. 1998: *The New Zealand Weather Book*, Craig Potton Publishing, Nelson.

Brock, B. W. and Arnold, N. S. 2000: A Spreadsheet-Based (Microsoft Excel) Point Surface Energy Balance Model for Glacier and Snow Melt Studies, *Earth Surface Processes and Landforms*, 25, 649-658.

Brodrick, T. N. 1891: Report on the Tasman Glacier, *Appendix to the Journal of the House of Representatives of New Zealand*, Vol 1, C-1A, 39-43.

Bureau of Meteorology 2005: 'Monthly Southern Oscillation Index', 17/10/2005, ftp://ftp.bom.gov.au/anon/home/ncc/www/sco/soi/soiplaintext.html.

Chinn, T. J. 1995: Glacier Fluctuations in the Southern Alps of New Zealand Determined from Snowline Elevations, *Arctic and Alpine Research*, 27, 187-198.

Chinn, T. J. 1999: New Zealand glacier response to climate change of the past 2 decades, *Global and Planetary Change*, 22, 155-168.

Chinn, T. J. 2001: Distribution of the glacial water resources of New Zealand, *Journal of Hydrology (NZ)*, 40, 139-187.

Chinn, T. J., Heydenrych, C. and Salinger, M. J. 2002a: *A Method of Calculating Annual Glacier Ice Volume Changes in New Zealand Southern Alps*, Ice in the Environment: Proceedings of the 16th IAHR International Symposium on Ice, Dunedin.

Chinn, T. J., Heydenrych, C. and Salinger, M. J. 2002b: *Glacier Snowline Survey 2002*, National Institute of Water and Atmospheric Research, Auckland.

Chinn, T. J., Heydenrych, C. and Salinger, M. J. 2003: *Glacier Snowline Survey 2003*, National Institute of Water and Atmospheric Research, Auckland.

Chinn, T. J., Willsman, A. and Salinger, M. J. 2005: *Glacier Snowline Survey 2005*, National Institute of Water and Atmospheric Research Ltd, Auckland.

Clare, G. R., Fitzharris, B. B., Chinn, T. J. and Salinger, M. J. 2002: Interannual Variation in End-of-Summer Snowlines of the Southern Alps of New Zealand, and Relationships with Southern Hemisphere Atmospheric Circulation and Sea Surface Temperature Patterns, *International Journal of Climatology*, 22, 107-120.

Coates, G. and Chinn, T. J. 1992: *The Franz Josef and Fox Glaciers*, Institute of Geological and Nuclear Sciences Ltd, Kahu Publishing, Wellington.

Denton, G. H. and Hendy, C. H. 1994: Younger Dryas Age Advance of Franz Josef Glacier in the Southern Alps of New Zealand, *Science*, 264, 1434-1436.

Department of Conservation 2001: *Westland Tai Poutini National Park Management Plan*, 3, Department of Conservation *Te Papa Atawhai*, Hokitika.

Douglas, C. 1896: Report on Cook's River District, *Appendix to the Journal of the House of Representatives of New Zealand*, Vol 1, C-1, 110-112.

Evans, E. 2003: *Ablation at the terminus of the Franz Josef Glacier*, Bachelor of Science (Honours), Otago University.

Fitzharris, B. B., Hay, J. E. and Jones, P. D. 1992: Behaviour of New Zealand glaciers and atmospheric circulation changes over the past 130 years, *The Holocene*, 2, 97-106.

Fitzharris, B. B., Chinn, T. J. and Lamont, G. N. 1997: Glacier Balance Fluctuations and Atmospheric Circulation Patterns over the Southern Alps, New Zealand, *International Journal of Climatology*, 17, 745-763.

Fitzharris, B. B., Lawson, W. and Owens, I. F. 1999: Research on glaciers and snow in New Zealand, *Progress in Physical Geography*, 23, 469-500.

Fitzharris, B. B. 2001: Global Energy and Climate Processes, in Sturman, A P and Spronken-Smith, Rachel, *The Physical Environment - A New Zealand Perspective*, Oxford University Press, Melbourne, 62-75.

Fitzsimons, S. J. 1997: Late-Glacial and Early Holocene Glacier Activity in the Southern Alps, New Zealand, *Quaternary International*, 38/39, 69-76.

Gellatly, A. F. and Norton, D. A. 1984: Possible warming and glacier recession in the South Island, New Zealand, *New Zealand Journal of Science*, 27, 381-388.

Gellatly, A. F., Chinn, T. J. and Röthlisberger, F. 1988: Holocene Glacier Variations in New Zealand: A Review, *Quaternary Science Reviews*, 7, 227-242.

Goodsell, B. 2005: *Long and short-term velocity variations at Franz Josef Glacier*, New Zealand Snow and Ice Research Group, Proceedings from the 3rd annual workshop held at Harihari, Westland, 15th-17th January 2005-01-18,

Goodsell, B., Anderson, B., Lawson, W. and Owens, I. F. 2005: Outburst flooding at Franz Josef Glacier, South Westland, New Zealand, *New Zealand Journal of Geology and Geophysics*, 48, 95-104.

Griffiths, G. and McSaveney, M. J. 1983: Distribution of mean annual precipitation across some steepland regions of New Zealand, *New Zealand Journal of Science*, 26, 197-209.

Gunn, B. M. 1964: Flow Rates and Secondary Structures of Fox and Franz Josef Glaciers, New Zealand, *Journal of Glaciology*, 5, 173-190.

Hagen, J. O., Zanon, G. and Martinez de Pison, E. 1998: Glaciers in Europe, in Haeberli, Wilfried, Hoelzle, Martin and Suter, S, *Into the second century of worldwide glacier monitoring- prospects and strategies.*, UNESCO, Paris, 147-166.

Harbor, J., Sharp, M., Copland, L., Hubbard, B., Nienow, P. and Mair, D. 1997: Influence of subglacial drainage conditions on the velocity distribution within a glacier cross section, *Geology*, 25, 739-742.

Hay, J. E. and Fitzharris, B. B. 1988: The Synoptic Climatology of Ablation on a New Zealand Glacier, *Journal of Climatology*, 8, 201-215.

Hessell, J. W. D. 1983: Climatic effects on the recession of the Franz Josef Glacier, *New Zealand Journal of Science*, 26, 315-320.

Hooke, R., Calla, P., Holmlund, P., Nilsson, M. and Stroeven, A. 1989: A 3 Year Record of seasonal variations in Surface Velocity, Storglaciären, Sweden, *Journal of Glaciology*, 35, 235-247.

Hooke, R. 2005: *Principles of Glacier Mechanics*, Cambridge University Press, Cambridge.

Hooker, B. L. 1995: *Advance and Retreat of Franz Josef Glacier in Relation to Climate*, Postgraduate Diploma of Science in Geography, Otago University.

Hooker, B. L. and Fitzharris, B. B. 1999: The correlation between climatic parameters and the retreat and advance of Franz Josef Glacier, New Zealand, *Global and Planetary Change*, 22, 39-48.

Hubbard, B. and Glasser, N. F. 2005: *Field Techniques in Glaciology and Glacial Geomorphology*, John Wiley & Sons Ltd, West Sussex.

Iken, A., Rothlisberger, H., Flotron, A. and Haeberli, W. 1983: The uplift of Unteraargletscher at the beginning of the melt season - a consequence of water storage at the bed?, *Journal of Glaciology*, 29, 28-47.

Ishikawa, N., Owens, I. F. and Sturman, A. P. 1992: Heat Balance Characteristics During Fine Periods on the Lower Parts of the Franz Josef Glacier, South Westland, New Zealand, *International Journal of Climatology*, 12, 397-410.

Johannesson, T., Raymond, C. and Waddington, E. 1989: Time-Scale for Adjustment of Glaciers to Changes in Mass Balance, *Journal of Glaciology*, 35, 355-369.

Kamb, B. and Engelhardt, H. 1987: Waves of accelerated motion in a glacier approaching surge: The mini surges of Variegated Glacier, Alaska, U.S.A, *Journal of Glaciology*, 33, 27-46.

Kelliher, F. M., Owens, I. F., Sturman, A. P., Byers, J. N., Hunt, J. E. and McSeveny, T. M. 1996: Radiation and ablation on the névé of Franz Josef Glacier, *Journal of Hydrology (NZ)*, 35, 131-150.

Kirkbride, M. P. 1995a: Relationships between temperature and ablation on the Tasman Glacier, Mount Cook National Park, New Zealand, *New Zealand Journal of Geology and Geophysics*, 38, 17-27.

Kirkbride, M. P. 1995b: Ice flow vectors on the debris-mantled Tasman Glacier 1957-1986, *Geografiska Annaler*, 77A, 147-157.

Knight, P. 1999: *Glaciers*, Stanley Thornes Ltd, Cheltenham.

Krimmell, R. and Vaughn, B. 1987: Columbia Glacier, Alaska: Changes in Velocity 1977-1986, *Journal of Geophysical Research*, 92, 8961-8968.

Langton, G. 2000: *Mr Explorer Douglas*, Canterbury University Press, Christchurch.

Lawson, W. and Fitzsimons, S. J. 2001: Glaciers and the Environment, in Sturman, A P and Spronken-Smith, Rachel, *The Physical Environment - A New Zealand Perspective*, Oxford University Press, Melbourne, 269-289.

Mair, D. 1997: *Hydrological Influences on the Dynamics of Valley Glaciers*, Doctor of Philosophy, St. Catherine's College.

Mair, D., Nienow, P., Willis, I. and Sharp, M. 2001: Spatial patterns of glacier motion during a high-velocity event: Haut Glacier d'Arolla, Switzerland, *Journal of Glaciology*, 47, 9-20.

Marcus, M. G., Moore, R. D. and Owens, I. F. 1985: Short-term estimates of surface energy transfers and ablation on the lower Franz Josef Glacier, South Westland, New Zealand, *New Zealand Journal of Geology and Geophysics*, 28, 559-567.

McGlone, M., Salinger, M. J. and Moar, N. T. 1993: Paleovegetation Studies of New Zealand's Climate since the Last Glacial Maximum, in Wright, H, *Global Climates Since the Last Glacial Maximum*, University of Minnesota Press, Minneapolis, 294-317.

McSaveney, M. J. and Gage, M. 1968: Ice Flow Measurements on Franz Josef Glacier, New Zealand, in 1966, *New Zealand Journal of Geology and Geophysics*, 11, 564-592.

Mercer, J. H. 1988: The age of the Waiho Loop terminal moraine, Franz Josef Glacier, Westland, *New Zealand Journal of Geology and Geophysics*, 31, 95-99.

Moore, R. D. and Owens, I. F. 1984: Controls on Advective Snowmelt in a Maritime Alpine Basin, *Journal of Climate and Applied Meteorology*, 23, 135-141.

Müller, F. and Keeler, C. M. 1969: Errors in Short-Term Ablation Measurements on Melting Ice Surfaces, *Journal of Glaciology*, 8, 91-105.

Nakawo, M. and Young, G. J. 1981: Field experiments to determine the effect of a debris layer on ablation of glacial ice, *Annals of Glaciology*, 2, 85-91.

Nesje, A. and Dahl, S. 2000: *Glaciers and Environmental Change*, Arnold, London.

Nienow, P., Sharp, M. and Willis, I. 1998: Seasonal changes in the morphology of the subglacial drainage system, Haut Glacier d'Arolla, Switzerland, *Earth Surface Processes and Landforms*, 23, 825-843.

NIWA 2005: *Climate Summaries*, National Institute of Water and Atmospheric Research,

Odell, N. E. 1960: The Mountains and Glaciers of New Zealand, *Journal of Glaciology*, 3, 739-741.

Oerlemans, J. 1997: Climate Sensitivity of Franz Josef Glacier, New Zealand, as Revealed by Numerical Modelling, *Arctic and Alpine Research*, 29, 233-239.

Oerlemans, J. 2001: *Glaciers and Climate Change*, A.A. Balkema Publishers, Lisse.

Ommanney, C., Demuth, M. and Meier, M. F. 1998: Glaciers in North America, in Haeberli, Wilfried, Hoelzle, Martin and Suter, S, *Into the second century of worldwide glacier monitoring- prospects and strategies*, UNESCO, Paris, 113-123.

Owens, I. 2005: *GPS observations of recent terminus behaviour of the Franz Josef*, New Zealand Snow and Ice Research Group Proceedings from the 3rd annual workshop held at Harihari, Westland, 15th-17th January 2005-01-18,

Owens, I. F., Sturman, A. P. and Ishikawa, N. 1992: *High Rates of Ablation on the Lower Part of the Franz Josef Glacier, South Westland*, Proceedings of the New Zealand Geographical Society, Hamilton.

Paterson, W. S. B. 1964: Variations in velocity of Athabasca Glacier with time, *Journal of Glaciology*, 5, 277-285.

Paterson, W. S. B. 1969: *The Physics of Glaciers*, Pergamon Press Ltd, Oxford.

Paterson, W. S. B. 1994: *The Physics of Glaciers*, Butterworth-Heinemann, Oxford.

Pelto, M. 2000: *Mass balance of adjacent debris-covered and clean glacier ice in the North Cascades, Washington.*, Debris-Covered Glaciers, Seattle, Washington, USA.

Purdie, J. M. 1996: *Ice loss at the terminus of the Tasman Glacier*, Master of Science, Otago University.

Ruddell, A. R. 1995: *Recent Glacier and Climate Change in the New Zealand Alps*, Doctor of Philosophy, University of Melbourne.

Salinger, M. J., Heine, M. and Burrows, C. J. 1983: Variations of the Stocking (Te Wae Wae) Glacier, Mount Cook, and climatic relationships, *New Zealand Journal of Science*, 26, 321-338.

Salinger, M. J. 2005: *New Zealand glaciers continue to recover*, National Institute of Water and Atmospheric Research, Auckland.

Sara, W. A. 1968: Franz Josef and Fox Glaciers, 1951-1967, *New Zealand Journal of Geology and Geophysics*, 11, 768-780.

Sara, W. A. 1970: *Glaciers of Westland National Park*, Government Printer, Wellington.

Singh, P., Kumar, N., Ramasatri, K. S. and Singh, Y. 2000: *Influence of a fine debris layer on the melting of snow and ice on a Himalayan glacier.*, Debris-Covered Glaciers, Seattle, Washington, USA.

Speight, R. 1935: Notes on the Franz Josef Glacier, February, 1934, *Transactions of the New Zealand Institute*, 64, 315-322.

Spronken-Smith, R. 2001: Microclimates and Earth-surface Energy Exchanges, in Sturman, A P and Spronken-Smith, Rachel, *The Physical Environment - A New Zealand Perspective*, Oxford University Press, Melbourne, 113-129.

Sturman, A. P. 2001a: Local and Regional Weather and Climate, in Sturman, A P and Spronken-Smith, Rachel, *The Physical Environment - A New Zealand Perspective*, Oxford University Press, Melbourne, 94-112.

Sturman, A. P. 2001b: Synoptic Controls on the Weather, in Sturman, A P and Spronken-Smith, Rachel, *The Physical Environment - A New Zealand Perspective*, Oxford University Press, Melbourne, 76-93.

Suggate, R. P. 1950: Franz Josef and other Glaciers of the Southern Alps, New Zealand, *Journal of Glaciology*, 1, 422-429.

Suggate, R. P. 1952: Franz Josef Glacier, March, 1951, *New Zealand Journal of Science and Technology*, 33B, 299-304.

Suggate, R. P. 1990: Late Pliocene and Quaternary Glaciations of New Zealand, *Quaternary Science Reviews*, 9, 175-197.

Summerfield, M. 1991: *Global Geomorphology*, Pearson Education Limited, Essex.

Swift, D. A., Nienow, P., Hoey, T. and Mair, D. 2005: Seasonal evolution of runoff from Haut Glacier d'Arolla, Switzerland and implications for glacial geomorphic processes, *Journal of Hydrology*, Article in Press, 1-16.

Takeuchi, Y., Naruse, R., Satow, K. and Ishikawa, N. 1999: Comparison of heat balance characteristics at five glaciers in the Southern Hemisphere, *Global and Planetary Change*, 22, 201-208.

Takeuchi, Y., Kayastha, R. B. and Nakawo, M. 2000: *Characteristics of ablation and heat balance in debris-free and debris-covered areas on Khumbu Glacier, Nepal Himalayas, in the pre-monsoon season.*, Debris-Covered Glaciers, Seattle, Washington, USA.

The Press. 31 August, 2005, 5.

Tippett, J. M. and Kamp, J. J. 1995: Geomorphic Evolution of the Southern Alps, New Zealand, *Earth Surface Processes and Landforms*, 20, 177-192.

Tyson, P. D., Sturman, A. P., Fitzharris, B. B., Mason, S. J. and Owens, I. F. 1997: Circulation Changes and Teleconnections Between Glacial Advances on the West Coast of New Zealand and Extended Spells of Drought Years in South Africa, *International Journal of Climatology*, 17, 1499-1512.

Willis, I. 1995: Intra-annual variations in glacier motion: a review, *Progress in Physical Geography*, 19, 61-106.

Willis, I., Mair, D., Hubbard, B., Nienow, P., Fischer, U. H. and Hubbard, A. 2003: Seasonal variations in ice deformation and basal motion across the tongue of Haut Glacier d'Arolla, Switzerland, *Annals of Glaciology*, 36, 157-167.

Wilson, W. 1896: The Fox Glacier, *Appendix to the Journal of the House of Representatives of New Zealand*, Vol 1, C-1, 108-109.

Woo, M. and Fitzharris, B. B. 1992: Reconstruction of Mass Balance for Franz Josef Glacier, New Zealand, 1913 to 1989, *Arctic and Alpine Research*, 24, 281-290.